Climate and vegetation dynamics of Central Europe during the Eocene greenhouse: Palynological investigations of lacustrine sediments from the Sprendlinger Horst (Hesse, Southwest Germany)

TECHNISCHE UNIVERSITÄT DARMSTADT

Dissertation approved by
the Department of Materials- and Geosciences,
Technical University of Darmstadt
in fulfilment of the requirements for the degree of
Doctor rerum naturalium (Dr. rer. nat.)

by
Maryam Moshayedi
M.Sc. in Geology

Referee: PD. Dr. Olaf Klaus Lenz
Co- referee: Prof. Dr. Christoph Schüth
Submission: April 2021
Oral exam: 12.07.2022

Darmstadt 2023

Maryam Moshayedi: Climate and vegetation dynamics of Central Europe during the Eocene greenhouse: Palynological investigations of lacustrine sediments from the Sprendlinger Horst (Hesse, Southwest Germany)
Darmstadt, Technische Universität Darmstadt
Year thesis published in TUprints 2023
Date of the viva voce 12.07.2022

Maryam Moshayedi

Dissertation
Thema “Climate and vegetation dynamics of Central Europe during the Eocene greenhouse: Palynological investigations of lacustrine sediments from the Sprendlinger Horst (Hesse, Southwest Germany)”

Referee: PD. Dr. Olaf Klaus Lenz
Co- referee: Prof. Dr. Christoph Schüth
Prüfer 1: Prof. Dr. Matthias Hinderer
Prüfer 2: Prof. Dr. Nico Blüthgen

Eidesstattliche Erklärung (Declaration of authorship)

Hiermit erkläre ich, Maryam Moshayedi (Matrikel-Nr. 2394057), dass ich die vorliegende Doktorarbeit

"Climate and vegetation dynamics of Central Europe during the Eocene greenhouse: Palynological investigations of lacustrine sediments from the Sprendlinger Horst (Hesse, Southwest Germany)"

ohne Hilfe Dritter und ohne Benutzung anderer als der angegebenen Hilfsmittel angefertigt habe; die aus fremden Quellen direkt oder indirekt übernommenen Gedanken sind als solche kenntlich gemacht. Die Arbeit wurde bisher in gleicher oder ähnlicher Form keiner anderen Prüfungsbehörde vorgelegt und nicht veröffentlicht.

I hereby certify that the complete work to this PhD thesis was done by myself and only with the use of the referenced literature and the described methods.

Darmstadt, den

Maryam Moshayedi

Contents

Supplementary material - chapter 4 (available on electronic media)

List of figures

List of tables

Acknowledgements

Undertaking this PhD has been a truly life-changing experience for me and it would not have been possible to do without the support and guidance that I received from many people.

First of all, I would like to express my sincere gratitude to Prof. Matthias Hinderer of the Applied Sedimentology working group at the Technische Universität Darmstadt, who enabled the thesis and for giving me the opportunity to realize my research ideas. It is always a pleasure to work with him and to be a member of his working group.

Equally my sincere thanks go to my advisor PD. Dr. Olaf Lenz of the Senckenberg Gesellschaft für Naturforschung in Frankfurt for the continuous support of my PhD study and related research, for his patience, motivation, and immense knowledge. His guidance helped me in all the time of research and writing of this thesis. I could not have imagined having a better advisor and mentor for my PhD study.

Besides my advisor, I would like to thank PD Dr. Volker Wilde of the Senckenberg Forschungsinstitut und Naturmuseum in Frankfurt not only for his support and encouragement, but also for insightful comments and discussions which incented me to widen my research from various perspectives.

I would like to express my gratitude to Karin Schmidt and all the student assistants for their excellent work in the field of time-consuming sample processing.

Special thanks go to the staffs and my colleagues from the working group of Applied Sedimentology, who gave me such a good time in Darmstadt.

I would acknowledge the people who mean a lot to me, my parents, Davood and Fereshteh, for giving me liberty to choose what I desired. I salute you for the selfless love, care, pain and sacrifice you did to shape my life.

I owe thanks to a very special person, my husband, Pouyan for his continued and unfailing love, support and understanding during my pursuit of PhD degree that made the completion of the thesis possible. I greatly value his contribution and deeply appreciate his belief in me. I appreciate my son, my little Sorena, for being a source of motivation and the patience he showed during my work. Words would never say how grateful I am to both of you.

Last but not least, the German Academic Exchange Service (DAAD) is thanked for funding this project.

Preface

One of the periods, which may represent a past analog of a future warmer climate on earth and which was in the focus of several palaeoclimate studies during the last 20 years, is the Paleogene. In this time interval pronounced climate changes occurred, most notably the Eocene/Oligocene greenhouse/icehouse transition and in the early Paleogene several short term hyperthermal events. In this cumulative PhD thesis palynological analyzes have been used to provide new contributions to the research of vegetation dynamics during the Paleogene greenhouse of Central Europe and the associated effects on the palaeoenvironment, especially in relation to climate dynamics. Sedimentological studies were applied as additional methods. The thesis can be divided into 5 chapters:

Chapter 1 (Introduction) introduces this thesis by giving an overview of the research aim.

Chapter 2 (Methods) presents methods and analytical tools applied during the study.

Chapter 3 (Geological background) discuss the paleogeography and geology of Upper Rhine Graben and Sprendlinger Horst and the evolution of the Paleogene lacustrine deposits in this area.

Chapter 4 (Results and publications) presents a systematic list of recorded species during this study as well as published and unpublished results of the studies:

Chapter 4. 5 (Publication 1) is a published quantitative palynological study of lacustrine sediments taken from a research core (B/98-BK 1E) drilled in the center of the maar lake of Offenthal and provide different pollen and spore assemblages that can be used for the reconstruction of the palaeoenvironment and changes within the vegetation. Furthermore, the palynomorph assemblages from Offenthal are compared in this study with already published assemblages from Messel by multivariate analysis to reveal similarities and differences during the recolonization of volcanically disturbed habitats on the Sprendlinger Horst during Paleogene greenhouse conditions. This chapter has been published as:
Moshayedi, M., Lenz, O.K., Wilde, V., Hinderer, M., 2020. The recolonization of volcanically disturbed habitats during the Eocene of Central Europe: The maar lakes of Messel and Offenthal (SW Germany) compared. Palaeobiodiversity and Palaeoenvironments, 100**,** 951–973 (2020). https://doi.org/10.1007/s12549-020-00425-4

Chapter 4. 6 (Publication 2) discusses the control mechanisms of sedimentary changes and vegetational changes within the small pull-apart basin at “Grube Prinz von Hessen” (PvH) on the Sprendlinger Horst during Paleogene greenhouse conditions. In this paper statistical analysis of the palynoflora, revealed by a study of lacustrine sediments taken from a drill core (B/97-BK 9) in the center of the lake basin, show 5 distinct palynomorph associations representing different vegetation communities. It could be proven that throughout the sedimentary record there is a strong correlation between major changes in vegetation and lithology which were controlled mainly by changes in humidity together with tectonic activity. Furthermore, based on biostratigraphic analysis based on palynomorphs, it has been proven that the basin is older than previously assumed and of Lower Eocene age. This chapter has been published as:
Moshayedi, M., Lenz, O.K., Wilde, V., Hinderer, M., 2018. Controls on sedimentation and vegetation in an Eocene pull-apart basin (Prinz von Hessen, Germany): evidence from palynology. Journal of the Geological Society, 175, 757-773.

Chapter 4. 7 (Publication 3) focuses on a palynological study of a specific part of the lacustrine filling in the core B/97-BK 9 of the Eocene pull-apart basin "Grube Prinz von Hessen", characterized by a regular alternation of lignite layers and mudstones. Multivariate statistical analyses of the microflora reveal strong differences between the palynomorph assemblages of lignite and mudstone beds. The lake was influenced probably by tectonic activity, such as earthquake tremor, resulting in the redeposition of lignite and mudstone. The same subordinate trends in the vegetation are obvious in the microflora of both lithologies. Slight qualitative changes in the vegetation may be explained by climate change. This chapter has been accepted for publication as:
Moshayedi, M., Lenz, O.K., Wilde, V., Hinderer, M., 2021. Lake level fluctuation and allochthonous lignite deposition in the Eocene pull-apart basin "Prinz von Hessen" (Hesse, Germany) – A palynological study. Syntheses in Limnogeology, Rosen, M.R., Finkelstein, D., Park Boush, L., Pla-Pueyo, S. (eds.): Limnogeology: Progress, challenges and apportunities: A tribute to Beth Gierlowski-Kordesch, Chapter 3. Springer Nature article in press.

Chapter 4. 8 (Manuscript in preparation 1) presents a small palynological study of 6 lignite samples from the lake basin of Grube "Prinz von Hessen", which were taken east of the drill site. The palynomorph assemblages are compared with assemblages from core Prinz von Hessen to provide chronological control for the sedimantry sequences in the basin. The results underline age differences between lignites revealed in the core and the lignites that have been mined in the last century in parts of the lake basin. This chapter is considered to be prepared for publication in the near future.

Chapter 4. 9 (Manuscript in preparation 2) discusses a complete overview on the evolution of the vegetation on the Sprendlinger Horst during the Lower and Middle Eocene by comparing the palynological assemblages from the maar lakes at Messel, Offenthal and Groß Zimmern and the pull-apart basin Prinz von Hessen. Furthermore, the study sheds new light on the history of volcanism in the area of the Sprendlinger Horst east of the Upper Rhine Graben. This chapter is considered to be prepared for publication.

Chapter 5 (Synthesis) presents a final discussion and summary of the results obtained during this study as well as delineating perspective on future directions.

Abbreviations

CA	Correspondence Analysis
CoA	Coexistence Approach
cm	Centimeter
DCA	Detrended Correspondence Analysis
DIC	Dissolved Inorganic Carbon
EILP	Early Initial Lake Phase
GDR	German Democratic Republic
HCl	Hydrochloric acid
HF	Hydrofluric acid
HNO_3	Nitric acid
H_2O_2	Hydrogen peroxide
Hu	Helmstedt Unterflöze
ka	Thousand years
KOH	Potassium hydroxide
Kyr	Thousand years
Li	Lignite
LILP	Late Initial Lake Phase
LMA	Leaf Margin Analysis
LMF	Lower Messel Formation
LZ	Lithozone
Ma	Million years
m	Meter
mm	Millimeter/ 10^{-3} m
MMF	Middle Messel Formation
MP	Mammal Paleogene Zone
Mu	Mudstone
MZN	Messel Fault Zone
NMDS	Non-Metric Multidimentional Scaling
NLR	nearest living relatives
PvH	Prinz von Hessen
PCA	Principle Component Analysis
PZ	Palynozone
SD	Units of average standard deviation of species turnover
SO_4	Sulphate
TOC	Total Organic Carbon
UNESCO	United Nations Educational, Scientific and Cultural Organization
UPGMA	Unweighted Pair Group Average
^{39}Ar	Instable Argon isotope
^{40}Ar	stable Argon isotope
$\delta^{13}C$	stable Carbon isotope
$\delta^{18}O$	stable Oxygen isotope
%	Percentage
µm	Micrometer/10^{-6} m
cps	Counts per seconds

1- Introduction

The palynological research of the Eocene of Central Europe began almost 85 years ago with a paper by R. Potonié (1934) on the brown coal of the Geiseltal in eastern Germany. During the 1950s, this pioneering work has been extended mainly by Pflug (1952) and Thomson and Pflug (1953). Later, this relevant knowledge was substantially enhanced during the intensive brown coal exploration on the territory of the GDR in the 1960s and 1970s particularly by Krutzsch (e.g. Krutzsch 1959, 1976, 1992). Together with following studies that focused on different localities from Germany (e.g. Thiele-Pfeiffer 1988; Schuler 1990; Nickel 1996a, 1996b; Hammer-Schiemann 1998; Lenz 2005), a worldwide unique data base on the systematics and taxonomy of pollen and spores from the Paleogene of Central Europe has been established, which provided an excellent basis for further paleoclimate and paleoecological analysis of appropriate material.

The focus particularly of the older studies from the last century was primarily on the systematic-taxonomic inventory of the palynoflora with the aim to implement a biostratigraphic base for the correlation of isolated basins with a filling of mainly lacustrine sediments and for the correlation of coal seams within individual lignite deposits. The principles of the stratigraphic subdivision of the Paleogene, which are essentially based on the conditions within the Central German brown coal deposits have been summarized by Krutzsch (1992) and Pflug (1986).

Since classification and taxonomy of the Paleogene palynoflora of Central Europe is now very well known, today a systematic-taxonomic inventory of the microflora in other hitherto not investigated deposits from Central Europe is unproblematic for this time interval. Therefore, in recent studies from the last decade the focus was placed more on the reconstruction of the palaeoenvironment (e. g. Lenz 2005; Lenz et al. 2007; Riegel et al. 2012). This is mostly done by high-resolution studies of sediments with a high number of analyzed samples to capture short- and long-term trends in climate and vegetation dynamics. In particular, the recent palynological studies from the maar lake of Messel provide important contributions on climate and vegetation dynamics within the terrestrial greenhouse climate of Central Europe (Lenz 2005; Lenz et al. 2007; 2009; 2010; 2011, 2015; Lenz and Wilde 2018).
In this cumulative PhD thesis the palynological composition of two small Eocene lakes at Prinz von Hessen and Offenthal on the Spendlinger Horst in Southwest Germany were studied and additionally compared with existing data of two other nearby lakes at Messel and Groß Zimmern for understanding the evolution of the vegetation in Central Europe during Paleogene greenhouse conditions with respect to regional tectonic and volcanic influence. A further task of the thesis is also the application of numerical methods on palynological data for the study of interactions between palaeoclimate, palaeoenvironment and vegetation.
Except Prinz von Hessen, which is most probably a small pull-apart basin, the other basins are maar lakes and formed as a consequence of phreathomagmatic eruptions. Based on revised $^{40}Ar/^{39}Ar$ dates the eruptions at Offenthal (47.71/47.87 ± 0.3 Ma) and Messel (48.11/48.27 ± 0.22 Ma) are nearly of the same age around the Lower/Middle Eocene boundary. Based on the palynostratigraphic work of Mutzl (2017) it seems likely that Lake Groß Zimmern has a similar age as the adjacent crater lakes of Messel and Offenthal, but this must be confirmed by radiometric dating in the near future. With the comparison of these three adjacent and coeval lakes and the palynostratigraphically dated lower Eocene pull-apart basin Prinz von Hessen (Moshayedi et al. 2018), it is possible to reconstruct the evolution of the vegetation and the paleoclimate on the Sprendlinger Horst across the lower to middle Eocene. Furthermore, a chronostratigraphic scenario for volcanic and tectonic activity in the region can be presented.

The results of the studies are condensed in 5 original papers (3 of them are published), which are presented here in this PhD thesis.

References:

Hammer-Schiemann, G. (1998). Palynologische Untersuchungen zur Fazies und Ökologie der Unterflözgruppe im Tagebau Schöningen (Untereozän, Helmstedt, Bezirk Braunschweig). – *Diss. Univ. Göttingen*: 1-146.

Krutzsch, W. (1959). Mikropaläontologische (sporenpaläontologische) Untersuchungen in der Braunkohle des Geiseltales. – *Geologie Beih*., 21/22: 1-425.

Krutzsch, W., (1976) Die Mikroflora der Braunkohle des GeiseltalesTeil IV: Die stratigraphische Stellung des Geiseltalprofils im Eozän und die sporenstratigraphische Untergliederung des mittleren Eozäns. – *Abh. Zentr. Geol. Inst*., 26: 47-92.

Krutzsch, W. (1992). Paläobotanische Klimagliederung des Alttertiärs (Mitteleozän bis Oberoligozän) in Mitteldeutschland und das Problem der Verknüpfung mariner und kontinentaler Gliederungen (klassische Biostratigraphien - paläobotanisch-ökologische Klimastratigraphie - Evolutions-Stratigraphie der Vertebraten). – *N. Jb. Geol. Paläont. Abh*., 186, 1-2: 137-253.

Lenz, O.K. (2005). Palynologie und Paläoökologie eines Küstenmoores aus dem Mittleren Eozän Mitteleuropas Die Wulfersdorfer Flözgruppe aus dem Tagebau Helmstedt, Niedersachsen. *Palaeontographica B*, *271*, 1–157.

Lenz, O.K., Wilde, V., Riegel, W. (2007). Recolonization of a Middle Eocene volcanic site: quantitative palynology of the initial phase of the maar lake of Messel (Germany). *Review of Palaeobotany and Palynology*, *145*, 217–242.

Lenz, O.K., Wilde, V., Riegel, W. (2009). Potential of palynostratigraphic resolution in a homogeneous lacustrine succession: the Middle Eocene Messel Formation. *Neues Jahrbuch für Geologie und Paläontologie, Abhandlungen*, 251 (3): 285-301.

Lenz, O.K., Wilde, V., Riegel, W., Harms, F.-J. (2010). A 600 k.y. record of El Niño–Southern Oscillation (ENSO): Evidence for persisting teleconnections during the Middle Eocene greenhouse climate of Central Europe. *Geology*, 38 (7): 627-630.

Lenz, O.K., Wilde, V., Riegel, W. (2011). Short-term fluctuations in vegetation and phytoplankton during the Middle Eocene greenhouse climate: a 640-kyr record from the Messel oil shale (Germany). *International Journal of Earth Sciences*, 100: 1851 -1874. DOI 10.1007/s00531-010-0609-z.

Lenz, O.K., Wilde, V., Mertz, D.F., Riegel, W. (2015). New palynology-based astronomical and revised 40Ar/39Ar ages for the Eocene maar lake of Messel (Germany). *International Journal of Earth Science*, *104*, 873-889.

Lenz, O. K., and Wilde, V. (2018). Changes in Eocene plant diversity and composition of vegetation: the lacustrine archive of Messel (Germany). *Paleobiology*, *44(4)*, 709-735.

Nickel, B. (1996a). Die mitteleozäne Mikroflora von Eckfeld bei Manderscheid/Eifel. – *Mainzer naturwiss. Archiv, Beih*., 18: 1-148.

Nickel, B. (1996b). Palynofazies und Palynostratigraphie der Pechelbronn Schichten im nördlichen Oberrheintalgraben. – *Palaeontographica B*, 240: 1-151.

Schuler, M. (1990). Palynologie et biostratigraphie de l´Eocène et de l´Oligocène inférieur dans les fossés rhénan, rhodanien et de Hesse. – *Doc. B.R.G.M*., 190: 1-503.

Pflug, H. (1952). Palynologie und Stratigraphie der Braunkohlen von Helmstedt. – *Paläont. Z*., 26: 112-137.

Pflug, H. (1986). Palyno-Stratigraphy of the Eocene/Oligocene in the Area of Helmstedt, in North Hessia and in the adjacent southern Range. In: Tobien, A.[Ed.]: *Beiträge zur regionalen Geologie der Erde (Nordwestdeutschland im Tertiär)*., 38: 567-583; Berlin-Stuttgart (Gebr. Bornträger).

Potoniè, R. (1934). Zur Mikrobotanik des eozänen Humodils des Geiseltales. – Arb. Inst. Paläobot. Petrogr. Brennsteine, *Preuß. Geol. L.-A*., 4: 25-125.

Riegel, W., Wilde, V., Lenz, O.K. (2012). The Early Eocene of Schöningen (N-Germany) – an interim report. *Austrian Journal of Earth Sciences*, 105 (1): 88 – 109.

Thiele-Pfeiffer, H. (1988). Die Mikroflora aus dem mitteleozänen Ölschiefer von Messel bei Darmstadt. *Palaeontographica B*, *211*, 1–86.

Thomson, P.W., Pflug, H. (1953). Pollen und Sporen des mitteleuropäischen Tertiärs. Gesamtübersicht über die stratigraphisch und paläontologisch wichtigen Formen. *Palaeontographica B*, *94*, 1–138.

2- Methods

2-1 Palynology

The wall of palynomorphs is made of a mixture of cellulose and polymer with saturated and unsaturated hydrocarbons and phenolics called sporopollenin (Suthworth 1990). Sporopollenin is resistant to most forms of chemical and physical degradation, except oxidation (Bennett and Willis 2001). Therefore, palynomorphs may be preserved indefinitely in anaerobic environments and strong chemicals such as hydrofluoric acid (HF) or hydrochloric acid (HCl) can be used during sample processing to remove other components of sediments. The palynological preparation used in the here presented studies followed the standard procedures as described by Kaiser and Ashraf (1974) including treatment with hydrochloric acid (HCl), hydrofluoric acid (HF), and potassium hydroxide (KOH). To remove flocculating organic matter and improve the transparency of the palynomorphs, the residue was briefly oxidized with nitric acid (HNO_3) or hydrogen peroxide (H_2O_2) after sieving with a mesh size of 10 µm. Remaining sample material and slides are stored at the Palaeobotanical Section of the Senckenberg Research Institute and Museum in Frankfurt, Germany.
Palynological analysis was undertaken using a transmitted light microscope (Olympus BX40). To obtain a representative dataset for robust statistical analysis, at least 300 individual palynomorphs were counted per sample at ×400 magnification (raw data are included in the Supplementary material). The palynomorphs were mainly identified on the basis of the systematic-taxonomic studies of Thomson and Pflug (1953), Thiele-Pfeiffer (1988), Nickel (1996) and Lenz (2005). Poorly preserved palynomorphs that could not be identified were counted as 'Varia'. Morphologically similar sporomorph taxa, which have been assigned to the same parent plant family, were lumped to minimize potential errors in the identification and counting of individual species.

2-2 Statistics

2-2-1 Data preparation

Palynological studies generate large amount of data. Therefore, it is vital to evaluate the data by different multivariate statistical methods to simplify the interpretation of the data and identify hidden structures in the data set. For this reason, an important focus of this thesis is to apply a varity of multivariate statistical methods and to find for every situation the appropriate method. For the analysis of palynomorphs of "Lake Prinz von Hessen" (publication 2) I used abundance classes to eliminate minor abundance fluctuation of palynomorphs and remove dependence of variables.
In the other studies (publication 1, 3 and manuscript in preparation) I used Wisconsin double standardized raw data values of counted samples (Bray and Curtis 1957; Cottam et al. 1978; Gauch and Scruggs 1979; Oksanen 2007). Hence, the species counts are standardized by dividing the empirical value by the maximum counting value across all samples for each species; then, sample counts are standardized by finding the proportion of each species versus the total sum for each sample. This equalizes the effects of rare and abundant taxa, and removes the influence of sample size on the analysis (Bray and Curtis 1957; Cottam et al. 1978).

2-2-2 Zonation of pollen diagrams

The pollen diagrams, produced by PanPlot 11.04 (Alfred Wegener Institut für Polare und Marine Forschung, PANGEA), show the abundance of the most important palynomorphs in percentages. Taxa are arranged according to their weighted average value (WA regression; ter Braak and Looman 1995) in relation to depth by using the software C2 1.7.6 (Juggins 2007). This arrangement led to a structured pollen diagram showing the major patterns of compositional variation in relation to depth and revealed the steps in the progression of the

plant community (Janssen and Birks 1994). Pollen and spores were calculated to 100% whereas algae such as *Botryococcus* and *Ovoidites* were added as additional percentages (in percent of the total pollen sum). For the Offenthal paper (publication 1) a robust zonation of the pollen diagram constrained cluster analysis was carried out using the unweighted pair group average method (UPGMA), an agglomerative hierarchical clustering method. The agglomerative clustering is the most common type of hierarchical clustering used to group objects in clusters based on their similarity (Kasambara 2017). For the analysis of palynomorphs of "Lake Prinz von Hessen" (publication 2) a robust zonation of the pollen diagram was established by constrained cluster analysis using Ward's minimum variance method (software PAST 3.06, Hammer et al. 2001). In the second paper of Prinz von Hessen (publication 3) a robust zonation of the pollen assemblages in the lignite and mudstone samples was reached by using two-way cluster analyses (Q- and R-mode) resulting in a cluster matrix to identify samples with similar palynomorph contents (Q-mode) and to reveal which pollen-spore taxa group together (R-mode). Bootstrapped Q-mode cluster analysis was established by constrained cluster analysis using the unweighted pair-group average (UPGMA) method and an Eucledian distance, whereas R-mode cluster analysis applied the unconstrained UPGMA method with the Euclidean distance (software PAST 3.06, Hammer et al. 2001). Bootstrapped constrained analysis for Q-mode defined sample clusters was chosen to group only stratigraphically adjacent samples during the clustering procedure to identify a zonation in the lithological succession and to test if the multiple phases (clusters) are robust or just produced by change (detailed results of the bootstrapping analysis are presented in the supplementary material). Rare species with a maximum value less than 1% which do not show any significant pattern throughout the pollen diagram were excluded from cluster analyses.

2-2-3 Paleoenvironmental analysis

For the statistical analysis of Prinz von Hessen data (publication 2) detrended correspondence analysis (DCA) has been used to reveal the underlying pattern as well as ecological gradients. It was implemented by using software PAST 3.06 (Hammer et al. 2001). DCA was chosen as the appropriate multivariate model, because a gradient lengths analysis (DCA, Hill and Gauch 1980) using the software Canoco for windows 4.56 (ter Braak and Smilauer 2009) determined a length of 3.0 SD (units of average standard deviation of species turnover) for the samples. Following ter Braak and Smilauer (2002) a gradient length of more than 2 SD indicates monotonic trends in species composition. Therefore, the unimodal response model of the DCA should be used rather than a linear response model such as a principal component analysis (PCA). DCA has been used instead of correspondence analysis (CA), because DCA corrects the arch effect and compression of data points at the edges of the ordination space (Hill and Gauch, 1980) and is therefore a technique that is commonly used in ecological ordination (e.g., Lenz et al., 2011; Daly et al. 2011; Galloway et al. 2015; Vellekoop et al. 2015). In contrast to cluster analysis that has been performed by using all palynomorph taxa, for DCA only taxa with an overall assemblage value of more than 0.5% were included in the analysis to reduce statistical noise (Stukins et al. 2013; Galloway et al. 2015).

For the other studies (publication 1, 3 and manuscript in preparation) as an alternative to the DCA non-metric multidimensional scaling (NMDS) has been used with the standardized raw data values and the Bray-Curtis dissimilarity (Bray and Curtis 1957; Hair et al. 2010; software PAST). This ordination method was chosen as the appropriate multivariate model, because NMDS is the most robust unconstrained ordination method in ecology (Minchin 1987) and has been successfully applied to palynological data in previous studies (e.g., Jardine and Harrington 2008, Mander et al. 2010, Broothaerts et al. 2014). NMDS avoids the assumption of a linear or unimodal response model between the palynomorph taxa and the underlying

environmental gradients, and also avoids the requirement that data must be normally distributed.

References:

Bray, J.R., Curtis, J.T. (1957). An ordination of the upland forest communities of southern Wisconsin. *Ecological Monographs*, *27*, 325-349.

Bennett, K.D., Willis, K.J. (2001). 2. Pollen. In: Smol JP, Birks HJB,Last WM (eds) Tracking environmental change using lakesediments. Volume 3: *terrestrial, algal, and siliceous indi-cators*. Kluwer Academic Publishers, Dordrecht, pp 5–32

Broothaerts, N., Verstraeten, G., Kasse, C., Bohncke, S., Notebaert, B., Vandenberghe, J. (2014). Reconstruction and semi-quantification of human impact in the Dijle catchment, central Belgium: a palynological and statistical approach. *Quaternary Science Reviews*, 102: 96-110.

Cottam, G., Goff, F.G., Whittaker, R.H. (1978). Wisconsin Comparative Ordination, in Whittaker RH, ed., Ordination of Plant Communities. Handbook of Vegetation Science, *5-2*, 185-213.

Daly, R.J., Jolley, D.W., Spicer, R.A. and Ahlberg, A., (2011). A palynological study of an extinct arctic ecosystem from the Palaeocene of Northern Alaska. *Review of Palaeobotany and Palynology*, 166, 107-116.

Gauch, H. G. and Scruggs, W. M. (1979). Variants of polar ordination, Veg-etatio, 40, 147–153, 1979.

Hair JR JF, Black WC, Babin BJ, Anderson RE (2010). *Multivariate data analysis, 7th edition*, London, Pearson, p 761.

Hammer, Ø., Harper, D.A.T., Ryan, P.D. (2001). PAST: paleontological statistics software package for education and data analysis. *Palaeontologia Electronica 4(1)*, https://palaeo-electronica.org/2001_1/past/issue1_01.htm

Galloway, J.M., Tullius, D.N., Evenchick, C.A., Swindles, G.T., Hadlari, T. and Embry, A. (2015). Early Cretaceous vegetation and climate change at high latitude: Palynological evidence from Isachsen Formation, Arctic Canada. *Cretaceous Research*, 56, 399-420.

Hill, M.O. and Gauch, H.G. (1980). Detrended Correspondence Analysis: an improved ordination technique. *Vegetatio*, 42, 47-58.

Janssen, C.R., Birks, H.J.B. (1994). Recurrent groups of pollen types in time. *Review of Palaeobotany and Palynology*, *82*, 165–173.

Jardine, P.E., Harrington, GJ., (2008). The Red Hills Mine palynoflora: A diverse swamp assemblage from the Late Paleocene of Mississippi, U.S.A. Palynology 32: 183-204.

Juggins, S. (2007). *C2 Software for ecological and palaeoecological data analysis and visualization.* User guide Version *1.5*, p 73.

Kaiser, M.L., Ashraf, R. (1974). Gewinnung und Präparation fossiler Pollen und Sporen sowie anderer Palynomorphae unter besonderer Berücksichtigung der Siebmethode. *Geologisches Jahrbuch*, *25*, 85–114.

Kassambara, A. (2017). Practical guide to cluster analysis in R: Unsupervised machine learning. (Vol. 1). Sthda.

Lenz, O.K. (2005). Palynologie und Paläoökologie eines Küstenmoores aus dem Mittleren Eozän Mitteleuropas Die Wulfersdorfer Flözgruppe aus dem Tagebau Helmstedt, Niedersachsen. *Palaeontographica B*, *271*, 1–157.

Lenz, O. K., Wilde,V. and Riegel, W. (2011). Short-term fluctuations in vegetation and phytoplankton during the Middle Eocene greenhouse climate: a 640-kyr record from the Messel oil shale (Germany). *International Journal of Earth Sciences*, *100*, 1851–1874.

Mander, L., Kürschner, W.M., McElwain, J.C. (2010). An explanation for conflicting records of Triassic–Jurassic plant diversity. Proceedings of the National Academy of Sciences of the United States of America 107: 15351–15356.

Minchin, P.R. (1987). An evaluation of the relative robustness of techniques for ecological ordination. *Vegetation*, 69: 89-107.

Nickel, B. (1996). Die mitteleozäne Mikroflora von Eckfeld bei Manderscheid/Eifel. *Mainzer Naturwissenschaftliches Archiv. Beiheft*, *18*, 1–121.

Oksanen, J. (2007). Standardization methods for community ecology. Documentation and user guide for package Vegan, 1.8-6.

Southworth, D. (1990). Exine biochemistry In: Blackmore S, Knox RB, eds. Microspores: evolution and ontogeny.

Stukins, S., Jolley, D.W., McIlroy, D. and Hartley, A.J. (2013). Middle Jurassic vegetation dynamics from allochthonous palynological assemblages: an example from a marginal marine depositional setting; Lajas Formation, Neuquén Basin, Argentina. *Palaeogeography, Palaeoclimatology, Palaeoecology*, 392, 117-127.

Thiele-Pfeiffer, H. (1988). Die Mikroflora aus dem mitteleozänen Ölschiefer von Messel bei Darmstadt. *Palaeontographica B*, *211*, 1–86.

ter Braak, C.J.F. and Looman, C.W.N. (1995). Regression. In: Jongman, R.H.G., Ter Braak, C.J.F. and Tongeren, O.F.R. (eds). *Data Analysis in Community and Landscape Ecology*. Cambridge University Press, Cambridge, 29–77.

ter Braak, C.J.F. and Smilauer, P. (2002). CANOCO Reference Manual and CanoDraw for Windows User's Guide: Canonical Community Ordination (version 4.5). *Microcomputer Power*, Ithaca, New York.

ter Braak, C.J.F. and Smilauer, P. (2009). Canoco. *Wageningen: Biometris Plant Research International.*

Thiele-Pfeiffer, H. (1988). Die Mikroflora aus dem mitteleozänen Ölschiefer von Messel bei Darmstadt. *Palaeontographica B*, 211, 1–86.

Thomson, P.W., Pflug, H. (1953). Pollen und Sporen des mitteleuropäischen Tertiärs. Gesamtübersicht über die stratigraphisch und paläontologisch wichtigen Formen. *Palaeontographica B*, *94*, 1–138.

Vellekoop, J., Smit, J., van de Schootbrugge, B., Weijers, J.W., Galeotti, S., Damste, J.S.S. and Brinkhuis, H. (2015). Palynological evidence for prolonged cooling along the Tunisian continental shelf following the K–Pg boundary impact. *Palaeogeography, Palaeoclimatology, Palaeoecology*, 426, 216-228.

3- Geological background

3.1 Paleogene palaeogeography of Central Europe

Contemporaneously with Tertiary tectonic phases of the Alpine orogeny, an extensive rift system developed in western and central Europe from the Mediterranean Sea to the North Sea. The middle Eocene origin and later development of this still active graben complex, known as the European Cenozoic Rift System, and the changes in kinematics of its individual segments is probably linked to stages of the convergence of the African and European plates (Ziegler, 1994; Prodehl et al., 1995).

Most part of northwestern Europe was covered by a shallow sea during the Paleogene, whereas Central Europe was represented by the Central European Island which was composed of the Rhenish and Bohemian Massifs and therefore without any marine influence (Fig. 3.1.1). Noteworthy for this area is especially the Upper Rhine Graben (URG) as part of the Cenozoic rift system. The northeastern shoulder of the URG is formed by the Sprendlinger Horst. Here, a series of isolated Paleogene deposits can be found, such as Messel, Prinz von Hessen, Offenthal and Groß Zimmern, which were selected to study the terrestrial climate evolution and the palaeoenvironment of the Paleogene in Central Europe.

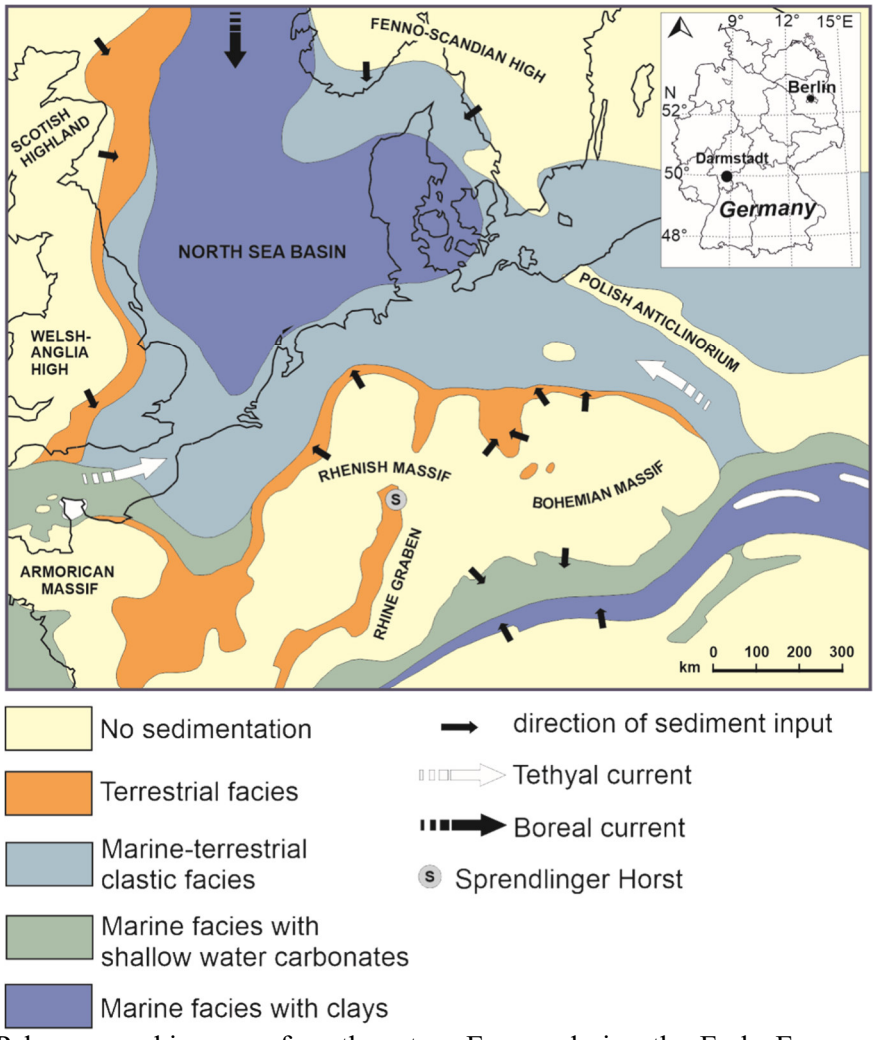

Fig. 3. 1. 1. Paleogeographic map of northwestern Europe during the Early Eocene (adapted from Ziegler 1990) showing the position of Sprendlinger Horst (S).

3.2 Geology

3.2.1 Upper Rhine Graben

The Upper Rhine graben (URG) represents the Central part of the European Cenozoic Rift System (ECRS), a complex of rift structures in the European continent, which trends from the North Sea coast to the Mediterranean (e.g. Ziegler 1994, Schumacher 2002, Dezes et al. 2004, Fekiacova et al. 2007, Reinhold et al. 2016). The NNE-SSW striking URG extends to about 300 km in length and 30-40 km in width. During the rift basin development two major phases of rift-related tectonic activity and subsidence rates are distinguished in the northen RRG (Fig. 3.2.1).

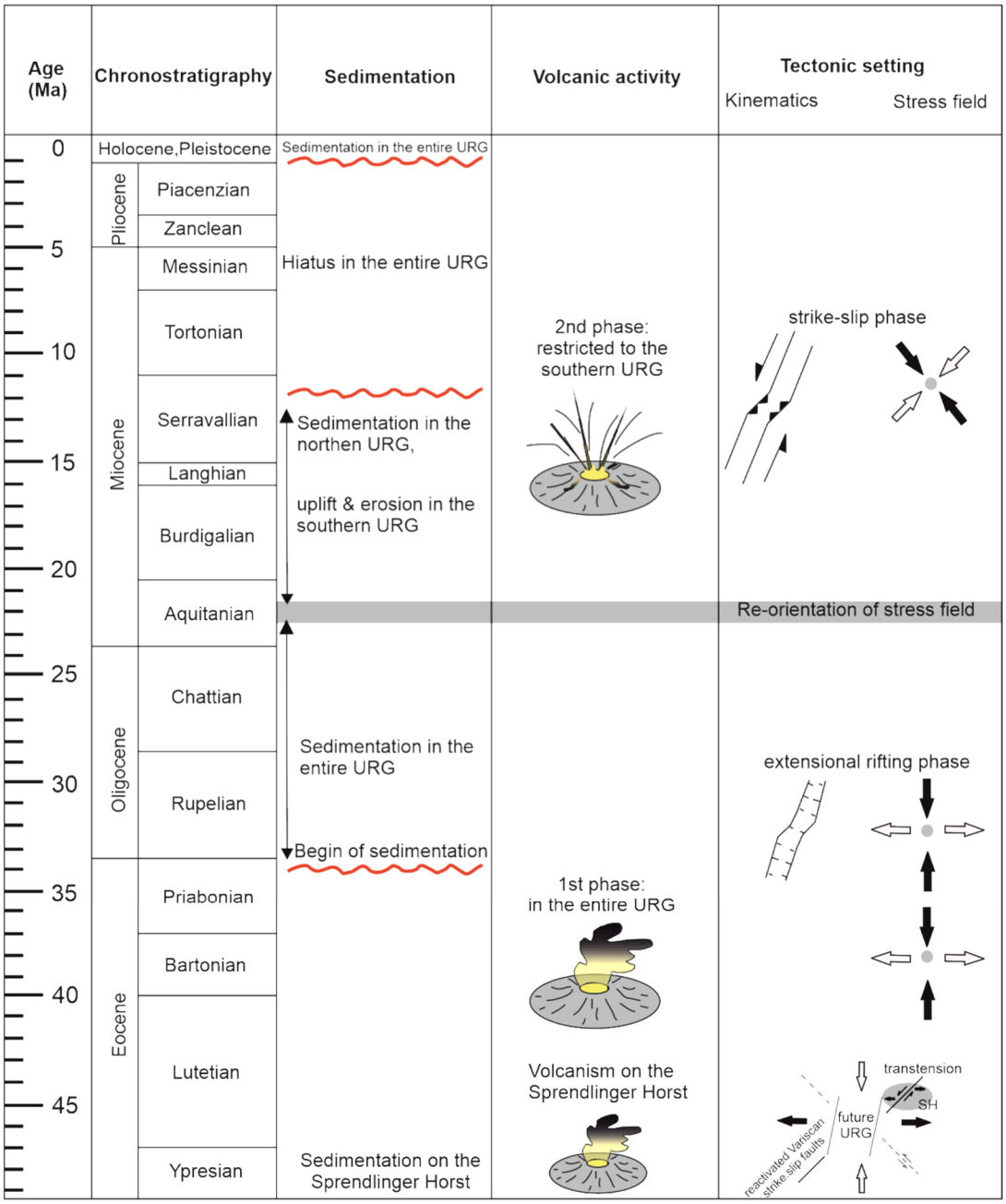

Fig. 3. 2. 1. Sedimentation record, tectonic setting and volcanism in the Upper Rhine Graben (modified after Perner 2018).

The late Eocene to early Oligocene subsidence phase (Villemin and Coletta 1990, Schumacher 2002) occurred due to a WNW-ESE oriented extension (Meier and Eisbacher 1991, Schumacher 2002). Active tilted fault blocks and horst-graben structures throughout the graben are the result of intense syn-rift graben tectonics. A second major phase of subsidence took place in the early Miocene (Aquitanian) and a third during the Pliocene and Quaternary.
Volcanic activity took place prior and during the rifting processes of the URG. Rifting was not caused by volcanism, as it originated from tectonic stress (passive rifting) and not by plume activity (active rifting) (Achauer and Masson 2002, Glahn and Granet 1992, Schwarz 2005). Two phases of volcanic activity are distinguished during syn-rift times (Fig. 3.2.1): the first phase, in the early to middle Eocene, is identified in the entire URG; maximum activity was reached during the middle Eocene, directly prior to the initiation of rifting (Horn et al. 1972, Keller et al. 2002). The second volcanic phase is assigned to the middle Miocene (Baranyi et al. 1976) and is restricted to the southern URG (e.g. Kaiserstuhl volcanics, Ziegler 1992).

3.2.2. The Sprendlinger Horst

The study sites within this PhD project are lower to middle Eocene lacustrine fillings of small basins located on the Sprendlinger Horst at the northern end of the Odenwald basement, immediately to the east of the URG. The Odenwald is part of the Mid-German Crystalline Rise, a magmatic arc formed during the Variscan Orogeny by the collision of the Rhenohercynian and Saxothuringian terranes after the collapse of the Rheic Ocean (Zeh and Will 2010).
Miocene uplift of the shoulders of the URG led to the erosion of Mesozoic and younger sediments that covered most of the basement rocks of the Mid-German Crystalline Rise and exposed Variscan basement (Schumacher 2002, Schwarz and Henk 2005, Ziegler and Dèzes 2005). The thickness of the late Paleozoic (Permian) cover, including Rotliegend basalts, sedimentary breccias, conglomerates and sandstones, decreases from 250 m in the northern part of the Sprendlinger Horst to zero south of Darmstadt (Marell 1989, Kowalczyk 2001). The southern Sprendlinger Horst is underlain by the Frankenstein Complex and consists of granites, granodiorites, tonalities, diorites and gabbros; the last of latest Devonian to earliest Carboniferous age (ca. 360 Ma; Stein 2001). Mesozoic rocks are followed by a stratigraphic gap that lasts to the early Palaeogene.
Lower Eocene extensional tectonics in the URG was accompanied by basaltic and trachytic volcanism on the Sprendlinger Horst that led to the formation of maar craters and pull-apart basins in the area (Fig. 3.2.1). They were filled by lacustrine deposits, such as the famous fossil-rich oil shale of Messel, as well as lesser known occurrences at Prinz von Hessen, Gross-Zimmern and Offenthal (Felder et al. 2001). The Messel and Prinz von Hessen deposits are aligned along the steep gravimetric gradient. Photo lineations within that zone are aligned parallel the Bouguer anomaly isolines (Jacoby et al. 2000, 2005). According to Jacoby et al. (2000) the gravity gradient reflects a 2 km wide, NE–SW-striking sinistral strike-slip fault zone, the so-called Messel Fault Zone (MFZ), which could have originated as a NW-directed thrust fault during the Variscan Orogeny.
The MFZ is thought to be reactivated during the development of the Saar-Nahe Trough in the Permian (Marell 1989) and the Eocene rifting of the URG (Fig. 3.2.1, Jacoby et al. 2000). 7 km to the SW of the MFZ a transfer zone existed within the URG, acting as a relay ramp connecting half-grabens with different polarity (Derer et al. 2005). The influence of Eocene tectonic activity in the URG on the Sprendlinger Horst (Fig. 3.2.1) is indicated by coeval deposition of the oil shale in Messel (47–45 Ma) and adjacent Prinz von Hessen (Backhaus and Rahnama-Rad 1991, Derer et al. 2005).

3.2.3 Paleogene lacustrine deposits

A series of about half a dozen isolated occurrences of Paleogene sediments can be found on the Sprendlinger Horst (Fig. 3.2.2). Geophysical data and evidence from cores penetrating some of these small Paleogene basins suggested that most of them represent the filling of volcanic structures which can be related to initial tectonic activity around the northern part of the future URG (Fig.3.2.1. e.g, Harms et al. 1999; Jacoby et al. 2000; Felder and Harms 2004).

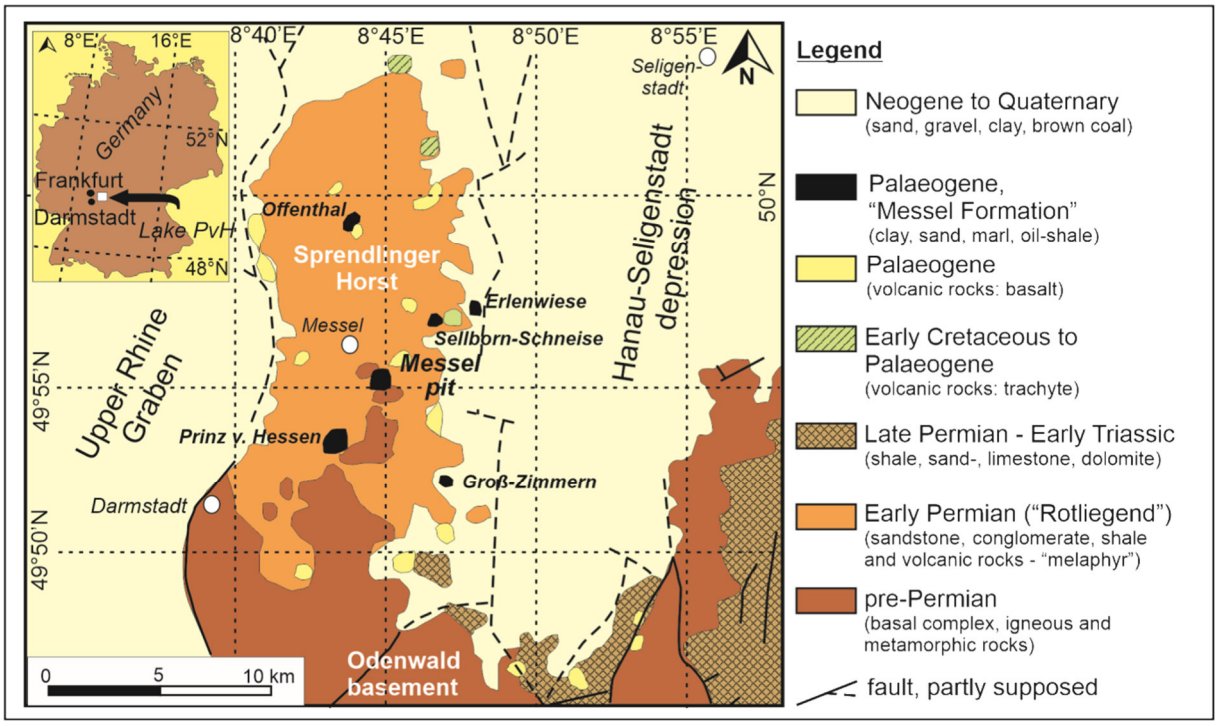

Fig. 3. 2. 2. Geological map of the Sprendlinger Horst (modified after Harms et al. 1999; Lenz et al. 2017; Lenz and Wilde 2018)

3.2.3.1 Pull-apart basin

Prinz von Hessen

Three of the volcanic basins (Messel, Erlenwiese, Sellborn-Schneise; Fig. 3.2.2) are aligned with the structure at Prinz von Hessen in SW-NE direction along a major concealed fault, the Messel Fault Zone (MZN; Mezger et al. 2013). However, the character of the basin at Prinz von Hessen remained unclear (Harms 1999; Felder et al. 2001; Jacoby et al. 2005). It has been discussed that it could represent either another maar structure or a small pull-apart basin (Felder et al. 2001, Hofmann et al. 2005).

Lake Prinz von Hessen had a semi-circular shape with a diameter of 600-800 m and was surrounded by sediments of Permian age (Felder et al. 2001). A scientific core (B/97-BK 9/9A) with a total thickness of 150 m was drilled in 1997 in the centre of the lake basin (49°53'56.64" N, 8°43'48.31"E) and has been described by Felder et al. (2001). In the lower 55 m the core revealed a mixed allochthonous succession with lapilli in the upper part. Of importance is that the drilling penetrated clayey sediments of the Rotliegend (Felder et al. 2001), which are probably not reworked. This is clear evidence that the drilling did not reached rocks of a vent breccia. Therefore, a volcanic origin of the basin is unlikely. Furthermore, the proportion of volcanic components is very low so that according to Felder et al. (2001) an assignment of the succession to the maar lithozones of Pirrung (1998) is not possible. This clearly indicates that Prinz von Hessen is not a maar lake but a pull-apart basin.

In the upper part of the core a succession of 95 m of lacustrine sediments can be recognized (Fig. 3.2.3). It starts with a unit of 34 m of graded and occasionally cross-bedded sandstones and siltstones, interbedded with several thin, cm-thick mudstones that were deposited in a shallow lake environment (Fig. 3.2.3; Felder et al. 2001; Hofmann et al. 2005). The succeeding unit is characterized by 15 m of black, bituminous shale with high TOC content (30-45%; Hofmann et al. 2005), followed by approximately 15 m of interbedded grey-green mudstones and lignite and 25 m of mostly laminated bituminous shale in the upper part (Fig. 3.2.3). The top of the core consists of 5 m of deeply weathered bituminous shale.

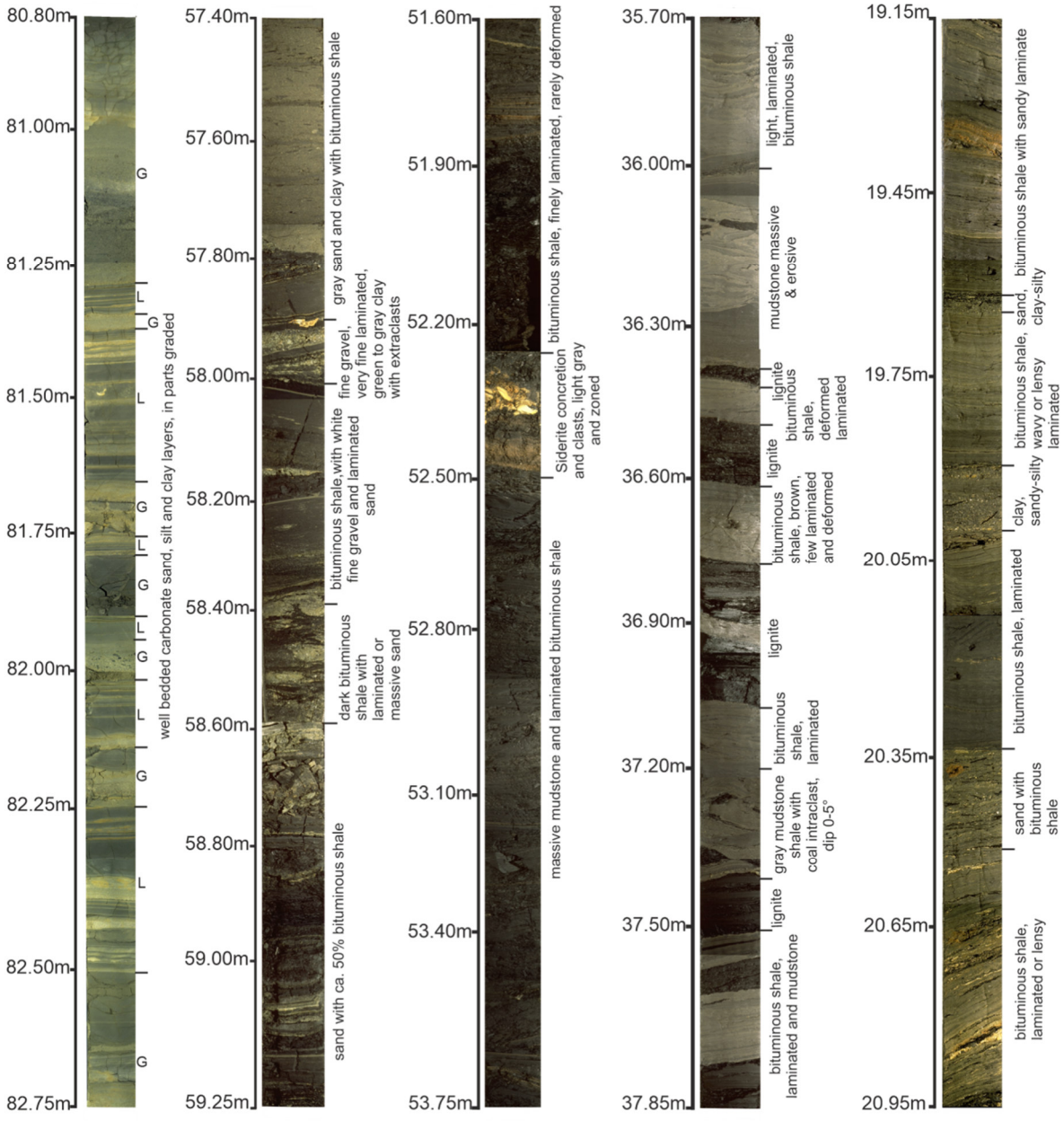

Fig. 3. 2. 3. Selected sections of core Prinz von Hessen illustrate various stages of sedimentation.

A further evidence that Lake Prinz von Hessen filled a small pull-apart basin is that the isotopic values of siderite (δ^{13}Carbon and δ^{18}Oxygen) in the lacustrine sediments at Prinz von Hessen are significantly lower than typical values for deep maar lakes which are characterized by long-lasting and stable meromictic conditions (Felder and Gaupp 2006). Low δ^{13}C and

$\delta^{18}O$ values can be interpreted as a consequence of the position of the redox boundary near the sediment surface within an open holomictic system, such as a river delta or an alluvial plain (Felder and Gaupp 2006). Therefore, it has been concluded that Lake Prinz von Hessen was significantly shallower than a typical deep maar lake (Fig. 3.2.4; Felder et al. 2001, Felder and Gaupp 2006).

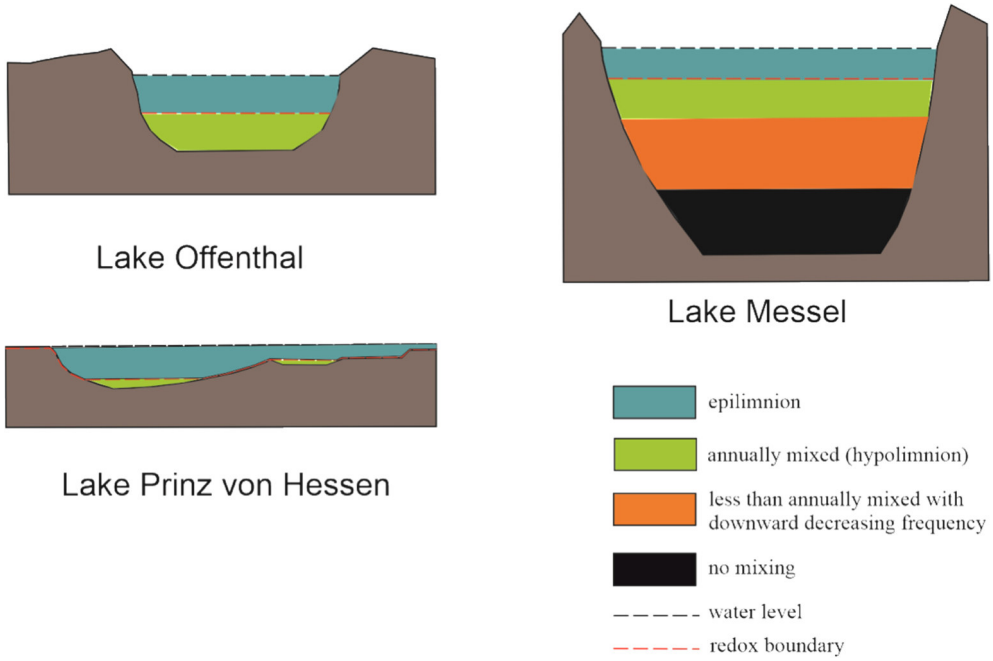

Fig. 3. 2. 4. Sketches of lake types (modified after Felder and Gaupp 2006)

In addition, the palynological results show that Lake Prinz von Hessen is considerably older than previously assumed (Moshayedi et al. 2018). Lacustrine sedimentation started in the latest Early Eocene almost coeval with deposition of the Lower Messel Formation at Messel. A mammal age for Prinz von Hessen from the mined part of the succession (Franzen 2006) possibly even ranges into the late Eocene and points to a considerable hiatus between the lake sediments in core Prinz von Hessen and the thick lignite which was originally mined at the top of the succession. The existence of the basin at Prinz von Hessen may therefore have lasted for more than 7 million years in contrast to less than a million years for the maar lake at Messel.

3.2.3.2 Maar Lakes

Messel

The Messel pit is located about 10 km NE of Darmstadt on the Sprendlinger Horst (49°55'03" N, 8°45'24"E; Fig. 3.2.2). Lake Messel is the best known among the isolated occurrences of Paleogene sediments on the Sprendlinger Horst and became worldwide known for an exceptionally well preserved assemblage of fossils, such as early mammals, vertebrates, insects and plants of early Middle Eocene age (Smith et al. 2018). This was the reason that the abandoned oil shale mine of Messel was added to the UNESCO list of World Nature Heritage Sites as a window to the past in 1995. In 2001 a continuous core was received from a research well in the center of the Paleogene basin at Messel. Starting with typical “Messel Oil shale”at the top it shows a differentiated lacustrine succession overlying some volcanoclastics and ends in some kind of a vent breccia. This finally proved that the oil shale was deposited in a meromictic maar lake with a diameter of 650 – 1100 m, which formed due to phreatomagmatic activity (Fig. 3.2.4, Lorenz 2000; Felder et al. 2001; Schulz et al. 2002;

Harms et al. 2003; Felder and Harms 2004). The reactivation of Variscian fault zone during the initial opening of the URG was probably the cause for the eruption (Mezger et al. 2013). A basaltic clast from the volcaniclastic material was dated radiometrically at 47.8 ± 0.2 Ma (Mertz and Renne 2005), Nevertheless this $^{40}Ar/^{39}Ar$ age have been revised by Lenz et al. (2015). The initial eruption can now be dated at 48.11 ± 0.22 or 48.27 ± 0.22 Ma. This date may serve as a good estimate for the time of the eruption and proofs that maar formation started already in the upper Lower Eocene (Lenz et al. 2015).

The sedimentary filling of the Messel Maar is subdivided into the Lower, Middle and Upper Messel Formations (Felder and Harms 2004). The early phase of lake Messel is represented by the Lower Messel Formation (LMF). During that time instability of the crater wall resulted in frequent mass movements as reflected by turbidites and slump deposits in the core. The lower part of the LMF between 230 and 140 m is characterized by alternating breccias, tuffs and layers of sand, silt and clay (Figs. 3.2.5).

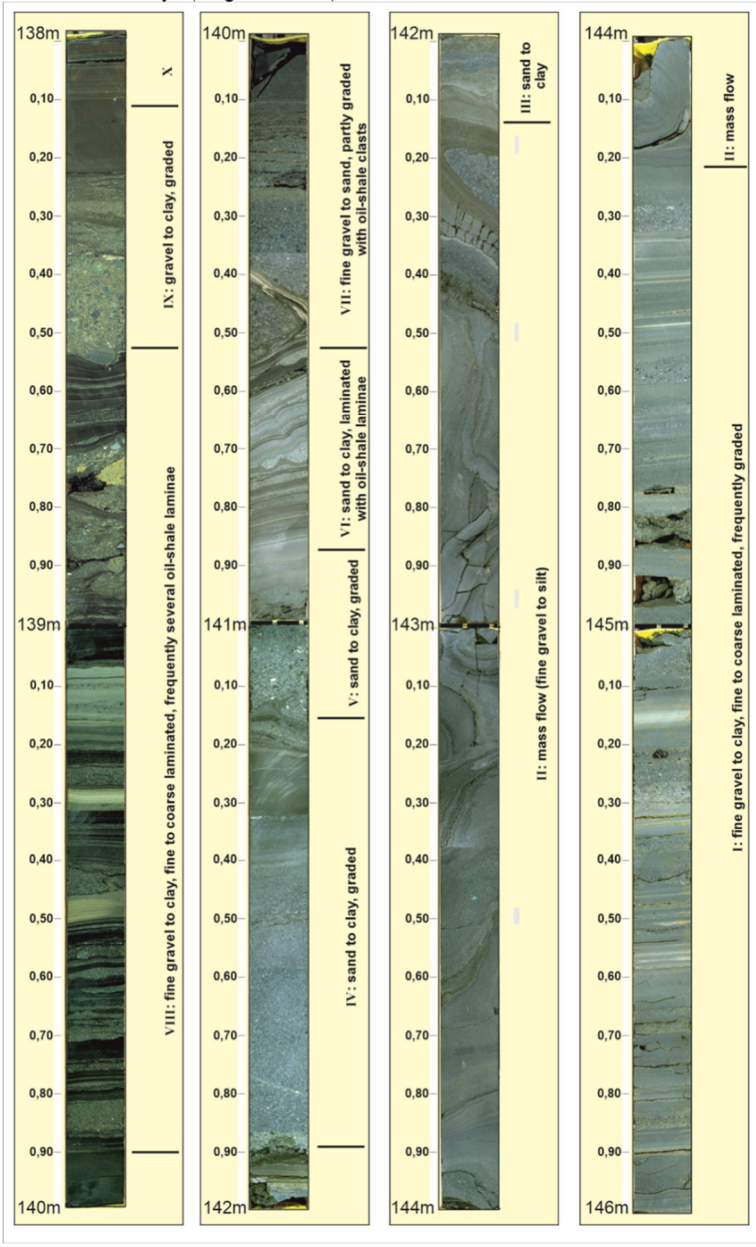

Fig. 3. 2. 5. Selected sections of core Messel 2001 illustrate various stages of sedimentation (modified after Lenz et al. 2007).

Because of more or less permanent turbulence holomictic conditions existed within the water body. Increasing stability of the crater wall and decreasing turbulence led to the onset of meromictic conditions and the beginning of deposition of oil shale layer in the upper part of the LMF at around 140 m depth in the core (Figs. 3.2.5). The LMF represents the initial lake phase according to Lenz et al. (2007), and is terminated by event beds of redeposited blocks of oil-shale, oil shale debris and clay between 110 and 94 m in the core, representing a turbidite deposit, probably a seismite (Fig. 3.2.5; Liebig 2002, Felder and Harms 2004).
The succeeding Middle Messel Formation (MMF) is characterized by a continuous succession of finely laminated oil shale, the classical "Messel oil shale", which is almost unaffected by turbidites and redeposition and represents long-term stable meromictic conditions in the lake (Fig. 3.2.5). The MMF is unconformably overlain by the Upper Messel Formation, an intercalation of inorganic claystones of various colors and coal beds restricted to three troughs in the south and east of the basin (Matthess 1966).

Offenthal
Among the Paleogene maar lakes on the Sprendlinger Horst Lake Offenthal is one of the smallest with a diameter of only 200 – 400 m (Felder et al. 2001). In order to find unequivocal proof for the origin of the basin, a scientific well (B/98-BK 1E) was drilled 1998 in the centre of the basin (49°58'52.37" N, 8°44'40.88" E) to penetrate the lake sediments. A total of 80 m was cored of which the lower 51 m consist of volcanic rocks that can be separated from a lacustrine succession in the upper 29 m (Fig. 3.2.6).

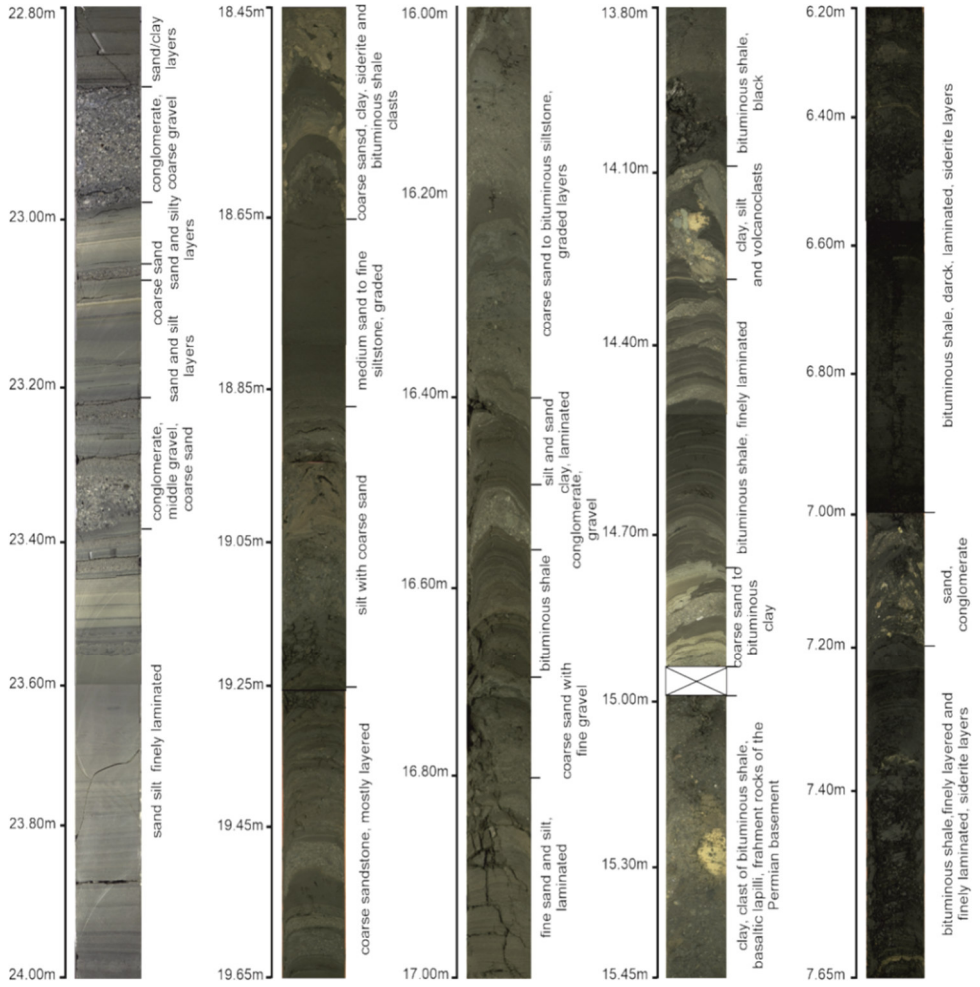

Fig. 3. 2. 6. Selected sections of core Offenthal illustrate various stages of sedimentation (modified after Moshayedi et al. 2020).

A basaltic clast from the top of volcanoclastic material of LZ 2 that may serve as evidence for the time of the eruption was dated at 47.4 ± 0.3 Ma applying the $^{40}Ar/^{39}Ar$ incremental heating technique (Mertz and Renne 2005). However, according to a revised calibration of the $^{40}Ar/^{39}Ar$ system in the Fish Canyon sanidine as age reference material (FCs; see Lenz et al. 2015 for details) the eruption at Offenthal happened 300 to 500 ka earlier than previously assumed at 47.71 ± 0.3 Ma using a new FCs age of Kuiper et al. (2008), and 47.87 ± 0.3 Ma using a recalibrated FCs age provided by Renne et al. (2011). Low $\delta^{18}O$ values with significant variability, point to a varying but short residence time of deep water at Offenthal (Felder and Gaupp 2006). From the small lake diameter and depth, as well as a paleolatitude higher than 40° N it can be suggested, that the intermediate carbon isotopic values in combination with the oxygen isotopic signature may be typical for a lake characterized by annual overturn (Felder and Gaupp 2006; Fig. 3.2.4).

Groß Zimmern

Lake Groß Zimmern is another small Paleogene maar structure on the Sprendlinger Horst. Scientific drilling (B/97-BK 8) in the center of the structure revealed a reference core (49°52' N, 8°50' E), including 80 m of a volcanoclastic breccia overlain by 30 m of a lacustrine succession of clastic sediments and finely laminated bituminous shale (Fig. 3.2.7).

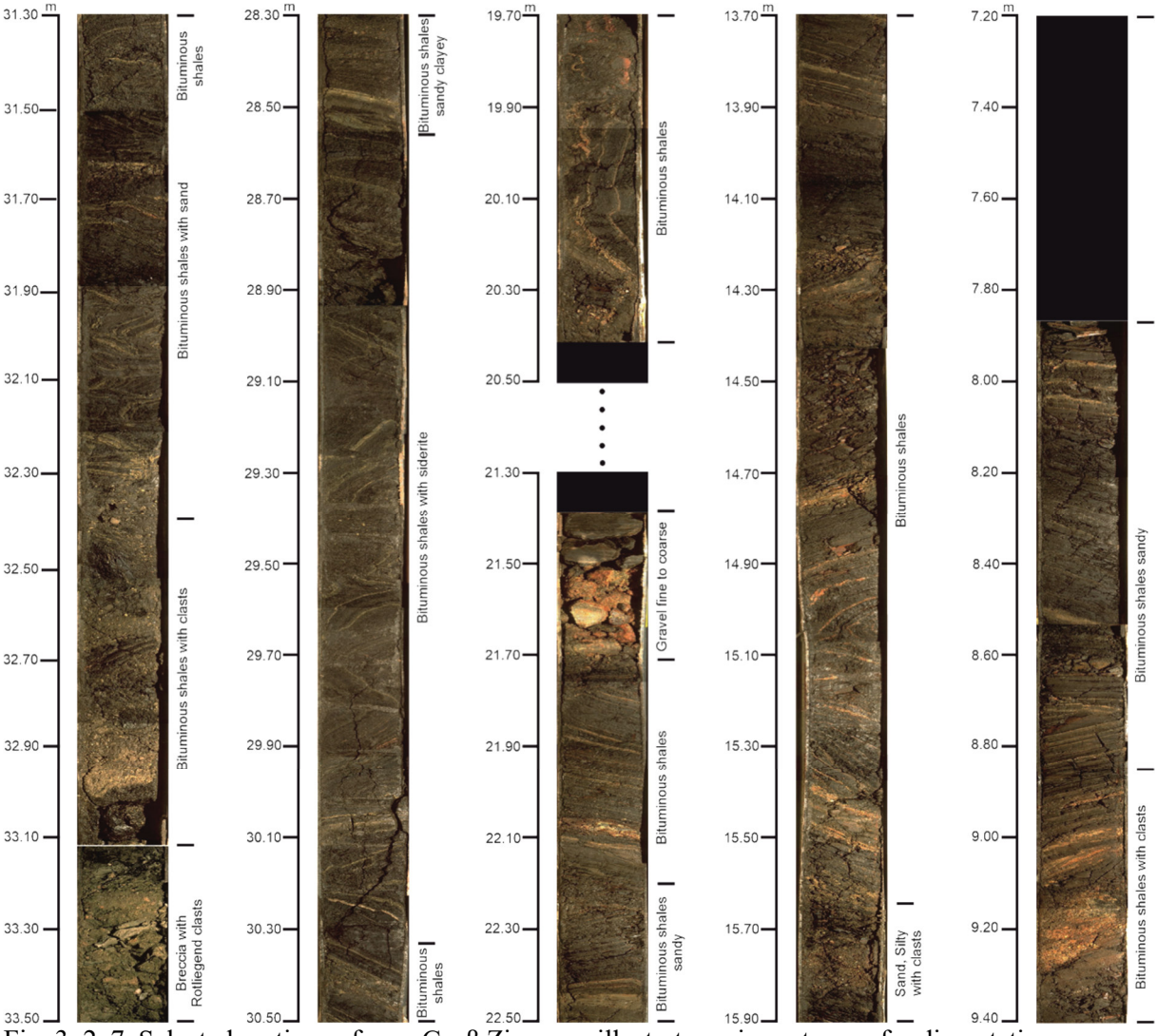

Fig. 3. 2. 7. Selected sections of core Groß Zimmern illustrate various stages of sedimentation.

The whole lacustrine succession shows signs of slumping, redeposition or in-situ deformation. The discovery of massive volcanoclastic deposits proved that the lake sediments have been deposited within a small maar structure with a diameter of 250 to 400 m. However, sediments of a holomictic lake phase which are typical for the initial phase of maar lakes are completely missing. Comparable studies of oxygen and carbon isotope values as done for the other Paleogene lakes on the Sprendlinger Horst are missing. Nevertheless, because of the similar diameter and thickness of the lacustrine succession it can be assumed that Lake Groß Zimmern was similar to Lake Offenthal. A first palynological study by Mutzl (2017) indicated that the lake sediments are of Early to Middle Eocene age.

3.3 Palaeoclimate evolution of the Paleogene

The Cenozoic climate is characterized by significant changes and a complex evolution. This can be seen in the global deep-sea oxygen isotope record based on data from a variety of DSDP and ODP sites revealing the evolution of deep-sea temperatures of the last 65 Ma (Zachos et al. 2001, 2008, Fig. 3.3.1). The early Cenozoic was characterized by noticeably higher concentrations of greenhouse gases in comparison to the present (Royer 2006). The most important change is the Early Eocene Climate Optimum (EECO), about 52 to 50Ma, when there was a high concentration of CO_2 and the global temperature reached a long-term maximum (Zachos et al 2001, Fig. 3.3.1). Subtropical forests of the northern hemisphere spread beyond 60° palaeolatitude (Harrington 2001). The correlation between extreme greenhouse climate and high CO_2 concentration during this time may be a model for the present global warming. Afterwards a gradual cooling is obvious before the Eocene/Oligocene boundary with a strong temperature drop (Fig. 3.3.1, Zachos et al. 2001). This change from greenhouse climate of Paleogene to icehouse climate of Neogene led to continental-scaled glaciations of Antarctica and finally Northern Hemisphere. Megafloras of the terrestrial climate of Central Europe also reflected this evolution of global temperature in Cenozoic (Mosbrugger et al. 2005).

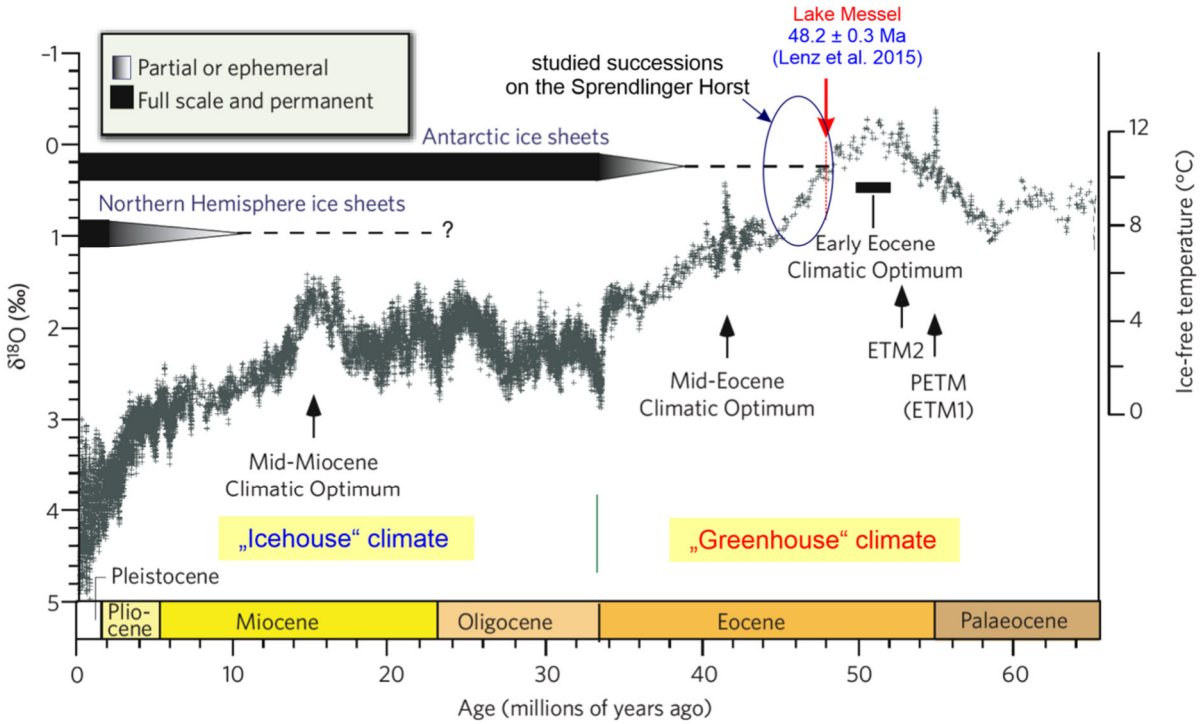

Fig. 3. 3. 1. Evolution of the global climate over the past 65 million years (adapted from Zachos et al. 2008).

However, the long-term climate trend in Cenozoic was interrupted by series of short-term hyperthermal fluctuations. The Paleocene Eocene Thermal Maximum (PETM) was a period with more than 5–8 ˚C global average temperature rise across the event (McInherney and Wing 2011). The associated period of massive carbon release into the atmosphere has been estimated to have lasted 20,000 to 50,000 years. The entire warm period lasted for about 200,000 years (McInherney and Wing 2011). Detailed studies of the carbon isotope excursion (CIE) suggest that $\delta^{13}C$ steps down within 20 kyr and returns in a roughly logarithmic pattern to near-initial values over ~220 kyr (Norris and Röhl 1999; Röhl et al. 2000). The magnitude, shape, and global nature of the CIE indicate a massive injection of ^{13}C-depleted carbon into the ocean-atmosphere system, followed by sequestering of excess carbon into carbonate and organic matter (Dickens 2000; 2001a). Methane released from seafloor gas hydrate systems provides the most probable source (Dickens et al. 1995; Katz et al. 1999; Dickens 2000; 2001a). Somehow associated with intense warming and excess carbon at the PETM are numerous changes in marine and terrestrial biota. Well-documented changes include a benthic foraminiferal extinction event (Kennettand Stott 1991; Thomas 1998), turnovers in planktonic organisms (Kelly et al. 1996; Aubry 1998a; Bralower 2002), and diversification of terrestrial mammal orders (Clyde and Gingerich 1998; Bowen et al. 2002).

A variety of climate-related palaeobotanical studies focused on PETM, particularly on the question whether an important floral turnover was associated with this hyperthermal event. Significant migrations of vegetation in response to the PETM have been reported along potential pathways in the American Rocky Mountains region (Wing et al. 2005). Also a radical floristic change with extirpation of the local or regional mesothytic flora and the recolonization of the area by thermophilic and dry-tolerant taxa during the PETM has been described for the Bighorn Basin in the USA (Wing and Currano 2013). A rapid and distinct increase in plant diversity and origination rates can be recognized in tropical forests of Colombia and Venezuela in the lowermost Eocene in response to the PETM (Jaramillo et al. 2010). However in other regions contemporaneous vegetation changes appear to be minor in comparison or cannot be directly related to this hyperthermal event (Harrington 2001; 2008; Wing and Harrington 2001; Wing et al. 2003; Jaramillo 2002).

The Eocene Thermal Maximum 2 (ETM-2), also called H-1 or ELMO (Eocene Layer of Mysterious Origin) event, was a transient period of global warming that occurred approximately 53.7 million years ago (Ma). It appears to be the second major hyperthermal that punctuated the long-term warming trend from the Late Paleocene through the early Eocene Eocene (58 to 50 Ma) (Zachos et al. 2008). PETM or ETM-1, occurred about 1.8 million years before ETM-2, at approximately 55.5 Ma. Other hyperthermals likely followed ETM-2 at nominally 53.6 Ma (H-2), 53.3 (I-1), 53.2 (I-2) and 52.8 Ma (informally called K, X or ETM-3). The number, nomenclature, absolute ages and relative global impact of the Eocene hyperthermals are the source of current research (Slotnick et al. 2012; Abels et al. 2012). The presence of at least five intervals with similar isotope records suggests a mechanism that repeatedly injected large masses of isotopically depleted carbon during the early Eocene.

Some studies attributed the Eocene transition from the greenhouse to the icehouse climate to the tectonic opening of Southern Ocean gateway, but also declining atmospheric greenhouse gas concentration may have played an important role (Bijl et al. 2013). This cooling trend was only interrupted at ~40 Ma by another short but striking thermal event, the so called Middle Eocene Climatic Optimum (MECO, Bohaty and Zachos 2003). Stable oxygen isotope records show that within 400 ka both surface and deep ocean temperatures increased by 4-6˚C (Bohaty et al. 2009). The warming is coincided with a worldwide decline in carbonate compensation depth (Bohaty et al. 2009). The synchroneity of deep-water acidification and extensive warming points to a link between increased pCO_2 and the MECO event (Bohaty and Zachos 2003; Bohaty et al. 2009; Bijl et al. 2010). In contrast to the PETM and the other Early Eocene hyperthermal events a $\delta^{18}O$ deviation is not accompanied by a corresponding

negative carbon isotope excursion. Therefore, Bohaty and Zachos (2003) conclude that not the dissociation of methane hydrates is possible cause for the MECO, but rather pCO_2 increase resulted from increased volcanism at active plate margins.
Age determination of the four studied successions on the Sprendlinger Horst reveals that these records are outside of the mentioned thermal events (Fig. 9). A basaltic clast from the top of volcano-clastic material of Offenthal that may serve as evidence for the time of the eruption was dated at 47.4 ± 0.3 Ma applying the $^{40}Ar/^{39}Ar$ incremental heating technique (Mertz and Renne 2005). Compared to the eruption at Messel with an age of 48.27 ± 0.22 (based on the FCs age of Kuiper et al. 2008, see Lenz et al. 2015) or 48.11 ± 0.22 (FCs age of Renne et al. 2011, see Lenz et al. 2015) the eruption at Offenthal happened *c.* 300 ka later. Palynological studies show that lacustrine sedimentation at Prinz von Hessen started in the latest Early Eocene almost coeval with the deposition of the Lower Messel Formation at Messel and in Groß Zimmern the palynoassemblages represent Middle Eocene age. Therefore, the recorded vegetation changes of the Paleogene on the Sprendlinger Horst are not influenced by the extreme warming events but indicative for a more balanced warm greenhouse climate.

References

Abels, H. A., Clyde, W. C., Gingerich, P. D., Hilgen, F. J., Fricke, H. C., Bowen, G. J., and Lourens, L. J. (2012). Terrestrial carbon isotope excursions and biotic change during Palaeogene hyperthermals. *Nature Geoscience*, 5(5), 326-329.

Achauer, U., and Masson, F. (2002). Seismic tomography of continental rifts revisited: from relative to absolute heterogeneities. *Tectonophysics*, 358(1-4), 17-37.

Aubry, M. P. (1998). Early Paleogene calcareous nannoplankton evolution: a tale of climatic amelioration. *Late Paleocene-Early Eocene climatic and biotic events in the marine and terrestrial records*, 158-203.

Backhaus, E., and Rahnama-Rad, J. (1991). Die Rutschgefährdung der Messel-Formation (Fundstätte Messel; Mittel-Eozän). Einflüsse der Tektonik, der Hydrogeologie und der Materialeigenschaften der Gesteine. *Cour. Forsch.-Inst. Senckenberg*, 139, 1-69.

Baranyi, H.J. Lippolt, W. Todt. (1976). Kalium-Argon-Altersbestimmungen an tertiären Vulkaniten des Oberrheingebietes: II die Alterstraverse vom Hegau nach Lothringen *Oberrheinische geologische Abhandlungen*, 25 (1976), pp. 41-62

Bijl, P. K., Houben, A. J., Schouten, S., Bohaty, S. M., Sluijs, A., Reichart, G. J., and Brinkhuis, H. (2010). Transient Middle Eocene atmospheric CO2 and temperature variations. *Science*, 330(6005), 819-821.

Bijl, P. K., Bendle, J. A., Bohaty, S. M., Pross, J., Schouten, S., Tauxe, L., ... and Sluijs, A. (2013). Eocene cooling linked to early flow across the Tasmanian Gateway. *Proceedings of the National Academy of Sciences*, 110(24), 9645-9650.

Bohaty, S. M., and Zachos, J. C. (2003). Significant Southern Ocean warming event in the late middle Eocene. *Geology*, 31(11), 1017-1020.

Bohaty, S. M., Zachos, J. C., Florindo, F., and Delaney, M. L. (2009). Coupled greenhouse warming and deep-sea acidification in the middle Eocene. *Paleoceanography*, 24(2).

Bowen, G. J., Clyde, W. C., Koch, P. L., Ting, S., Alroy, J., Tsubamoto, T., ... and Wang, Y. (2002). Mammalian dispersal at the Paleocene/Eocene boundary. *Science*, 295(5562), 2062-2065.

Bralower, T. J. (2002). Evidence of surface water oligotrophy during the Paleocene-Eocene thermal maximum: Nannofossil assemblage data from Ocean Drilling Program Site 690, Maud Rise, Weddell Sea. *Paleoceanography*, 17(2), 13-1.

Clyde, W. C., and Gingerich, P. D. (1998). Mammalian community response to the latest Paleocene thermal maximum: an isotaphonomic study in the northern Bighorn Basin, Wyoming. *Geology*, 26(11), 1011-1014.

Derer, C. E., Schumacher, M. E., and Schäfer, A. (2005). The northern Upper Rhine Graben: basin geometry and early syn-rift tectono-sedimentary evolution. *International Journal of Earth Sciences*, 94(4), 640-656.

Dèzes, P., Schmid, S. M., and Ziegler, P. A. (2004). Evolution of the European Cenozoic Rift System: interaction of the Alpine and Pyrenean orogens with their foreland lithosphere. *Tectonophysics*, 389(1-2), 1-33.

Dickens, G. R. (2000). Methane oxidation during the late Palaeocene thermal maximum. *Bulletin de la Société géologique de France*, 171(1), 37-49.

Dickens, G. R. (2001). The potential volume of oceanic methane hydrates with variable external conditions. *Organic geochemistry*, 32(10), 1179-1193.

Dickens, G. R., O'Neil, J. R., Rea, D. K., and Owen, R. M. (1995). Dissociation of oceanic methane hydrate as a cause of the carbon isotope excursion at the end of the Paleocene. *Paleoceanography*, 10(6), 965-971.

Fekiacova, Z., Mertz, D. F., and Renne, P. R. (2007). Geodynamic setting of the tertiary Hocheifel volcanism (Germany), Part I: 40 Ar/39 Ar geochronology. *In Mantle Plumes* (pp. 185-206). Springer, Berlin, Heidelberg.

Felder, M. and Gaupp, R. 2006. The δ13C and δ18O signatures of siderite a tool to discriminate mixis patterns in ancient lakes. *Zeitschrift der Deutschen Gesellschaft für Geowissenschaften*, 157, 397-410.

Felder, M., Harms, F.J. (2004). Lithologie und genetische Interpretation der vulkano-sedimentären Ablagerungen aus der Grube Messel anhand der Forschungsbohrung Messel 2001 und weiterer Bohrungen. *Courier Forschungsinstitut Senckenberg*, *252*, p 151-203.

Felder, M., Harms, F.J. and Liebig, V. (2001). Lithologische Beschreibung der Forschungsbohrungen Groβ-Zimmern, Prinz von Hessen und Offenthal sowie zweier Lagerstättenbohrungen be Eppertshausen (Sprendlinger Horst, Eozän, Messel-Formation, Süd-Hessen). *Geologische Jahrbuch Hessen*, *128*, 29–82.

Franzen, J.L. 2006. *Eurohippus parvulus parvulus* (Mammalia, Equidae) aus der Grube Prinz von Hessen bei Darmstadt (Süd-Hessen, Deutschland). *Senckenbergiana lethaea*, 86, 265-269.

Glahn, A., and Granet, M. (1992). 3-D structure of the lithosphere beneath the southern Rhine Graben area. *Tectonophysics*, 208(1-3), 149-158.

Harrington, G., (2001). Impact of Paleocene/Eocene greenhouse warm-ing on North American paratropical forests. *Palaios*, 16, 266–278.

Harrington, G. J. (2008). Comparisons between Palaeocene–Eocene paratropical swamp and marginal marine pollen floras from Alabama and Mississippi, USA. *Palaeontology*, 51(3), 611-622.

Harms, F.-J. (1999) mit Beitr. von Wallner, H. and Jacoby, W.: Verbreitungder Messel-Formation und der Tiefenlage der Basis desDeckgebirges (Miozän, Pliozän und Quartär) am Ostrand des Sprendlinger Horst es.–1 Kt. Hessisches Landesamt für Bodenforschung.

Harms, F.J., Aderhold, G., Hoffmann, I., Nix, T., Rosenberg, F. (1999). Erläuterungen zur Grube Messel bei Darmstadt, Südhessen. *Schriftenreihe der Deutschen Geologischen Gesellschaft*, 8, 181-222.

Harms, F. J., Nix, T., and Felder, M. (2003). Neue Darstellungen zur Geologie des Ölschiefer-Vorkommens Grube Messel. *Natur und Museum*, 133(5), 140-148.

Hofmann, P., Duckensell, M., Chpitsglous, A. and Schwark, L. 2005. Geochemical and organic petrological characterization of the organic matter of lacustrine Eocene oil shales (Prinz von Hessen, Germany): reconstruction of the depositional environment. *Paleolimnology*, 33, 155–168.

Horn, P., Lippolt. H.J., Todt. W. (1972). Kalium-Argon-Altersbsestimmungen an tertiären Vulkaniten des Oberrheingrabens: I Gesteinsalter. *Eclog geol Helv* 65:131–156

Jacoby, W., Wallner, H., Smilde, P. (2000). Tektonik und Vulkanismus entlang der Messeler-Sto¨ rungszone auf dem Sprendlinger Horst: geophysikalische Ergebnisse. *Zeitschrift der Deutschen Gesellschaft für Geowissenschaften*, 151–154, 493–510.

Jacoby,W., Sebazungu, E., Wallner, H., Gabriel, G., Pucher R. (2005).Potential field data for the Messel Pit and surroundings Courier Forschungsinstitut Senckenberg, 255 (2005), pp. 1-9

Jaramillo, C. A. (2002). Response of tropical vegetation to Paleogene warming. *Paleobiology*, 28(2), 222-243.

Katz, M. E., Pak, D. K., Dickens, G. R., and Miller, K. G. (1999). The source and fate of massive carbon input during the latest Paleocene thermal maximum. *Science*, 286(5444), 1531-1533.

Keller, J., Kraml, M., and Henjes-Kunst, F. (2002). 40Ar/39Ar single crystal laser dating of early volcanism in the Upper Rhine Graben and tectonic implications. *Schweizerische Mineralogische und Petrographische Mitteilungen*, 82, 1-10.

Clay Kelly, D., Bralower, T. J., Zachos, J. C., Silva, I. P., and Thomas, E. (1996). Rapid diversification of planktonic foraminifera in the tropical Pacific (ODP Site 865) during the late Paleocene thermal maximum. *Geology*, 24(5), 423-426.

Kennett, J. P., and Stott, L. D. (1991). Abrupt deep-sea warming, palaeoceanographic changes and benthic extinctions at the end of the Palaeocene. *Nature*, 353(6341), 225-229.

Kowalczyk, G. (2001). Permokarbon des Sprendlinger Horstes und der westlichen Wetterau (Exkursion I am 20. April 2001). *Jahresberichte und Mitteilungen des Oberrheinischen Geologischen Vereins*, 211-236.

Kuiper, K.F., Deino, A., Hilgen, F.J., Krijgsman, W., Renne, P.R., Wijbrans, J.R. (2008). Synchronizing rock clocks of Earth history. *Science*, 320, 500–504

Lenz, O.K., Wilde, V., Riegel, W. (2007). Recolonization of a Middle Eocene volcanic site: quantitative palynology of the initial phase of the maar lake of Messel (Germany). *Review of Palaeobotany and Palynology*, 145, 217–242.

Lenz, O.K., Wilde, V., Mertz, D.F., Riegel, W. (2015). New palynology-based astronomical and revised 40Ar/39Ar ages for the Eocene maar lake of Messel (Germany). *International Journal of Earth Science*, 104, 873-889.

Lenz, O.K., Wilde, V. and Riegel, W. (2017). ENSO-and solar-driven sub-Milankovitch cyclicity in the Paleogene greenhouse world: high resolution pollen records from Eocene Lake Messel, Germany. *Journal of the Geological Society*, 174, 110-128.

Lenz, O. K., and Wilde, V. (2018). Changes in Eocene plant diversity and composition of vegetation: the lacustrine archive of Messel (Germany). *Paleobiology*, 44(4), 709-735.

Liebig, W. 2002. Neuaufnahme der Forschungsbohrungen KB 1,2, 4, 5, und 7 von 1980 aus der Grube Messel (Sprendlinger Horst, Stidhessen). – *Kaupia*, 11: 3-68

Lorenz V (2000) Formation of maar-diatreme volcanoes. Terra Nostra 2000/6:284-291

Marell, D. (1989). Das Rotliegende zwischen Odenwald und Taunus: *Geologische Abhandlungen Hessen*.

Matthess, G. (1966). Zur Geologie des Ölschiefervorkommens von Messel bei Darmstadt: Abhandlungen des Hessischen Landesamtes für Bodenforschung.

McInerney, F. A., and Wing, S. L. (2011). The Paleocene-Eocene Thermal Maximum: a perturbation of carbon cycle, climate, and biosphere with implications for the future. *Annual Review of Earth and Planetary Sciences*, 39, 489-516.

Meier, L., and Eisbacher, G. H. (1991). Crustal kinematics and deep structure of the northern Rhine Graben, Germany. *Tectonics*, 10(3), 621-630.

Mertz, D.F., and Renne, P.R. (2005). A numerical age for the Messel fossil deposit (UNESCO World Heritage Site) derived from 40Ar/39Ar dating on a basaltic rock fragment. *Courier Forschungsinstitut Senckenberg*, *255*, 67-75.

Mezger, J.E., Felder, M. and Harms, F.-J. 2013. Crystalline rocks in the maar deposits of Messel: key to understand the geometries of the Messel Fault Zone and diatreme and the post-eruptional development of the basin fill. *Zeitschrift der Deutschen Gesellschaft für Geowissenschaften*, 164, 639–662.

Mosbrugger, V., Utescher, T., and Dilcher, D. L. (2005). Cenozoic continental climatic evolution of Central Europe. *Proceedings of the National Academy of Sciences*, 102(42), 14964-14969.

Moshayedi, M., Lenz, O.K., Wilde, V., Hinderer, M. (2018). Controls on sedimentation and vegetation in an Eocene pull-apart basin (Prinz von Hessen, Germany): evidence from palynology. *Journal of the Geological Society*, 175, 757-773.

Moshayedi, M., Lenz, O.K., Wilde, V., Hinderer, M., (2020). The recolonization of volcanically disturbed habitats during the Eocene of Central Europe: The maar lakes of Messel and Offenthal (SW Germany) compared. *Palaeobiodiversity and Palaeoenvironments*, 100**,** 951–973. https://doi.org/10.1007/s12549-020-00425-4

Mutzl, J., (2017). Klima und Vegetationsdynamik während der eozänen Treibhausphase in Mitteleuropa: Palynologische Untersuchungen der lakustrinen Sedimente aus dem Maar-See von Groß Zimmern. Masrearbeit, Institut für Angewandte Geowissenschaften, TU Darmstadt

Norris, R. D., and Röhl, U. (1999). Carbon cycling and chronology of climate warming during the Palaeocene/Eocene transition. *Nature*, 401(6755), 775-778.

Pirrung, M. 1998. Zur Entstehung isolierter alttertiärer Seesedimente in zentraleuropäischen Vulkanfeldern. *Mainzer Naturwissenschaftliches Archiv, Beiheft*, 20, 117.

Prodehl, C., Mueller, St., Haak, V. (1995). The European CenozoicRift System. In: Olsen, K.H. (Ed.), Continental Rifts: Evolution,Structure, *Tectonics, Developments in Geotectonics*, vol. 25.Elsevier, Amsterdam, pp. 133–212.

Reinhold, C., Schwarz, M., Bruss, D., Heesbeen, B., Perner, M. and Suana, M. (2016). The northern Upper Rhine Graben – Re-dawn of a mature petroleum province?Swiss Bulletin, 21, 35–56

Renne, P.R., Balco, G., Ludwig, K.R., Mundil, R., Min, K.W. et al. (2011). Response to the comment by W.H. Schwarz, on "Joint determination of 40 K decay constants and 40Ar*/40 K for the Fish Canyon sanidine standard, and improved accuracy for 40Ar/39Ar chronology" by PR Renne et al. (2010). *Geochim Cosmochim Acta, 75*, 5097–5100

Rohl, U., Bralower, T. J., Norris, R. D., and Wefer, G. (2000). New chronology for the late Paleocene thermal maximum and its environmental implications. *Geology*, 28(10), 927-930.

Royer, D. L. (2006). CO2-forced climate thresholds during the Phanerozoic. *Geochimica et Cosmochimica Acta*, 70(23), 5665-5675.

Schulz R, Harms FJ, Felder M (2002) Die Forschungsbohrung Messel 2001: Ein Beitrag zur Entschlüsselung der Genese einer Ölschieferlagerstätte. *Z Angew Geol*, 48:9–17

Schumacher, M. E. (2002). Upper Rhine Graben: role of preexisting structures during rift evolution. Tectonics, 21(1), 6-1

Schwarz, M. (2005). Evolution und Struktur des Oberrheingrabens: quantitative Einblicke mit Hilfe dreidimensionaler thermomechanischer Modellrechnungen (Doctoral dissertation, Verlag nicht ermittelbar).

Schwarz, M., and Henk, A. (2005). Evolution and structure of the Upper Rhine Graben: insights from three-dimensional thermomechanical modelling. *International Journal of Earth Sciences*, 94(4), 732-750.

Slotnick, B. S., Dickens, G. R., Nicolo, M. J., Hollis, C. J., Crampton, J. S., Zachos, J. C., and Sluijs, A. (2012). Large-amplitude variations in carbon cycling and terrestrial weathering during the latest Paleocene and earliest Eocene: The record at Mead Stream, New Zealand. *The journal of geology*, 120(5), 487-505.

Smith, K.T., Schaal, S.F.K., Habersetzer, J. (2018): Messel – An Ancient Greenhouse Ecosystem. Senckenberg-Buch 80, E. *Schweizerbart'sche Verlagsbuchhandlung*, Stuttgart.

Stein, E. (2001): Die magmatischen Gesteine des Bergsträßer Odenwaldes und ihre Inplatznahme-Geschichte. – Jber. Mitt. Oberrhein. *Geol*. Ver., N.F., 83, 267–283.

Thomas, E. (1998). Biogeography of the late Paleocene benthic foraminiferal extinction. Late Paleocene-Early Eocene climatic and biotic events in the marine and terrestrial records, 214-243.

Villemin, T., and Coletta, B. (1990, March). Subsidence in the Rhine Graben: a new compilation of borehole data. In Symposium on Rhine-Rhone Rift System; ICL-WG-3. *Symp*, (Vol. 31).

Wing, S. L., and Harrington, G. J. (2001). Floral response to rapid warming in the earliest Eocene and implications for concurrent faunal change. *Paleobiology*, 27(3), 539-563.

Wing, S. L., Harrington, G. J., Bowen, G. J., and Koch, P. L. (2003). Floral change during the initial Eocene thermal maximum in the Powder River Basin, Wyoming. *SPECIAL PAPERS-GEOLOGICAL SOCIETY OF AMERICA*, 425-440.

Wing, S. L., Harrington, G. J., Smith, F. A., Bloch, J. I., Boyer, D. M., and Freeman, K. H. (2005). Transient floral change and rapid global warming at the Paleocene-Eocene boundary. *Science*, 310(5750), 993-996.

Wing, S. L., and Currano, E. D. (2013). Plant response to a global greenhouse event 56 million years ago. *American Journal of Botany*, 100(7), 1234-1254.

Zeh, A., and Will, T. M. (2010). The mid-German crystalline zone. Pre-Mesozoic Geology of Saxo-Thuringia–from the Cadomian Active Margin to the Variscan Orogen. Schweizerbart, Stuttgart, 195-220.

Zachos, J., Pagani, M., Sloan, L., Thomas, E., and Billups, K. (2001). Trends, rhythms, and aberrations in global climate 65 Ma to present. *science*, 292(5517), 686-693.

Zachos, J. C., Dickens, G. R., and Zeebe, R. E. (2008). An early Cenozoic perspective on greenhouse warming and carbon-cycle dynamics. *Nature*, 451(7176), 279-283.

Ziegler, P. A. (1992). European Cenozoic rift system. Geodynamics of rifting, 1, 91-111.

Ziegler, P. A. (1994). Cenozoic rift system of Western and Central-Europe-an overview. *Geologie en Mijnbouw*, 73(2-4), 99-127

Ziegler, P. A., and Dèzes, P. (2005). Evolution of the lithosphere in the area of the Rhine Rift System. *International Journal of Earth Sciences*, 94(4), 594-614.

4- Results and publications

4-1 Systematic list of recorded species

The complete list of palynomorphs of lakes Prinz von Hessen and Offenthal including their systematic and ecological affinities is presented in following. They all have been identified through the morphological appearance. A picture of each taxa can be found on plates 1 to 9.

Supergroup Spores

Group Trilites

Azonotrilite Spores

1-	*Leiotriletes microadriennis* KRUTZSCH 1959	Schizaeaceae
2-	*Leiotriletes maxoides* KRUTZSCH 1962	Schizaeaceae
3-	*Toroisporis irregularis* KRUTZSCH 1959	Unknown
4-	*Toroisporis torus* PFLUG 1953	Unknown
5-	*Toripunctisporis* sp.	Unknown
6-	*Echinatisporis longechinus* KRUTZSCH 1959	Selaginellaceae
7-	*Trilites menatensis* KEDVES 1982	Schizaeaceae
8-	*Cicatricosisporites paradorogensis* KRUTZSCH 1959	Schizaeaceae
9-	*Cicatricosisporites dorogensis* R. POTONIÉ and GELLETICH 1933	Schizaeaceae
10-	*Baculatisporites primarius* (WOLF 1934) THOMSON and PFLUG 1953	Osmundaceae
11-	*Baculatisporites gemmatus* KRUTZSCH, 1959	Osmundaceae
12-	*Stereisporites breviancoris* KRUTZSCH 1963	Sphagnaceae
13-	*Stereisporites minor* (RAATZ) KRUTZSCH 1959	Sphagnaceae
14-	*Tegumentisporis sculpturoides* (KRUTZSCH 1959)	Selaginellaceae
15-	*Tegumentisporis tegumentis* (KRUTZSCH 1959) KRUTZSCH 196	Selaginellaceae

Zonotrilite Spores

16-	*Polypodiaceoisporites gracillimus* NAGY 1963	Polypodiaceae
17-	*Polypodiaceoisporites lusaticus* KRUTZSCH 1967	Polypodiaceae
18-	*Camarozonosporites semilevis* KRUTZSCH 1963	Lycopodiaceae
19-	*Camarozonosporites decorus* (WOLFF 1934) KRUTZSCH 1959	Lycopodiaceae
20-	*Camarozonosporites heskemensis* (PFLANZL 1955) KRUTZSCH 1959	Lycopodiaceae

Group Monoletes

21-	*Laevigatosporites discordatus* PFLUG 1953	Polypodiaceae
22-	*Laevigatosporites haardtii* (R. POTONIÉ and VENITZ 1934)	Polypodiaceae
23-	*Punctatosporites palaeogenicus* KRUTZSCH 1959	Polypodiaceae
24-	*Verrucatosporites favus* (R. POTONIÉ 1931) THOMSON and PFLUG 1953	Polypodiaceae

Supergroup Pollen

Group Saccates

25- *Pityosporites labdacus* (R. POTONIÉ 1931) THOMSON and PFLUG 1953 Pinaceae

Group Inapertures

26- *Inaperturopollenites concedipites* (WODEHOUSE 1933) KRUTZSCH 1971 Cupressaceae
27- *Inaperturopollenites dubius* (R. POTONIÉ and VENITZ 1934) THOMSON and PFLUG 1953 Cupressaceae

Group Monoporates

28- *Milfordia minima* KRUTZSCH 1970 Restionaceae
29- *Sparganiaceapollenites sp.* Sparganiaceae
30- *Emmapollis pseudoemmaensis* KRUTZSCH 1970 Chloranthaceae

Group Monocolpates

31- *Monocolpopollenites crassiexinus* THIELE-PFEIFFER 1988 Nymphaeaceae
32- *Monocolpopollenites tranquillus* (R. POTONIÉ 1934) THOMSON and PFLUG 1953 Nymphaeaceae

Group Brevaxones

33- *Nudopollis terminalis hastaformis* (THOMSON and PFLUG 1953) PFLUG 1953 ssp. *hastaformis* THOMSON and PFLUG 1953 Normopapolles
34- *Interpollis supplingensis* (PFLUG 1953) KRUTZSCH 1961 Normapapolles
35- *Interpollis microsupplingensis* KRUTZSCH 1961 Normapapolles
36- *Plicapollis pseudoexcelsus* (KRUTZSCH 1957) KRUTZSCH 1961 ssp. *turgidus* PFLUG 1953 Normapapolles
37- *Plicapollis pseudoexcelsus* (KRUTZSCH 1957) KRUTZSCH 1961 ssp. *semiturgidus* PFLUG 1953 Normapapolles
38- *Plicapollis pseudoexcelsus* (KRUTZSCH 1957) KRUTZSCH 1961 ssp. *microturgidus* PFLUG 1953 Normapapolles
39- *Triatriopollenites bitutus* (R. POTONIÉ 1931) THOMSON and PFLUG 1953 Myricaceae
40- *Triatriopollenites rurensis* THOMSON and PFLUG 1953 Myricaceae
41- *Plicatopollis plicatus* (R. POTONIÉ 1934) KRUTZSCH 1962 Juglandaceae
42- *Plicatopollis hungaricus* KEDVES 1974 Juglandaceae
43- *Plicatopollis lunatus* KEDVES 1974 Juglandaceae
44- *Plicatopollis* sp. Juglandaceae
45- *Momipites punctatus* (R. POTONIÉ 1931) NAGY 1969 Juglandaceae
46- *Platycaryapollenites platycaryoides* (ROCHE 1969) KEDVES 1982 Juglandaceae
47- *Platcacaryapollenites semicyclus* (KRUTZSCH and VANHOORNE 1977) THIELE-PF. 1988 Juglandaceae
48- *Caryapollenites triangulus* (PFLUG 1953) KRUTZSCH 1961 Juglandaceae

49- *Subtriporopollenites magnoporatus* (THOMSON and PFLUG 1953) KRUTZSCH 1961 Unknown
50- *Subtriporopollenites constans* PFLUG 1953 Juglandaceae
51- *Triporopollenites rhenanus*(THOMSON IN R. POTONIÉ; THOMSON and THIERGART 1950) THOMSON and PFLUG 1953 Corylaceae
52- *Triporopollenites robustus* PFLUG 1953 Corylaceae
53- *Triporopollenites undolatus* PFLUG 1953 Corylaceae
54- *Intratriporopollenites microinstructus* KRUTZSCH and VAN HOORNE 1977 Malvaceae
55- *Bombacacidites kettingensis* (PFLUG 1953) KRUTZSCH 1961 ssp. *minimus* KRUTZSCH 1970 Malvaceae
56- *Porocolpopollenites rarobaculatus* THIELE-PFEIFFER 1980 Symplocaceae
57- *Porocolpopollenites vestibulum* (R. POTONIÉ 1931) THOMSON and PFLUG 1953 Symplocaceae
58- *Symplocospollenites orbis* (THOMSON and PFLUG 1953) R. POTONIÉ 1960 Symplocaceae
59- *Celtipollenites laevigatus* THIELE-PFEIFFER 1988 Ulmaceae
60- *Celtipollenites intrastructurus* (KRUTZSCH and VAN HOORNE 1977) THIELE-PFEIFFER 1980 Ulmaceae
61- *Polyporopollenites verrucatus* THIELE PFEIFFER 1980 spp. minor THIELE PFEIFFER 1980 Ulmaceae
62- *Labrapollis labraferus* (R. POTONIÉ 1931) KRUTZSCH 1968 Unknown
63- *Compositoipollenites rhizophorus* (R. POTONIÉ 1934) R. POTONIÉ 1960 Icacinaceae
64- *Trivestibulopollenites betuloides* PFLUG 1953 Betulaceae
65- *Pentapollis pentangulus* (PFLUG 1953) KRUTZSCH 1957 Unknown

Group Longaxones

66- *Tricolpopollenites liblarensis* (THOMS. in R. POT., THOMS. and THIERG. 1950) TH. and PF. 1953 *liblarensis* (THOMS. in R. POT., THOMS. and THIERG. 1950) TH. and PF. 1953 Fagaceae
67- *Tricolpopollenites liblarensis* (THOMS. in R. POT., THOMS. and THIERG. 1950) TH. and PF. 1953 *fallax* (R. POTONIÉ 1934) THOMSON and PFLUG 1953 Fagaceae
68- *Trocolpopollenites quisqualis* (R. POTONIÉ 1934) THOMSON and PFLUG 1953 Fagaceae
69- *Tricolpopollenites asper* THOMSON and PFLUG 1953 Fagaceae
70- *Tricolpopollenites microhenrici* (R. POTONIÉ 1931) THOMSON and PFLUG 1953 Fagaceae
71- *Tricolpopollenites retiformis* THOMSON and PFLUG 1953 Salicaceae
72- *Tricolpopollenites vegetus* (R. POTONIÉ 1934) THOMSON and PFLUG 1953 Hamamelidaceae
73- *Tricolporopollenites cingulum* (POTONIE´ 1931) THOMSON and PFLUG 1953 *fusus* (R. POTONIÉ 1931) THOMSON and PFLUG 1953 Fagaceae
74- *Tricolporopollenites cingulum* (R. POTONIÉ 1931) THOMSON and PFLUG 1953 *pusillus* (R. POTONIÉ 1934) THOMSON and PFLUG 1953 Fagaceae
75- *Tricolporopollenites cingulum* (R. POTONIÉ 1931) THOMSON and PFLUG 1953 *oviformis* (R. POTONIÉ 1931) THOMSON and PFLUG 1953 Fagaceae
76- *Tricolporopollenites pseudocingulum* (R. POTONIÉ 1931) THOMSON and PFLUG 1953 Unknown

77- *Tricolporopollenites megaexactus* (R. POTONIÉ 1931) THOMSON and PFLUG 1953 Cyrillaceae
78- *Tricolporopollenites satzveyensis* PFLUG 1953 Mastixiaceae
79- *Tricolporopollenites edmundi* (R. POTONIÉ 1931) THOMSON and PFLUG 1953 Mastixiaceae
80- *Tricolporopollenites marcodurensis* THOMSON and PFLUG 1953 Typ A and B Vitaceae
81- *Tricolporopollenites microreticulatus* THOMSON and PFLUG 1953 Oleaceae
82- *Tricolporopollenites parmularius* (R. POTONIÉ 1934) KRUTZSCH in KRUTZSCH, PCHALEK and SPIEGLER 1960 Eucommiaceae
83- *Tricolporopollenites sole de portai* KEDVES 1965 Anacardiaceae/Rosaceae
84- *Tricolporopollenites crassiexinus* KRUTZSCH and VANHOORNE 1977 Celastraceae
85- *Tricolporopollenites eofagoides* KRUTZSCH and VANHOORNE 1977 Unknown
86- *Tricolporopollenites vancampoae* KEDVES 1964 Unknown
87- *Tricolporopollenites mansfeldensis* KRUTZSCH 1969 Rhizophoraceae
88- *Tricolporopollenites quercioides* KRUTZSCH and VANHOORNE 1977 Unknown
89- *Tricolporopollenites splendidus* THIELE-PFEIFFER 1988 Unknown
90- *Tricolporopollenites megaporatus* KRUTZSCH and VANHOORNE 197 Unknown
91- *Tricolporopollenites crassostriatus* NICKEL 1996 Solanaceae
92- *Tricolporopollenites abbreviates* (R. POTONIÉ 1934) KRUTZSCH 1961 Unknown
93- *Tricolporopollenites microporitus* THOMSON and PFLUG 1953 Hamaelidaceae/Verbenaceae/Oleaceae?
94- *Pistillipollenites mcgregorii* ROUSE 1962 Gentianaceae
95- *Nyssapollenites kruschii* (R. POT. 1931) R. POT., TH. and THIERG. 1950 *accessorius* (R. POT. 1934) R. POT., TH. and THIERG. 1950 ex SIMONCSICS 1969 Nyssaceae
96- *Ilexpollenites margaritatus* (R. POTONIÉ 1931) THIERGART 1937 ex R. POTONIÉ 1960 Aquifoliaceae
97- *Ilexpollenites iliacus* (R. POTONIÉ 1931) THIERGART 1937 ex R.POTONIÉ 1960 Aquifoliaceae
98- *Araliaceoipollenites reticuloides* THIELE-PFEIFFER 1980 Araliaceae
99- *Lythraceaepollenites minimus* THIELE-PFEIFFER 1988 Lythraceae
100- *Reticulataepollenites intergranulatus* (R. POTONIÉ 1934)KRUTZSCH 1959 Unknown
101- *Tetracolporopollenites kirchheimeri* THOMSON and PFLUG 1953 Sapotaceae
102- *Tetracolporopollenites sapotoides* THOMSON and PFLUG 1953 Sapotaceae
103- *Tetracolporopollenites obscurus* THOMSON andPFLUG 1953 Sapotaceae
104- *Ericipites callidus* (R. POTONIÉ 1931) KRUTZSCH 1970 Ericaceae
105- *Ericipites ericius* (R. POTONIÉ 1931) R. POTONIÉ 1960 Ericaceae

Super Group Algae

106- *Botryococcus* cf. *braunii* KÜTZING 1849 Chlorophyta
107- *Ovoidites* POTONIÉ 1951 Chlorophyta
108- *Entophlyctis lobate* WILLOUGHBY AND TOWNLEY 1961 Endochytriaceae

4-2 Stratigraphic range of species

A stratigraphic range chart (Fig. 4.2.1) presents the occurrences of long- and short-living palynological taxa at Prinz von Hessen and Offenthal. The data for chart are extracted from the database Palynodata (https://paleobotany.ru/palynodata) and include the occurrences of the specific palynomorphs in Central Europe. Some taxa therefore may have occurred in other areas at other times. Of the total of 105 pollen and spore species 92 taxa are could be classified stratigraphically (Fig. 4.2.1).

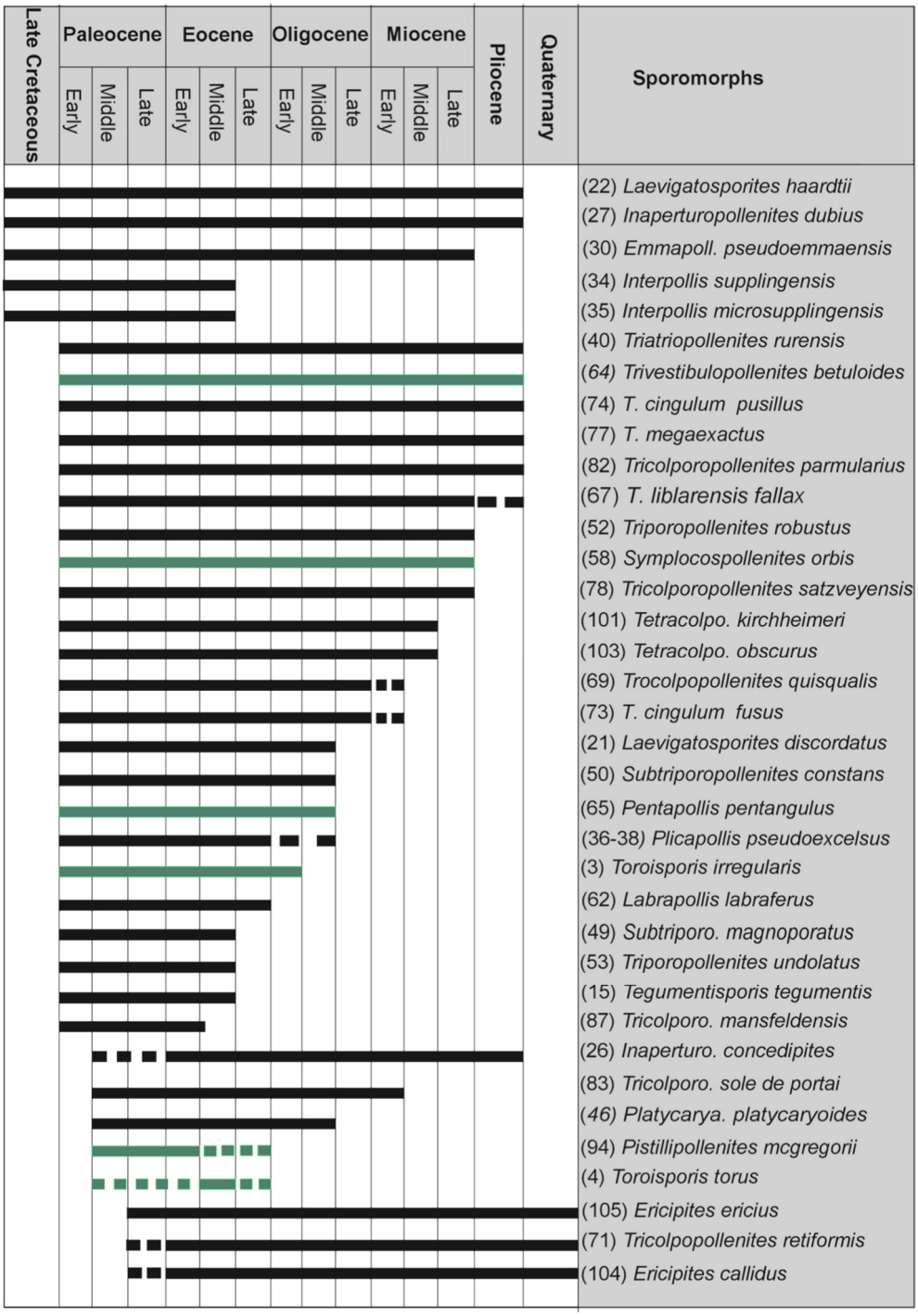

Fig. 4. 2. 1 Stratigraphic range of palynomorphs in Prinz von Hessen and Offenthal. Green colums present species which have been observed only in Prinz von Hessen.

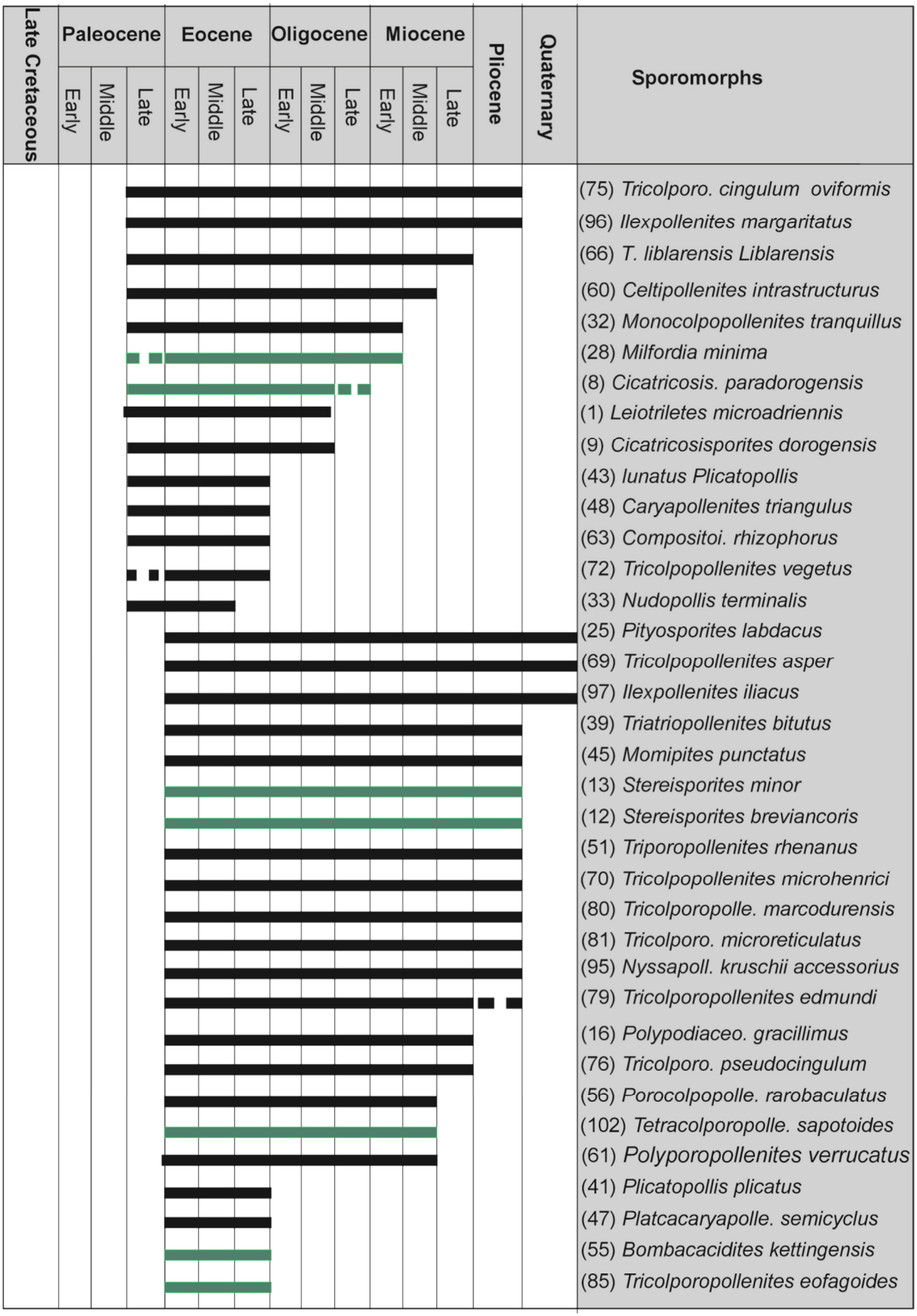

Fig. 4.2.1. (Continue)

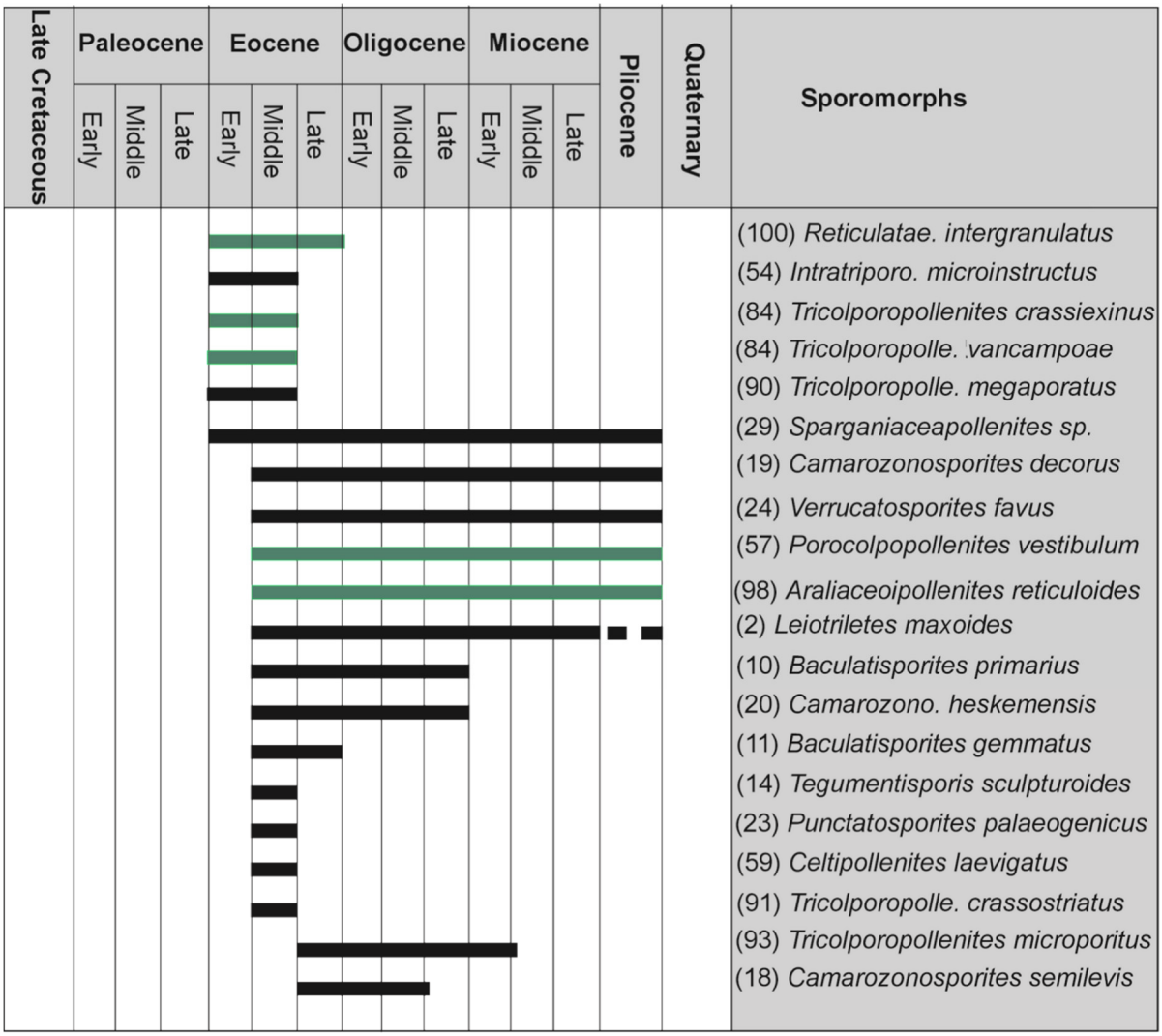

Fig. 4.2.1. (Continue)

Quantitative distributions of individual taxa, which do not have important stratigraphic statements, are not taken into account in this representation. 45.65% of taxa have been observed first in the Eocene and 48.91% of forms are appeared for the first time in the Paleocene (Fig. 4.2.2a) with 26.63% disappearing in Eocene and 15.56% becoming extinct in the Oligocene (Fig. 2b). However, nearly half of the taxa can still be observed in Neogene records and over 6 % occur almost unchanged even more recently (Fig. 4.2.2b). Nevertheless, taking into account the stratigraphic relevant taxa the palynomorph assemblages clearly point to a Lower to Middle Eocene age of the records.

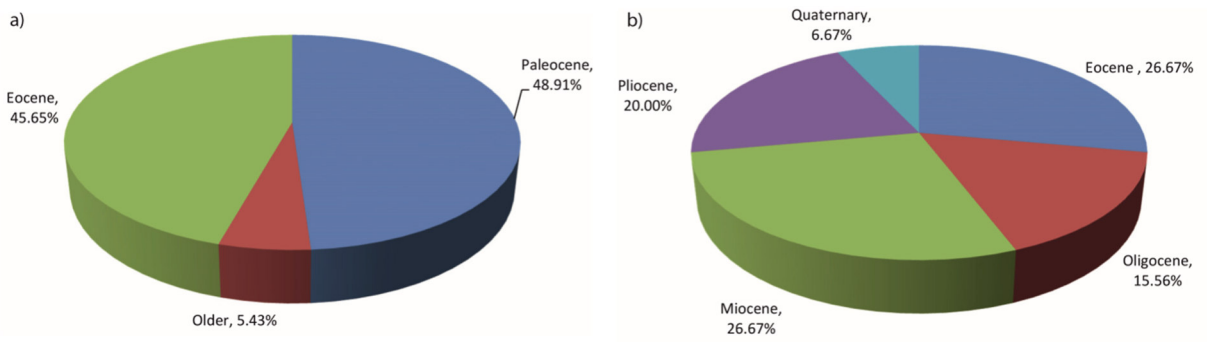

Fig. 4. 2. 2. Diagram of the stratigraphic occurrence of the taxa: a) first appearance, b) last appearance.

It is important to note that only morphologically distinct taxa such as *Pistillipollenites mcgregorii* are stratigraphically important and can be used for age determination whereas other species, especially collective taxa such as *Tricolpopollenites liblarensis* or *Tricolporopollenites cingulum* are very often represented in Paleogene and Neogene samples. Therefore, the stratigraphic relevance of these pollen species is limited, but, however, they are important for facies and paleoenvironment interpretations.

4-3 Climatic indicators

With the palynological zonation of Krutzsch and Majewski (1967), it is possible to divide the taxa into groups with similar climatic and ecologic demands. It can be distinguished between thermophilic, temperate, intermediate and facies elements.

Thermophilic elements	
• *Leiotriletes microadriennis*	• *Leiotriletes maxoides*
• *Toroisporis irregularis*	• *Toroisporis torus*
• *Tegumentisporis sculpturoides*	• *Tegumentisporis tegumentis*
• *Cicatricosisporites paradorogensis*	• *Cicatricosisporites dorogensis*
• *Polypodiaceoisporites gracillimus*	• *Polypodiaceoisporites lusaticus*
• *Camarozonosporites decorus*	• *Camarozonosporites semilevis*
• *Camarozonosporites heskemensis*	• *Verrucatosporites favus*
• *Emmapollis pseudoemmaensis*	• *Monocolpopollenites crassiexinus*
• *Monocolpopollenites tranquillus*	• *Nudopollis terminalis hastaformis*
• *Interpollis supplingensis*	• *Interpollis microsupplingensis*
• *Triatriopollenites bitutus*	• *Triatriopollenites rurensis*
• *Plicatopollis plicatus*	• *Plicatopollis hungaricus*
• *Plicatopollis lunatus*	• *Plicatopollis* sp.
• *Platycaryapollenites platycaryoides*	• *Platcacaryapollenites semicyclus*
• *Platycaryapollenites platycaryoides*	• *Bombacacidites kettingensis*
• *Triporopollenites robustus*	• *Porocolpopollenites vestibulum*
• *Porocolpopollenites rarobaculatus*	• *Symplocospollenites orbis*
• *Labrapollis labraferus*	• *Tricolporopollenites megaexactus*
• *Compositoipollenites rhizophorus*	• *Tricolporopollenites edmundi*
• *Tricolporopollenites satzveyensis*	• *Tricolporopollenites marcodurensis B*
• *Tricolporopollenites marcodurensis A*	• *Tricolporopollenites parmularius*
• *Tricolporopollenites sole de portai*	• *Tetracolporopollenites kirchheimeri*
• *Tetracolporopollenites sapotoides*	• *Tricolporopollenites crassiexinus*
• *Tetracolporopollenites obscurus*	• *Plicapollis pseudoexcelsus turgidus*
• *Echinatisporis longechinus*	• *Pentapollis pentangulus*
• *Tricolporopollenites pseudocingulum*	• *Araliaceoipollenites reticuloides*
• *Lythraceaepollenites minimus*	

Intermediate elements	
• *Milfordia minima*	• *Caryapollenites triangulus*
• *Subtriporopollenites magnoporatus*	• *Subtriporopollenites constans*
• *Trivestibulopollenites betuloides*	• *Tricolpopollenites microhenrici*
• *Tricolpopollenites asper*	• *Tricolpopollenites vegetus*
• *Tricolporopollenites cingulum fusus*	• *Tricolporopollenites cingulum pusillus*
• *Tricolporopollenites cingulum oviformis*	

Temperate elements	
• *Baculatisporites primaries*	• *Baculatisporites gemmatus*
• *Triporopollenites rhenanus*	• *Intratriporopollenites microinstructus*
• *Celtipollenites laevigatus*	• *Celtipollenites intrastructurus*
• *Tricolpopollenites retiformis*	• *Polyporopollenites verrucatus*

Facies elements	
• *Laevigatosporites discordatus*	• *Laevigatosporites haardtii*
• *Pityosporites labdacus*	• *Inaperturopollenites concedipites*
• *Inaperturopollenites dubius*	• *Punctatosporites palaeogenicus*
• *Nyssapollenites kruschii accessories*	• *Ilexpollenites margaritatus*
• *Ilexpollenites iliacus*	• *Ericipites callidus*
• *Ericipites ericius*	

Fig. 4. 3. 1. Diagram of distribution of climatic indicators.

83 taxa have been considered for the climate indicator species diagram (Fig. 4.3.1) with 53 thermophilic elements, 11 intermediate elements, 8 temperate elements and 11 facies elements. It shows a dominance of thermophilic elements with 63.86% versus 9.67% of temperate elements. Therefore, the climate can be interpreted as a being warm and (sub)tropical. The percentual composition indicates a paratropical rain forest. According to Wolfe (1979) a paratropical rain forest has a confused history of nomenclature, being sometimes grouped with tropical rain forest and sometimes excluded. The paratropical rain forest is preponderantly broad-leaved evergreen, but broad-leaved deciduous trees and conifers may be minor elements (particularly in secondary vegetation). To the casual observer, a paratropical rain forest might resemble the tropical rain forest. The most critical distinction is in the number of closed canopies.
Application of methods for calculating absolute climate data for temperature and precipitation based on palynomorphs which are common in use for Neogene records such as the NLR method (nearest living relatives) are problematic for Paleogene records, because of the general assignment of palynomorph taxa only to plant families and not to specific genera or species (Greib et al. 2001). However, Greib et al. (2001) presented a quantitative analysis on temperate, precipitation and humidity for the middle Eocene of Messel based on plant macrofossils (mainly leaves). The study obtained with the CA (Coexistence Approach) and LMA (Leaf Margin Analysis) methods indicates a mean annual temperature of opproximatley 22 °C (up to ~16.8- 23.9 °C) with a mean temperature of the coldest month clearly ranging above 10 °C. Mean annual precipitation rates reached values of 803- 2540 mm and mean relative air humidity reached 73- 77% at most. In spite of some uncertainities caused by the comparison on family level and potential changes in the climatic limitations of the respective families, they confirmed comparatively warm and humid, frost-free climate for the middle Eocene of Messel.

4-4 Comparison of the palynomorph assemblages in the four lakes

Table 1 presents a complete list of palynomorphs obtained in Lake Messel, Lake Prinz von Hessen, Lake Offenthal and Lake Groß Zimmern. The information is based on more than 700 samples from Lake Messel (Lenz et al. 2007; 2011; 2015 and 2017), 99 samples from Lake Prinz von Hessen (Moshayedi et al. 2018; 2020 in press), 68 samples from Lake Offenthal (Moshayedi et al. 2020) and 17 samples from Lake Groß Zimmern (Mutzl 2017). The record at Messel starts with a pioneering vegetation that is followed by a progressive recolonization of a paratropical forest (Lenz and Wilde 2018). Therefore, the palynomorph assemblages at Messel present an almost complete picture of the vegetation and its evolution between the

initial and the climax of the vegetation. Therefore, a high number of 103 different species have been identified from Messel (Lenz et al. 2007; 2011). The palynomorph assemblages of the other lakes show clear differences. In Lake Offenthal, 78 taxa have been described 75% of them are also known from Messel. In the lake Prinz von Hessen 105 taxa have been identified and 72% of them are similar with Messel. However, among the assemblage of fern spores there are differences (see table 4.4.1) which may point to differences in the composition of the pioneering vegetation. A total number of 20 different fern species have been observed in Messel whereas they are 25 in Prinz von Hessen, 19 in Offenthal and only 7 in Groß Zimmern. For the record of Groß Zimmern only 49 taxa have been described by Mutzl (2017). 80 % of them are known from Messel, but the diversity of palynomorph taxa seems to be significantly lower. However, this may be due to the low number of samples that were studied for Lake Groß Zimmern, which represent not the complete vegetation in the record.

References:

Krutzsch, W., Majewski, J. 1967. Zur Methodik der pollenstratigraphischen Zonengliederung im *Jungtertiär Mitteleuropas*. Abhandlungen des Zentralen Geologischen Instituts, 10: 83

Grein, M., Utescher, T., Wilde, V., and Roth-Nebelsick, A. (2011). Reconstruction of the middle Eocene climate of Messel using palaeobotanical data. *Neues Jahrbuch für Geologie und Paläontologie-Abhandlungen*, 260(3), 305-318.

Lenz, O.K., Wilde, V., Riegel, W. (2007). Recolonization of a Middle Eocene volcanic site: quantitative palynology of the initial phase of the maar lake of Messel (Germany). *Review of Palaeobotany and Palynology*, 145, 217–242.

Lenz, O. K., Wilde,V. and Riegel, W. (2011). Short-term fluctuations in vegetation and phytoplankton during the Middle Eocene greenhouse climate: a 640-kyr record from the Messel oil shale (Germany). *International Journal of Earth Sciences*, 100, 1851–1874.

Lenz, O.K., Wilde, V., Mertz, D.F., Riegel, W. (2015). New palynology-based astronomical and revised 40Ar/39Ar ages for the Eocene maar lake of Messel (Germany). *International Journal of Earth Science*, 104, 873-889.

Lenz, O.K., Wilde, V., Riegel, W. (2017). ENSO- and solar-driven sub-Milankovitch cyclicity in the Palaeogene greenhouse world; high-resolution pollen records from Eocene Lake Messel, Germany. *Journal of the Geological Society*, 174, 110-128.

Moshayedi, M., Lenz, O.K., Wilde, V., Hinderer, M. (2018). Controls on sedimentation and vegetation in an Eocene pull-apart basin (Prinz von Hessen, Germany): evidence from palynology. *Journal of the Geological Society*, 175, 757-773.

Moshayedi, M., Lenz, O.K., Wilde, V., Hinderer, M., (2020). The recolonization of volcanically disturbed habitats during the Eocene of Central Europe: The maar lakes of Messel and Offenthal (SW Germany) compared. Palaeobiodiversity and Palaeoenvironments, 100, 951–973. https://doi.org/10.1007/s12549-020-00425-4

Moshayedi, M., Lenz, O.K., Wilde, V., Hinderer, M. (2021): Lake-level fluctuations and allochthonous lignite deposition in the Eocene pull-apart basin "Prinz von Hessen" (Hesse, Germany) - A palynological study. *Syntheses in Limnogeology*, Rosen, M.R., Finkelstein, D., Park Boush, L., Pla-Pueyo, S. (eds.): Limnogeology: Progress, Challenges and Opportunities - A Tribute to Elizabeth Gierlowski-Kordesch, Chapter 3. Springer Nature (in press)

Mutzl, J., (2017). Klima und Vegetationsdynamik während der eozänen Treibhausphase in Mitteleuropa: Palynologische Untersuchungen der lakustrinen Sedimente aus dem Maar-See von Groß Zimmern. Masterearbeit, Institut für Angewandte Geowissenschaften, TU Darmstadt

Wolfe, J. A., and JA, W. (1979). Temperature parameters of humid to mesic forests of eastern Asia and relation to forests of other regions of the northern hemisphere and Australasia.

Table 4. 4. 1. Complete list of palynomorphs in Messel, Prinz von Hessen, Offenthal and Groß Zimmern.

Palynomorphs	Messel	Prinz von Hessen	Offenthal	Groß Zimmern
***Leiotriletes maxoides* KRUTZSCH, 1962**	+	+	+	
***Leiotriletes microadriennis* KRUTZSCH, 1959**	+	+	+	
***Toroisporis torus* PFLUG 1953**		+		
***Toroisporis arealis* KRUTZSCH, 1959**				+
***Toroisporis irregularis* KRUTZSCH, 1959**		+		
***Echinatisporis longechinus* KRUTZSCH, 1959**		+	+	
Toripunctisporis sp	+	+		
***Trilites solidus* (R. POTONIÉ 1934) KRUTZSCH, 1959**	+	+	+	+
***Trilites menatensis* KEDVES 1982**	+	+	+	
***Cicatricosisporites paradorogensis* KRUTZSCH 1959**	+	+		
***Cicatricosisporites dorogensis* R. POTONIÉ and GELLETICH 1933**	+	+	+	
***Baculatisporites primarius* (WOLF 1934) THOMSON and PFLUG 1953**	+	+	+	
***Baculatisporites gemmatus* KRUTZSCH, 1959**		+	+	
***Stereisporites minor* (RAATZ) KRUTZSCH, 1959**		+		
***Stereisporites breviancoris* KRUTZSCH 1963**		+		
***Tegumentisporis sculpturoides* (KRUTZSCH 1959) KRUTZSCH 1963**	+	+	+	+
***Tegumentisporis tegumentis* (KRUTZSCH 1959) KRUTZSCH 1963**		+	+	
***Tegumentisporis villosoides* (KRUTZSCH 1959) KRUTZSCH 1963**	+			
***Polypodiaceoisporites gracillimus* NAGY 1963**	+	+	+	+
***Polypodiaceoisporites lusaticus* KRUTZSCH 1967**	+	+	+	
***Camarozonosporites heskemensis* (PFLANZL 1955) KRUTZSCH**		+	+	
***Camarozonosporites decorus* (WOLFF 1934) KRUTZSCH 1959**		+	+	
***Camarozonosporites semilevis* KRUTZSCH 196**		+	+	
***Laevigatosporites haardtii* (R. POTONIÉ and VENITZ 1934) THOMSON and PFLUG 1953**	+	+	+	+
***Laevigatosporites discurdatus* Pflug 1953**	+	+	+	
***Punctatosporites palaeogenicus* KRUTZSCH 1959**		+	+	+
***Verrucatosporites favus* (R. POTONIÉ 1931) THOMSON and PFLUG 1953**	+	+	+	+(*V. microfavus*)
***Pityosporites labdacus* (R. POTONIÉ 1931) THOMSON and PFLUG 1953**	+	+	+	+
***Inaperturopollenites dubius* (R. POTONIÉ and VENITZ 1934) THOMSON and PFLUG 1953**		+	+	+
***Inaperturopollenites concedipites* (WODEHOUSE 1933) KRUTZSCH 1971**	+	+	+	+
***Milfordia minima* KRUTZSCH 1970**	+	+		+

Milfordia incerta **(THOMSON and PFLUG 1953) KRUTZSCH 1961**	+			
Sparganiaceapollenites sp.		+		
Zircipollenites globosus **KEDVES 1974**	+			
Emmapollis pseudoemmaensis **KRUTZSCH 1970**	+	+	+	+
Monocolpopollenites crassiexinus **THIELE-PFEIFFER**	+	+		
Monocolpopollenites tranquillus **(R. POTONIÉ 1934) THOMSON and PFLUG 1953**	+			+
Nudopollis terminalishastaformis **(THOMSON and PFLUG 1953) PFLUG 1953 ssp. *hastaformis* THOMSON and PFLUG 1953**	+	+	+	
Interpollis supplingensis **(PFLUG 1953) KRUTZSCH 1961**		+	+	
Interpollis microsupplingensis **KRUTZSCH 1961**		+	+	+
Plicapollis pseudoexcelsus **(KRUTZSCH 1957) KRUTZSCH 1961 ssp. *turgidus* PFLUG 1953**	+	+	+	+
Plicapollis pseudoexcelsus **(KRUTZSCH 1957) KRUTZSCH 1961 ssp. *semiturgidus* PFLUG 1953**	+	+	+	
Plicapollis pseudoexcelsus **(KRUTZSCH 1957) KRUTZSCH 1961 ssp. *microturgidus* PFLUG 1953**	+	+	+	
Triatriopollenites myricoides **(KREMP 1949) THOMSON and PFLUG 1953**	+			
Triatriopollenites rurensis **THOMSON and PFLUG 1953**	+	+	+	+
Triatriopollenites bitutus **(R. POTONIÉ 1931) THOMSON and PFLUG 1953**	+	+	+	+
Plicatopollis plicatus **(R. POTONIÉ 1934) KRUTZSCH 1962**	+	+	+	+
Plicatopollis lunatus **KEDVES 1974**	+	+	+	+
Plicatopollis hungaricus **KEDVES 1974**	+	+	+	+
Momipites punctatus **(R. POTONIÉ 1931) NAGY 1969**	+	+	+	+
Momipites quietus (R. POTONIÉ 1931) NICHOLS 1973	+			+
Platycaryapollenites platycaryoides **(ROCHE 1969) KEDVES 1982**	+	+	+	+
Platycacaryapollenites semicyclus **(KRUTZSCH and VANHOORNE 1977) THIELE-PF. 1988**	+	+	+	
Caryapollenites triangulus **(PFLUG 1953) KRUTZSCH 1961**	+	+	+	
Caryapollenites circulus **(PFLUG 1953) KRUTZSCH 1961**	+			
Subtriporopollenites constans **PFLUG 1953**	+	+	+	+
Subtriporopollenites magnoporatus **(THOMSON and PFLUG 1953) KRUTZSCH 1961**		+	+	
Triporopollenites rhenanus**(THOMSON IN R. POTONIÉ THOMSON and THIERGART 1950) THOMSON and PFLUG 1953**	+	+	+	+
Triporopollenites robustus **PFLUG 1953**	+	+	+	+
Triporopollenites undolatus **PFLUG 1953**		+	+	
Celtipollenites intrastructurus **(KRUTZSCH and VANHOORNE 1977) THIELE-PFEIFFER 1980**	+	+	+	+
Celtipollenites laevigatus **THIELE-PFEIFFER 1988**	+	+	+	
Polyporopollenites verrucatus **THIELE PFEIFFER 1980 spp. minor THIELE PFEIFFER 1980**	+			

Intratriporopollenites microinstructus **KRUTZSCH and VANHOORNE 1977**				+
Intratriporopollenites minimus **MAI 1961**	+			
Bombacacidites kettingensis **(PFLUG 1953) KRUTZSCH 1961 ssp.** ***Minimus*** **KRUTZSCH 1970**		+		
Porocolpopollenites rarobaculatus **THIELE-PFEIFFER 1980**	+	+	+	+
Porocolpopollenites vestibulum **(R. POTONIÉ 1931) THOMSON and PFLUG 1953**		+		
Symplocospollenites orbis **(THOMSON and PFLUG 1953) R. POTONIÉ 1960**		+		
Labrapollis labraferus **(R. POTONIÉ 1931) KRUTZSCH 1968**	+	+	+	
Compositoipollenites rhizophorus **(R. POTONIÉ 1934)) R. POTONIÉ 1960**	+	+	+	
Trivestibulopollenites betuloides **PFLUG 1953**		+		
Pentapollis pentangulus **(PFLUG 1953) KRUTZSCH 1957**	+	+		
Tricolpopollenites liblarensis **(THOMS. in R. POT., THOMS. and THIERG. 1950) TH. and PF. 1953** ***liblarensis*** **(THOMS. in R. POT., THOMS. and THIERG. 1950) TH. and PF. 1953**	+	+	+	
Tricolpopollenites liblarensis **(THOMS. in R. POT., THOMS. and THIERG. 1950) TH. and PF. 1953** ***fallax*** **(R. POTONIÉ 1934) THOMSON and PFLUG 1953**	+	+	+	
Trocolpopollenites quisqualis **(R. POTONIÉ 1934) THOMSON and PFLUG 1953**	+	+	+	
Tricolpopollenites asper **THOMSON and PFLUG 1953**	+	+	+	
Tricolpopollenites microhenrici **(R. POTONIÉ 1931) THOMSON and PFLUG 1953**	+	+		
Tricolpopollenites retiformis **THOMSON and PFLUG 1953**	+	+	+	
Tricolpopollenites vegetus **(R. POTONIÉ 1934) THOMSON and PFLUG 1953**	+	+	+	+
Tricolporopollenites cingulum **(R. POTONI E´ 1931) THOMSON and PFLUG 1953** ***fusus*** **(R. POTONIÉ 1931) THOMSON and PFLUG 1953**	+	+	+	+
Tricolporopollenites cingulum **(R. POTONIÉ 1931) THOMSON and PFLUG 1953** ***pusillus*** **(R. POTONIÉ 1934) THOMSON and PFLUG 1953**	+	+	+	+
Tricolporopollenites cingulum **(R. POTONIÉ 1931) THOMSON and PFLUG 1953** ***oviformis*** **(R. POTONIÉ 1931) THOMSON and PFLUG 1953**	+	+	+	+
Tricolporopollenites pseudocingulum **(R. POTONIÉ 1931) THOMSON and PFLUG 1953**	+	+	+	+
Tricolporopollenites megaexactus **(R. POTONIÉ 1931) THOMSON and PFLUG 1953**	+	+	+	+
Tricolporopollenites satzveyensis **PFLUG 1953**	+	+	+	+
Tricolporopollenites edmundi **(R. POTONIÉ 1931) THOMSON and PFLUG 1953**	+	+	+	+
Tricolporopollenites marcodurensis **THOMSON and PFLUG 1953 Typ A and B**	+	+	+	+
Tricolporopollenites microreticulatus **THOMSON and PFLUG 1953**	+	+	+	+
Tricolporopollenites parmularius **(R. POTONIÉ 1934) KRUTZSCH in KRUTZSCH, PCHALEK and SPIEGLER 1960**	+	+	+	
Tricolporopollenites microporitus **THOMSON and PFLUG 1953**	+	+	+	
Tricolporopollenites sole de portai **KEDVES 1965**	+	+	+	
Tricolporopollenites crassiexinus **KRUTZSCH and VANHOORNE 1977**		+		+
Tricolporopollenites eofagoides **KRUTZSCH and VANHOORNE 1977**	+	+		

Tricolporopollenites vancampoae **KEDVES 1964**	+	+		+
Tricolporopollenites mansfeldensis **KRUTZSCH 1969**	+	+	+	+
Tricolporopollenites quercioides **KRUTZSCH and VANHOORNE 1977**	+	+		
Tricolporopollenites splendidus **THIELE-PFEIFFER 1988**	+	+		
Tricolporopollenites megaporatus **KRUTZSCH and VANHOORNE 1977**		+	+	
Tricolporopollenites crassostriatus **NICKEL 1996**		+	+	+
Tricolporopollenites abbreviates **(R. POTONIÉ 1934) KRUTZSCH 1961**		+		
Pistillipollenites mcgregorii **ROUSE 1962**	+	+		
Nyssapollenites kruschii **(R. POT. 1931) NAGY 1969** ***analepticus*** **(R. POT. 1934) NAGY 1969**	+			+
Nyssapollenites kruschii **(R. POT. 1931) R. POT., TH. and THIERG. 1950** ***accessorius*** **(R. POT. 1934) R. POT., TH. and THIERG. 1950 ex SIMONCSICS 1969**	+	+	+	+
Ilexpollenites iliacus **(R. POTONIÉ 1931) THIERGART 1937 ex R. POTONIÉ 1960**	+	+	+	
Ilexpollenites margaritatus **(R. POTONIÉ 1931) THIERGART 1937 ex R. POTONIÉ 1960**	+	+	+	+
Araliaceoipollenites euphorii **(R. POTONIÉ 1931a) R. POTONIÉ 1951**	+			
Araliaceoipollenites reticuloides **THIELE-PFEIFFER 1980**	+	+		
Lythraceaepollenites minimus **THIELE-PFEIFFER 1988**	+	+		
Reticulataepollenites intergranulatus **(R. POTONIÉ 1934) KRUTZSCH 1959**	+	+		
Tetracolporopollenites sapotoides **THOMSON and PFLUG 1953**	+	+		+
Tetracolporopollenites kirchheimeri **THOMSON and PFLUG 1953**		+	+	
Tetracolporopollenites obscurus **THOMSON and PFLUG 1953**		+	+	+
Ericipites callidus **(R. POTONIÉ 1931) KRUTZSCH 1970**	+	+	+	+
Ericipites ericius **(R. POTONIÉ 1931) R. POTONIÉ 1960**	+	+		
Botryococcus **cf.** ***braunii*** **KU¨ TZING 1849**	+	+	+	+
Ovoidites **POTONIÉ 1951**		+	+	+
Entophlyctis lobate **WILLOUGHBY AND TOWNLEY 1961**		+	+	+

Plate 1

The scale bar represents 20µm

Fig. 1, 2:	(1) *Leiotriletes microadriennis*
	Fig. 1, 2: Off- 62, 21.32 m
Fig. 3, 4, 5:	(2) *Leiotriletes maxoides*
	Fig. 3, 5: Prinz von Hessen 99A, 56.52 m. Fig. 4: Off-88, 19.80 m
Fig. 6:	(3) *Toroisporis irregularis*
	Prinz von Hessen- 31C, 75.68 m
Fig. 7:	(4) *Toroisporis torus*
	Prinz von Hessen- 24C, 79.77 m
Fig. 8:	(5) *Toripunctisporis* sp.
	Prinz von Hessen- 194A, 46.50 m
Fig. 9:	(6) *Echinatisporis longechinus*
	Off-126, 17.90 m

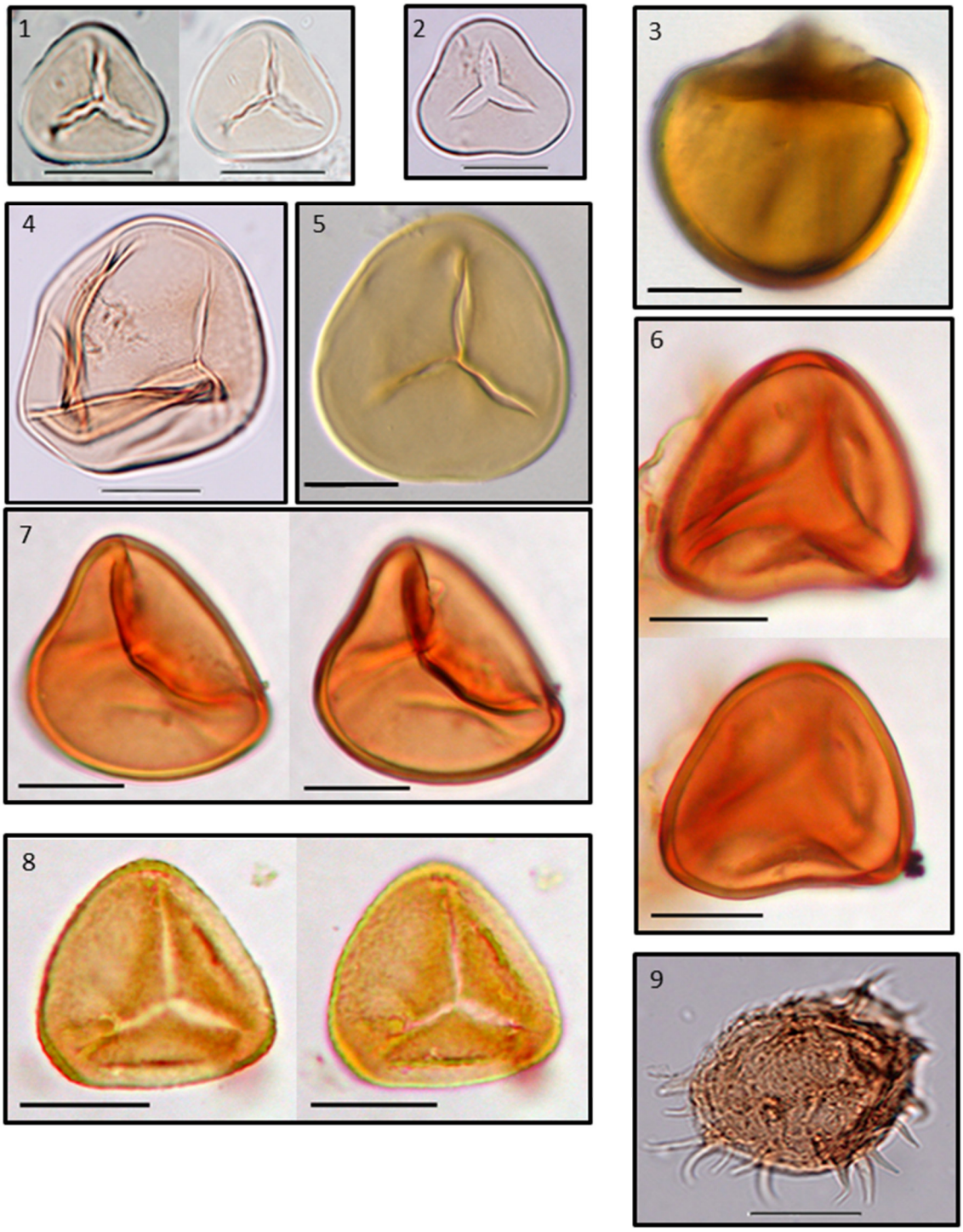
1
2
3
4
5
6
7
8
9

Plate 2

The scale bar represents 20µm

Fig. 1: (7) *Trilites menatensis*
Prinz von Hessen- 20C, 82.08 m

Fig. 2: (8) *Cicatricosisporites paradorogensis*
Off- 118, 18.30 m

Fig. 3: (9) *Cicatricosisporites dorogensis*
Prinz von Hessen- 194A, 46.50 m

Fig. 4: (10) *Baculatisporites primaries*
Prinz von Hessen- 174A, 48.50 m

Fig. 5: (11) *Baculatisporites gemmatus*
Prinz von Hessen- 365, 28.90 m

Fig. 6: (12) *Stereisporites breviancoris*
Prinz von Hessen- 329A, 32.50 m

Fig. 7: (13) *Stereisporites minor*
Prinz von Hessen- 159A, 50.50 m

Fig. 8: (14) *Tegumentisporis sculpturoides*
Prinz von Hessen- 194A, 46.50 m

Fig. 9, 10: (15) *Tegumentisporis tegumentis*
Fig. 9: Prinz von Hessen- 39K, 71.23 m. Fig. 10: Prinz von Hessen- 99A, 56.50 m

Fig. 11: (16) *Polypodiaceoisporites gracillimus*
Prinz von Hessen- 229A, 42.50 m

Fig. 12: (17) *Polypodiaceoisporites lusaticus*
Prinz von Hessen- 43C, 69.03 m

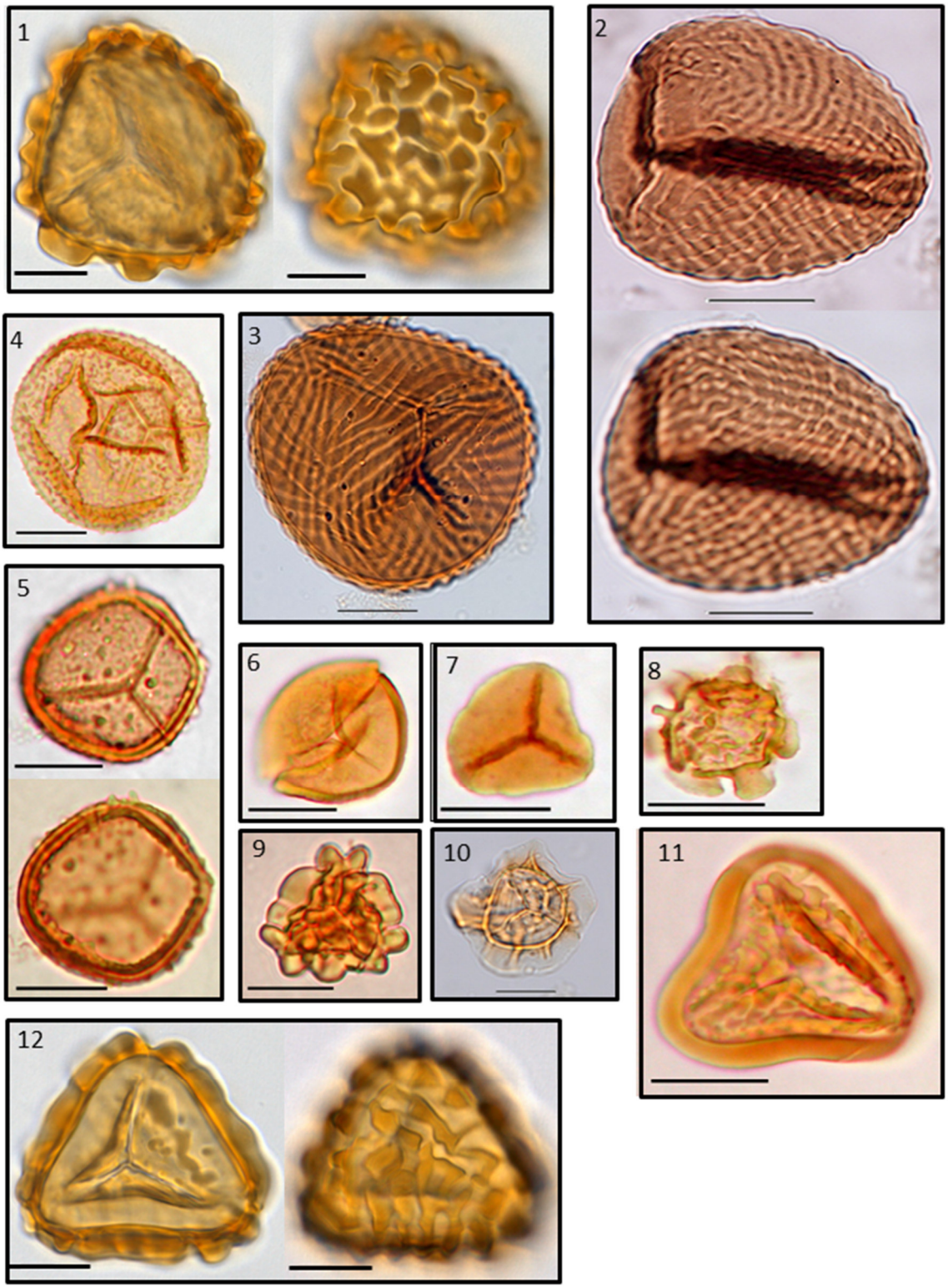
1
2
4
3
5
6
7
8
9
10
11
12

Plate 3

The scale bar represents 20µm

Fig. 1	(18) *Camarozonosporites semilevis*
	Prinz von Hessen- 444A, 15.80 m
Fig. 2	(19) *Camarozonosporites decorus*
	Prinz von Hessen- 229A, 42.50 m
Fig. 3	(20) *Camarozonosporites heskemensis*
	Prinz von Hessen 329A, , 32.50 m
Fig. 4:	(21) *Laevigatosporites discordatus*
	Prinz von Hessen- 174A, 48.50 m
Fig. 5:	(22) *Laevigatosporites haardtii*
	Prinz von Hessen- 269A, 38.50 m
Fig. 6, 7:	(23) *Punctatosporites palaeogenicus*
	Fig. 3: Prinz von Hessen- 289A, 36.50 m. Fig. 4: Off-126, 17.90 m
Fig. 8a, b:	(24) *Verrucatosporites favus*
	Off-62, 21.32 m
Fig. 9:	(25) *Pityosporites labdacus*
	Off-64, 21.00 m
Fig. 10:	(26) *Inaperturopollenites concedipites*
	Off-152, 16.60 m
Fig. 11:	(27) *Inaperturopollenites dubius*
	Off-64, 21.00 m
Fig. 12a, b, 13:	(28) *Milfordia minima*
	Fig. 9: Off-118, 18.30 m. Fig. 10: Prinz von Hessen- 56A
Fig. 14:	(29) *Sparganiaceapollenites sp.*
	Prinz von Hessen- 39L, 71.23 m

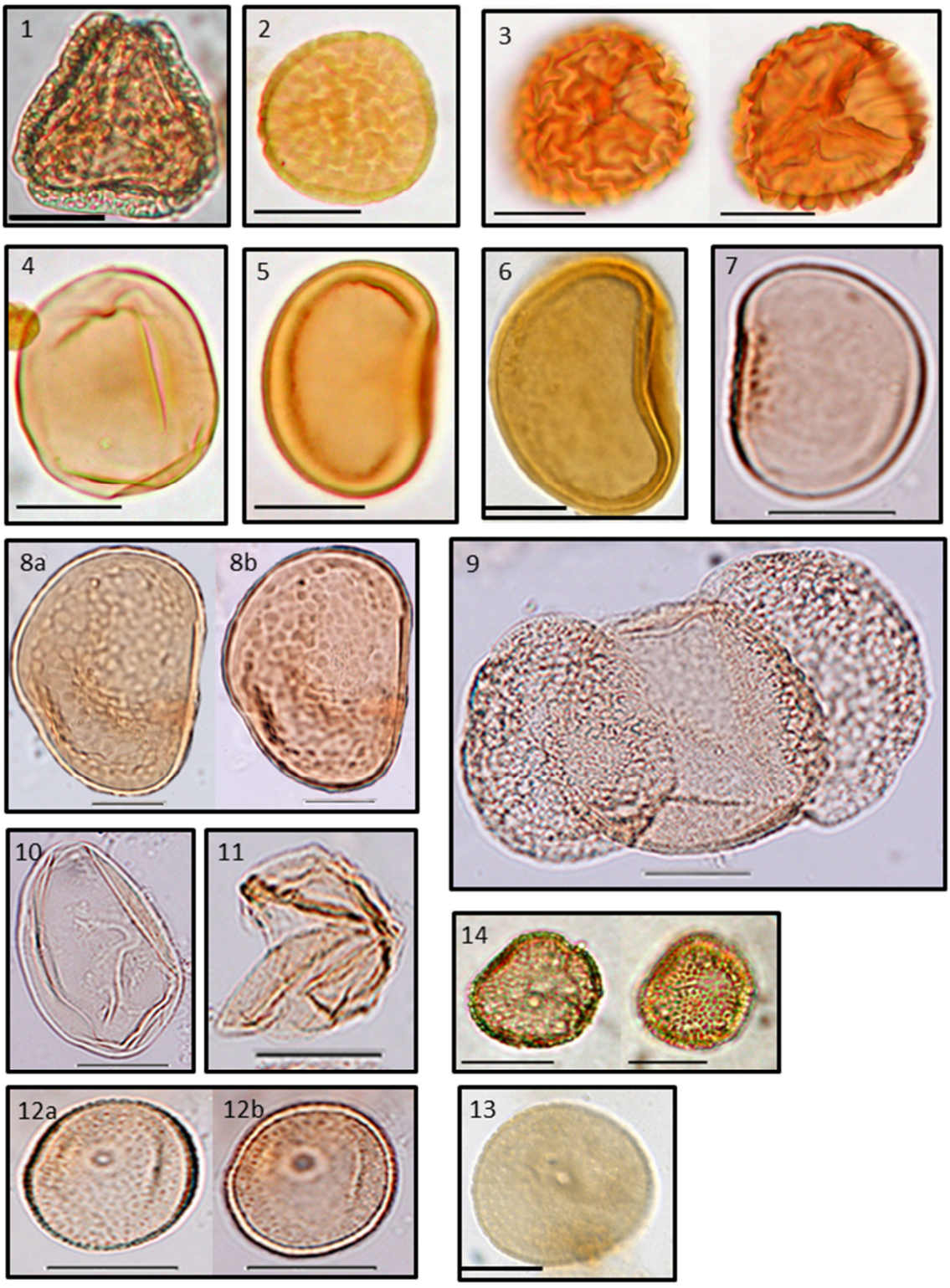
1
2
3
4
5
6
7
8a
8b
9
10
11
14
12a
12b
13

Plate 4

The scale bar represents 20µm

Fig. 1a, b: (30) *Emmapollis pseudoemmaensis*
Off-155, 16.45 m

Fig. 2: (31) *Monocolpopollenites crassiexinus*
Prinz von Hessen- 174A, 48.50 m

Fig. 3: (32) *Monocolpopollenites tranquillus*
Prinz von Hessen- 209B, 45.00 m

Fig. 4, 5a, b: (33) *Nudopollis terminalishastaformis*
Fig. 4: Off-62, 21.32 m. Fig. 5: Off- 88, 19.80 m

Fig. 6: (34) *Interpollis supplingensis*
Prinz von Hessen- 194A, 46.50 m

Fig. 7: (35) *Interpollis microsupplingensis*
Prinz von Hessen- 119A, 54.50 m

Fig. 8a, b: (36) *Plicapollis pseudoexcelsus turgidus*
Off-64, 21.00 m

Fig. 9a, b: (37) *Plicapollis pseudoexcelsus semiturgidus*
Prinz von Hessen- 139A, 52.50 m

Fig. 10: (38) *Plicapollis pseudoexcelsus microturgidus*
Prinz von Hessen- 269A, 38.50 m

Fig. 11: (39) *Triatriopollenites bitutus*
Prinz von Hessen- 349A, 30.50 m

Fig. 12, 13: (40) *Triatriopollenites rurensis*
Fig. 12: Prinz von Hessen- 194A, 46.50 m. Fig. 13: Off- 64, 21.00 m

Fig. 14: (41) *Plicatopollis plicatus*
Prinz von Hessen- 27C, 77.97 m

Fig. 15: (42) *Plicatopollis hungaricus*
Prinz von Hessen- 194A, 46.50 m

Fig. 16: (43) *Plicatopollis lunatus*
Prinz von Hessen- 139A, 52.50 m

Fig. 17: (44) *Plicatopollis* sp.
Off- 99, 19.25 m

Fig. 18: (45) *Momipites punctatus*
Prinz von Hessen- 119A, 54.50 m

Fig. 19, 20a. b: (46) *Platycaryapollenites platycaryoides*
Fig. 19: Off- 152, 16.60 m. Fig. 20: Off- 118, 18.30 m

Fig. 21: (47) *Platcacaryapollenites semicyclus*
Prinz von Hessen- 119A, 54.50 m

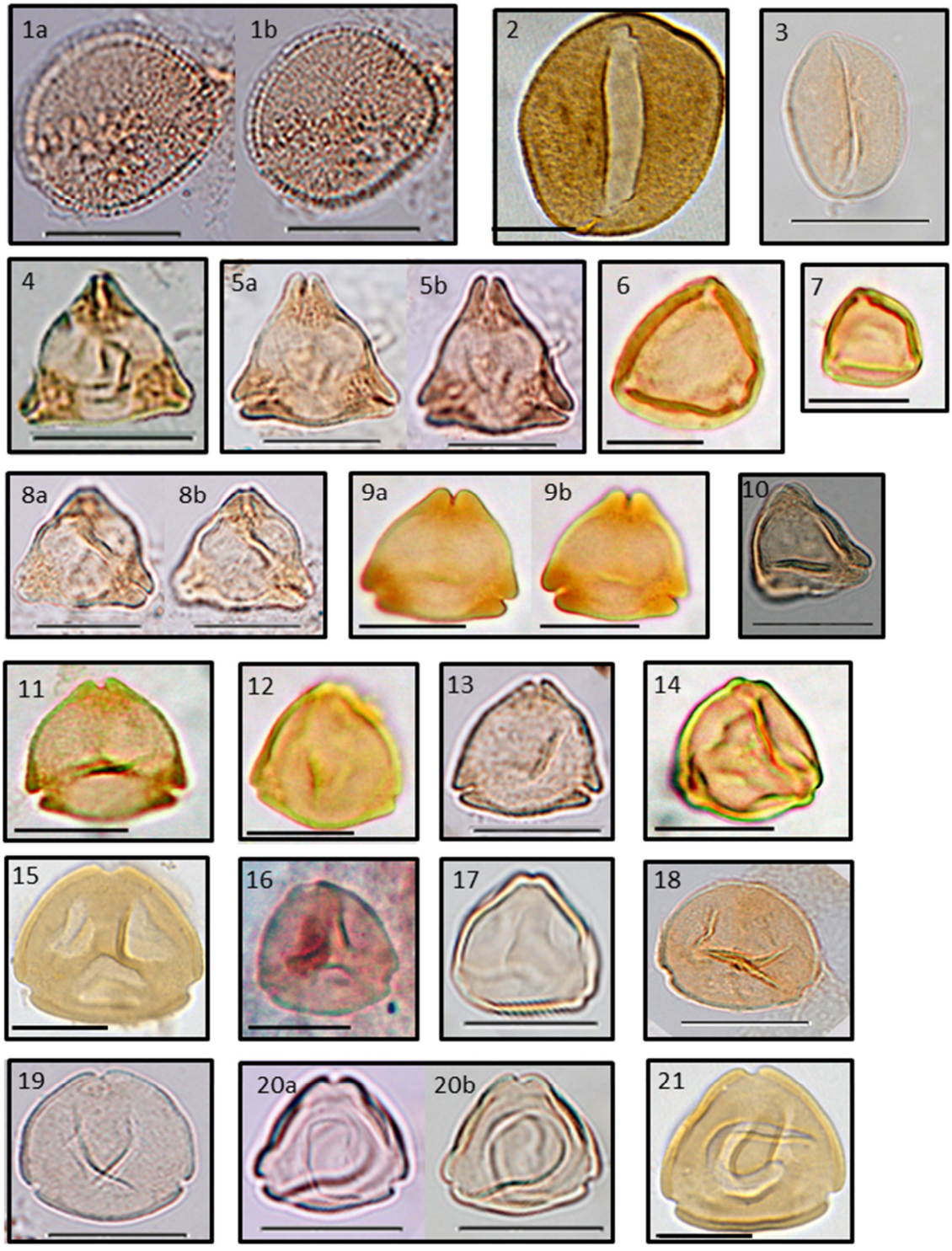
1a
1b
2
3
4
5a
5b
6
7
8a
8b
9a
9b
10
11
12
13
14
15
16
17
18
19
20a
20b
21

Plate 5

The scale bar represents 20µm

Fig. 1:	(48) *Caryapollenites triangulus*
	Prinz von Hessen- 174A, 48.50 m
Fig. 2a, b:	(49) *Subtriporopollenites magnoporatus*
	Off-62, 21.32 m
Fig. 3:	(50) *Subtriporopollenites constans*
	Prinz von Hessen- 56A, 60.51 m
Fig. 4:	(51) *Triporopollenites rhenanus*
	Prinz von Hessen- 174A, 48.50 m
Fig. 5:	(52) *Triporopollenites robustus*
	Prinz von Hessen- 159A, 50.50 m
Fig. 6:	(53) *Triporopollenites undolatus*
	Prinz von Hessen- 229A, 42.50 m
Fig. 7, 8a, b:	(54) *Intratriporopollenites microinstructus*
	Fig. 7: Prinz von Hessen- 139A, 52. 50 m. Fig. 8: Off-88, 19.80 m
Fig. 9a, b:	(55) *Bombacacidites kettingensis minimus*
	Off-99, 19.25 m
Fig. 10a, b, ,	(56) *Porocolpopollenites rarobaculatus*
11a, b 12a, b	Fig. 10: Prinz von Hessen- 229A, 52.50 m, Fig. 11: Off-126, 17.90 m,
	Fig. 12: Off 99, 19.25 m
Fig. 13a, b:	(57) *Porocolpopollenites vestibulum*
	Prinz von Hessen- 159A, 50.50 m
Fig. 14a, b:	(58) *Symplocospollenites orbis*
	Prinz von Hessen- 249A, 40.50 m
Fig. 15:	(59) *Celtipollenites laevigatus*
	Off-118, 18.30 m
Fig. 16:	(60) *Celtipollenites intrastructurus*
	Prinz von Hessen- 194A, 46.50 m

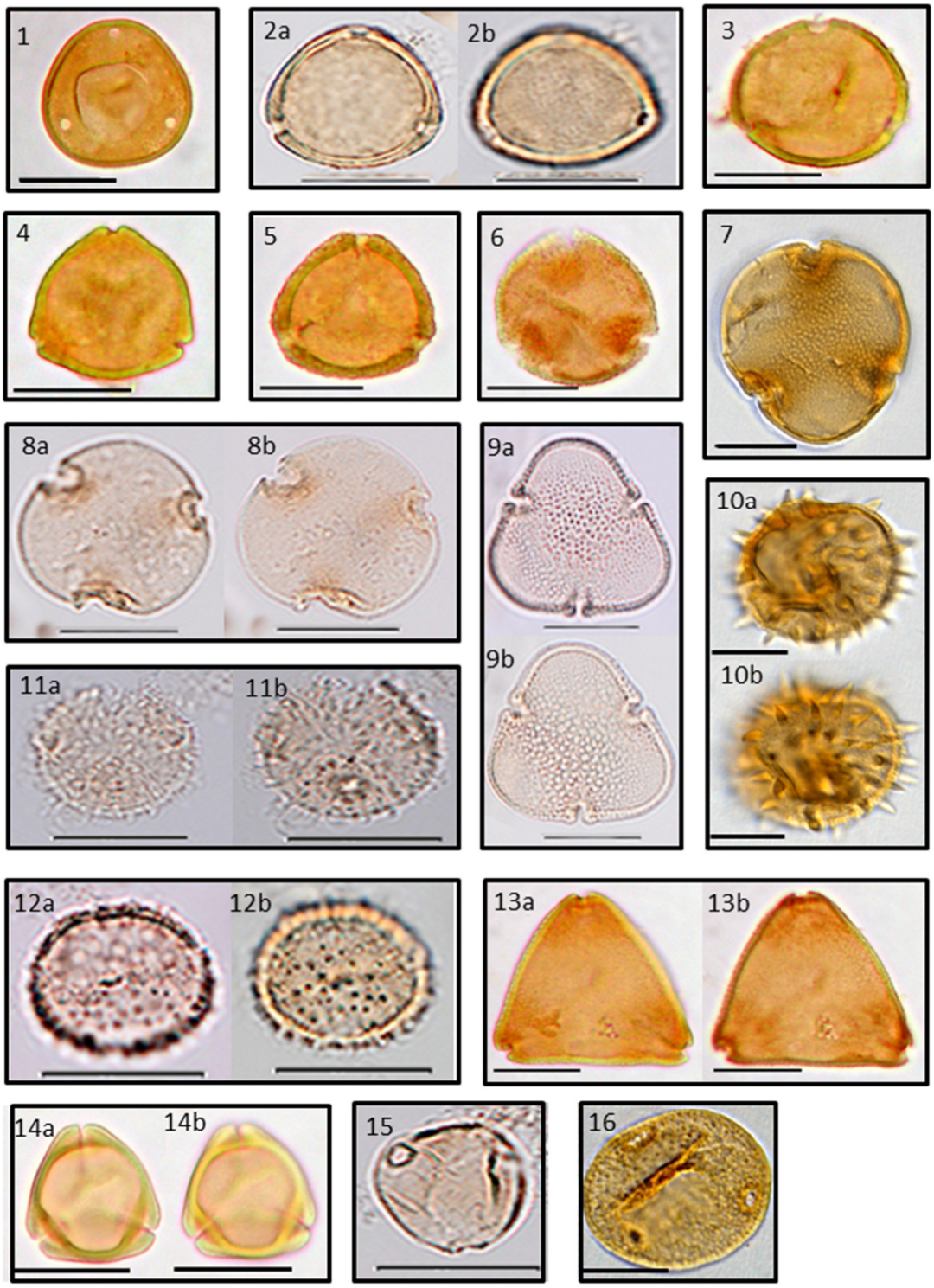
1
2a
2b
3
4
5
6
7
8a
8b
9a
9b
10a
10b
11a
11b
12a
12b
13a
13b
14a
14b
15
16

Plate 6

The scale bar represents 20µm

Fig. 1a, b: (61) *Polyporopollenites verrucatus*
Off- 88, 19.80 m

Fig. 2a, b: (62) *Labrapollis labraferus*
Prinz von Hessen- 269A, 38.50 m

Fig. 3a, b: (63) *Compositoipollenites rhizophorus*
Prinz von Hessen- 249A, 40.50 m

Fig. 4a, b: (64) *Trivestibulopollenites betuloides*
Prinz von Hessen- 2, 94.88 m

Fig. 5a, b: (65) *Pentapollis pentangulus*
Prinz von Hessen- 7, 90.98 m

Fig. 6a, b: (66) *Tricolpopollenites liblarensis liblarensis*
Off-99, 19.25 m

Fig. 7a ,b, 8a, b: (67) *Tricolpopollenites liblarensis fallax*
Fig. 7, 8: Off- 88, 19.80 m

Fig. 9: (68) *Trocolpopollenites quisqualis*
Prinz von Hessen- 119A, 54. 50 m

Fig. 10: (69) *Tricolpopollenites asper*
Prinz von Hessen- 31C, 75.68 m

Fig. 11: (70) *Tricolpopollenites microhenrici*
Prinz von Hessen- 119A, 54. 50 m

Fig. 12a, b, c: (71) *Tricolpopollenites retiformis*
Prinz von Hessen- 5C, 92. 57 m

Fig. 13a, b: (72) *Tricolpopollenites vegetus*
Off-126, 17.90 m

Fig. 14, 15a, b: (73) *Tricolporopollenites cingulum fusus*
Fig. 14: Off-62, 21.32 m. Fig. 15: Off-64, 21.00 m

Fig. 16a, b: (74) *Tricolporopollenites cingulum pusillus*
Fig. Off- 64, 21.00 m

Fig. 17: (75) *Tricolporopollenites cingulum oviformis*
Prinz von Hessen- 31C, 75.68 m

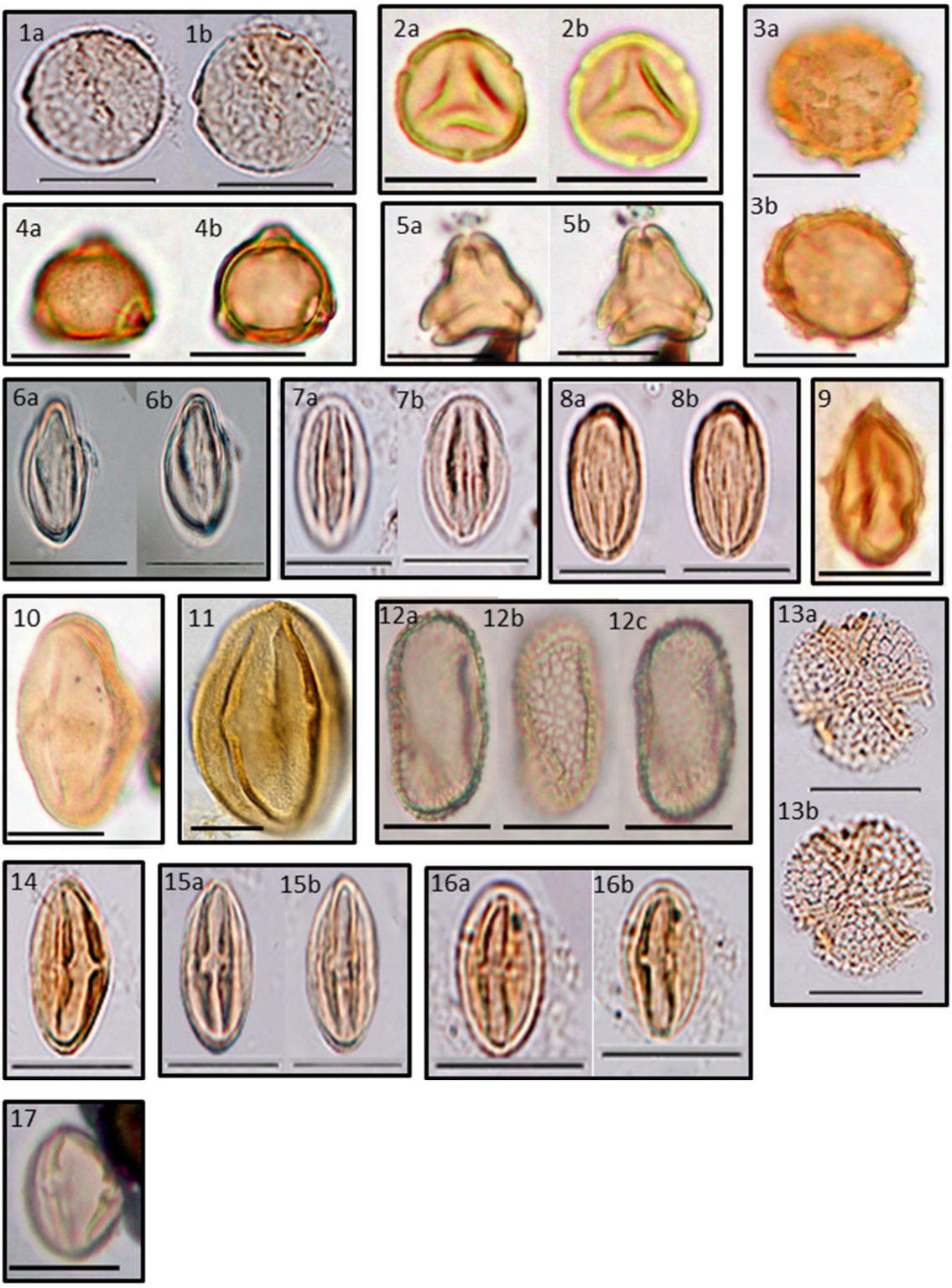
1a
1b
2a
2b
3a
3b
4a
4b
5a
5b
6a
6b
7a
7b
8a
8b
9
10
11
12a
12b
12c
13a
13b
14
15a
15b
16a
16b
17

Plate 7

The scale bar represents 20µm

Fig. 1, 2a, b: (76) *Tricolporopollenites pseudocingulum*
Fig. 1: Off- 80, 20.20 m. Fig. 2: Prinz von Hessen- 194A, 46.50 m

Fig. 3a, b: (77) *Tricolporopollenites megaexactus*
Prinz von Hessen- 289A, 36.50 m

Fig. 4a, b: (78) *Tricolporopollenites satzveyensis*
Off- 64, 21.00 m

Fig. 5a, b: (79) *Tricolporopollenites edmundi*
Off- 118, 18.30 m

Fig. 6a, b: (80) *Tricolporopollenites marcodurensis*
Off- 62, 21.32 m

Fig. 7a, b, 8a, b: (81) *Tricolporopollenites microreticulatus*
Fig. 7: Prinz von Hessen- 174A, 48.50 m. Fig. 8: Off-99, 19.25 m

Fig. 9a, b: (82) *Tricolporopollenites parmularius*
Off-62, 21.32 m

Fig. 10a, b: (83) *Tricolporopollenites sole de portai*
Off- 99, 19.25 m

Fig. 11a, b: (84) *Tricolporopollenites crassiexinus*
Prinz von Hessen- 46C, 67.30 m

Fig. 12: (85) *Tricolporopollenites eofagoides*
Prinz von Hessen- 24C, 79.77 m

Fig. 13: (86) *Tricolporopollenites vancampoae*
Prinz von Hessen- 159A, 50.50 m

Fig. 14a, b: (87) *Tricolporopollenites mansfeldensis*
Prinz von Hessen- 13C, 86.37 m


1
2a
2b
3a
3b
4a
4b
5a
5b
6a
6b
7a
7b
8a
8b
9a
9b
10a
10a
11a
11b
12
13
14a
14b

Plate 8

The scale bar represents 20µm

Fig. 1: (88) *Tricolporopollenites quercioides*
Prinz von Hessen- 159A, 50.50 m

Fig. 2: (89) *Tricolporopollenites splendidus*
Prinz von Hessen- 35C, 73.57 m

Fig. 3a, b: (90) *Tricolporopollenites megaporatus*
Off- 62, 21.32 m

Fig. 4a, b: (91) *Tricolporopollenites crassostriatus*
Prinz von Hessen- 99A, 56.50 m

Fig. 5a, b: (92) *Tricolporopollenites abbreviates*
Prinz von Hessen- 99A, 56.50 m

Fig. 6: (93) *Tricolporopollenites microporitus*
Prinz von Hessen- 249A, 40.50 m

Fig. 7, 8: (94) *Pistillipollenites mcgregorii*
Fig. 7: Prinz von Hessen- 139A, 52.50 m. Fig. 8: Prinz von Hessen- 56A, 60.51 m

Fig. 9a, b: (95) *Nyssapollenites kruschii accessories*
Off-52, 22.10 m

Fig. 10a, b, c: (96) *Ilexpollenites margaritatus*
Prinz von Hessen- 174A, 48.50 m

Fig. 11a, b: (97) *Ilexpollenites iliacus*
Prinz von Hessen- 5C, 92.57 m

Fig. 12: (98) *Araliaceoipollenites reticuloides*
Prinz von Hessen- 159A, 50.50 m

Fig. 13: (99) *Lythraceaepollenites minimus*
Prinz von Hessen- 7C, 90.98 m

Fig. 14 a, b: (100) *Reticulataepollenites intergranulatus*
Prinz von Hessen- 249A, 40.50 m

Fig. 15 a, b: (101) *Tetracolporopollenites kirchheimeri*
Prinz von Hessen- 99A, 56.50 m

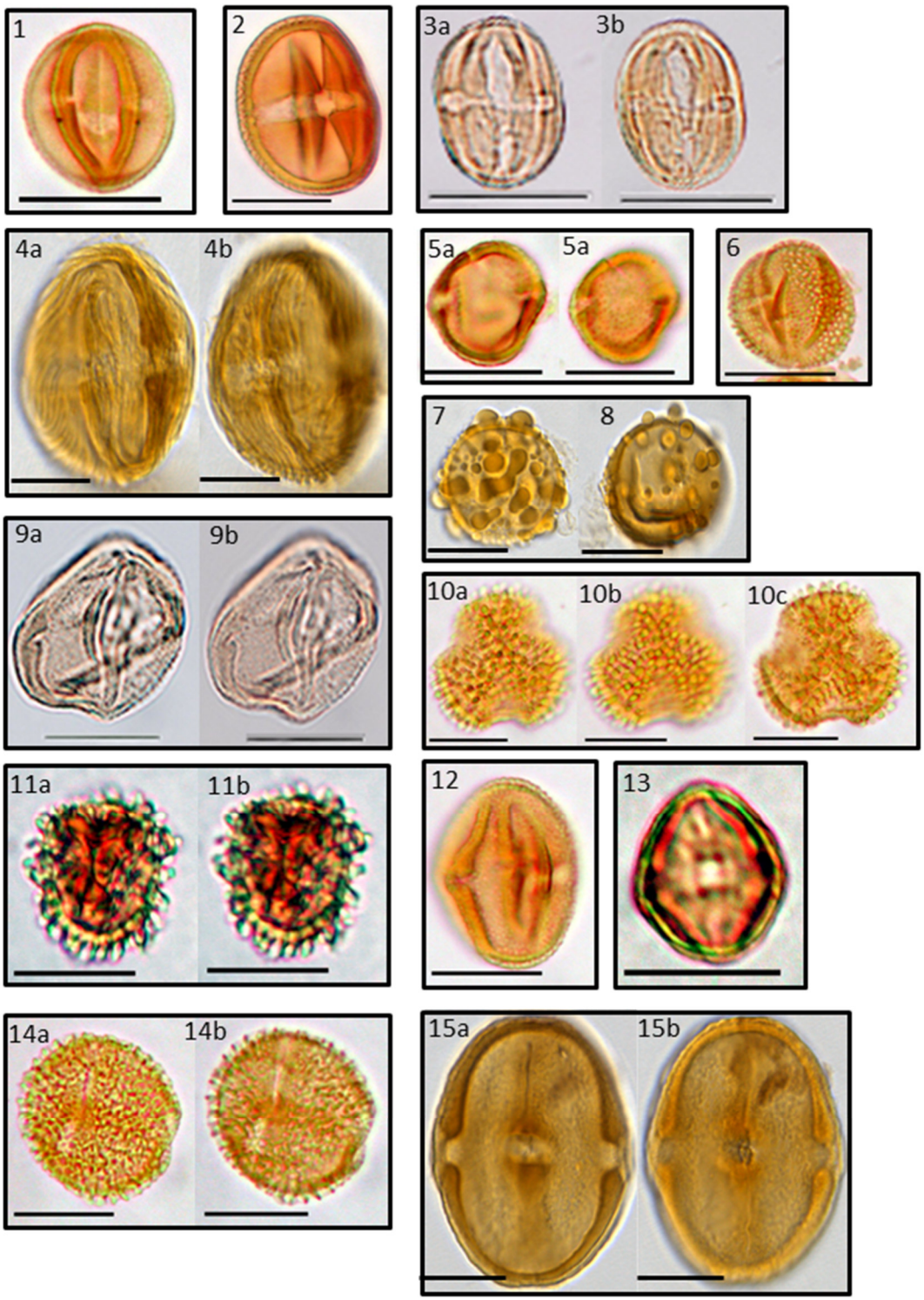
1
2
3a
3b
4a
4b
5a
5a
6
7
8
9a
9b
10a
10b
10c
11a
11b
12
13
14a
14b
15a
15b

Plate 9

The scale bar represents 20µm

Fig. 1: (101) *Tetracolporopollenites kirchheimeri*
Off- 62, 21.32 m

Fig. 2a, b, 3a, b: (102) *Tetracolporopollenites sapotoides*
Fig. 2, 3: Off- 80, 58.30 m.

Fig. 4a, b: (103) *Tetracolporopollenites obscurus*
Off- 64, 59.90 m

Fig. 5: (104) *Ericipites callidus*
Prinz von Hessen- 329A, 32.50 m

Fig. 6a, b: (105) *Ericipites ericius*
Off- 88, 19.80 m

Fig. 7: (106) *Botryococcus* cf. *braunii*
Off- 102, 19.10 m

Fig. 8: (107) *Ovoidites*
Off- 292A, 9.30 m

Fig. 9: (108) *Entophlyctis lobate*
Prinz von Hessen- 262D, 39.20 m

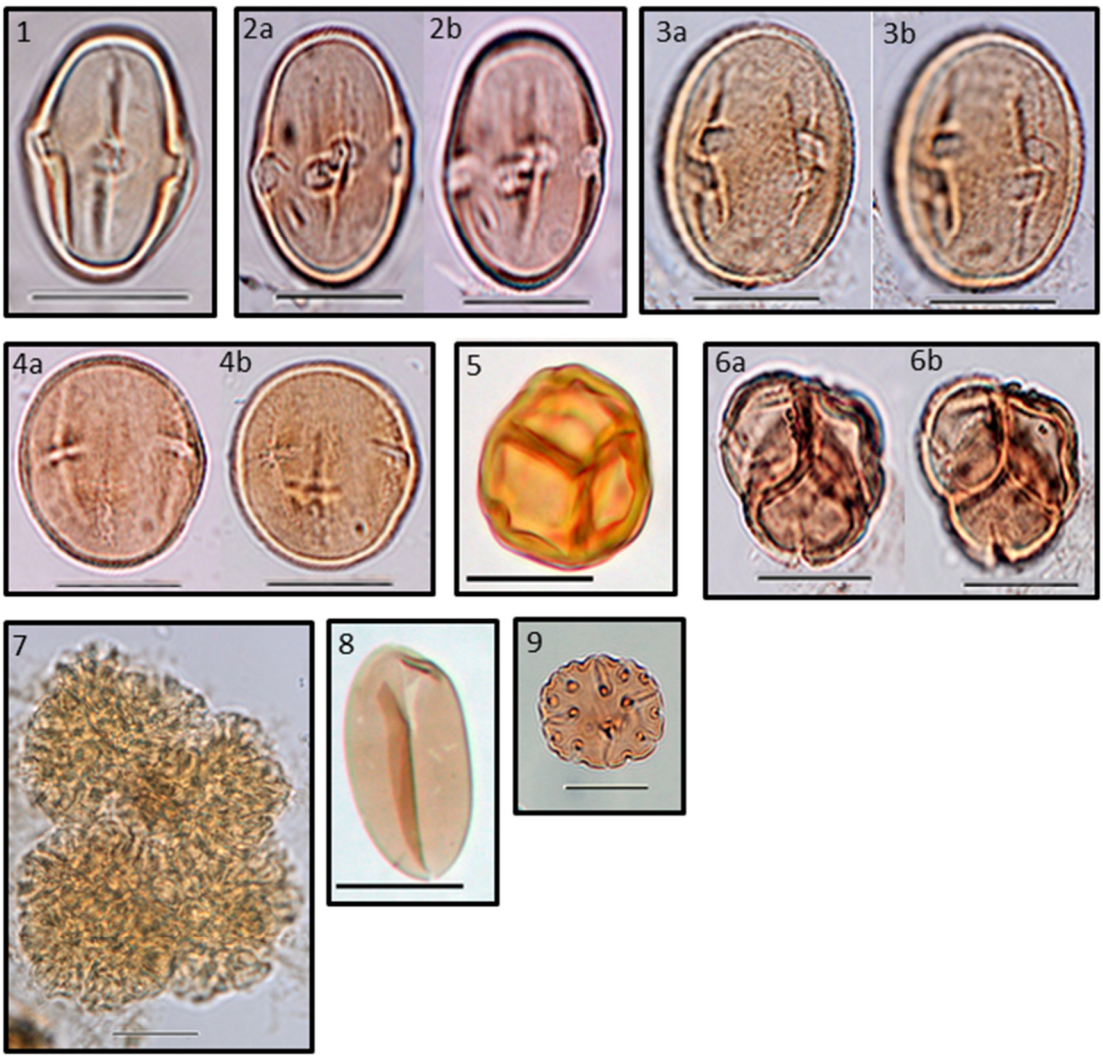
1
2a
2b
3a
3b
4a
4b
5
6a
6b
7
8
9

4-5 Publication 1: The recolonization of volcanically disturbed habitats during the Eocene of Central Europe: The maar lakes of Messel and Offenthal (SW Germany) compared

Published in Palaeobiodiversity and Palaeoenvironments, 100**,** 951–973 (2020). https://doi.org/10.1007/s12549-020-00425-4

Maryam Moshayedi[1*], Olaf K. Lenz[1, 2], Volker Wilde[3], Matthias Hinderer[1]
[1]Technische Universität Darmstadt, Institute of Applied Geosciences, Applied Sedimentology, Schnittspahnstrasse 9, 64287 Darmstadt, Germany.
[2]Senckenberg Gesellschaft für Naturforschung, General Directorate, Senckenberganlage 25, 60325, Frankfurt am Main, Germany.
[3]Senckenberg Forschungsinstitut und Naturmuseum, Sektion Paläobotanik, Senckenberganlage 25, 60325, Frankfurt am Main, Germany.

Author Contributions

Conceptualization: M. Moshayedi, Olaf K. Lenz, Volker Wilde, M. Hinderer
Data Curation: M.Moshayedi
Formal Analysis: M. Moshayedi
Funding Acquisition: M. Moshayedi
Investigation: M. Moshayedi,
Methodology: M. Moshayedi, Olaf K. Lenz, Volker Wilde
Project Administration: Olaf K. Lenz, Volker Wilde, M. Hinderer
Resources: M. Hinderer, V. Wilde
Validation: M. Moshayedi
Visualization: M. Moshayedi
Writing – Original Draft Preparation: M. Moshayedi
Writing – Review and Editing: Olaf K. Lenz, V. Wilde

Abstract
To reconstruct the paleoenvironment and changes within the vegetation 68 core samples were analyzed palynologically from the lacustrine filling of the Eocene maar lake of Offenthal (Hesse, SW-Germany). The lacustrine succession includes 16 m of clastic sediments overlain by 13 m of finely laminated bituminous shale. Based on a revised $^{40}Ar/^{39}Ar$ age of ~47.8 ± 0.3 Ma the lacustrine filling at Offenthal can be dated as uppermost Lower Eocene to lowermost Middle Eocene which is almost coeval to part of the nearby lacustrine succession at Messel. Cluster and NMDS analyses of well-preserved palynomorph assemblages reveal successional stages during the recolonization of the maar lake and its surroundings which are related to lithological changes. Furthermore, the palynomorph assemblages from Offenthal are compared to assemblages from Messel by NMDS analysis to find similarities and differences during the recolonization of volcanically disturbed habitats in Central Europe during Paleogene greenhouse conditions. Based on the similar succession in the vegetation at both lakes four different phases can be distinguished during recolonization and reestablishment of the vegetation at these sites: (1) an initial phase, (2) a recolonization phase, (3) a recovery phase, (4) a climax phase.

Key words: Palynology, Eocene, maar lake, recolonization, multivariate analysis

Introduction

Since it was the last greenhouse period on Earth and ecosystems already consisted of modern-type floras and faunas the Paleogene has been intensely studied to understand the response of ecosystems to environmental changes and climate variations. For the Eocene of Germany terrestrial ecosystems as described from the maar lake deposits of Messel (Gruber and Micklich 2007; Smith et al. 2018) and Eckfeld (Lutz et al. 2010) or the lignites of the Geiseltal (Krumbiegel et al. 1983) as well as sites characterized by paralic settings such as the mining district of Helmstedt-Schöningen (Riegel et al. 2015, Riegel and Wilde 2016) are the best known examples. Paleoenvironmental studies frequently focused on quantitative high-resolution palynology, e.g., for the maar lake of Messel (e.g., Lenz et al. 2007, 2015, 2017) or Lake Prinz von Hessen (Moshayedi et al. 2018).

There are at least half a dozen Eocene basins exposing lacustrine sediments known on the Sprendlinger Horst near Darmstadt in Southwest Germany (Fig. 4.5.1).

Most of them are fillings of maar structures resulting from hydro-volcanic activity, such as Messel, Offenthal and Groß Zimmern (Jacoby 1997; Harms et al. 1999; Jacoby et al. 2000; Felder et al. 2001; Felder and Harms 2004). Maar lake sediments are excellent for the preservation of paleoenvironmental information due to a considerable water depth in combination with a relatively small size of the lake. Anoxic conditions in the bottom water facilitate the excellent preservation of fossil remains (Sabel et al. 2005) and allow for high resolution studies due to undisturbed and frequently finely laminated, sometimes varved sediments (Lenz et al. 2010). Therefore, the Sprendlinger Horst is offering the rare opportunity to study and compare almost coeval and nearby fillings of Paleogene maar lakes. The present palynological study of lacustrine sediments from the maar lake of Offenthal not only introduces another Eocene archive in the area, but especially allows for a comparison to the maar deposits of Messel that are world-wide known for an excellent preservation of fossils (Smith et al. 2018). Such a combination of spatial and temporal resolution is almost unique for Paleogene volcanic settings.

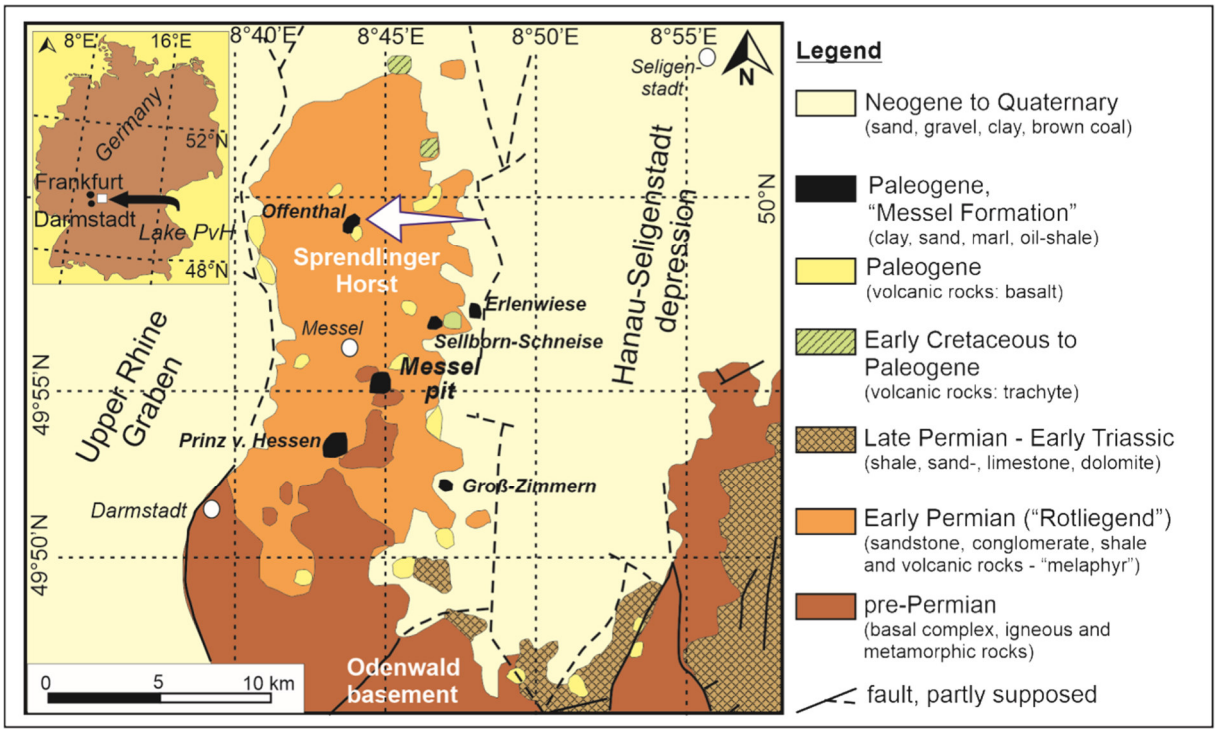

Fig. 4. 5. 1. Geological map of the Sprendlinger Horst (Southwest Germany) showing Lake Offenthal and other Palaeogene sites in the area (modified from Harms et al. 1999 and Lenz et al. 2007).

Our high-resolution palynological study is designed for providing insight into the recolonization of a volcanically disturbed area by plants. Furthermore, it should aim to investigate by statistical analyses, whether the long- and short-term compositional changes of the vegetation are related to local facies changes in the depositional basin.

The lacustrine succession at Offenthal

Among the Paleogene maar lakes on the Sprendlinger Horst Lake Offenthal is one of the smallest with a diameter of only 200 – 400 m (Felder et al. 2001). In order to find unequivocal proof for the origin of the basin, a scientific well (B/98-BK 1E) was drilled 1998 in the centre of the basin (49°58'52.37" N, 8°44'40.88" E) to penetrate the lake sediments. A total of 80 m was cored of which the lower 51 m consist of volcanic rocks that can be separated from a lacustrine succession in the upper 29 m (Fig. 4.5.2). Based on lithological changes Felder et al. (2001) divided the core in seven lithozones (LZ 1 to LZ 7), the lower two of them (LZ1 and 2; Felder at al. 2001) of purely volcanic origin.

This part of the succession is followed by lacustrine sediments in which Felder et al. (2001) distinguished four lithozones (LZ 3-6) that became the focus of our study (Fig. 4.5.3). Representative parts of these lithozones are presented in Fig. 4.5.4, however, the complete photo documentation of the lacustrine succession is included in the online supplementary material.

LZ 3 between 29.40 and 22.20 m is characterized by the dominance of turbiditic beds of conglomerates and graded sandstone to siltstone layers (Figs. 4.5.3, 4.5.4a). They document the fast post-eruptive filling of the crater by mass flows from the collapsing crater wall into the initial lake (Felder et al. 2001).

A first bituminous siltstone marks the boundary between LZ 3 and 4. The following LZ 4 between 22.20 and 14.07 m is characterized by a continuous decrease of grain size and an increase in layers of bituminous silt and clay, which appear massive to finely bedded or laminated (Fig. 4.5.3, 4.5.4b, c.). The increasing content of organic material in LZ 4 compared to LZ 3 is also indicated by the darker color of the sediment (Figs. 4.5.4b, c).

In LZ5 between 14.07 and 8.25 m bituminous shales are dominant (Felder et al. 2001). Beds with coarser clastic layers or individual turbidites occur only occasionally (Figs. 4.5.3, 4.5.4d).

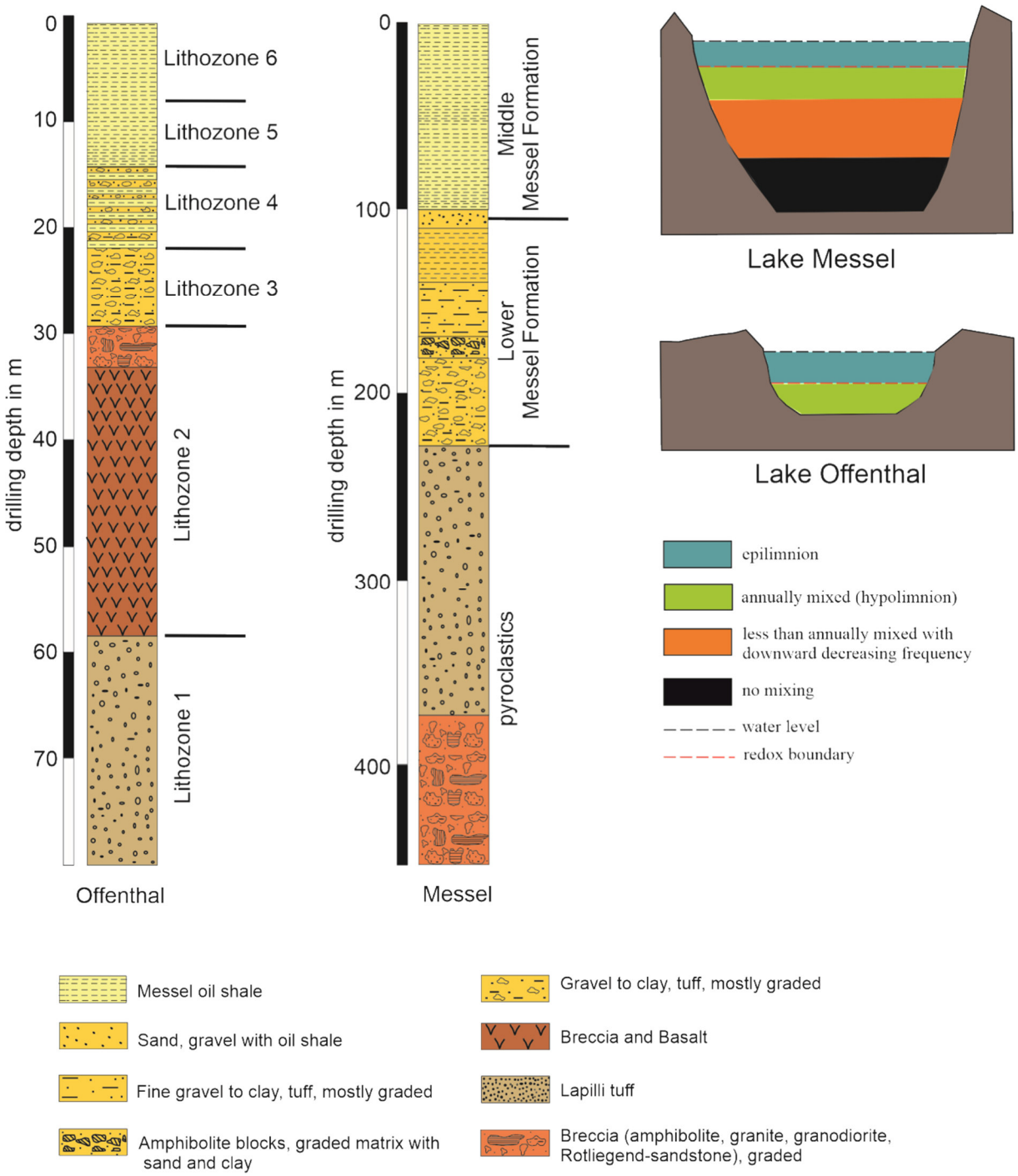

Fig. 4. 5. 2. **a** Generalized sections of the Messel and Offenthal cores modified after Felder et al. (2001) and Felder and Harms (2004). **b** Sketches of the maar lakes of Messel and Offenthal indicating meromixis and a permanently stratified lake at Messel and annual overturn with only seasonal stratification at Lake Offenthal (Modified from Felder and Gaupp 2006).

This indicates an increasing stability of the crater walls (see Lenz et al. 2007). The same as for LZ 5 also applies to LZ 6 between 8.25 and 1.8 m. However, in contrast to LZ 5, the bituminous shales are often finely laminated (Fig. 4.5.4e) and frequently interspersed with siderite laminae (Felder et al., 2001).

The lacustrine succession of LZ 3 to 6 documents the gradual and continuous filling of the basin without unconformities and disturbance. The succession is finally cut by Quaternary sediments at a depth of 1.8 m (Fig. 4.5.3).

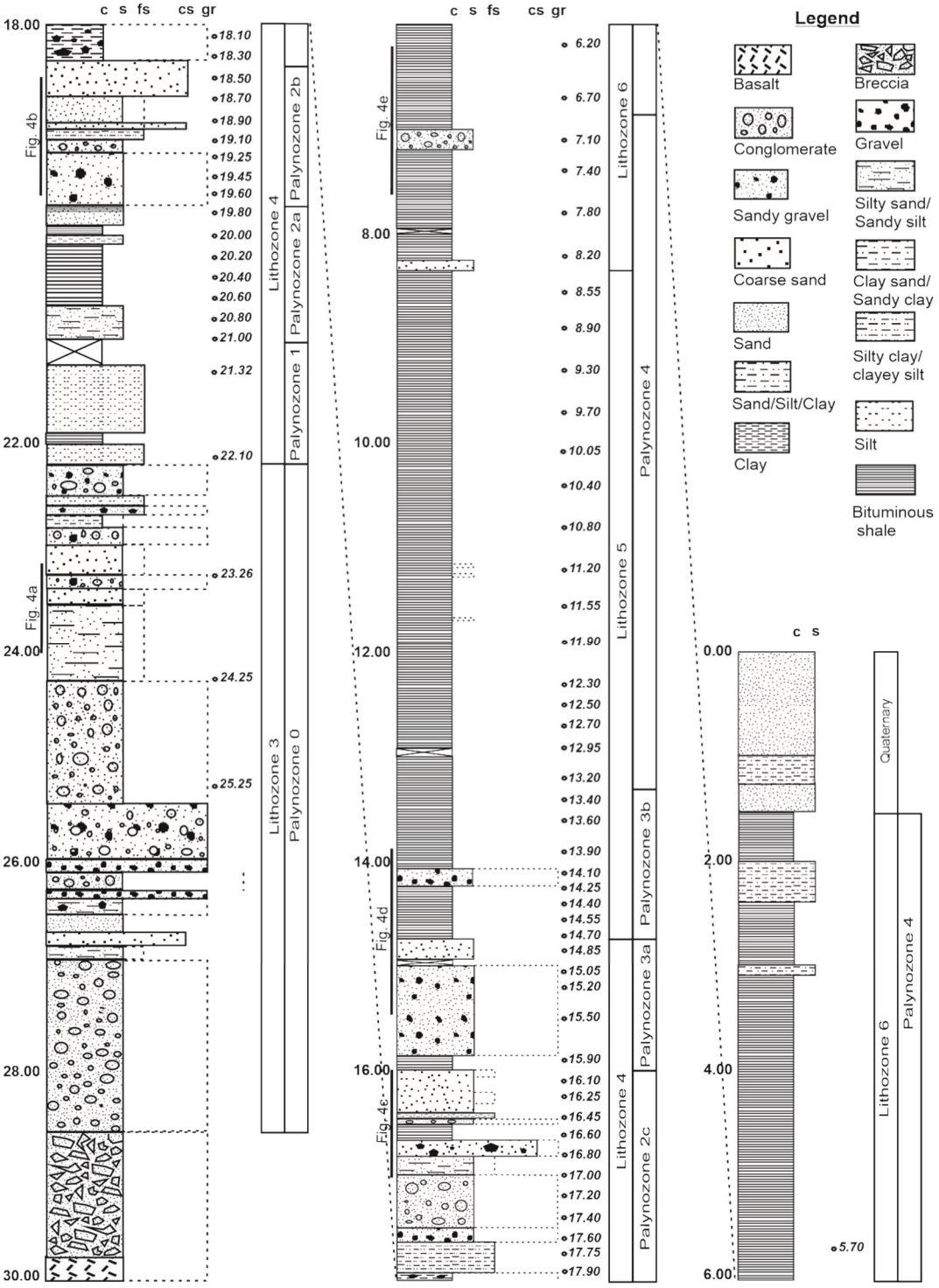

Fig. 4. 5. 3. Generalized section of the core Offenthal showing lithozones and palynozones as used in this paper. The position of core images as providedon Figure 4.5.4 is indicated.

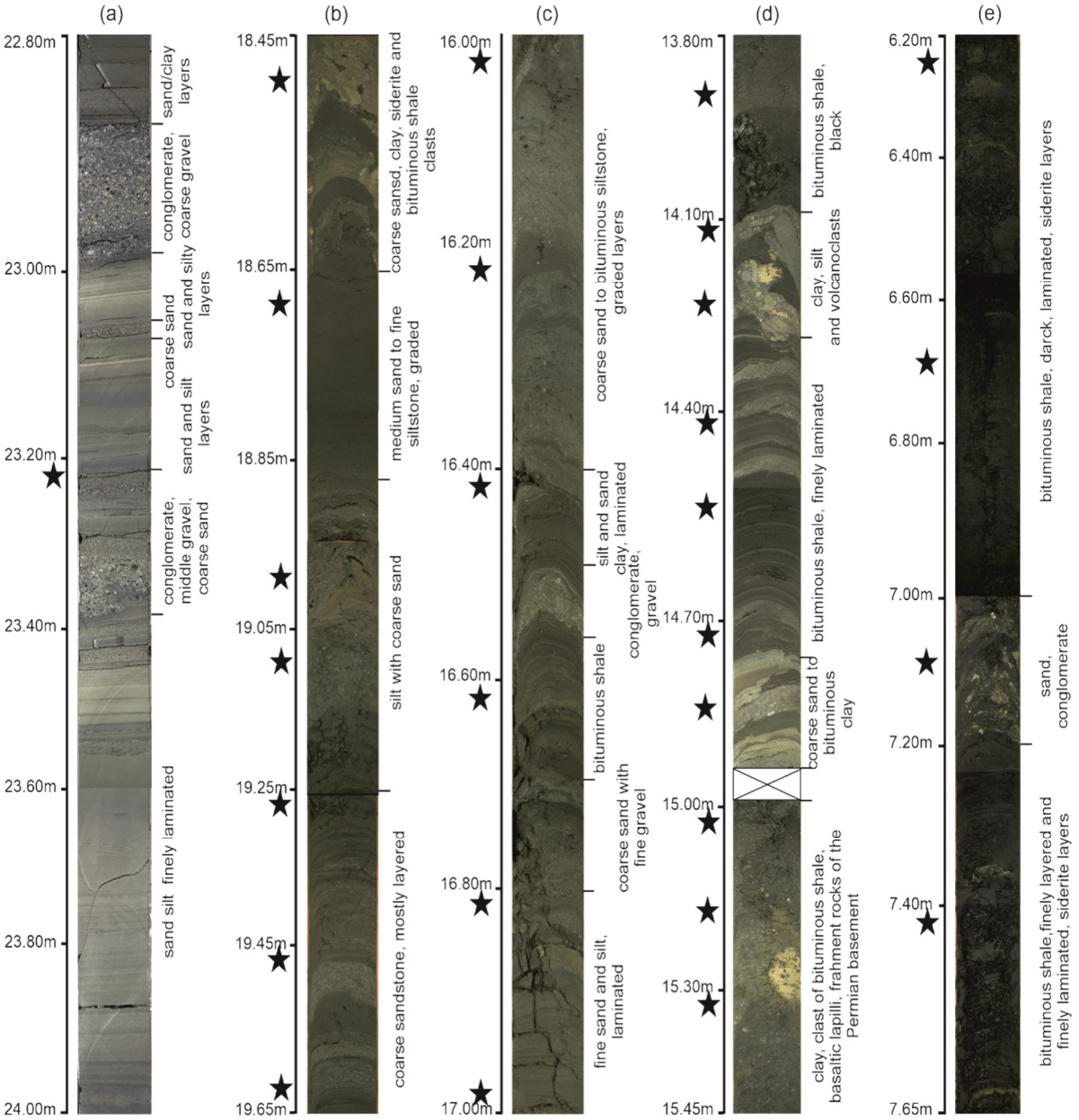

Fig. 4. 5. 4. Selected images of the core illustrating the lacustrine record of Offenthal and its lithozones. The position of the respective palynological samples is indicated by black stars. The pictures are based on photographs of FIS/HLUG (F.J Harms, W. Schiller and M. Stryj) from the core BK 1E. **a** LZ3, 11034.pcd-11037.pcd; **b** LZ4, 11024.pcd-11026.pcd; **c** LZ4, 11018.pcd-11020.pcd; **d** LZ4/5, 11013.pcd-11016.pcd; **e** LZ6, 10995.pcd-10998.pcd.

Material and methods

Sampling and sample processing

For palynological investigation of the lacustrine sediments of the Offenthal core between 25.25 m and 5.70 m, 68 samples were analyzed at approximately 20 cm intervals. Samples were prepared using standard palynological extraction techniques as described by Kaiser and Ashraf (1974). They were successively treated by hydrochloric acid (HCL), hydrofluoric acid (HF) and potassium hydroxide (KOH). To improve transparency of the palynomorphs after sieving through a 10 µm mesh screen, the residues were briefly oxidized by applying nitric acid (HNO_3) or hydrogen peroxide (H_2O_2). For each sample one or more permanent slides have been prepared by mixing the residue with glycerin jelly. Slides and residues are housed at the Senckenberg Research Institute und Natural History Museum, Section Paleobotany, Frankfurt am Main, Germany.

Quantitative palynological analysis

Palynological analysis was undertaken by using a transmitted light microscope (Olympus BX40). At least 250 individual palynomorphs per sample were identified and counted at x400 magnification to obtain a representative and robust dataset that can be used for statistical analysis. The raw data are included in the supplementary material. However, 10 to 15% of the total assemblages could not be determined due to poor preservation and were counted as "Varia". The palynomorphs (complete list in supplementary Table 1) were identified based on the systematic-taxonomic studies of Thomson and Pflug (1953), Thiele-Pfeiffer (1988), Nickel (1996) and Lenz (2005).

The pollen diagram, produced by PanPlot 11.04 (Alfred Wegener Institut für Polare und Marine Forschung, PANGEA), shows the abundance of the most important palynomorphs in percentages. To arrange the taxa according to their weighted average value (WA regression; ter Braak and Looman 1995) software C2 1.7.6 (Juggins 2007) was used because such an arrangement of pollen is necessary to obtain a structured pollen diagram that shows the major patterns of compositional variation in relation to depth and reveals progressive steps in the evolution of the plant community (Janssen and Birks 1994). Pollen and spores were calculated to 100%, whereas algae such as *Botryococcus* and *Ovoidites* were recorded as additional percentages in percent of the total pollen sum.

Statistical analysis (Cluster analysis and Non-Metric Multidimensional Scaling)

For a robust zonation of the pollen diagram constrained cluster analysis was carried out using the unweighted pair group average method (UPGMA), an agglomerative hierarchical clustering method. Furthermore, to illustrate compositional differences and ecological trends between the different vegetation phases at Offenthal and to compare the vegetation at Offenthal with the vegetation at Messel, non-metric multidimensional scaling (NMDS; Shepard 1962a, b; Kruskal 1964) has been performed. For Cluster analysis and NMDS software PAST 3.23 has been used (Hammer et al. 2001).

To avoid possible sources of error which can have an impact on the results, the palynological data set was simplified for statistical analysis. Some of the palynomorph taxa were lumped to minimize problems in the identification to "species level" and therefore potential identification errors, because of minor differences between some of the species, e.g., species of the juglandaceous genera *Plicatopollis* and *Plicapollis*. Furthermore, for cluster analysis and NMDS all taxa have been removed that did not reach 1% in any of the studied samples. Therefore, for multivariate analysis of the Offenthal data, a reduced number of 40 palynological "variables" was used (Supplementary Table 1). For the joint NMDS of the Offenthal and Messel data the number of palynological "variables", which are typical for both records, slightly increased to 54 (Supplementary Table 1).

Statistical analysis is based on the raw data, which have been standardized using the Wisconsin double standardization (Bray and Curtis 1957; Cottam et al. 1978; Gauch and Scruggs 1979; Oksanen 2007). This standardization method scales the abundance of each taxon to its maximum value and represents the abundance of each taxon by its proportion in the sample (Mander et al. 2010). This removes the influence of sample size on the analysis and equalizes the effects of rare and abundant taxa on clustering and NMDS (Van Tongeren 1995; Jardine and Harrington 2008). As a similarity measure we used the Bray-Curtis dissimilarity for all analyses.

NMDS has been chosen as the appropriate ordination method, because NMDS is the most robust unconstrained ordination method in ecology (Minchin 1987) and has been successfully applied to palynological data in previous studies (e.g., Oswald et al. 2007; Jardine and Harrington 2008; Mander et al. 2010; Ghilardi and O'Connell 2013; Broothaerts et al. 2014, Lenz and Wilde 2018). Compared to other ordination techniques of multivariate data such as principal component analysis or (detrended) correspondence analysis NMDS avoids the

assumption of a linear or a unimodal response model between the palynomorph taxa and the underlying environmental gradients, and as a non-parametric method it also avoids the requirement of normality of data. NMDS uses ranked, rather than absolute, distance values to project the data into a two- or three-dimensional coordinate system (ter Braak 1995; Hammer and Harper 2006).
For the joint NMDS of palynomorph assemblages from Lake Offenthal and Lake Messel, quantitative palynological data of 598 samples from Messel (Lenz and Wilde 2018) have been used. Compared to Lenz and Wilde (2018) the original Messel data set of 680 samples has been reduced by 82 samples by cutting off outliers in the data set which are characterized by specific palynomorph contents that do not represent typical assemblages of different evolutionary stages of the vegetation at Messel. Furthermore, the 10 different vegetation phases (Lenz et al. 2007, Lenz et al. 2011, Lenz and Wilde 2018) which have previously been distinguished at Messel were reduced to five phases including two phases from the Lower Messel Formation with the Early Initial Lake Phase (EILP) and the Late Initial Lake Phase (LILP) and three phases of the Middle Messel Formation (MMF). Phase "MMF base" includes phases MMF 1 and 2, "MMF center" phase MMF 3 and "MMF top" phases MMF 4 to 6 of Lenz and Wilde (2018).

Results

Age determination for Lake Offenthal

A basaltic clast from the top of volcanoclastic material of LZ 2 that may serve as evidence for the time of the eruption was dated at 47.4 ± 0.3 Ma applying the $^{40}Ar/^{39}Ar$ incremental heating technique (Mertz and Renne 2005). However, according to a revised calibration of the $^{40}Ar/^{39}Ar$ system in the Fish Canyon sanidine as age reference material (FCs; see Lenz et al. 2015 for details) the eruption at Offenthal happened 300 to 500 ka earlier than previously assumed at 47.71 ± 0.3 Ma using a new FCs age of Kuiper et al. (2008), and 47.87 ± 0.3 Ma using a recalibrated FCs age provided by Renne et al. (2011). According to the ICS International Chronostratigraphic Chart, the Ypresian/Lutetian boundary is now fixed almost exactly at 47.8 Ma (Cohen et al. 2013). Therefore, the lacustrine filling at Offenthal should be regarded as uppermost Lower Eocene to lowermost Middle Eocene in age.
Compared to the eruption at Messel with an age of 48.27 ± 0.22 (based on the FCs age of Kuiper et al. 2008, see Lenz et al. 2015) or 48.11 ± 0.22 (FCs age of Renne et al. 2011, see Lenz et al. 2015) the eruption at Offenthal happened *c.* 300 ka later. However, since deposition at Messel lasted *c.* 900 ka (Lenz et al. 2015) the lacustrine sediments at Offenthal probably were deposited contemporaneously to the younger part of the Middle Messel Formation at Messel.

Palynology of Lake Offenthal

The occurrence and distribution of the most abundant palynomorphs throughout the lacustrine succession of Lake Offenthal is shown in the pollen diagram (Fig. 4.5.5). Based on constrained cluster analysis, five palynozones (PZ 1 to 5) have been distinguished (Fig. 4.5.6). They are characterized by specific palynomorph assemblages and can be correlated to the LZs of Felder et al. (2001) (Figs. 4.5.3, 4.5.6). A sixth, and lowest palynozone (PZ 0) is created in the pollen diagram for the lowermost three samples at 25.25, 24.25 and 23.26 m from the lacustrine part of the core (Fig. 4.5.5). These samples rarely show any palynomorphs and counts are without any statistical significance. In the lower two samples only 14 and 12 palynomorphs and in the sample at 23.26 m depth only 135 palynomorphs have been identified by scanning several slides. Therefore, they have been separated from the other samples which contain abundant and well-preserved palynomorphs.

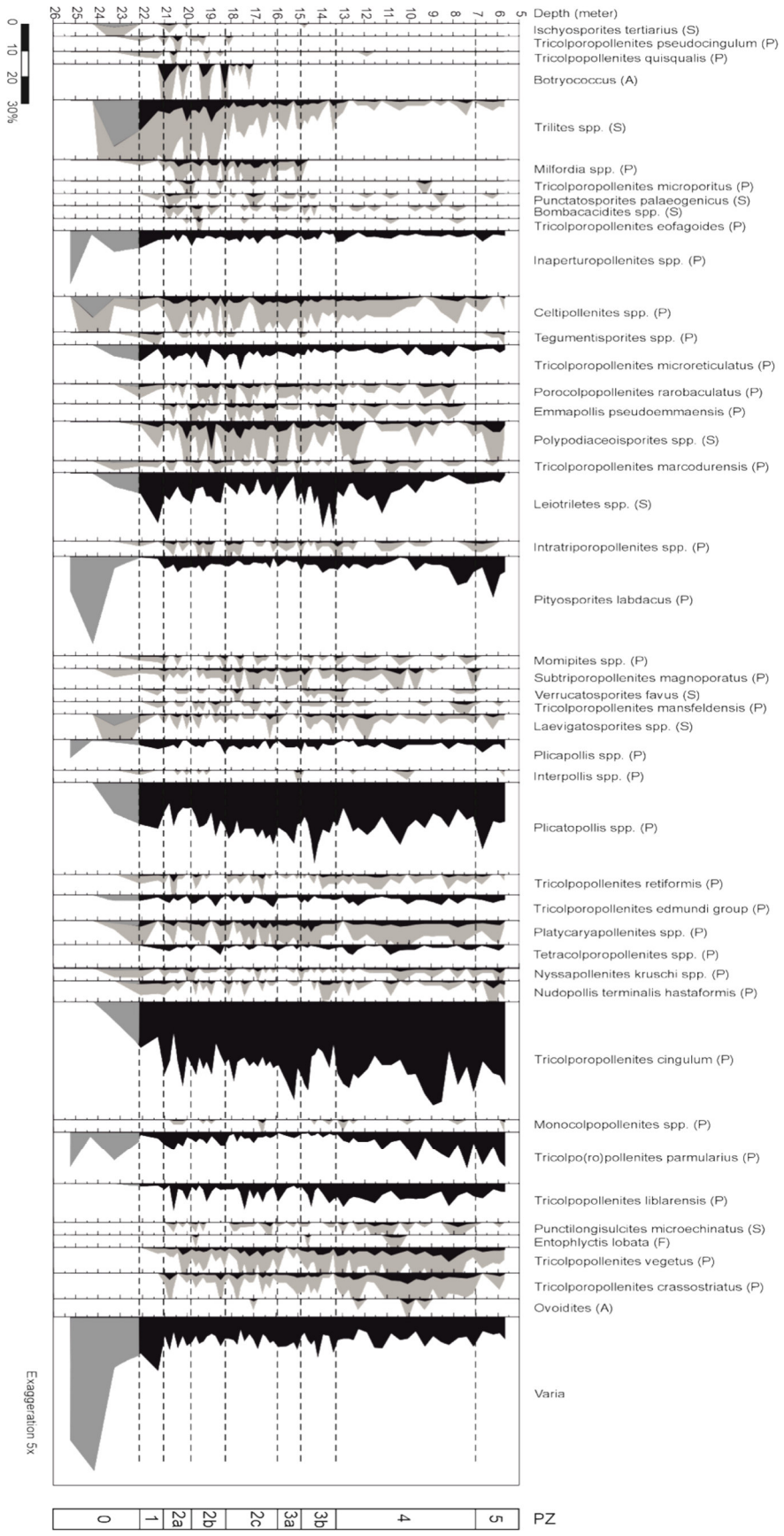

Fig. 4. 5. 5. Pollen diagram showing the most important taxa in the lacustrine succession of Lake Offenthal. The diagram shows the five palynological zones as derived from constrained cluster analysis (see Fig.4.5. 6). A, algae; P, pollen; S, spore; F, fungal spore.

Compositional differences between the pollen assemblages in PZ 1 to 5 become evident in the NMDS plot (Fig. 4.5.7), because samples from the oldest PZ 1 up to the youngest PZ 5 are ordered from right to left in the ordination space of the NMDS plot.

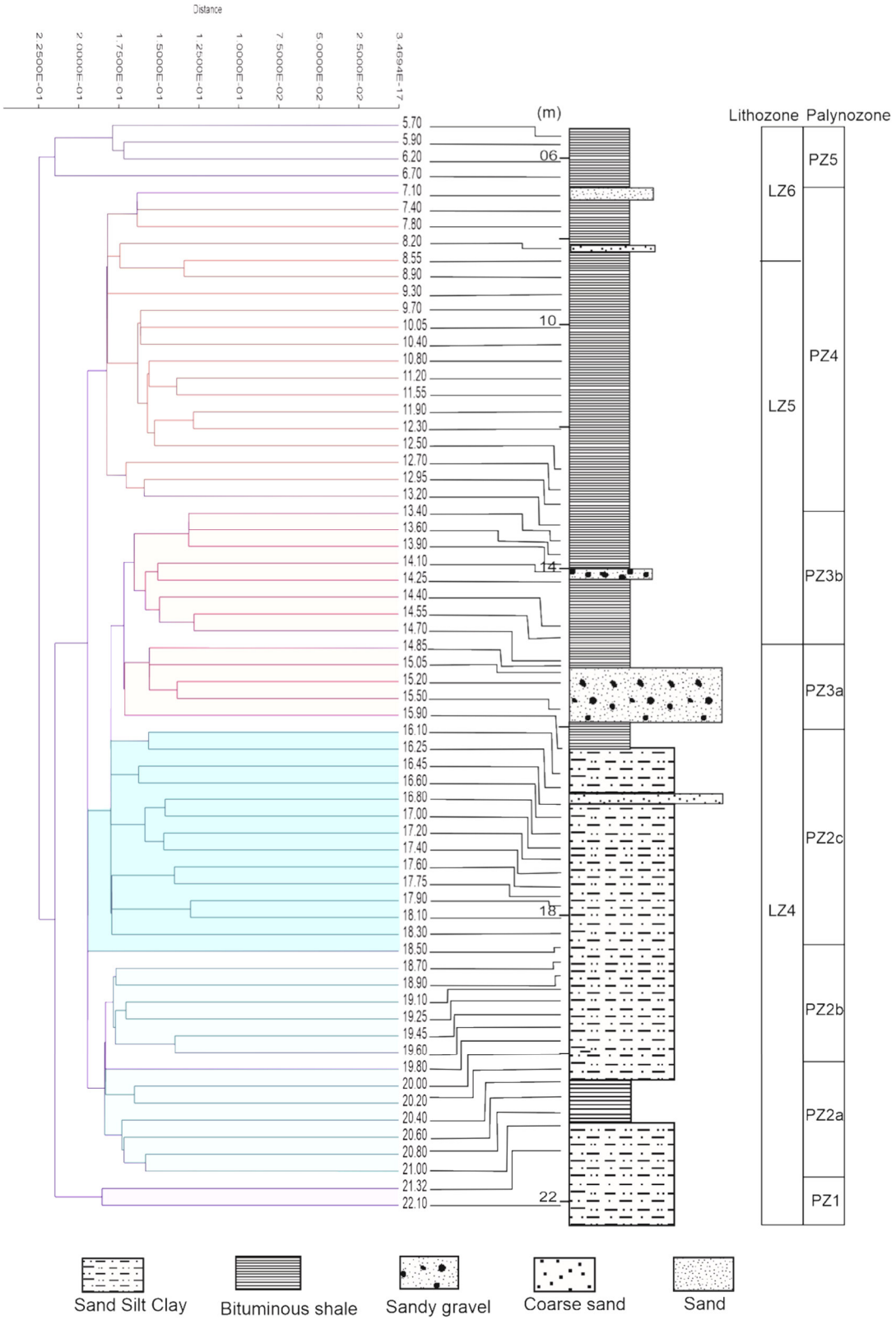

Fig. 4. 5. 6. Results of a constrained cluster analysis (UPGMA) of 68 samples between 21.10 and 5.70 m. Samples are labelled with their core depth in meters. The separation into five pollen zones correlates well with lithological changes.

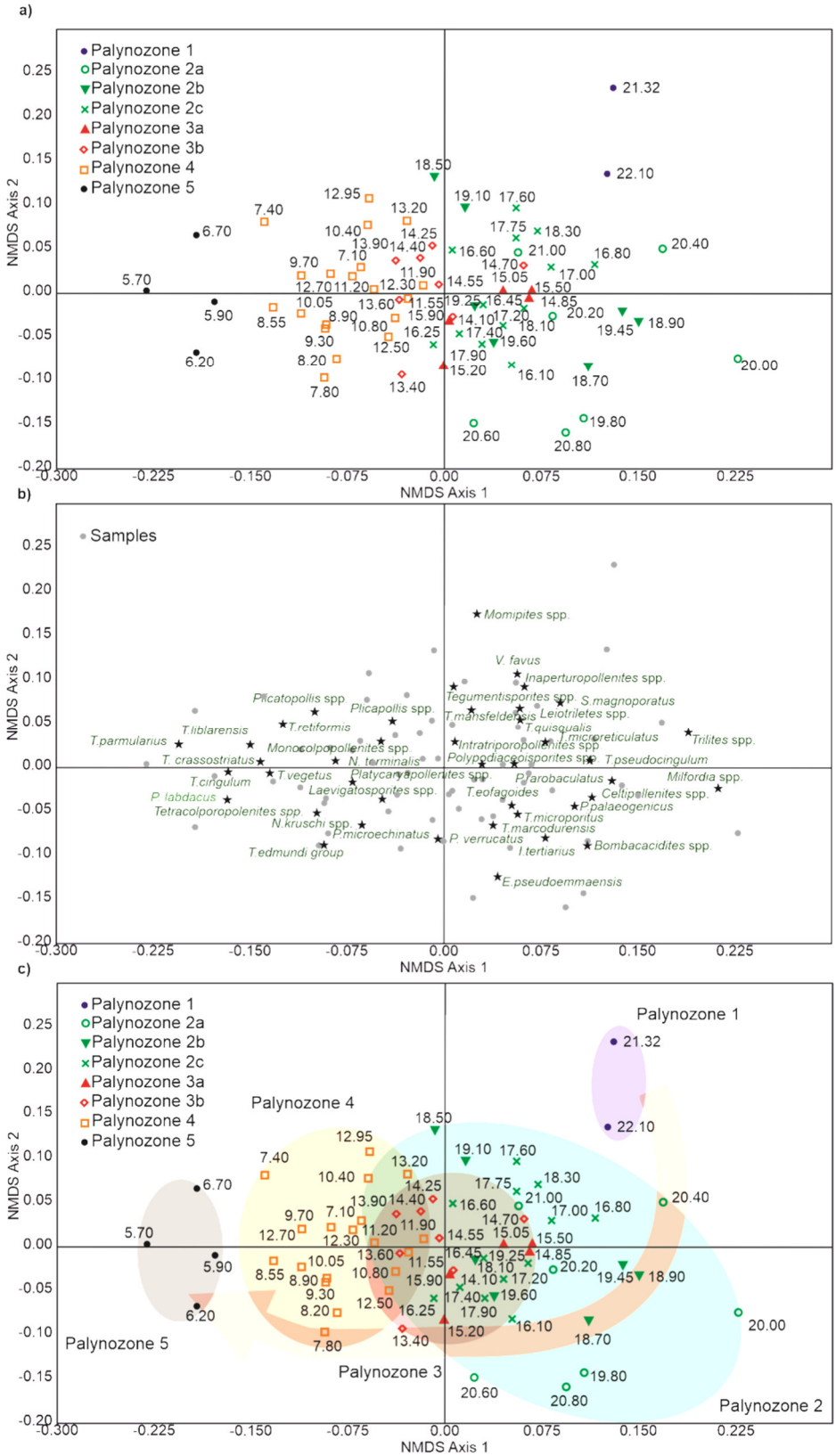

Fig. 4. 5. 7. Non-metric multidimensional scaling (NMDS) of palynological data of 68 samples from the lacustrine succession of the Offenthal maar lake using the Bray-Curtis dissimilarity and the Wisconsin double standardized raw data values. **a** Scatter plot of the first two axes showing the arrangement of samples. The different symbols represent samples from the five different palynozones. **b** Scatter plot of the first two axes showing the arrangement of taxa. The dots represent the different samples (see a). **c** Scatter plot of the first two axes showing the arrangement of palynozones and samples. The arrow illustrates the temporal succession of palynozones.

Palynozone 1

PZ1 is represented by only two samples from 22.10 and 21.32 m depth from the lower part of LZ4 (Figs. 4.5.3, 4.5.6). These samples plot in the upper right corner of the NMDS ordination space clearly separate from the other samples due to significant differences in composition compared to the palynomorph assemblages of the other samples (Fig. 4.5.7a). Spores of Schizaeaceae with different species of *Leiotriletes* spp. (up to 28%, Figs. 4.5.8d, e) and *Trilites* spp. (up to 12%) are particularly abundant. These taxa have also been recognized with some grains in PZ 0. Other fern spores such as *Tegumentisporites* spp. (Selaginellaceae, up to 2%) and *Polypodiaceoisporites* spp. (Polypodiaceae, up to 3%, Fig. 4.5.8i) appear also regular in this PZ.

Among the swamp forest elements *Inaperturopollenites* spp. (Cupressaceae, Figs. 4.5.8b, c) reach their maximum for the complete section with 7%. Further dominant elements are *Plicatopollis* spp. (Juglandaceae, up to 18%, Fig. 4.5.9i) and *Tricolporopollenites cingulum* (Fagaceae, up to 18%, Figs. 4.5.9k, l).

Remarkable is the poor preservation of palynomorphs in these two samples which is indicated by the highest amount of unidentified palynomorphs ("Varia") in the record at Offenthal.

Palynozone 2 and its subdivisions

PZ2 occurs between 21.00 and 16.10 m depth and consists of 27 samples (Fig. 4.5.6). Due to minor differences in the palynomorph composition it can be subdivided in three parts: PZ 2a with 7 samples between 21.00 and 19.80 m, followed by PZ 2b with 6 samples up to a depth of 18.70 m and finally PZ 2c with 14 samples in the upper 2.60m of PZ2. The zone comprises most of LZ 4 in which bituminous shales become more and more abundant.

In the NMDS the samples are plotted at the right side of the ordination space (Fig. 4.5.7a). Most samples of PZ 2a are in the lower right corner, whereas samples of zones PZ 2b and 2c are plotted near the center of the ordination space. Therefore, a continuous change within the palynomorph assemblages between PZ 2a and PZ 2c is indicated.

The dominant fern spores of PZ1 such as *Trilites* spp. and *Leiotriletes* spp. are still present in PZ2, but steadily decreasing towards PZ 2c. Other fern spores, such as *Punctatosporites palaeogenicus* (Fig. 4.5.8k), a spore of the Polypodiaceae, are limited to PZ 2 with a maximum value of 3%. Spores of other Polypodiaceae (*Polypodiaceoisporites* spp.) which are distributed throughout the Offenthal record, reach their maximum here.

Some taxa such as, e. g., *Milfordia* spp. (Restionaceae, up to 5%; Fig. 4.5.9a), *Emmapollis pseudoemmaensis* (Chloranthaceae, up to 3%; Fig. 4.5.9q), *Pityosporites labdacus* (Pinaceae, up to 5%; Fig. 4.5.8a), *Intratriporopollenites* spp. (Malvaceae, up to 4%; Fig. 4.5.8g), *Tricolporopollenites crassostriatus* (Solanaceae, up to 2%) and *Tricolpopollenites vegetus* (Hamamelidaceae, up to 6%; Fig. 4.5.9b) have their first appearance for Offenthal in this PZ.

Among the dominant elements the increase of *Tricolporopollenites cingulum* in comparison to zone PZ 1 is noteworthy. With up to 32% this taxon is by far the most common in PZ 2. *Plicatopollis* spp. (up to 24%) is also much more common than in PZ 1 and increases continuously from PZ 2a to PZ 2c.

The subdivision of PZ 2 is in mainly based on the decreasing abundance of fern spores and increasing values of *Plicatopollis* spp. However, also the occurrence of less abundant palynomorphs differs between the three subzones. PZ2a, for example, is characterized by the regular appearance of *Bombacacidites* spp. (Malvacaceae; Fig. 4.5.8l), *Tricolporopollenites pseudocingulum* and *Tricolporopollenites quisqualis* (both fagaceous alliance), while these elements disappear in zones PZ2b and PZ2c. Furthermore, the coccal green alga *Botryococcus* is relatively abundant in PZ2a and PZ 2b with a maximum value of 9%, but lacks completely in PZ 2c and the rest of the core.

Fig. 4. 5. 8. Pollen and spores from the lacustrine record at Lake Offenthal. The scale bar represents 20µm. Slide numbers and related depths are given in brackets.
a *Pityosporites labdacus* (Pinaceae; Off-64, 21.00 m); **b** *Inaperturopollenites dubius* (Cupressaceae; Off-64, 21.00 m); **c** *Inaperturopollenites magnus* (Cupressaceae; Off-152, 16.60 m); **d** *Leiotriletes microadriennis* (Schizaeaceae; Off-62, 21.32 m); **e** *Leiotriletes maxoides* (Schizaeaceae; Off-64, 21.00 m); **f** *Verrucatosporites favus* (Polypodiaceae; Off-62, 21.32 m); **g** *Intratriporopollenites microinstructus* (Malvaceae; Off-88, 19.80 m); **h** *Tricolporopollenites marcodurensis* (Vitaceae; Off-62, 21.32 m); **i** *Polypodiaceoisporites lusaticus* (Polypodiaceae; Off-88, 19.80 m); **j** *Echinatisporites longiechinatus* (Selaginellaceae; Off-126, 17.90 m); **k** *Punctatosporites palaeogenicus* (Polypodiaceae; Off-126, 17.90 m); **l** *Bombacacidites* sp. (Malvaceae; Off-99, 19.25 m); **m** *Tricolporopollenites microreticulatus* (Oleaceae; Off-99, 19.25 m);

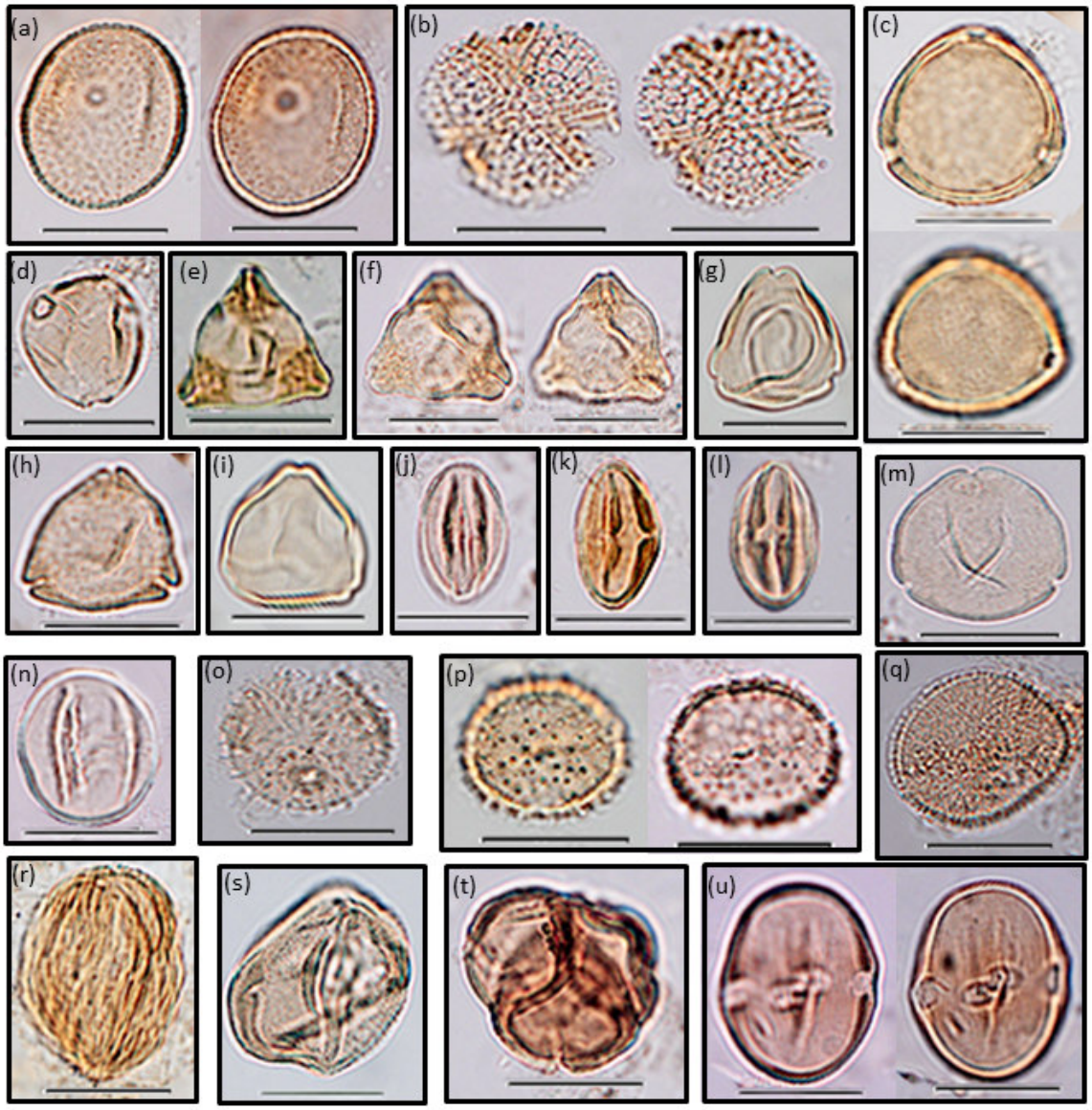

Fig. 4. 5. 9. Pollen and spores from the lacustrine record at Lake Offenthal. The scale bar represents 20µm. Slide numbers and related depths are given in brackets.
a *Milfordia minima* (Restionaceae; Off-118, 18.30 m); **b** *Tricolpopollenites vegetus* (Hamamelidaceae; Off-126, 17.90 m); **c** *Subtriporopollenites magnoporatus* (unknown botanical affinity; Off-62, 21.32 m); **d** *Celtipollenites intrastructurus* (Cannabaceae; Off-118, 18.30 m); **e** *Nudopollis terminalis hastaformis* (Normapolles with unknown botanical affinity; Off-62, 21.32 m); **f** *Plicapollis pseudoexcelsus turgidus* (Juglandaceae?; Off-64, 21.00 m); **g** *Playcaryapollenites semicyclus* (Juglandaceae; Off-118, 18.30 m), **h** *Triatriopollenites rurensis* (Myricaceae; Off-64, 21.00 m); **i** *Plicatopollis* sp. (Juglandaceae; Off-99, 19.25 m); **j** *Tricolpopollenites liblarensis* (Fagaceae, Fabaceae, Combretaceae, Verbenaceae; Off-99, 19.25 m); **k**, **l** *Tricolporopollenites cingulum* (Fagaceae; Off-62, 21.32 m; Off-64, 21.00 m); **m** *Playcaryapollenites platycaryoides* (Juglandaceae; Off-152, 16.60 m); **n** *Tricolpo(ro)pollenites parmularius* (Eucommiaceae; Off-62, 21.32 m); **o** *Porocolpopollenites rarobaculatus* (Symplocaceae; Off-126, 17.90 m); **p** *Compositoipollenites rhizophorus* (Icacinaceae; Off-99, 19.25 m); **q** *Emmapollis pseudoemmaensis* (Chloranthaceae; Off-155, 16.45 m); **r** *Tricolporopollenites sole de portai* (Anacardiaceae, Rosaceae; Off-99, 19.25 m); **s** *Nyssapollenites kruschii* (Nyssaceae; Off-52, 22.10 m); **t** *Ericipites ericius* (Ericaceae; Off-88, 19.80 m); **u** *Tetracolporopollenites sapotoides* (Sapotaceae; Off-80, 20.20 m)

Palynozone 3 and its subdivisions

PZ 3 consists of 13 samples between 15.90 and 13.40 m depth and is subdivided in subzones PZ 3a (5 samples up to 14.85 m) and PZ 3b (8 samples up to 13.40 m). This subdivision clearly correlates to the lithological change between LZ 4 and LZ 5 (Figs. 4.5.3, 4.5.6). LZ 5 is characterized by the deposition of bituminous shales.

The samples of PZ 3 are plotted near the center of the NMDS ordination space, but samples of zone PZ 3a more on the positive side of NMDS axis 1 together with samples from PZ 2c, whereas samples of zone PZ 3b are more on the negative side of axis 1 together with samples from the following PZ 4 (Fig. 4.5.7a). This shows that PZ 3 is a transitional phase between the older (PZ 2) and the younger (PZ 4) vegetation.

A transitional phase is indicated by the complete disappearance of Restionaceae (*Milfordia* spp.) at the end of PZ 3a, while fern spores of *Trilites* spp. nearly disappear at the end of PZ 3b. Both elements are among the dominant species in the older zones PZ 1 and PZ 2. In contrast, taxa such as *Tricolpopollenites liblarensis* (Fig. 4.5.9j) or *T. vegetus* start to increase in abundance in PZ 3b towards values which are characteristic for the younger zones PZ 4 and PZ 5.

Among the dominant elements *Tricolporopollenites cingulum* and *Plicatopollis* spp. also increase in abundance in comparison to the older PZs. *T. cingulum* reaches a peak abundance with 37% in PZ 3a, while *Plicatopollis* spp. have their highest abundance for the complete record with 30% in PZ 3b. Furthermore, fern spores of *Leiotriletes* spp. (up to 21%) also have their maximum in PZ 3b. Another polypodiaceous spore (*Verrucatosporites favus*; Fig. 4.5.8f) occurs regularly in PZ 3b but is almost missing otherwise at Offenthal.

Palynozone 4

PZ 4 between 13.20 and 7.10 m includes 19 samples of LZ 5 and the lower part of LZ 6 (Figs. 4.5.3, 4.5.6). The samples are plotted in the NMDS at the left negative side of axis 1 in the ordination space, clearly separate from samples of the younger PZs 1 to 3b (Fig. 4.5.7a). Only samples of PZ 3b are plotted together with some samples of PZ 4 at the center of the ordination space, indicating similar palynomorph assemblages.

Some palynomorph taxa show a strong increase in their abundance compared to older PZs (Fig. 4.5.5). *Tricolpo(ro)pollenites parmularius* (Eucommiaceae; Fig. 4.5.9n) regularly occurs with low values in PZ 1 to PZ 3 but increases strongly in its abundance from *c*. 3% at the base of PZ 4 to 14% at the top of the PZ. *Tricolporopollenites cingulum* (up to 40%), *T. vegetus* (up to 6%) and *Pityosporites* spp. (up to 11%) also increase in abundance from the lower to the upper part of PZ 4. *Plicatopollis* spp. (up to 24%) and *Tricolpopollenites liblarensis* (up to 9%) are characterized by keeping high values.

In contrast ferns spores of *Trilites* spp. and especially of *Leiotriletes* spp. show a strong decrease to relatively low numbers compared to PZ3 and 2. *Milfordia* spp., prominent in PZ 2 and PZ 3, is completely missing in PZ 4.

Also remarkable is the occurrence of *Ovoidites* which represents cysts of freshwater algae (Zygnemataceae) in some samples of PZ 4.

Palynozone 5

Four samples from the top of the studied section between 6.70 to 5.70 m (LZ 6) have been put together in PZ 5. In the cluster analysis these samples are clearly distinguished from all other samples (Fig. 4.5.6) and plot on the left side of the NMDS ordination space relatively far away from the other samples on the negative end of axis 1 indicating significant compositional differences compared to the other samples (Fig. 4.5.7a). This depends mainly on the maximum distribution of *Pityosporites labdacus* (up to 16%) in combination with high values of *Tricolpo(ro)pollenites parmularius* (up to 13%), *Tricolporopollenites cingulum* (up to 25%) and *Plicatopollis* spp. (up to 15%). Furthermore, the Normapolles element

Nudopollis terminalis (myricaceous/juglandaceous alliance; Fig. 4.5.9e) has its peak abundance in PZ 5 with up to 3%.

Discussion

Reconstruction of the paleoenvironment at Lake Offenthal

After the eruption(s) at Offenthal had ceased, the newly formed barren surface of the crater wall and the surrounding devastated area were gradually re-occupied by the vegetation in a similar way as described for Lake Messel by Lenz et al. (2007). Recolonization at Offenthal started with elements of a pioneering vegetation such as different ferns (Fig. 4.5.5). During the recolonization process the zonal vegetation re-advanced and completely re-occupied the area at the end of the time which is documented in the lacustrine deposits of the crater. This is seen in the pollen record as presented in the pollen diagram (Fig. 4.5.5) and especially in the NMDS plot of the taxa. Samples from the oldest PZ 1 up to the youngest PZ 5 are ordered from right to left in the ordination space of the NMDS plot indicating a continuous change in the composition of the vegetation throughout the different palynozones (Fig. 4.5.7c).

The different distributions of early colonizers such as ferns represented by spores such as *Leiotrilites* spp., *Trilites* spp., *Verrucatosporites favus* and *Polypodiaceoisporites* spp. in PZ1, PZ2 and PZ3a, which are plotted on the right side of the NMDS ordination space (Fig. 4.5.7b) reveal a successive vegetational recolonization in the lower part of the record. During PZ 3b, PZ 4 and PZ 5 the re-advance of the (para)tropical rainforest in the crater area is obvious. This is indicated especially by pollen of the Juglandaceae (e.g. *Plicatopollis* spp., *Plicapollis* spp.) and Fagaceae (e.g. *Tricolporopollenites cingulum*, *Tricolporopollenites liblarensis*), which became more and more dominant in the younger PZs and are therefore plotted at the left side of NMDS axis 1 (Fig. 4.5.7b). At the same time the herbaceous pioneering community represented by diverse fern spores decreased. Taking into account the sediments at the base of the lacustrine succession, which are almost free of palynomorphs (PZ 0), three phases can be distinguished in the recolonization of the volcanically disturbed site at Offenthal by plants.

1) Initial phase

An initial recolonization phase is represented by PZ 0, composed of three samples from the lowermost part of the lacustrine succession. Except for single badly preserved pollen of Pinaceae (*Pityosporites* spp.), Cupressaceae (*Inaperturopollenites* spp.), Juglandaceae (*Plicatopollis* spp.), Eucommiaceae (*Tricolpo(ro)pollenites parmularius*) and a couple of fern spores, these samples are barren of palynomorphs.

Since these three samples originate from the base of the lacustrine succession which is lithologically characterized mainly by coarse-grained turbidites (LZ 3, Felder et al. 2001), it can be assumed that the sediments were deposited rapidly after the end of the eruption while a lake formed in the crater and material was sliding from the unstable crater slopes into the lake. During this phase the crater area was almost free of vegetation. However, rare but diverse fern spores such as *Ischyosporites tertiarius*, *Trilites* sp., *Leiotriletes* spp., and *Laevigatosporites* spp. probably indicate that initial colonization of the area by ferns already had started (Fig. 10a). Few pollen grains were transported into the lake by wind from the zonal vegetation surviving in the distance (Fig. 4.5.10a). This is especially supported by pinaceous pollen, which is wind dispersed and may be transported over longer distances. The deposition of wind-dispersed pollen such as those of Pinaceae or Cupressaceae may even be regarded as typical for the basal part of lacustrine successions in crater lakes (Rampino and Koeberl 2006). Rare evidence of pollen of Juglandaceae or Eucommiaceae can also be regarded as representing the distant (para)tropical forest (Boulter and Hubbard 1982; Harrington et al. 2004; Lenz et al. 2011).

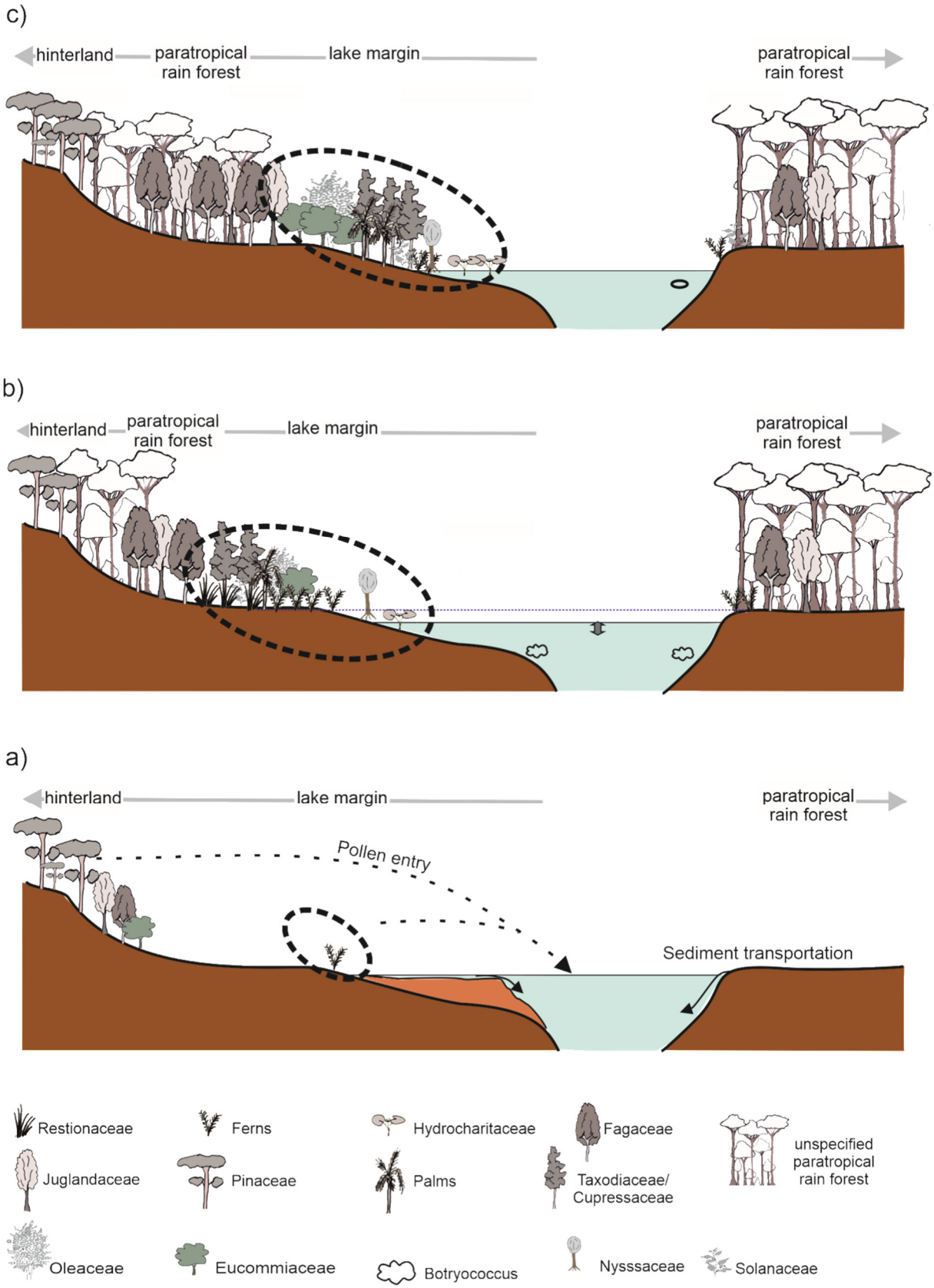

Fig. 4. 5. 10. Reconstruction of the palaeoenvironment in the lacustrine succession of the Offenthal maar lake. The lake basin model is based on Felder and Gaupp (2006).

PZs 1, 2 und 3a represent the recolonization phase, in which mainly pioneering plants colonized the crater area. Ferns like Schizaeaceae (*Leiotriletes* spp. *Trilites* spp.) and Polypodiaceae (*Laevigatosporites* spp.) in various combinations were important in the initial herbaceous communities of PZ 1 colonizing the crater walls and the shoreline (Fig. 4.5.10b). Due to a rapid dispersal of spores by wind and reproduction via gametophytes, ferns flourished at the beginning probably without competitors (Lenz et al. 2007). Accordingly, they have repeatedly been recorded today as early colonizers of volcanic sites in the tropics, such as the Krakatao (Richards 1996) or Motmot (Harrison et al. 2001). The well-known spike of fern-spores at the Cretaceous/Paleogene boundary is another example of initial recolonization of deeply devastated habitats by ferns (Tschudy et al. 1984, Fleming and Nichols, 1990).
Later during PZ 2 Restionaceae followed and invaded the herbaceous communities since their pollen (*Milfordia* spp.) is only found in this part of the lacustrine succession and disappeared finally in PZ 3b. On Krakatao and on crater walls of volcanoes on Papua New Guinea grasses followed the early fern communities on volcanic substrates (Taylor, 1957). However, since grasses were rare during the Eocene but pollen of Restionaceae is regularly present in Europe they may have occupied the role of today's grasses and were growing within the marginal vegetation at Messel and Offenthal (Lenz et al. 2007, this paper). Today they grow preferably in lowlands on wet and nutrient-poor soils and favor seasonally wet habitats that may dry out each year (Heywood 1993). Therefore, at Lake Offenthal relatively shallow habitats may have existed at the lake shore which were occasionally flooded during phases of a higher lake level (Fig. 4.5.10b). Furthermore, the relatively high values for Cupressaceae (*Inaperturopollenites* spp.) and Nyssaceae (*Nyssapollenites* spp., Fig. 4.5.9s) during the recolonization phase indicate that populations of *Nyssa* and *Taxodium* existed around the lake. The littoral zones in front of the swampy margin were colonized by sustaining floating and submersed aquatic plants such as Hydrocharitaceae (*Punctilongisulcites microechinatus*), which occur regularly in PZ 2 and the succeeding palynozones.
The high proportion of allochthonous pollen and spores derived from the regional vegetation such as pollen of Fagaceae (*Tricolpopollenites liblarensis*, *Tricolporopollenites cingulum*) as well as Juglandaceae (*Plicatopollis* spp.) already at the beginning of the recolonization phase is striking. This indicates that the surrounding forest was not affected to a greater distance by the phreatomagmatic explosion and maar formation at Offenthal. During the recolonization phase algae established within the lake. *Botryococcus* is regularly found and became temporarily frequent in PZ 2 (Fig. 4.5.5), but disappeared later in PZ 3. This shows that the distribution of *Botryococcus* is restricted to the holomictic lake phase. Formation of a stratified lake during the following recovery phase may have altered the water chemistry, as *Botryococcus* favors alkaline conditions (Wetzel 1983). Furthermore, *Botryococcus* prefers oligothrophic conditions (Jankovská and Komárek 2000), suggesting that nutrient supply to the lake was limited during PZ 2.

2) Recovery phase

PZs 3b, 4 and 5 represent the recovery phase (Fig. 4.5.10c). Palynomorphs from an initial pioneer vegetation decrease (ferns, e.g., *Trilites* spp.) or disappear completely (Restionaceae) (Fig. 4.5.5). Botanically, this reflects the change from a pioneering vegetation to a mixed forest successively invading the area around the crater. Therefore, elements of the (para)tropical rainforest increase significantly and dominate the pollen assemblages (Fig. 4.5.5), such as the pollen of Fagaceae (*Tricolporopollenites cingulum* and *Tricolpopollenites liblarensis*), Juglandaceae (*Plicatopollis spp.* and *Plicapollis spp.*) and Eucommiaceae (*Tricolpo(ro)pollenites parmularius*). Since all of these taxa have already been recorded in lower numbers in the samples from the previous recolonization phase a gradual colonization of the crater area by the thermophilic forest is documented. Some of the arboreal elements,

such as *Celtis* (Cannabaceae, Fig. 4.5.9d), are slightly decreasing in their abundance compared to the recolonization phase where they are even found in the earliest zones. This could indicate that some trees may have advanced into the crater area more quickly.
However, since some of the pioneering plants, such as some of the ferns, still persist in low numbers during the recovery phase, the transition to a complete reoccupation of the crater area by the forest vegetation with the total disappearance of the pioneer elements, as seen at Messel (Lenz et al. 2007) is not documented at Offenthal. A final climax state has therefore not been reached in the vegetation as recorded in the succession preserved at Offenthal.
Although most fern spores disappear throughout the recovery phase, some spores remain very abundant and show frequency maxima in PZs 3b and 4. This is especially true for *Leiotriletes* spp. which may have been derived from *Lygodium* (Schizaeaceae). They are known today as light-loving climbers (Tryon and Tryon 1982) and from volcanic terrains where they colonize open and disturbed habitats (Collinson 2002). Occasional collapse of minor sections of the crater wall or falling trees may have resulted in new open habitats which were then colonized by *Lygodium*-type ferns.
It is important that the change from the recolonization to the recovery phase coincides with the change from a holomitic to a seasonally stratified lake that is documented in the change in lithology between LZs 4 and 5 (Fig. 4.5.3). This indicates that a denese vegetation with deeply rooting trees led to a stabilization of the crater walls. As a consequence sediment input decreased to a minimum and mixing of the water body in the lake due to slope failure ceased. Therefore, the main influencing factor for the composition of the vegetation as well as the depositional conditions in the maar lake, which is represented by axis 1 of the NMDS (Fig. 4.5.7), has been the stability of the crater walls. Correspondingly, the pioneer elements and samples of the holomictic lake phase are plotted on the right side of the NMDS plot separate from elements of the rainforest and samples from the period with a stratified lake on the left side of the NMDS plot.
Among the algal flora in the lake the disappearance of *Botryococcus* and the regular occurrence of Zygnemataceae of the *Spirogyra*-type as recorded by their cysts (*Ovoidites* sp.) are noteworthy. Since Zygnemataceae prefer shallow and stagnant water (Colbath 1996, van Geel 2002), this can probably also be explained by the stabilization of the crater slopes and the formation of an at least temporarily stratified lake with low turbidity and a shallow shoreline.

Comparison of the maar lakes at Offenthal and Messel
Compared to the nearby maar lake of Messel the maar lake at Offenthal has only a third of the diameter and size (Felder et al. 2001). Therefore, the thickness of the lacustrine filling at Messel is by a factor of 8 higher than in Offenthal. Nevertheless, Lake Offenthal and Lake Messel are generally characterized by a similar succession of lithological units starting with volcanic material (Fig. 4.5.2) providing proof that the respective lake sediments have been deposited within maar structures which were formed by one or more phreatomagmatic eruption(s) (Felder et al. 2001, Liebig 2001, Felder and Harms 2004).
At Messel 230 m of lacustrine sediments have been cored (Felder and Harms 2004) while there are only 29 m in the core from Offenthal. The different thicknesses imply that a significant longer period of time is documented in the lacustrine filling at Messel.
In Messel the lower 90 m of the lacustrine maar filling are composed of clastic sediments (Lower Messel Formation), which represent the holomictic stage of the lake. In the upper part of the Lower Messel Formation, layers of oil-shale become more frequent and dominate above 139 m, reflecting the change from holomictic to meromictic conditions in the lake. In Offenthal, a similar sedimentary succession is found at the base of the lacustrine filling, albeit with a significantly lower thickness. Only in the lower 7 m of the lacustrine sequence (LZ 3), sands and silt, which are mostly graded, as well as turbidites dominate. The first layers of

bituminous shale appear at a depth of 22 m, which, as in Messel, indicate an increasing stability of the crater slopes with at least short meromictic phases.
The deposition of the classical "Messel Oil-shale" of the Middle Messel Formation started at a depth of 110 m in the core from Messel. This is a finely laminated, highly bituminous shale which was formed during the stable meromictic phase of the lake (Felder and Harms 2004) and resulted from annual algal blooms of the coccal green alga *Tetraedron minimum* (Irion 1977; Goth 1990; Lenz et al. 2010, 2015). The upper 14 m of the lacustrine succession at Offenthal also show some kind of a bituminous shale (LZ 5 and 6), which is often also finely laminated and appears similar to the Messel oil shale. However, *Tetraedron* has not been recovered by SEM studies of selected samples and an annual varve-like stratification cannot be proven in this portion of the Offenthal core. Interestingly, sponge spicules were frequently found in some of the Offenthal samples.
Accordingly, different depositional conditions can be assumed for both lakes, which is confirmed by the isotopic values of siderite (δ^{13}Carbon and δ^{18}Oxygen) from both lakes (Felder and Gaupp 2006). At Offenthal intermediate carbon isotopic values in combination with the oxygen isotopic signature may be regarded as typical for a holomictic lake with annual overturn (Felder and Gaupp 2006) (Fig. 4.5.2). The high values for δ^{18}O and for δ^{13}C at Messel with a comparatively wide range are typical for a meromictic lake with stagnant water at the bottom (Felder and Gaupp 2006).
In order to compare the vegetation around the maar lake of Offenthal with the almost coeval vegetation in the vicinity of the nearby maar lake at Messel, NMDS was carried out including the 68 samples from Offenthal and 598 samples from core Messel 2001 (Lenz and Wilde 2018).
In the ordination space of the NMDS, the samples from Messel are generally ordered from right to left reflecting the stratigraphical succession of different vegetational stages and indicating a gradual and continuous change in the composition of the vegetation (Fig. 4.5.11a). The oldest samples from Lake Messel from the Early Initial Lake Phase (EILP; Lenz et al. 2007) are plotted at the positive end of NMDS axis 1 mainly in the lower right corner of the ordination space (Fig. 4.5.11a). They are preferentially characterized by fern spores, which occur in high diversity in the EILP. Accordingly, trilete spores, such as *Cictricosisporites* spp., *Ischyosporites* sp. and *Punctatosporites* sp. as well as monolete spores, such as *Laevigatosporites* spp. and *Verrucatosporites* spp. are plotted at the positive end of NMDS axis 1 indicating that these spores reach their maximum values in samples from the EILP (Fig. 4.5.11b). The samples reflect the beginning of the recolonization of the devastated area around Lake Messel by a pioneer vegetation (Lenz et al. 2007, Lenz and Wilde 2018). In samples from the Late Initial Lake Phase (LILP; Lenz et al. 2007), which are mainly plotted in the center of the ordination space (Fig. 4.5.11a), the spores decrease significantly in frequency. Characteristic elements that reach their abundance maximum in the LILP at Messel are, for example, Restionaceae (*Milfordia* sp.), Juglandaceae (*Carya*), Cannabaceae (*Celtis*), Ulmaceae and Myricaceae (Fig. 4.5.11b). The pioneer vegetation almost completely disappeared at the end of the LILP and was replaced by a mixed forest indicating the termination of recolonization around the maar lake at Messel (Lenz et al. 2007, Lenz and Wilde 2018). Samples from the succeeding Middle Messel Formation (MMF) are plotted (Fig. 4.5.11a) to the left, negative side of NMDS axis 1 with a gradual change from the base to the top (Lenz et al. 2011, Lenz and Wilde 2018) (Fig. 4.5.11a). Furthermore, a general separation of samples from the MMF along NMDS axis 2 is obvious (Fig. 4.5.11a). The MMF is characterized by the dominance of pollen of the juglandaceous alliance (*Plicatopollis* spp., *Platycaryapollenites* spp., *Plicapollis pseudoexcelsus*, *Pterocaryapollenites* sp., *Momipites* spp.) as well as of fagaceous pollen (*Tricolporopollenites cingulum, Tricolpopollenites liblarensis*), which are all plotted on the negative side of NMDS axis 1 (Fig. 4.5.11b). These elements represent a thermophilic climax vegetation at Messel,

which is typical for inland sites of western and central Europe during the middle Eocene greenhouse climate (Mai 1981, 1995; Schaarschmidt 1988; Wilde 1989; Collinson et al. 2012).

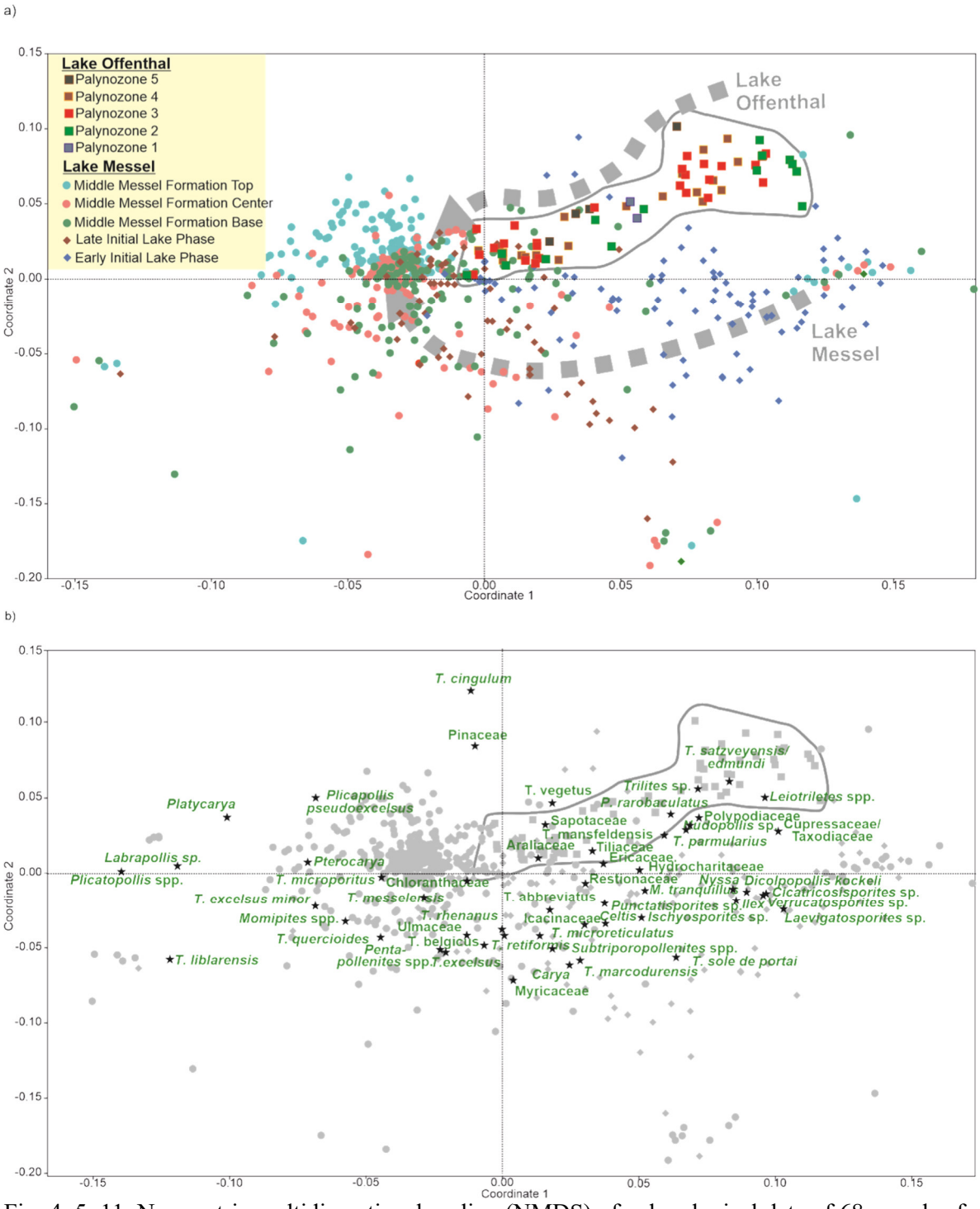

Fig. 4. 5. 11. Non-metric multidimentional scaling (NMDS) of palynological data of 68 samples from the lacustrine succession of the Offenthal maar lake and 598 samples from the lacustrine succession of the Messel maar lake using the Bray-Curtis dissimilarity and the Wisconsin double standardized raw data values. **a** Scatter plot of the first two axes showing the arrangement of samples. The different symbols represent samples from the different palynozones at Offenthal and phases at Messel (see Lenz and Wilde 2018); **b** Scatter plot of the first two axes showing the arrangement of taxa. The dots represent the different samples (see a).

The continuous gradual compositional changes within the vegetation communities at Messel during the recolonization of the crater area and the establishment of a climax vegetation are comparable to the vegetational changes at Lake Offenthal. Therefore, the evolution of the vegetation at Lake Messel can be assigned to similar vegetational phases. The *recolonization phase* is characterized by a herbaceous and shrubby pioneer vegetation represented by the EILP of the Lower Messel Formation (Lenz et al. 2007). The *recovery phase* during the LILP is marked by the reoccupation of the crater area by a mixed tropical rainforest and within the lake by a change from holomictic to meromictic conditions (Lenz et al. 2007). However, the forest of the *recovery phase* differs in composition and diversity from the climax vegetation which is established later in the *climax phase* during the subsequent Middle Messel Formation (Lenz and Wilde 2018).

The NMDS reveals that palynomorph assemblages from Offenthal are slightly different compared to the assemblages of the *recolonization phase* at Messel (Figs. 4.5.11, 4.5.12), because the samples are separated from the samples of the EILP in the upper right corner of the NMDS plot. This indicates that the composition of the pioneer vegetation was slightly different during the recolonization of the crater areas at Offenthal and Messel. However, differences mainly correspond to the composition of the fern communities. At Offenthal, fern spores of the Schizaeaceae, such as *Trilites* spp. or *Leiotriletes* spp. are more abundant than spores of the Polypodiaceae, such as *Laevigatosporites* spp, *Verrucatosporites* spp., which are common in the EILP at Messel (Lenz et al. 2007). Another spore of the Schiazeazeae (*Cicatricosisporites* spp.) occurs frequently during the EILP at Messel but is completely absent at Offenthal. However, other elements of the *recolonization phase* such as Restionaceae (*Milfordia* spp.) are important elements at both sites. Also, general vegetational trends, such as the establishment of a *Nyssa/Taxodium* community relatively early at the beginning of the *recolonization phase* are seen at Offenthal and Messel.

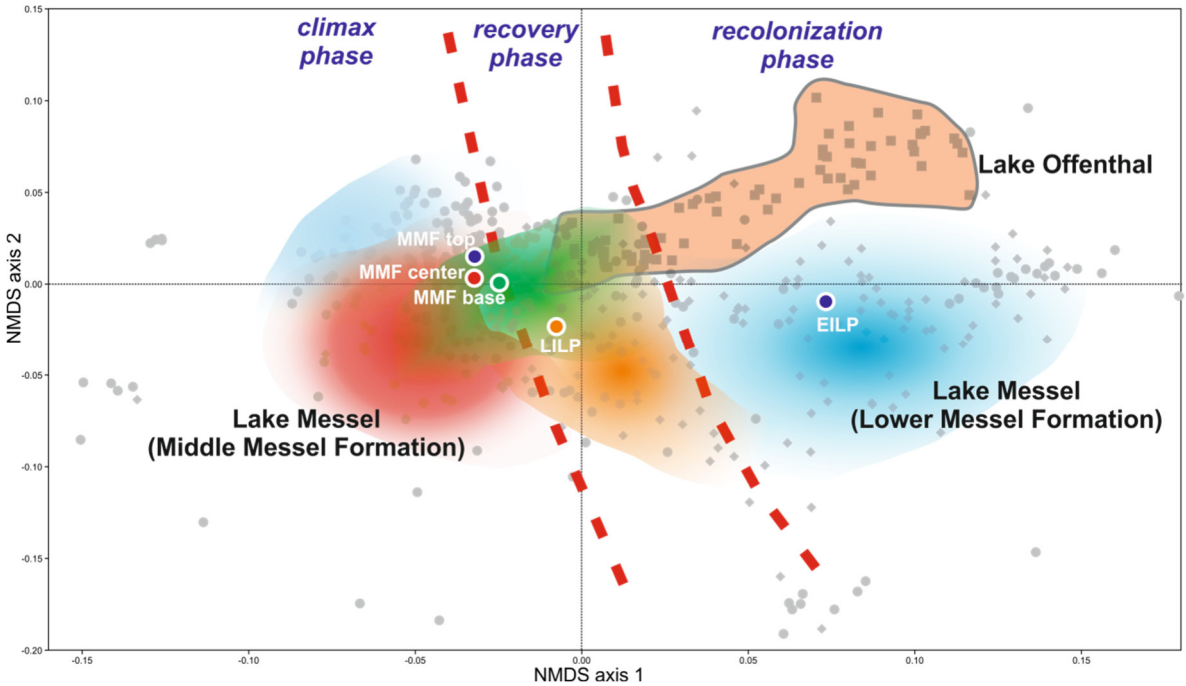

Fig. 4. 5. 12. Non-metric multidimensional scaling (NMDS) of palynological data of 68 samples from the lacustrine succession of the Offenthal maar lake and 598 samples from the lacustrine succession of the Messel maar lake showing the different vegetational phases during the recolonization of the volcanically disturbed sites. The colored dots indicate the median NMDS scores of the different vegetation phases at Messel (see Lenz and Wilde 2018).

Therefore, the recolonization of the devastated areas at both sites follows a similar pattern with palynological assemblages that reflect typical vegetation communities for the recolonization of Eocene maar lakes. This is supported by similar general trends which are today found in the recolonization of volcanically disturbed sites, e.g. the Krakatao (Richards 1996). Slight differences between Offenthal and Messel, for example in the composition of the fern communities, are probably related to local factors.
Most samples from the *recovery phase* at Offenthal are plotted in the NMDS with samples from the *recovery phase* at Messel (LILP) together in the center of the ordination space (Fig. 4.5.12) indicating that the forests, which reoccupied the crater areas of both maar lakes, had a similar composition. However, this is not surprising, as both lakes are almost coeval and located relatively close to each other on the Sprendlinger Horst (Fig. 4.5.1) which was most probably covered by a uniform zonal vegetation.
A fundamental difference between the successions at Offenthal and Messel becomes obvious in the NMDS by the fact that the samples from the Middle Messel Formation (MMF) are plotted on the left side of the ordination space clearly separate from all of the Offenthal samples on the right side (Fig. 4.5.12). During the MMF, at Messel, a robust climax vegetation existed for several hundred thousand years which was characterized by pollen assemblages without significant qualitative changes (Lenz et al., 2011, Lenz and Wilde 2018). Only quantitative changes in the dominance of individual pollen species occurred. Such a vegetation, which can be attributed to a *climax phase* and which follows the *recovery phase* in a natural vegetational succession by absence of further disturbance of the crater area, is not documented at Offenthal. The climax vegetation at Messel is dominated especially by fagaceous (*Tricolporopollenites cingulum, Tricolpopollenites liblarensis*) and juglandaceous (e.g,. *Plicatopollis* spp., *Plicapollis* spp.) plants (Lenz et al., 2011, Lenz and Wilde 2918). Although these pollen taxa are also very common in Offenthal, they are not as dominant as in Messel indicating that the final climax phase is not reached in the succession at Offenthal.
At Offenthal the maar lake was much smaller and thus the thickness of the sedimentary filling of the lake basin by a factor of 8 lower than at Messel. Therefore, probably a much shorter time interval is documented at Offenthal. Based on calculations of the sedimentation rate, it can be assumed that a time interval of 800 to 900 ka is documented at Messel by the lacustrine succession of the Lower and Middle Messel Formation including a deposition time of *c.* 640 ka for the MMF (Lenz et al. 2015). Due to the lack of an annual signature in the oil shale, a calculation of the time of deposition is impossible at Offenthal. Nevertheless, it can be assumed that a significantly shorter time was needed for the complete filling of the small lake basin, especially since the clastic sequences of LZs 3 and 4 with many turbidites were probably deposited in a very short time of a few hundred years. A *climax phase* such as the one at Messel is not documented at Offenthal, most probably since the succession is cut off by a Quarternary cover.

Conclusion

The nearly coeval phreatomagmatic eruptions at Offenthal and Messel on the Sprendlinger Horst in Southwestern Germany not only led to the formation of maar crater structures but also to destruction and disturbance of the Lower to Middle Eocene paratropical vegetation around. Based on the comparison of palynological assemblages as preserved in the maar lake sediments from cores at both localities similar processes during the recolonization of the volcanically disturbed sites can now be recognized.
During an *initial phase*, which is distinguished at Offenthal pollen of the zonal vegetation was transported only in small amounts from the distance into the crater lake. Wind-dispersed pollen of the Pinaceae or Cupressaceae and extremely rare grains of other elements from the forest, which survived in the distance, point to the composition of the vegetation prior to the eruption(s). In the succeeding *recolonization phase*, which is preserved at Offenthal and

Messel, plants can be attributed to a pioneering succession. The pioneering flora invaded the disturbed areas around the maar lakes in successional stages. Ferns flourished at the beginning without competitors and were followed by Restionaceae, both forming a herbaceous cover. Woody swamp elements such as *Nyssa* and *Taxodium* early established at the margin of the lakes. With increased stability of the slopes, the zonal vegetation reestablished around the lakes and within the crater area during the *recovery phase*. In both lakes, the increasing stability of the slopes is reflected sedimentologically by decreasing input of sediment causing the change from holomictic to meromictic conditions at Messel or at least to a seasonally stratified lake at Offenthal. In both lakes this change is characterized by the first appearance of laminated oil shale. The succeeding *climax phase* which is only preserved in the Middle Messel Formation at Messel is characterized by a robust climax vegetation without further fundamental changes in the vegetation.

The recolonization of different habitats such as the lake margin, the slopes of the crater wall and the disturbed areas around the lake reveals a similar pattern of distinct vegetational phases obviously representing the chronological succession of various plant communities at Messel and Offenthal. Therefore, both records can be regarded as textbook examples for the recolonization of volcanically disturbed areas during the Paleogene greenhouse period of Central Europe.

Acknowledgement and Funding

Our study has been carried out as a project funded by the Deutscher Akademischer Austauschdienst (DAAD) under the grant 110207-54900347 including the PhD appointment of the first author. The help of Karin Schmidt, Palaeobotanical Section, Senckenberg Research Institute and Natural History Museum Frankfurt, in sampling and sample preparation is acknowledged. We also acknowledged the Department for Messel Research and Mammalogy, Senckenberg Research Institute and Natural History Museum Frankfurt for supplying the core photographs of FIS/HLUG from the core B/98-BK 1E. Finally, we thank two reviewers, Dr. Torsten Utescher and Dr. Steven R. Manchester, for their comments and suggestions which greatly helped to improve this paper.

Disclosure of potential Conflict of interest

The authors declare that they have no conflict of interest.

References

Bray, J.R., Curtis, J.T. (1957). An ordination of the upland forest communities of southern Wisconsin. *Ecological Monographs*, 27, 325-349.

Broothaerts, N., Verstraeten, G., Kasse, C., Bohncke, S., Notebaert, B., and Vandenberghe, J. (2014). Reconstruction and semi-quantification of human impact in the Dijle catchment, central Belgium: a palynological and statistical approach. *Quaternary Science Reviews*, 102, 96-110.

Boulter, M. C., and Hubbard, R. N. (1982). Objective paleoecological and biostratigraphic interpretation of Tertiary palynological data by multivariate statistical analysis. *Palynology*, *6(1)*, 55-68.

Cohen, K.M., Finney, S.C., Gibbard, P.L., Fan, J.X. (2013). *The ICS international chronostratigraphic chart*, Episodes 36, 199–204.

Colbath, G. K. (1996). Chapter 7. Green and Blue-Green Algae. Introduction. *Palynology: Principles and applications*, American Association of Stratigraphic Palynologists Foundation, 1, 171-172.

Collinson , M.E. (2002). The Ecology of Cainozoic ferns. *Review of Palaeobotany and Palynology*, 119, 51-68.

Collinson, M.E., Smith, S.Y., Manchester, S.R., Wilde, V., Howard, L.E., Robson, B.E., Ford, D.S., Marone, F., Fife, J.L., Stampanoni, M. (2012). The value of X-ray approaches in the study of the Messel fruit and seed flora. *Palaeobiodiversity and Palaeoenvironments*, 92(4), 403-416.

Cottam, G., Goff, F.G., Whittaker, R.H. (1978). Wisconsin Comparative Ordination, in Whittaker RH, ed., Ordination of Plant Communities. Handbook of Vegetation Science, *5-2*, 185-213.
Felder, M., Harms, F.J. (2004). Lithologie und genetische Interpretation der vulkano-sedimentären Ablagerungen aus der Grube Messel anhand der Forschungsbohrung Messel 2001 und weiterer Bohrungen. *Courier Forschungsinstitut Senckenberg*, 252, p 151-203.
Felder, M., Gaupp, R. (2006). The δ13C and δ18O signatures of siderite – a tool to discriminate mixis patterns in ancient lakes. *Zeitschrift der Deutschen Gesellschaft für Geowissenschaften*, 157, 397-410.
Felder, M., Harms, F.J. and Liebig, V. (2001). Lithologische Beschreibung der Forschungsbohrungen Groβ-Zimmern, Prinz von Hessen und Offenthal sowie zweier Lagerstättenbohrungen be Eppertshausen (Sprendlinger Horst, Eozän, Messel-Formation, Süd-Hessen). *Geologische Jahrbuch Hessen*, 128, 29–82.
Fleming, R.F., Nichols, D.J., 1990. The fern-spore abundance anomaly at the Cretaceous–Tertiary boundary: a regional bioevent in western North America. In: Kauffman, E.G.,Walliser, O.H. (Eds.), Extinction events in Earth history. Lecture Notes in Earth Sciences, vol. 30. Springer, New York, pp. 351–364.
Gauch, H.G., Scruggs, W.M. (1979). Variants of polar ordination. *Vegetation*, 40, 147-153.
Ghilardi, B., and O'connell, M. (2013). Fine resolution pollen analytical study of Holocene woodland dynamics and land use in north Sligo, Ireland. *Boreas*, 42(3), 623-649.
Goth, K. (1990). Der Messeler Ölschiefer- ein Algenlaminit. *Couierr Forschungsinstitut Senckenberg*, 131, 1-143.
Gruber, G., and Micklich, N. (2007) Messel—Treasures of the Eocene. Darmstadt: Hessisches Landesmuseum p 158.
Hammer, Ø., Harper, D.A.T., Ryan, P.D. (2001). PAST: paleontological statistics software package for education and data analysis. *Palaeontologia Electronica*, 4(1), https://palaeo-electronica.org/2001_1/past/issue1_01.htm
Hammer, O., Harper, D. A. T., and Ryan, P. D. (2006). *Paleontological statistics*, version 1.57.
Harms, F.J., Aderhold, G., Hoffmann, I., Nix, T., Rosenberg, F. (1999). Erläuterungen zur Grube Messel bei Darmstadt, Südhessen. *Schriftenreihe der Deutschen Geologischen Gesellschaft*, 8, 181-222.
Harrington, G., Kemp, S., and Koch, P. (2004). Palaeocene–Eocene paratropical floral change in North America: responses to climate change and plant immigration. *Journal of the Geological Society*, 161(2), 173-184.
Harrison, R.D., Banka, R., Thornton, I.W.B., Shanahan, M., Yamuna, R., (2001). Colonization of an island volcano, Long Island, Papua New Guinea, and an emergent island, Motmot, in its caldera lake.II. The vascular Flora. *Journal of Biogeography*, 28, 1311–1337.
Heywood, V.H., (1993). *Flowering plants of the world. Updated edition*. Oxford University Press, New York.
Irion, G. (1977). Der eozäne See von Messel. *Natur Museum*, 107, 213-218.
Jacoby, W. (1997). Tektonik und Eozäner Vulkanismus des Sprendlinger Horstes, NE-Flanke des Oberrheingrabens. *Schriftenreihe dt. Geol*, 2, 66–67.
Jacoby, W., Wallner, H., Smilde, P. (2000). Tektonik und Vulkanismus entlang der Messeler-Sto¨ rungszone auf dem Sprendlinger Horst: geophysikalische Ergebnisse. *Zeitschrift der Deutschen Gesellschaft für Geowissenschaften*, 151–154, 493–510.
Jankovská, V., Komárek, J. (2000). Indicative value of *Pediastrum* and other coccal green algae in palaeoecology. *Folia Geobotanica*, 35, 59-82.
Janssen, C.R., Birks, H.J.B. (1994). Recurrent groups of pollen types in time. *Review of Palaeobotany and Palynology*, 82, 165–173.
Jardine, P. E., and Harrington, G. J. (2008). The Red Hills Mine palynoflora: A diverse swamp assemblage from the Late Paleocene of Mississippi, *USA. Palynology*, *32(1)*, 183-204.
Juggins, S. (2007). *C2 Software for ecological and palaeoecological data analysis and visualization.* User guide Version 1.5, p 73.
Kaiser, M.L., Ashraf, R. (1974). Gewinnung und Präparation fossiler Pollen und Sporen sowie anderer Palynomorphae unter besonderer Berücksichtigung der Siebmethode. *Geologisches Jahrbuch*, 25, 85–114.

Krumbiegel, G., Rüffle, L. and Haubold, H. (1983). *Das eozäne Geiseltal, ein mitteleuropäisches Braunkohlevorkommen und seine Pflanzen- und Tierwelt*. Neue Brehm-Bücherei, 273, A. Ziemsen, Wittenberg.

Kruskal, J.B. (1964). Nonmetric multidimensional scaling: a numerical method. *Psychometrika*, 29, 115-129.

Kuiper, K.F., Deino, A., Hilgen, F.J., Krijgsman, W., Renne, P.R., Wijbrans, J.R. (2008). Synchronizing rock clocks of Earth history. *Science*, 320, 500–504

Lenz, O.K. (2005). Palynologie und Paläoökologie eines Küstenmoores aus dem Mittleren Eozän Mitteleuropas Die Wulfersdorfer Flözgruppe aus dem Tagebau Helmstedt, Niedersachsen. *Palaeontographica B*, 271, 1–157.

Lenz, O.K., Wilde, V., Riegel, W. (2007). Recolonization of a Middle Eocene volcanic site: quantitative palynology of the initial phase of the maar lake of Messel (Germany). *Review of Palaeobotany and Palynology*, 145, 217–242.

Lenz, O.K., Wilde, V., Riegel, W., Harms, F.J. (2010). A 600 k.y.record of El Niño-Southern Oscillation (ENSO): Evidence for persisting teleconnections during the Middle Eocene greenhouse of Central Europe. *Geology*, 38(7), 627-630.

Lenz, O. K., V. Wilde, and W. Riegel (2011). Short-term fluctuations in vegetation and phytoplankton during the Middle Eocene greenhouse climate: a 640-kyr record from the Messel oil shale (Germany). *International Journal of Earth Sciences*, 100, 1851–1874.

Lenz, O.K., Wilde, V., Mertz, D.F., Riegel, W. (2015). New palynology-based astronomical and revised 40Ar/39Ar ages for the Eocene maar lake of Messel (Germany). *International Journal of Earth Science*, 104, 873-889.

Lenz, O.K., Wilde, V., Riegel, W. (2017). ENSO- and solar-driven sub-Milankovitch cyclicity in the Palaeogene greenhouse world; high-resolution pollen records from Eocene Lake Messel, Germany. *Journal of the Geological Society*, 174, 110-128.

Lenz, O. K., and Wilde, V. (2018). Changes in Eocene plant diversity and composition of vegetation: the lacustrine archive of Messel (Germany). *Paleobiology*, 44(4), 709-735.

Liebig, V. (2001). Neuaufnahme der Forschungsbohrungen KB 1, 2, 4 und 7 von 1980 aus der Grube Messel (Sprendlinger Horst, Südhessen). *Kaupia*, 11, 3–68.

Lutz, H., Kaulfuss, U., Wappler, T., Löhnertz, W., Wilde, V., Mertz, D.F., Mingram, J.F., Franzen, J.L., Frankenhäuser, H. and Kozil, M. (2010). Eckfeld Maar: Window into an Eocene terrestrial habitat in Central Europe. *Acta Geologica Sinica*, 84, 984-1009.

Mai, D.H. (1981). Entwicklung und klimatische Differenzierung der Laubwaldflora Mitteleuropas im Tertiär. *Flora*, 171, 525–582.

Mai, D.H. (1995). *Tertiäre Vegetationsgeschichte Europas—Methoden und Ergebnisse*, Gustav Fischer Verlag, Jena, p 691.

Mander, L., Kürschner, W.M., McElwain, J.C. (2010). An explanation for conflicting records of Triassic–Jurassic plant diversity. *Proceedings of the National Academy of Sciences of the United States of America*, 107, 15351–15356.

Mertz, D.F., and Renne, P.R. (2005). A numerical age for the Messel fossil deposit (UNESCO World Heritage Site) derived from 40Ar/39Ar dating on a basaltic rock fragment. *Courier Forschungsinstitut Senckenberg*, 255, 67-75.

Minchin, P.R. (1987). An evaluation of the relative robustness of techniques for ecological ordination. *Vegetation*, 69, 89-107.

Moshayedi, M., Lenz, O.K., Wilde, V., Hinderer, M. (2018). Controls on sedimentation and vegetation in an Eocene pull-apart basin (Prinz von Hessen, Germany): evidence from palynology. *Journal of the Geological Society*, 175, 757-773.

Nickel, B. (1996). Die mitteleozäne Mikroflora von Eckfeld bei Manderscheid/Eifel. *Mainzer Naturwissenschaftliches Archiv. Beiheft*, 18, 1–121.

Oksanen, J. (2007). Standardization methods for community ecology. Documentation and user guide for package Vegan, 1.8-6.

Oswald, W., Faison, E.K., Foster, D.R., Doughty, E.D., Hall, R.R. and Hansen, B.C.S. (2007). Post-glacial changes in spatial patterns of vegetation across southern New England. *Journal of Biogeography*, 34, 900-913.

Rampino, M.R., Koeberl, C. (2006). Comparison of Bosumtwi Impact Crater (Ghana) and Crater Lake Volcanic Caldera (Oregon, USA): Implications for Biotic Recovery after Catastrophic Events. *In*:

Cockell C., Gilmour I., Koeberl C. (eds) Biological Processes Associated with Impact Events. Impact Studies. Springer, Berlin, Heidelberg.
Renne, P.R., Balco, G., Ludwig, K.R., Mundil, R., Min, K.W. et al. (2011). Response to the comment by W.H. Schwarz, on "Joint determination of 40 K decay constants and 40Ar*/40 K for the Fish Canyon sanidine standard, and improved accuracy for 40Ar/39Ar chronology" by PR Renne et al. (2010). *Geochim Cosmochim Acta,* 75, 5097–5100
Richards, P.W., 1996. The tropical rain forest; an ecological study, 2nd ed. Cambridge Univ. Press, Cambridge.
Riegel, W., Lenz, O.K. and Wilde, V. (2015). From open estuary to meandering river in a greenhouse world: an ecological case study from Middle Eocene of Helmstedt, Northen Germany. *Palaios*, 30, 304-326.
Riegel, W. and Wilde, V. (2016). An early Eocene Sphagnum bog at Schöningen, northern Germany. *International Journal of Coal Geology*, 159, 57-70.
Sabel, M., Bechtel, A., Püttmann, W., Hoernes, S. (2005). Palaeoenvironment of the Eocene Eckfeld Maar lake (Germany): implication from geochemical analysis of the oil shale sequence. *Organic Geochemistry*, 36, 873-891.
Schaarschmidt, F. (1988). *Der Wald, fossile Pflanzen als Zeugen eines warmen Klimas*, *In*: Schaal, S. and Ziegler, W. (eds) Messel - ein Schaufenster in die Geschichte der Erde und des Lebens. Waldemar Kramer, Frankfurt am Main, p 27-52.
Shepard, R.N. (1962a). Analysis of proximities: Multidimensional scaling with an unknown distance function. I. *Psychometrica*, 27, 125–140.
Shepard, R.N. (1962b). Analysis of proximities: Multidimensional scaling with an unknown distance function. II. *Psychometrica*, 27, 219–246.
Smith, K.T., Schaal, S.F.K., Habersetzer, J. (2018): Messel – An Ancient Greenhouse Ecosystem. Senckenberg-Buch 80, E. Schweizerbart'sche Verlagsbuchhandlung, Stuttgart.
Taylor, B.W., 1957. Plant succession on recent volcanoes in Papua. *Journal of Ecology*, *45*, 233–243.
ter Braak, C. J. F. (1995). *Ordination. In Data analysis in community and landscape ecology*, 91-274. Cambridge University Press.
ter Braak, C.J.F. and Looman, C.W.N. (1995). Regression. In: Jongman, R.H.G., Ter Braak, C.J.F. and Tongeren, O.F.R. (eds). *Data Analysis in Community and Landscape Ecology*. Cambridge University Press, Cambridge, 29–77.
Thiele-Pfeiffer, H. (1988). Die Mikroflora aus dem mitteleozänen Ölschiefer von Messel bei Darmstadt. *Palaeontographica B*, 211, 1–86.
Thomson, P.W., Pflug, H. (1953). Pollen und Sporen des mitteleuropäischen Tertiärs. Gesamtübersicht über die stratigraphisch und paläontologisch wichtigen Formen. *Palaeontographica B*, 94, 1–138.
Tryon, R.M., Tryon, A.F. (1982). *Ferns and allied plants with special reference to tropical America*. Springer-Verlag, New York, Heidelberg, Berlin.
Tschudy, R.H., Pillmore, C.L., Orth, C.J., Gilmore, J.S., Knight, J.D. (1984). Disruption of the terrestrial plant ecosystem at the Cretaceous–Tertiary boundary, Western Interior. *Science*, 225, 1030–1032.
Van Geel, B. (2002). *Non-pollen palynomorphs. In Tracking environmental change using lake sediments*, pp. *99*-119, Springer, Dordrecht.
Van Tongeren, O. F. (1995). Data analysis or simulation model: a critical evaluation of some methods. *Ecological modelling*, 78(1-2), 51-60.
Wilde, V. (1989). Untersuchungen zur Systematik der Blattreste aus dem Mitteleozän der Grube Messel bei Darmstadt (Hessen, Bundesrepublik Deutschland). *Courier Forschungsinstitut Senckenberg*, 115, 1–123.

4-6 Publication 2: Controls on sedimentation and vegetation in an Eocene pull-apart basin (Prinz von Hessen, Germany): evidence from palynology

Published in Journal of the Geological Society London 175, 757-773 (2018).
https://doi.org/10.1144/jgs2017-128

Maryam Moshayedi[1*], Olaf K. Lenz[1, 2], Volker Wilde[3], Matthias Hinderer[1]
[1]Technische Universität Darmstadt, Institute of Applied Geosciences, Applied Sedimentology, Schnittspahnstrasse 9, 64287 Darmstadt, Germany.
[2]Senckenberg Gesellschaft für Naturforschung, General Directorate, Senckenberganlage 25, 60325, Frankfurt am Main, Germany.
[3]Senckenberg Forschungsinstitut und Naturmuseum, Sektion Paläobotanik, Senckenberganlage 25, 60325, Frankfurt am Main, Germany.

Author Contributions

Conceptualization: M. Moshayedi, Olaf K. Lenz, Volker Wilde, M. Hinderer
Data Curation: M.Moshayedi
Formal Analysis: M. Moshayedi
Funding Acquisition: M. Moshayedi
Investigation: M. Moshayedi,
Methodology: M. Moshayedi, Olaf K. Lenz, Volker Wilde
Project Administration: Olaf K. Lenz, Volker Wilde, M. Hinderer
Resources: M. Hinderer, V. Wilde
Validation: M. Moshayedi
Visualization: M. Moshayedi
Writing – Original Draft Preparation: M. Moshayedi
Writing – Review and Editing: Olaf K. Lenz, V. Wilde

Abstract
Tectonically controlled lakes may experience a complex history of deposition and subsidence which can influence their ecology and environment. To correlate controls on sedimentation with changes in vegetation within a small pull-apart basin at "Grube Prinz von Hessen" (Hessen, Germany) during Paleogene greenhouse conditions, 47 core samples were analysed palynologically. The Lower Eocene succession includes 34 m of clastic sediments overlain by 54 m of massive mudstone, finely laminated bituminous claystone and lignite. A fluvial-lacustrine and a profundal (deep lake) facies association are distinguished. Statistical analysis of the diverse and well-preserved palynoflora reveals 5 distinct associations. Throughout the sedimentary record there is a strong correlation between major changes in vegetation and lithology which were controlled mainly by changes in humidity together with tectonic activity which led to lake basin subsidence and a rise in lake level. Based on the association of pollen and spores which are typical for the Lower Eocene, it can be shown that the basin is older than previously assumed.

Supplementary material: A complete list of variables and palynomorphs used for pollen diagrams and statistical analyses, as well as their abundance percentages is available at https://doi.org/10.6084/m9.figshare.c.4108016

Key words: Palynomorphs, Central Europe, Lacustrine sediments, Tectonic activity, Humidity changes, Palaeoenvironment

Reconstructions of Eocene terrestrial ecosystems are abundant, because they allow a valuable insight into a greenhouse world where modern-type faunas and floras already existed. Some of the best-known examples have been described from the Middle Eocene of Germany, including Messel (Schaal and Ziegler 1988; Gruber and Micklich, 2007), the Geiseltal (Krumbiegel et al. 1983), Eckfeld (Lutz et al. 2010) and Helmstedt (Riegel et al. 2015). These records represent small isolated inland sites, most of them with vertebrate and invertebrate faunas of a unique preservation. Therefore, ecosystem reconstructions from such assemblages tend to be based mainly on faunal evidence and some plant megafossils, but the potential of palynological studies has rarely been employed (Riegel et al. 2015).
The present case study of lacustrine sediments from the former Lake Prinz von Hessen (PvH) introduces not only a new Eocene archive from Germany, but furthermore provides a rare insight into a basin that was influenced by tectonic activity and therefore experienced a complex history of deposition and subsidence. The detailed palynological analysis from a tropical mid-latitude lowland site therefore allows to assess temporal changes within the vegetation that have taken place in such an environment.
A number of small, isolated basins containing lacustrine sediments of Paleogene age are known from the Sprendlinger Horst, which consists of a Palaeozoic metamorphic and magmatic basement with a Rotliegend (Lower Permian) sediment cover (Marell 1989) and which flanks as the northern extension of the Odenwald basement the Upper Rhine Graben to the northeast in Southwest Germany (Fig. 4.6.1). Most of these structures are maar craters resulting from hydro-volcanic activity (Jacoby 1997; Harms et al. 1999; Jacoby et al. 2000; Felder et al. 2001; Felder and Harms 2004), particularly the maar lake of Messel, well-known for the perfect preservation of fossils and the focus of numerous studies. The undisturbed deposition of annually laminated sediments at Messel over a period of 640 ka during the Paleogene allowed studies on the evolution of palaeoenvironment and vegetation at an unprecedented resolution (e.g., Thiele-Pfeiffer 1988; Lenz et al. 2007, 2011, 2015, 2017). It was possible to prove the sensitivity of Paleogene vegetation to climate variations in relation to orbital and sub-orbital cyclicity, shedding new light on the interactions between

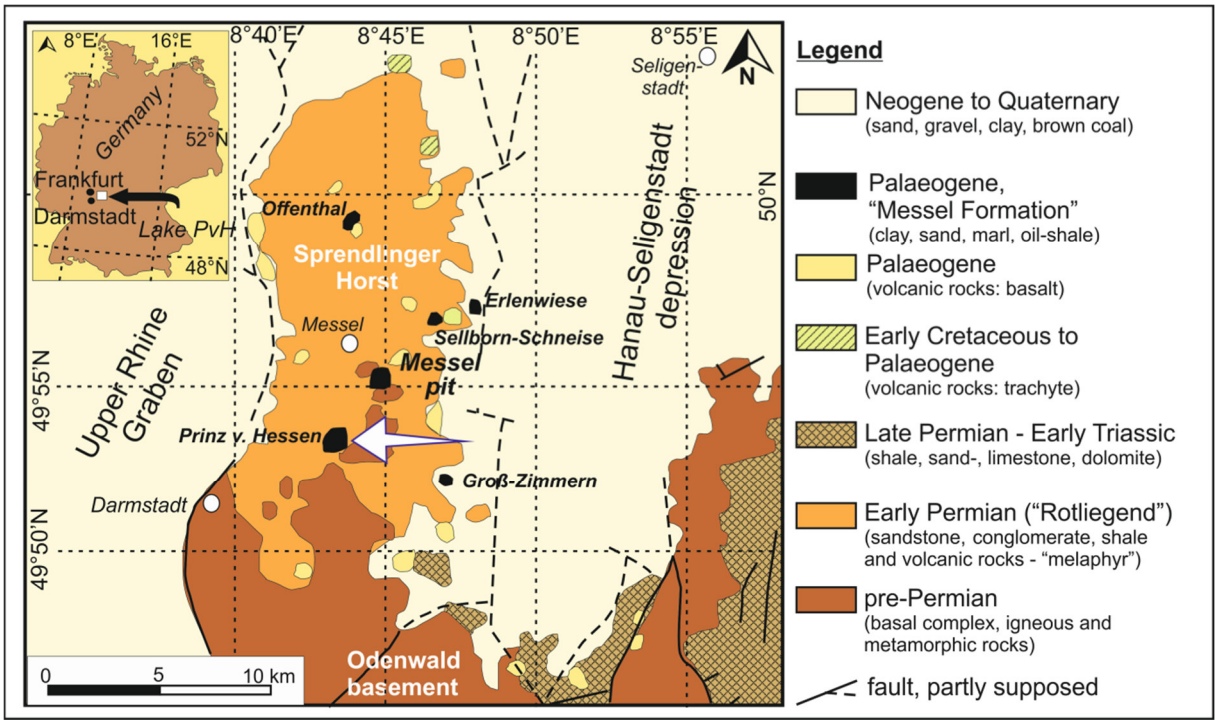

Fig. 4. 6. 1. Geological map of the Sprendlinger Horst (Southwest Germany) showing the location of Eocene Lake Prinz von Hessen and other sites of Palaeogene age in the area (modified after Lenz et al. 2007; Harms et al. 1999).

paratropical greenhouse vegetation and short-term climate variability (Lenz et al. 2011, 2017). Little is known however, regarding the Paleogene vegetation around the structure at the historic opencast mine "Grube Prinz von Hessen" (PvH) 5 km northeast of Darmstadt (Hessen, Germany) and 2 km southwest of the maar structure of Messel (Fig. 4.6.1). In contrast to the other structures of phreatomagmatic origin which contained deep meromictic lakes, PvH may have been a more shallow pull-apart-structure (Felder and Gaupp 2006). Our study is designed to unveil both long- and short-term changes in vegetation over the entire time of deposition of the lacustrine sediments at PvH, and link the vegetation record to the changing environments of deposition. It aims to show whether factors other than climate, such as tectonic activity, influenced the distribution of the vegetation around Lake PvH. Additionally, we demonstrate that environment reconstructions can be highly resolved on the basis of sedimentology and palynology alone even in the absence of faunal evidence.

Geological situation

Geophysical data and evidence from cores penetrating some of the small Paleogene basins on the Spendlinger Horst suggest that they are mostly related to volcanogenic structures and tectonic activity of the Upper Rhine Graben. Three of the basins (Messel, Erlenwiese, Sellborn-Schneise, Fig. 4.6.1) are aligned with the structure at PvH in SW-NE direction along a major concealed fault, the Messel Fault Zone (MZN; Mezger et al. 2013). However, the character of the basin at PvH remains unclear (Harms 1999; Felder et al. 2001; Jacoby et al. 2005). It has been discussed that it could represent either another maar structure or a small pull-apart basin (Felder et al. 2001, Hofmann et al. 2005). The isotopic values of siderite (δ^{13}Carbon and δ^{18}Oxygen) in the sediments at PvH are significantly lower than typical values for deep maar lakes which are characterized by long-lasting and stable meromictic conditions (Felder and Gaupp 2006). Low δ^{13}C and δ^{18}O values can be interpreted as a consequence of the position of the redox boundary near the sediment surface within an open holomictic system, such as a river delta or an alluvial plain (Felder and Gaupp 2006). Therefore, it has been concluded that the lake at PvH (Lake PvH) was significantly shallower than a typical

deep maar lake and probably filled a small pull-apart basin (Felder et al. 2001; Felder and Gaupp 2006).

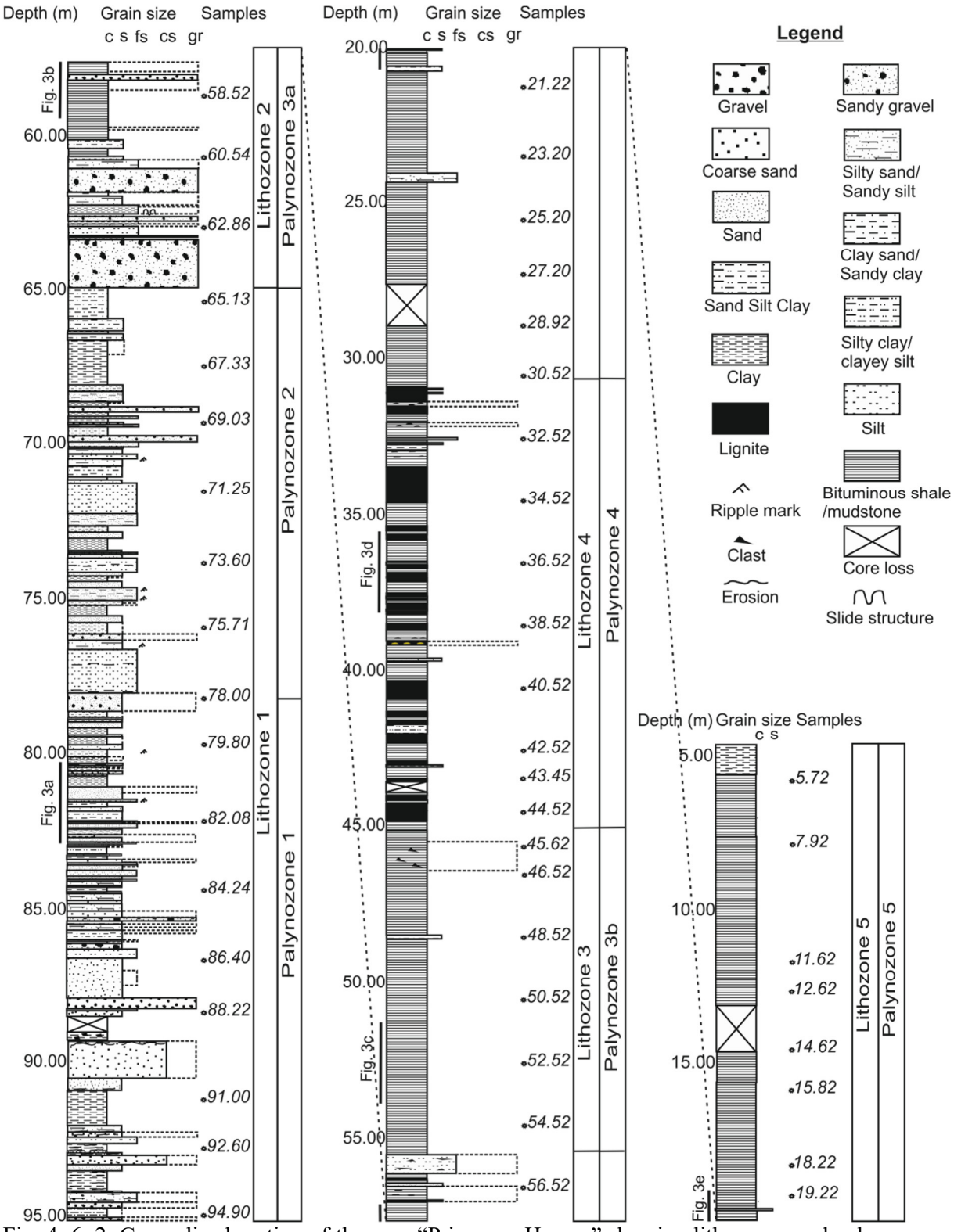

Fig. 4. 6. 2. Generalized section of the core "Prinz von Hessen" showing lithozones and palynozones used in this paper. The positions of core pictures given in Fig. 4.6.3 are indicated.

Lake PvH had a semi-circular shape with a diameter of 600-800 m and was surrounded by sediments of Permian age (Felder et al. 2001). A scientific core with a total thickness of 150

m was drilled in 1997 from the centre of the lake basin and has been described by Felder et al. (2001). In the lower 55 m the core revealed a mixed allochthonous succession with frequent lapilli in the upper part. This part is followed by 95 m of lacustrine sediments (Fig. 4.6.2). It starts with a unit of 34 m of graded and occasionally cross-bedded sandstones and siltstones, interbedded with several thin, cm-thick mudstones that were deposited in a shallow lake environment (Fig. 4.6.2; Felder et al. 2001; Hofmann et al. 2005). The succeeding unit is characterized by 15 m of black, bituminous shale with high TOC content (30-45%; Hofmann et al. 2005), followed by approximately 15 m of interbedded grey-green mudstones and lignite and 25 m of mostly laminated bituminous shale in the upper part (Fig. 4.6.2). The top of the core consists of 5 m of deeply weathered bituminous shale.
Although lignite was mined for several years during the 1920's in an area 250 m east of the drill site, the succession as exposed in the mine has never been described in detail. An early equid specimen (*Eurohippus parvulus parvulus*) that was found during mining activities pointed to a late Middle Eocene to middle Late Eocene age (European mammal chronology zones MP13-MP16; Franzen 2006) thus indicating a younger age than that for the deposits at Messel, which have an age between *c.* 48.5 and *c.* 47.9 Ma (Lenz et al. 2015).
A geochemical and organic petrological study on a part of the core PvH between 61 and 30 m depth suggested that lake level changes, associated with oxygenation levels and distribution of sedimentary facies were largely controlled by a combination of tectonic activity and climate variations (Hofmann et al. 2005).

Material and methods

Sampling and sample processing

The core was drilled in the centre of the PvH-basin (49°53'56.64" N, 8°43'48.31"E) as part of a scientific drilling campaign in cooperation between the Senckenberg Gesellschaft für Naturforschung (SGN, Frankfurt/M.), the Hessisches Landesamt für Umwelt und Geologie (HLUG, Wiesbaden) and the Institut für Geowissenschaftliche Gemeinschaftsaufgaben (now LIAG, Hannover). For a general overview of the entire lacustrine succession, 47 samples with an interval spacing of *c.* 2 m (based on lithological changes) were selected for the present study between 5 and 95 m.
Palynological preparation of the samples including treatment with hydrochloric acid (HCl), hydrofluoric acid (HF) and potassium hydroxide (KOH) followed the standard method as described by Kaiser and Ashraf (1974). After sieving through a 10 µm mesh screen, residues were oxidized using nitric acid (HNO_3) or hydrogen peroxide (H_2O_2) in order to improve transparency of the palynomorphs. For each sample one or more slides have been prepared using a mixture of the residue and glycerine jelly. All residues and slides are stored at the Senckenberg Forschungsinstitut und Naturmuseum, Sektion Paläobotanik, Frankfurt am Main, Germany.

Quantitative palynological analysis

Palynological analysis was undertaken using a transmitted light microscope (Olympus BX40). In order to get a representative dataset for robust statistical analysis, at least 300 individual palynomorphs were counted per sample at 400 times magnification. Poorly preserved individual palynomorphs which could not be identified were counted as "Varia". The palynomorphs were mainly identified on the basis of the systematic-taxonomic studies of Thomson and Pflug (1953), Thiele-Pfeiffer (1988), Nickel (1996) and Lenz (2005).
The pollen diagram (Fig. 4.6.4) shows the abundance of the most important palynomorphs in percentages. Taxa are arranged according to their weighted average value (WA regression, ter Braak and Looman 1995) in relation to depth by using the software C2 1.7.6 (Juggins 2007).

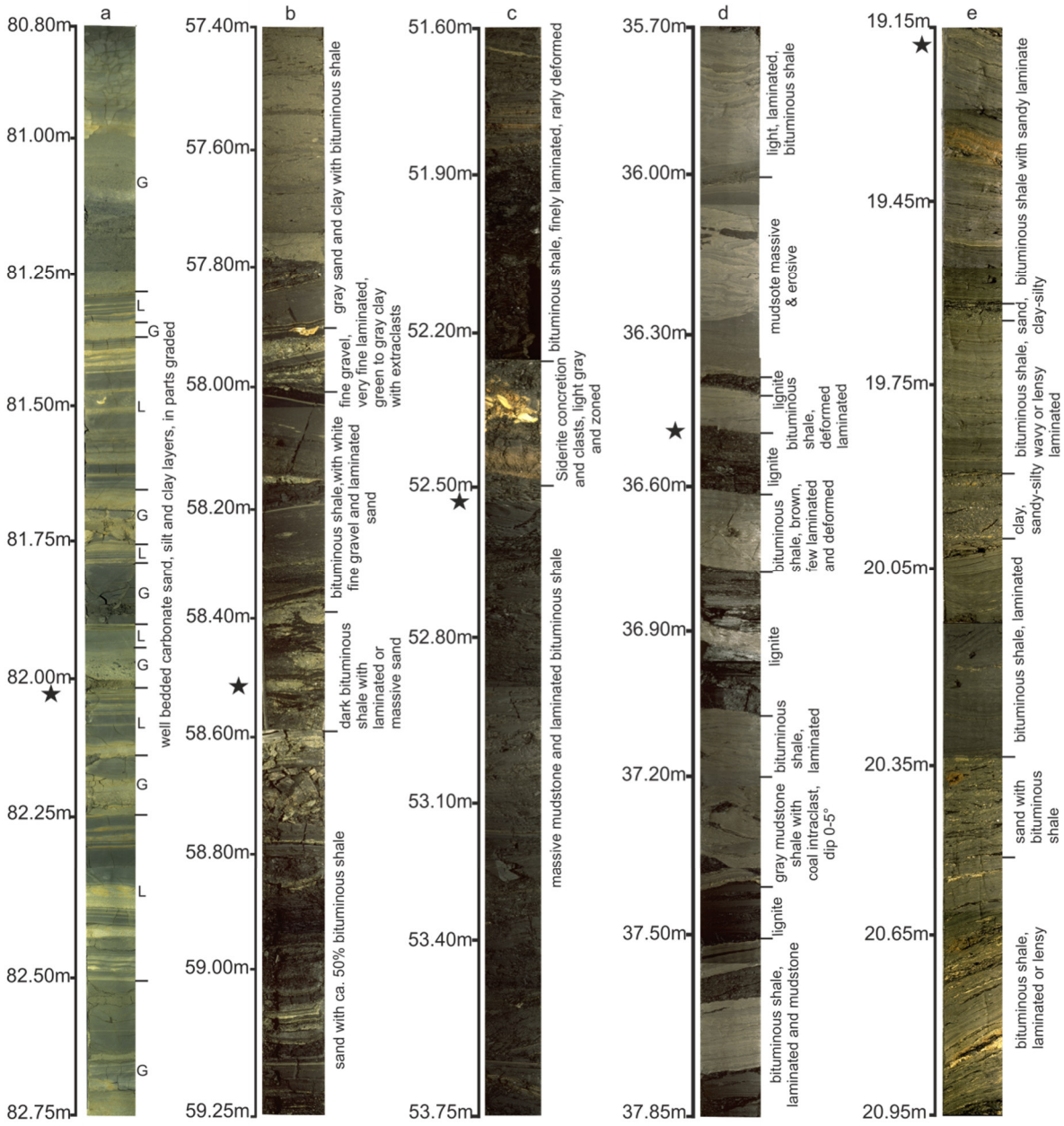

Fig. 4. 6. 3. Selected images of the core illustrating the lacustrine record of PvH with its different lithozones. The positions of the respective palynological samples are indicated by black stars. G: Graded and L: Laminated. The pictures are based on photographs of FIS/HLUG (Borges, Schiller and Stryj) from the core B/97- BK9: (**a**) LZ1, 10737.pcd - 10733.pcd, (**b**) LZ2, 10670.pcd - 10666.pcd, (**c**) LZ3, 10651.pcd - 10645.pcd (**d**) LZ4, 10598.pcd - 10592.pcd and (**e**) LZ5, 10546.pcd - 10552.pcd

This arrangement led to a structured pollen diagram showing the major patterns of compositional variation in relation to depth and revealed the different steps in the progression of the plant community (Janssen and Birks 1994). Pollen and spores were calculated to 100% while algae such as *Botryococcus* and *Ovoidites* were added as additional percentages (in % of the total pollen sum).

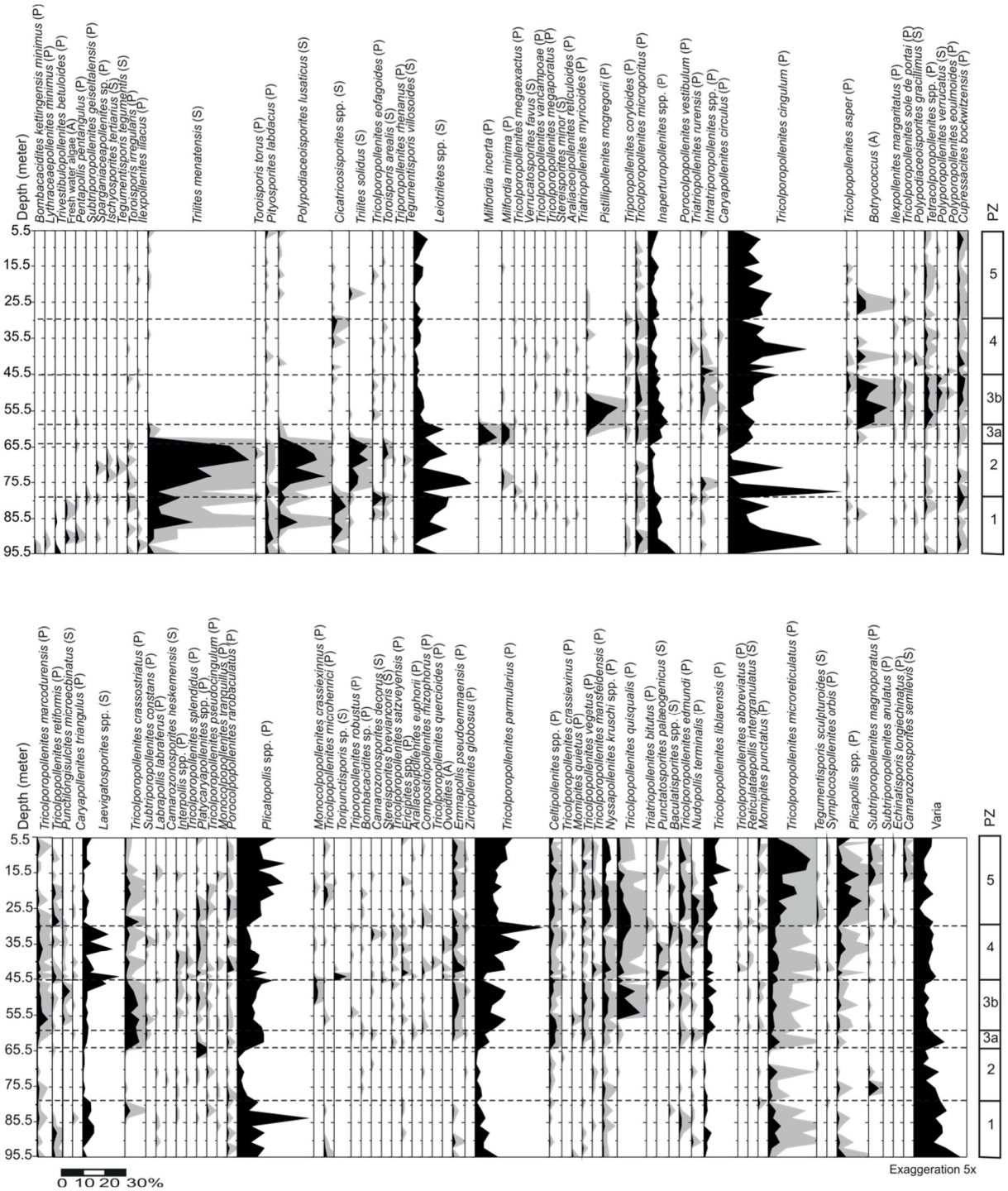

Fig. 4. 6. 4. . Pollen diagram of most important palynomorph taxa in the lacustrine succession of Eocene Lake Prinz von Hessen. The diagram shows five palynological zones, derived from constrained cluster analysis (Fig. 4.6.5). Abbreviations behind the species names: (A) alga, (P) pollen, (S) spore

Statistical analysis

Following Gauch (1982) nine cut levels (0%, 0.5%, 1%, 2%, 4%, 8%, 16%, 32% and 64%) were defined for distinguishing abundance classes to eliminate minor fluctuation and remove dependency of variables. Minor fluctuations in the pollen rain are probably due to regular variation in pollen precipitation related to random effects such as differential pollen

production, dispersal and deposition (Prentice 1980) and therefore do not reflect true changes in the frequency of the parent plants within the vegetation.
A robust zonation of the pollen diagram was established by constrained cluster analysis using Ward's minimum variance method (software PAST 3.06, Hammer et al. 2001). Rare species with a maximum value less than 1% which do not show any significant pattern throughout the pollen diagram were excluded from cluster analysis. Therefore, the number of taxa analysed has been limited to 104. Remains of algae were included in the numerical analysis since their dominance within parts of the section is important for the delineation of individual palynological zones.
To reveal the underlying pattern as well as ecological gradients, detrended correspondence analysis (DCA) was implemented by using software PAST 3.06 (Hammer et al. 2001). DCA was chosen as the appropriate multivariate model, because a gradient lengths analysis (DCA, Hill and Gauch 1980) using the software Canoco for windows 4.56 (ter Braak and Smilauer 2009) determined a length of 3.0 SD (units of average standard deviation of species turnover) for the samples. Following ter Braak and Smilauer (2002) a gradient length of more than 2 SD indicates monotonic trends in species composition. Therefore, the unimodal response model of the DCA should be used rather than a linear response model such as a principal component analysis (PCA). DCA has been used instead of correspondence analysis (CA), because DCA corrects the arch effect and compression of data points at the edges of the ordination space (Hill and Gauch, 1980) and is therefore a technique that is commonly used in ecological ordination (e.g., Lenz et al., 2011; Daly et al. 2011; Galloway et al. 2015; Vellekoop et al. 2015). In contrast to cluster analysis that has been performed by using all palynomorph taxa, for DCA only taxa with an overall assemblage value of more than 0.5% were included in the analysis to reduce statistical noise (Stukins et al. 2013; Galloway et al. 2015).

Results

Sedimentology

Based on lithological changes as seen in the photodocumentation and the description of the fresh core by Felder et al. (2001) we studied the remaining core material and distinguished five lithozones (LZ1-5; Fig. 4.6.2) in the lacustrine succession at PvH.
Between 95 m and 64.80 m (LZ1) the sediments are characterized by layers of well bedded to laminated carbonate sand, silt and clay (Fig. 4.6.3a). Occasionally ripple marks are present in sandy layers. In the lower part of LZ1, graded turbidites are frequent (Felder et al. 2001) as well as sandstones which are occasionally cross-bedded (Hofmann et al. 2005). The lithological composition suggests proximity to the source of clastic material. The sediment was transported to the lake probably by river(s) and settled to the lake bottom forming layers of different grainsize depending on current velocity. The sediment was occasionally remobilized producing graded bedding.
LZ2 between 64.80 and 55.40 m (Fig. 4.6.2) is characterized by frequent changes in lithology (Fig. 4.6.3b) including bituminous shales with interbedded turbidities, grainflows and mudflows (Hofmann et al. 2005). The latter dominate in the lower part and contain angular to sub-angular clasts of unconsolidated mudstones, cemented sandstones and wood fragments which are floating in a mud-supported matrix (Hofmann et al. 2005). The first layers of bituminous shale may be observed at a depth of 60.55 m. The lamination within the bituminous shales and a high total sulphur content with an average of 2.5% indicate that the lake at this stage was deep enough for a permanent chemocline and sub-oxic to euxinic conditions in its deep hypolimnion (Hofmann et al. 2005).
LZ3 between 55.40 and 44.70 m (Fig. 4.6.2) is characterized by massive mudstones and laminated bituminous shales without bioturbation (Fig. 4.6.3c; Felder et al. 2001). The bituminous shale indicates an open lake and increased water depth. The total sulphur content of <1 % still indicates anaerobic conditions in the sediment at the lake bottom and a poorly

oxygenated lower part of the water column (Hofmann et al. 2005). An increasing amount of quartz above 47.5 m as reported by Hofmann et al. (2005) may indicate shallowing of the lake.
Between 44.70 and 30.82 m (LZ4; Fig. 4.6.2) the core shows an alternation of lignite layers and interbedded grey-green mudstones. There are at least 20 layers of lignite with thicknesses between 5 and 50 cm (Fig. 4.6.3d; Felder et al. 2001; Hofmann et al. 2005). They consist primarily of woody organic matter of the huminite group which indicates a source either from terrestrial higher plants or from aquatic macrophytes which lived in the shallow littoral zone (Hofmann et al. 2005). The lignite layers on average contain less than 10% detrital mineral matter and show no traces of rootlets beneath them (Hofmann et al. 2005; personal observations). The thinner lignite beds are characterized in particular by erosional contacts with underlying sediment. The interbedded massive mudstones are poor in organic matter (<10 % TOC) compared to the lignites with up to 60% TOC (Hofmann et al. 2005).
LZ5 between 30.82 and 4.67 m is similar to LZ3 with sediments characterized by massive mudstones and sometimes laminated bituminous shales (Fig. 4.6.3e; Felder et al. 2001). The lignite layers which are typical of LZ4 disappear completely (Fig. 4.6.2) but lignite clasts can be found in some of the mudstones (Hofmann et al. 2005).A relative rise in lake level is probable for LZ5.

Palynology
The pollen diagram (Fig. 4.6.4) shows that several taxa vary significantly in frequency throughout the lacustrine succession. Based on constrained cluster analysis, five palynozones (PZ) were recognized (Fig. 4.6.5). They are characterized by distinct palynomorph assemblages and show an almost perfect correlation to our lithozones, with the exception of LZ1 (Figs. 4.6.2, 4.6.5) where two pollen zones can be distinguished (PZ 1 and 2).

Palynozone 1
PZ1, which covers more than half of LZ1 (about 17 metres from 94.9 m to 78 m), is represented by 9 samples. Dominant spores include Schizaeaceae (a family of climbing ferns) with different “species” of the genera *Leiotriletes* (up to 16%) and *Cicatricosisporites* (up to 6%). *Triletes menatensis*, another spore of affinity to Schizaeaceae, is particularly abundant in the upper part of PZ1, reaching a maximum of 20% while *Ischyosporites* is relatively rare (Fig. 4.6.4). Other fern spores such as those of Polypodiaceae (*Polypodiaceoisporites lusaticus,* Fig. 4.6.6b, and *Laevigatosporites* spp.) are found in lower quantities.
The high numbers of Cupressaceae (*Inaperturopollenites* spp., up to 13%; Fig. 4.6.6g) and the regular appearance of Nyssaceae (*Nyssapollenites* spp.) are evidence for a first *Nyssa-Taxodium* swamp community which established at the edge of the lake during the initial lake stage.
Among the dominant elements are juglandaceous (*Plicatopollis* spp., up to 35%, Fig. 4.6.6d) and fagaceous (*Tricolpopollenites cingulum*, up to 45%, Fig. 4.6.6e) pollen, which indicate that a (para)tropical forest vegetation (Boulter and Hubbard 1982; Harrington et al. 2004; Lenz et al. 2011) surrounded the lake basin already during the initial phase of the lake. Juglandaceae and Fagaceae are typical elements of Paleogene floras of Europe and North America (e.g. Manchester 1989). Accordingly, they are common in some of the other Central European Eocene pollen floras, such as at Geiseltal (Riegel and Wilde 2016), Eckfeld (Nickel 1996) or Helmstedt (Riegel et al. 2015). They also form the dominant elements within the forest vegetation in the nearby record of Messel (Lenz et al. 2011, 2017), such that a similar abundance in the pollen record of Lake PvH is not surprising. Together with an abundant macrofossil record of Juglandaceae at Messel (Wilde 1989, 2004), this is proof for the dominant role of these plants in the regional flora on the Sprendlinger Horst during the Eocene. In contrast, macroscopic remains of Fagaceae have never been found at Messel

(Wilde 1989, 2004). Therefore, the habitat of the Fagaceae is considered to have been outside the narrow catchment area of Lake Messel (Lenz et al. 2011). The same is most probably true for Lake PvH.

The pinaceous pollen *Pityosporites labdacus* appears only in relatively low numbers (0.5 to 4%). Nevertheless, this represents their maximum within the entire succession.

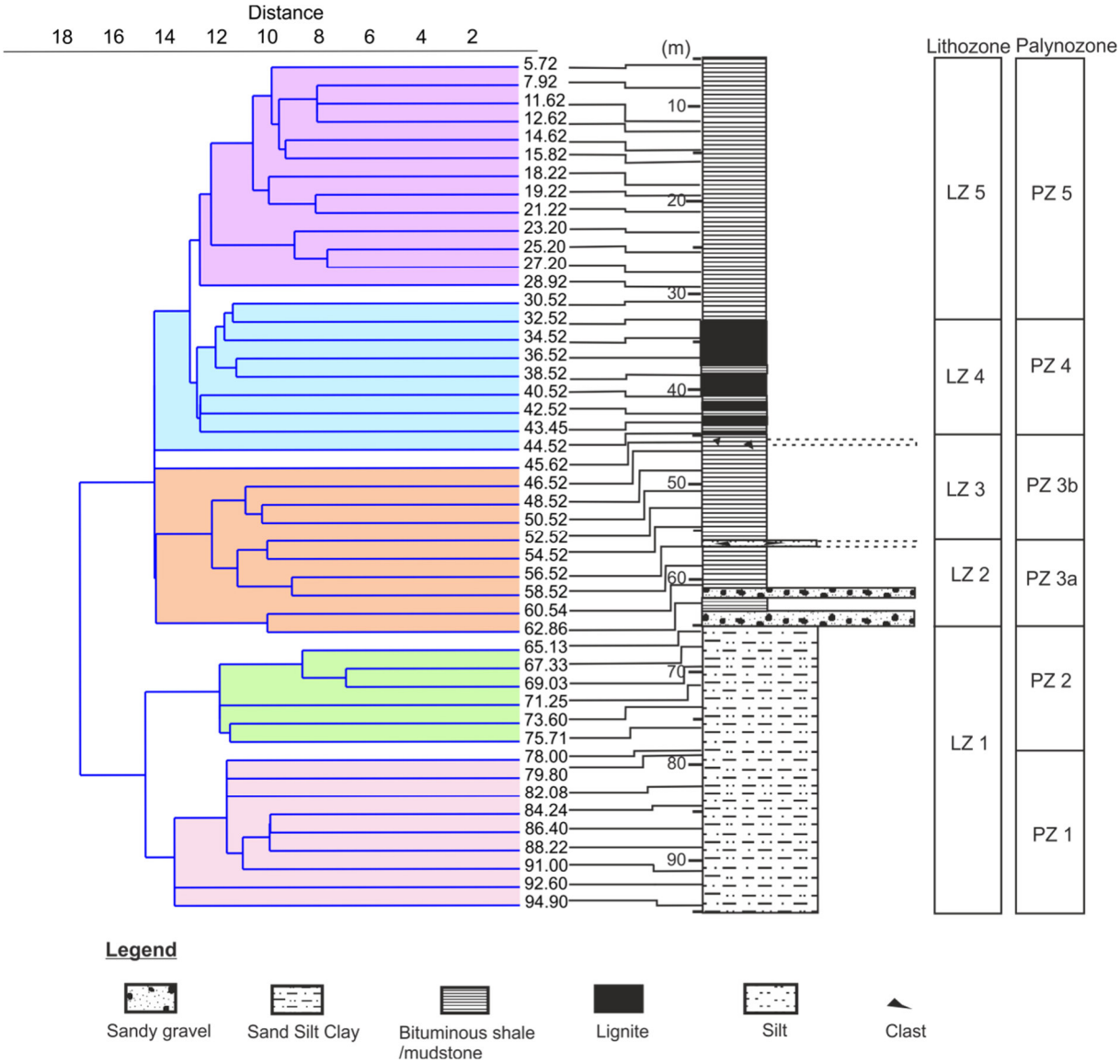

Fig. 4. 6. 5. Results of a constrained cluster analysis (Ward's method) of 47 samples between 94.9 and 5.72 m. Samples are labelled with their core depth in metres. The separation into 5 PZ correlates well with the lithological changes.

Palynozone 2

The upper part of LZ1 (13 metres from 78 m to 64.80 m depth) is represented by PZ2. Compared to PZ1, fern spores are still characteristic (Fig. 4.6.4). Nevertheless, the composition and diversity of the spore assemblage changes and the abundance of spores increases distinctly. Noteworthy are the high abundances of spores of polypodioid ferns, such as *Polypodiaceoisporites lusaticus* (up to 20%, Fig. 4.6.6b) or Schizaeaceae, e.g., *Trilites solidus* (up to 10%), *Trilites menatensis* (up to 47%, Fig. 4.6.6c) and *Leiotriletes* spp. (up to 25%, Fig. 4.6.6a).

Other dominant components of the palynomorph assemblage are the same as in PZ1 and typical for a (para)tropical rainforest, such as the juglandaceous pollen *Plicatopollis* spp. (up to 30%), and the fagaceous pollen *Tricolporopollenites cingulum* (up to 40%). A swamp forest is again indicated by, e.g., *Inaperturopollenites* spp. (Cupressaceae, up to 10%).

Palynozone 3

PZ3 (20 metres from 64.80 m to 45 m depth) is characterized by a sudden and abrupt decrease in fern spores, such as *Trilites menatensis* and *Polypodiaceoisporites lusaticus,* within two metres (Fig. 4.6.4). For example, *Trilites menatensis* decreases from 38% in PZ2 (65.13 m) to 0.58% in PZ3 (62.86 m).

In contrast *Milfordia minima* and *M. incerta* (Restionaceae, up to 4%; Fig. 4.6.6h), *Celtipollenites* spp. (Ulmaceae, starts with 4%, Fig. 4.6.6k) and *Tricolporopollenites crassostriatus* (Solanaceae, up to 7%; Fig. 4.6.6f) occur with high numbers. Restionaceae pollen have their peak abundance for the complete succession with 13% at the base of the zone. Restionaceae are a family of grass-like monocotyledons which are today widely distributed in the southern Hemisphere (Cronquist 1981; Campell 1983). They grow preferably in lowlands on wet and nutrient-poor soils and favour seasonally wet habitats which may dry out each year (Heywood 1993). During the Paleogene they were also common in the Northern Hemisphere. Prior to the expansion of grasses, sedges and rushes in marsh or wet meadow habitats with standing water at least for some time of the growing season, Restionaceae occupied such habitats in subtropical to tropical areas (Hochuli 1979; Lenz and Riegel 2001; Riegel et al. 2015; Riegel and Wilde 2016). At the top of PZ3 they disappear completely within a few meters together with most of the fern spores, such as *Triletes menatensis* and *T. solidus.*

Noteworthy in the upper part of PZ3 is the occurrence of *Pistillipollenites mcgregorii* (putative Gentianaceae, up to 15%; Fig. 4.6.6j), an index fossil for the Lower Eocene in Central Europe (Krutzsch 1966, 1970). Also other elements, such as *Tricolpopollenites quisqualis* (Fagaceae?, up to 10%), *Nyssapollenites* spp. (Nyssaceae, up to 3%; Fig. 4.6.6i), *Tricolpopollenites liblarensis* (Fagaceae, up to 6%), *Tetracolporopollenites* spp. (Sapotaceae, up to 4%; Fig. 4.6.7a) or *Tricolporopollenites marcodurensis* (Vitaceae, up to 5%, Fig. 4.6.7b) increase significantly in the upper part of PZ3. Among the non-pollen palynomorphs the coccal green alga *Botryococcus* is abundant in the upper part of PZ3 with a maximum value of 15%.

The cluster analysis shows that the samples of palynozone 3 (Fig. 4.6.5) are characterized by a similar palynomorph assemblage. Nevertheless, due to the striking difference in abundance for few species, such as *Milfordia* spp. and *Pistillipollenites mcgregorii*, the palynozone can be subdivided into two subzones, 3a and 3b.

Palynozone 4

Compared to PZ3 in PZ4 (about 12.5 metres from 45 m to 32.52 m depth) changes within the palynomorph assemblages are restricted to only a few elements (Fig. 4.6.4). Characteristic taxa are forest elements, such as *Tricolpo*(*ro*)*pollenites parmularius* (Eucommiaceae, up to 32%; Fig. 4.6.7h), *Tricolporopollenites edmundii* (Mastixiaceae, up to 6%; Fig. 4.6.7g), *Porocolpopollenites rarobaculatus* (Symplocaceae, up to 4%; Fig. 4.6.7j) or *Tricolpopollenites retiformis* (Salicaceae, up to 3%), which increase in abundance. Some spores of polypodioid ferns, such as *Laevigatosporites* spp. (up to 30%) or *Punctatosporites palaeogenicus* (up to 7%, Fig. 4.6.7f) are also abundant. In contrast, characteristic elements of PZ3 disappear completely (*Milfordia* spp.) or decrease significantly in abundance (*Pistillipollenites mcgregorii* from 15% to 1% and *Tricolporopollenites crassostriatus* from 7% to 1%).

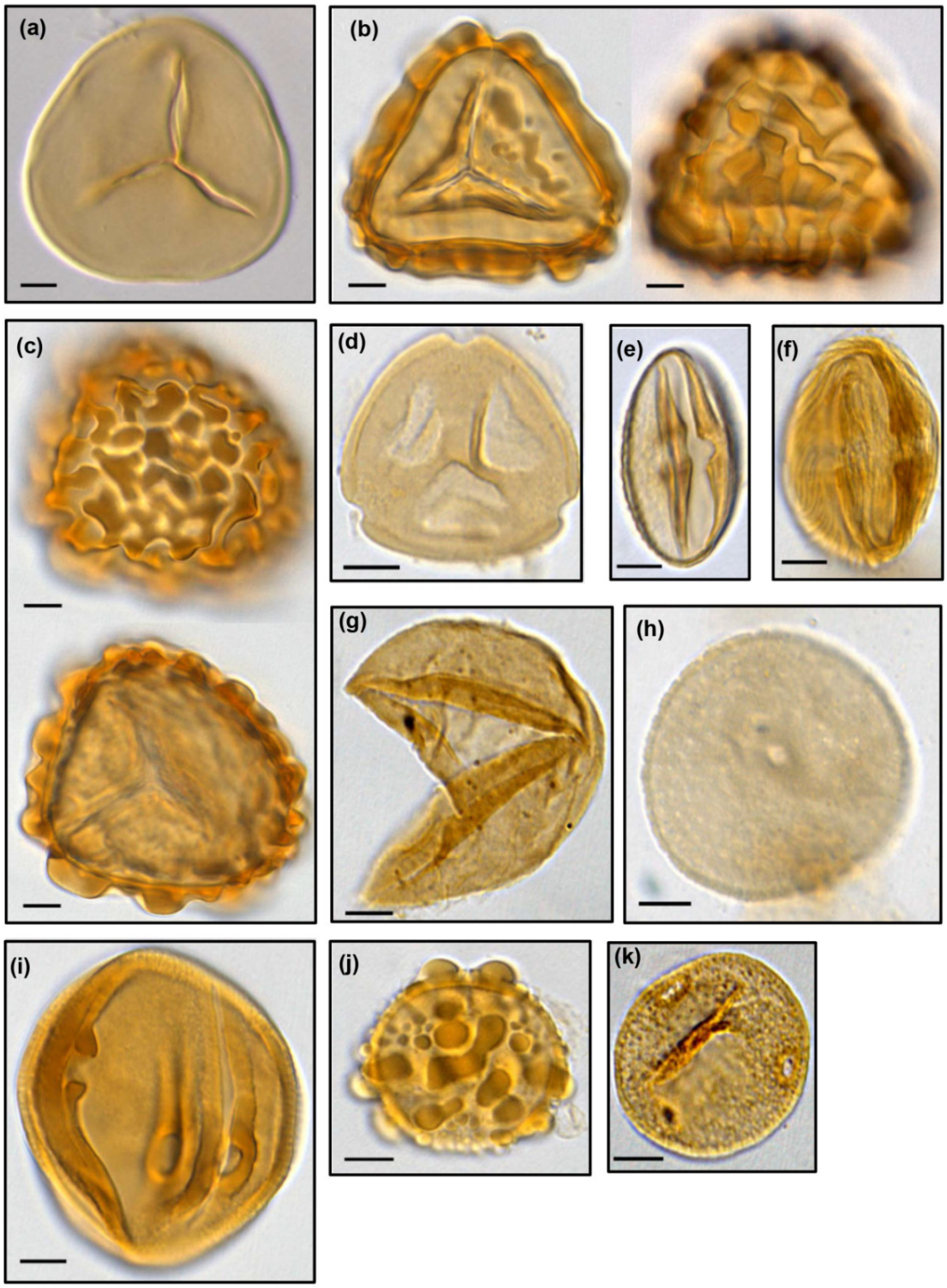

Fig. 4. 6. 6. Palynomorphs from Eocene Lake Prinz von Hessen. Sample and slide numbers with depth are given in brackets after the species name. The scale bars represent 10µm. Characteristic elements of PZ1 and 2: images (**a-e, g**), Characteristic elements of PZ 3a: (**f, h, k**) and Characteristic elements of PZ 3b: (**i, j**). (**a**): *Leiotriletes maxoides* (PvH-99A, 56,52m). (**b**): *Polypodiaceoisporites lusaticus* (PvH-43C, 69.03m). (**c**): *Trilites menatensis* (PvH-20C, 82.08m). (**d**): *Plicatopollis hungaricus* (PvH-194A, 46.52m). (**e**): *Tricolporopollenites cingulum* (PvH-20C, 82.08m). (**f**): *Tricolporopollenites crassostriatus* (PvH-99A, 56.52m). (**g**): *Inaperturopollenites sp.* (PvH-2C, 94.90m). (**h**): *Milfordia minima* (PvH-56A, 60.54m). (**i**): *Nyssapollenites kruschii* (PvH-229A, 42.52m). (**j**): *Pistillipollenites mcgregorii* (PvH-139A, 52.52m). (**k**): *Celtipollenites intrastructurus* (PvH-194A, 46.52m).

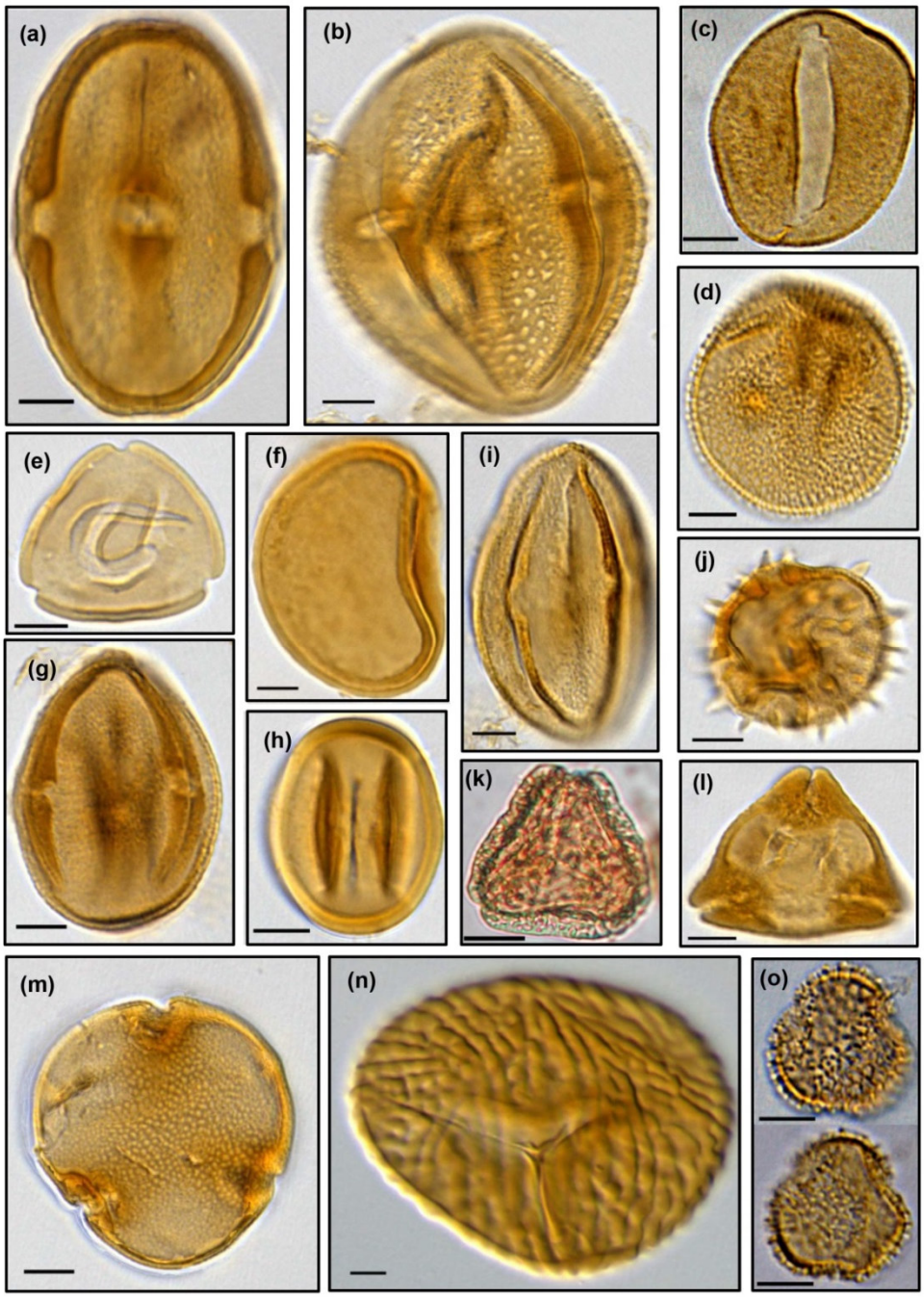

Fig. 4. 6. 7. Palynomorphs from Eocene Lake Prinz von Hessen. Sample and slide numbers with depth are given in brackets after the species name. The scale bars represent 10µm. Characteristic elements of PZ 3b: images (**a- d**), Characteristic elements of PZ 4: images (**e, f, g, h, j, and m**) and Characteristic elements of PZ 5: images: (**i, k, l**). (**a**): *Tetracolporopollenites kirchheimeri* (PvH-99A, 56.52m). (**b**): *Tricolporopollenites marcodurensis* (PvH-99A, 56.52m). (**c**): *Monocolpopollenites crassiexinus* (PvH-174A, 48.52m). (**d**): *Emmapollis pseudoemmaensis* (PvH-159A, 50.52m). (**e**): *Playcaryapollenites semicyclus* (PvH-229A, 42.52m). (**f**): *Punctatosporites palaeogenicus* (PvH-289A, 36.52m). (**g**): *Tricolporopollenites edmundii* (PvH-194A, 46.52m). (**h**): *Tricolporopollenites parmularius* (PvH-119A, 54.52m). (**i**): *Tricolpopollenites microhenrici* (PvH-119A, 54.52m). (**j**): *Porocolpopollenites rarobaculatus* (PvH-229A, 42.52m). (**k**): *Camarozonosporites semilevis* (PvH-444A, 15.82m). (**l**): *Nudopollis terminalis* (PvH-39A, 71.25m). (**m**): *Intratriporopollenites microinstructus* (PvH-139A, 52.52m). (**n**): *Cicatricosisporites cf. paradorogensis* (PvH-194A, 46.52m). (**o**): *Tricolporopollenites microreticulatus* (PvH-174A, 48.52m).

Palynozone 5

In PZ5 (26.8 metres from 32.52 m to 5.72 m depth) a strong increase in abundance for some of the taxa is especially noteworthy (Fig. 4.6.4). *Nyssapollenites* spp. (Nyssaceae, up to 4.5%), *Tricolporopollenites microreticulatus* (Oleaceae, up to 20%, Fig. 4.6.7o), *Tricolpopollenites microhenrici* (Fagaceae, up to 2.5%, Fig. 4.6.7i), *Plicapollis* spp. (Juglandaceae?, up to 12%), *Tricolpopollenites liblarensis* (Fagaceae, up to 13%), *Nudopollis terminalis* (Myricaceae/ Juglandaceae?, up to 5%, Fig. 4.6.7l) reach their highest values within the complete succession. In contrast, fern spores, such as *Laevigatosporites* spp., show a decrease to relatively low numbers compared to PZ4.

Discussion

Age of the succession

For palynostratigraphic analysis our palynomorph spectrum is compared to the distribution of stratigraphically relevant microfloras in Northwestern Central Germany (Pflug 1986) and Eastern Germany (Krutzsch 1966, 1970). Both of these authors divided the Paleogene into different palynostratigraphic zones (Fig. 4.6.8). The palynomorph assemblage from the core at PvH fits best to zones Hu1 to Hu3 of Pflug (1986) and 12 to 13b of Krutzsch (1966), which corresponds to the late Early Eocene (Fig. 4.6.8). Some stratigraphically relevant taxa from our material, such as *Pistillipollenites* or *Interpollis* are unkown from the Middle Eocene of Central Germany (Krutzsch 1970). Furthermore, our palynomorph assemblage is comparable to the well dated late Early Eocene Lower Messel Formation, but differs from the palynomorph assemblages of the Middle Eocene Middle Messel Formation where some taxa increase to mass abundances, such as *Tricolpopollenites liblarensis*, or decrease significantly, such as *Tricolpo*(*ro*)*pollenites parmularius* (Lenz et al. 2007, 2015).

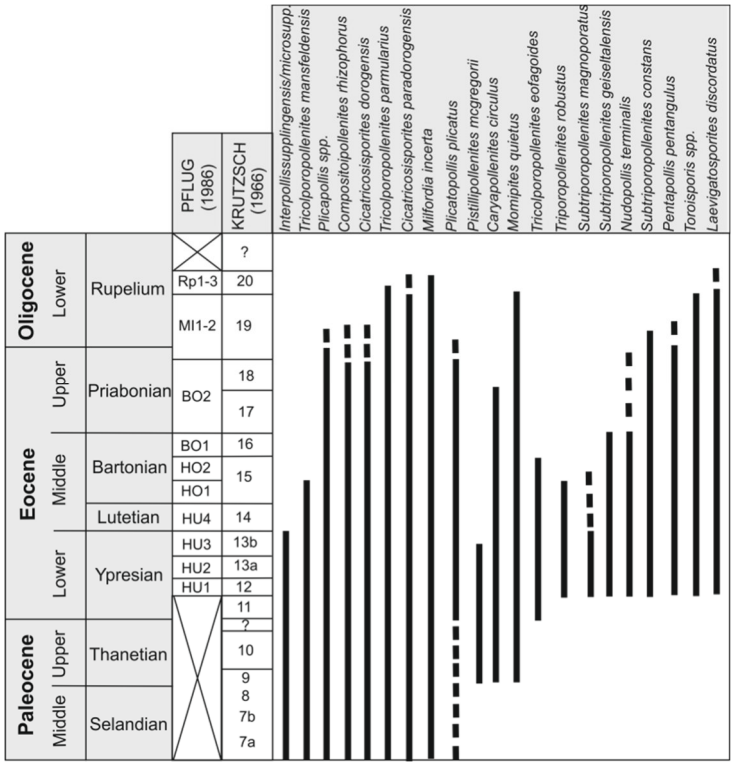

Fig. 4. 6. 8. Stratigraphic ranges of selected palynomorph taxa from Eocene Lake Prinz von Hessen. Taxa included are considered as important stratigraphic index species for the Eocene in Central and Eastern Germany (Krutzsch 1966; Pflug 1986). The last-appearance datum of *Pistillipollenites mcgregorii* and *Interpollis* spp. as well as the first appearance datum of some species, such as *Triporopollenites robustus* or *Subtriporopollenites magnoporatus,* indicate a late Early Eocene age of the succession.

An Early Eocene age for our succession contradicts the Middle to Late Eocene age which was assigned to PvH by mammal chronology (Fahlbusch 1976; Franzen 2006). This may be explained by the fact that the mammal material was discovered during mining activities at the beginning of the last century. According to old reports and photographs (Harms 2005), a considerable thickness of lignite was exposed in the opencast mine which is obviously missing in the core that is located a few hundred metres to the West. It is therefore probable that sedimentation of organic material in the basin lasted for a significantly longer time than that represented in the core.
Because of the correlation of core PvH with the Lower Messel Formation, Lake Messel and Lake PvH are likely to have coexisted for some time. This would explain the existence of a similar fauna and flora in both taphocoenoses, especially expressed by the fish assemblages (Micklich 2012) and the palynoflora (Lenz et al. 2007). Frequent accretionary lapilli between 116 and 96 m in the core are probably derived from an eruption in the vicinity of Lake PvH (Felder et al. 2001) and may therefore represent the Messel eruption, however, this has still to be proven.

Controls on sedimentation
Volcanoclastic deposits indicative of a maar lake, such as syn-eruptive and subaquatic breccias (e.g., Pirrung 1998; Felder et al. 2001), have not been recognized at PvH, suggesting a non-volcanic origin of the lake basin. This supports the interpretation of the basin at PvH as a small pull-apart basin.
Carroll and Bohacs (1999) and Bohacs et al. (2000) described different lake types with differing lacustrine facies associations. Their facies types were related to the interplay of (mostly tectonic) accommodation and the rate of sediment and water fill. Although the concept was developed for large modern lakes, similarities can be noted for the small Lake PvH. The lower part of the lacustrine succession (LZ1), which is composed of a mixture of gravel, sandstone and mudstone with a coarse lamination (Fig. 4.6.3a), is comparable to a fluvial-lacustrine facies association (Carrol and Bohacs 1999) typical for an overfilled lake, in which the influx of water and sediment generally exceeds potential accommodation. In LZ's 2 and 3 the deposition of laminated organic-rich bituminous shales and mudstones (Figs. 4.6.3b, c) with TOC-values above 20% (Hofmann et al. 2005) is typical for a fluctuating profundal (deep water) facies association with changing lake levels (Carroll and Bohacs 1999; Bohacs et al. 2000). In such balanced-filled lakes tectonic accommodation equals water and sediment fill (Carrol and Bohacs 1999). LZ4 with alternating layers of mudstone and lignite indicating a period with a very low lake level and a change to a more fluvial-lacustrine facies (Carroll and Bohacs 1999), whereas LZ5 with finely laminated mudstone and bituminous shale represents a further profundal facies association comparable to LZ's 2 and 3. Lacustrine basin fills often grade from one facies association into another, without major unconformities (Carrol and Bohacs 1999). However, the abrupt change between facies associations in Lake PvH suggests that tectonic activity has influenced the evolution of the basin by rapid uplift and subsidence. This is especially true for the change between LZ's 1 and 2, which records considerable deepening of the lake within a few metres of sediment. The frequent occurrence of mass flows and turbidites (Fig. 4.6.9), especially at the transitions between the individual facies associations and LZ's may therefore relate to distinct tectonic events such as earthquakes during the evolution of the lake. Other possible causes for remobilizing material from the littoral zone of the lake such as, e.g., wave activity or storm events should not have had a significant influence in such a small-sized lake.

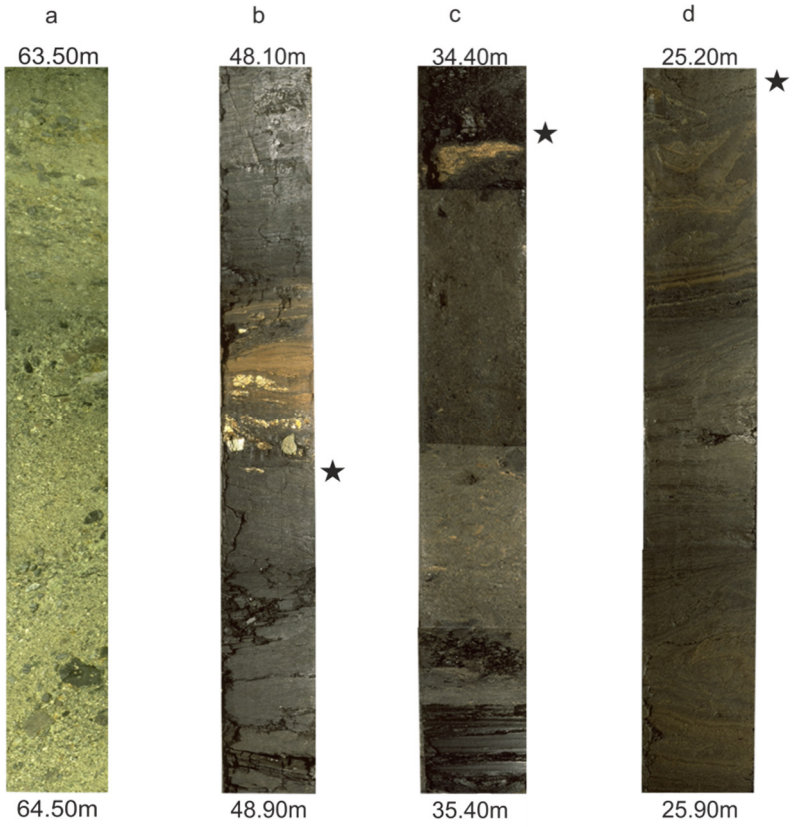

Fig. 4. 6. 9. Core sections showing event layers and redeposited sediments in the succession of Eocene Lake Prinz von Hessen, potentially related to tectonic activity. The position of palynological samples is given by black stars. (**a**): Segment of the event bed between 64.80 and 63.23 m showing a turbulent deposition of material of different grain sizes which point to remobilized sediments from the littoral zone of the lake transported towards the basin centre. (**b**): Section of core showing sediments mainly composed of bituminous shales and mudstones. The layer of green coloured sands and clays including cm-sized clasts of putative Permian rocks between 48.4 and 48.3 m indicate a redeposition event. (**c**): Section of core showing redeposition including the incorporation of clasts up to gravel size of different origin in mudflows (e.g., 35.20 and 34.50m). (**d**): Slumping and convolute bedding (e.g., 25.30 and 25.80 m) pointing to events that led to transport of unconsolidated sediments into the lake basin.
The pictures are based on photographs of FIS/HLUG (Borges, Schiller and Stryj) from the core B/97-BK9: (a) LZ2, 10688.pcd- 10686.pcd, (b) LZ3, 10636.pcd- 10634.pcd, (c) LZ4, 10590.pcd- 10587.pcd and (d) LZ5, 10565.pcd- 10563.pcd.

Reconstruction of the palaeoenvironment

Based on the qualitative and quantitative palynological data as well as on sedimentological evidence some general steps in the evolution of the palaeoenvironmental conditions can be recognized. Accordingly, during lacustrine sediment deposition as documented in the core, five stages in vegetation development that are associated with lithological changes have been distinguished by cluster analysis (Figs. 4.6.2, 4.6.4, 4.6.5). There is a clear difference between the palynomorph assemblages of the older two PZ's 1 and 2 (=LZ1) and the three younger PZ's 3 to 5, which is especially illustrated by the strong decline in different fern spores. Nevertheless, it is obvious that sedimentary processes changed fundamentally between LZ 1 (fluvial-lacustrine facies) and LZ's 2 to 5 (mainly profundal facies), since the coarse grained clastic sediments in the lower part are replaced by bituminous shales and mudstones indicating a rapid deepening of the lake basin between LZ1 and LZ2. Therefore, differential transportation and sorting of pollen and spores during transportation and deposition must be considered (Galloway et al. 2015), which prevents a direct comparison between the

palynomorph assemblages of PZ's 1 and 2 with PZ's 3 to 5. Therefore, LZ1 and LZ's 2 to 5 have been treated separately in the DCA (Fig. 4.6.10).

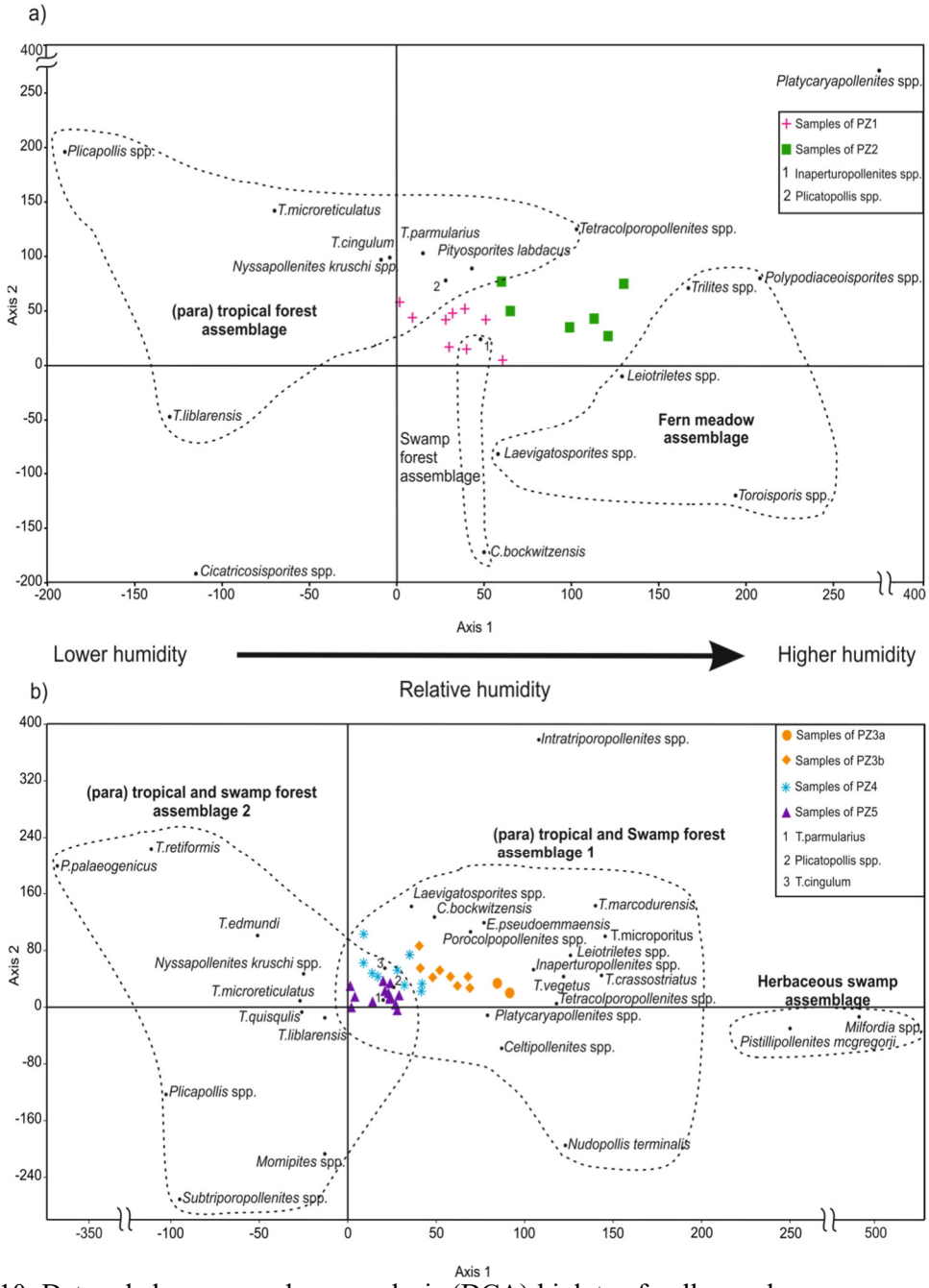

Fig. 4. 6. 10. Detrended correspondence analysis (DCA) biplots of pollen and spores occurring with a mean relative abundance of >0.5% in samples from the (**a**) fluvial-lacustrine facies (LZ 1) and samples from the (**b**) profundal facies association of LZ's 2 to 5. (**a**): The percentage variance of 41.59% and eigenvalue (0.137) of the x-axis are much higher than those of the y-axis (16.68%, 0.039), indicating that only variation along axis 1 represents a significant ecological factor. Three ecological groupings of taxa are delineated by dashed lines. Palynozones 1 and 2 defined by constrained cluster analysis are separated by different symbols. (**b**): The percentage variance of 22.54% and eigenvalue (0.074) of the x-axis are higher than those of the y-axis (14.56%, 0.035), indicating that mainly the variation along axis 1 represents a significant ecological factor. Three ecological groupings of taxa are delineated by dashed lines. Palynozones 3a to 5 defined by constrained cluster analysis are separated by different symbols. In both plots the x-axis is interpreted to represent a climate signal with an increase of relative humidity from left to right.

Fluvial-lacustrine facies (LZ1; PZ1, 2)

The DCA of samples from the fluvial-lacustrine facies association (Fig. 4.6.10a) reveals significant compositional differences between PZ's 1 and 2, because both zones are separated along DCA axis 1. Furthermore, three vegetation communities are separated by DCA (Fig. 4.6.10a). On the right side of the ordination space the different fern spores are plotted indicating widespread fern meadows in the vicinity of the lake. Typical swamp elements, such as the Cupressaceae (*Inaperturopollenites* spp., *Cupressacites bockwitzensis*) are separated from the group of dominating elements of a (para)tropical forest, which mainly plot on the left side of the DCA diagram. The community of the (para)tropical forest is characterized by elements of a climax stage of the Paleogene European vegetation, typical for inland sites of Western and Central Europe during the Eocene greenhouse climate (Mai 1981, 1995; Schaarschmidt 1988; Wilde 1989; Collinson et al. 2012), such as Fagaceae (*Tricolpopollenites liblarensis, Tricolporopollenites cingulum*) and Juglandaceae (*Plicapollis* spp., *Plicatopollis* spp.). This indicates that the regional climax vegetation already existed in the vicinity of Lake PvH during the initial phases of lake development.

The high numbers of fern spores may point to extended fern meadows flourishing under wet conditions at the shoreline or in marginal swamps (Lenz and Riegel 2001; Lenz et al. 2011) especially during PZ2. Fern spores generally show higher abundances in assemblages resulting from fluvial transport compared to wind transported assemblages and may therefore be overrepresented in PZ 1 and 2 in comparison to the wind transported pollen of the surrounding forest (DeBusk 1997). There is however, a strong increase in fern spores between PZ1 and 2 without a significant change in lithology and depositional environment. The separation of both PZ's along the first DCA axis is therefore probably not related to taphonomic processes and may represent a change in climate, in particular a change to more humid conditions from PZ1 to 2. DCA axis 1 therefore most likely records changes in relative humidity and the consequent effects on vegetation distribution (Fig. 4.6.10a).

A change to more humid conditions could also explain the decline in pinaceous pollen (*Pityosporites* spp.) between PZ1 and 2, because Pinaceae are generally regarded as more tolerant to less humid conditions and well-drained soils than most of the plants that form components of the regular PvH forest. Therefore, Pinaceae were probably more abundant in a slightly drier PZ1. Bisaccate pinaceous pollen are transported in greater numbers by fluvial processes than by wind (Suc and Drivaliari 1991). Their total disappearance in the successive zones of the profundal facies association (PZ's 3, 5) is thus in accordance with the decreasing fluvial influence.

Fluctuating profundal facies association (LZ2 to LZ5/ PZ3 to PZ5)

The DCA of the samples from LZ's 2 to 5, which represent a mainly profundal facies association, shows that the different palynozones are separated along DCA axis 1 (Fig. 4.6.10b) This indicates changes within the vegetation during lake evolution. Compared to the assemblages of the fluvial-lacustrine facies association of LZ 1 the strong decline or even disappearance of most fern spores is noteworthy. This could indicate a significant change in ecological conditions, resulting in suppression of ferns, e.g., by a change to less humid conditions. However, a change in climate towards drier conditions is not recognizable when comparing the pollen assemblages of PZ 2 and PZ 3.

It is obvious that the rapid and abrupt changes in pollen assemblages are coupled to lithology in Lake PvH. The abrupt frequency fluctuations of palynomorph taxa which occur between PZ's 2 and 3a are comparable to a coupling of Holocene vegetation dynamics and seismic events, which included sudden changes in ecological conditions such as a change from backswamp to open lake conditions in the Maramara Sea (Leroy et al. 2002) or the destruction of habitats in the vicinity of the Dead Sea (Neumann et al. 2009).

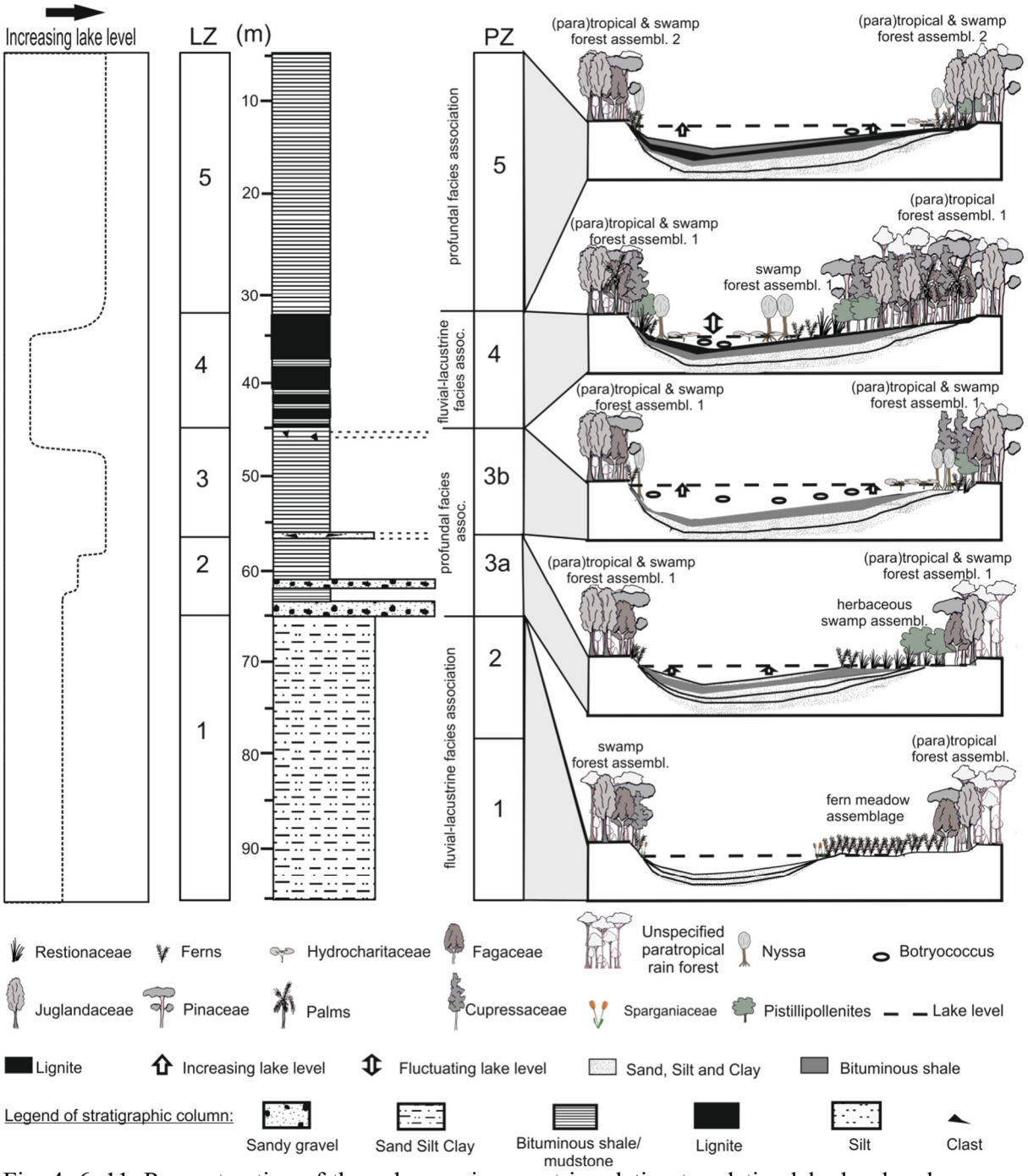

Fig. 4. 6. 11. Reconstruction of the palaeoenvironment in relation to relative lake level, palynozones and lithology. During the fluvial-lacustrine facies association a vegetation community was distributed in the vicinity of the lake which was characterized by widespread fern meadows (PZ1, 2). The profundal facies association, developed after an abrupt subsidence of the basin, is characterized by a herbaceous swamp dominated by Restionaceae (PZ3a). During PZ3 an increased lake level resulted in the littoral zone of the lake becoming inhabited by aquatic plants and a diverse swamp forest. The frequency of herbaceous elements in the palynoflora and especially the onset of lignite deposition indicate that during PZ4 wet areas were widely distributed around the lake in areas newly formed due to lake shrinkage following a drop in water level. A higher relative lake level was established again during PZ5 due following further subsidence of the lake basin. In comparison to PZ3 significant changes within the surrounding forest were triggered by a change in climate to slightly less humid conditions. Abbreviations: (LZ) lithozone, (PZ) palynozone.

Therefore, tectonic activity and related changes in the paleoenvironment may have played an important role for changes in the vegetation at PvH.

Another possibility is that the fern spores, which are mainly transported by rivers (DeBusk 1997) from habitats outside the immediate catchment area of the lake, are not transported to deeper lake environments, distal to distributary input points.
The strong rise of Restionaceae as typical herbaceous swamp elements in PZ3a is evidence for changes in the vegetation at the lakeside and in the surrounding forest. Restionaceae today favour seasonally wet habitats which may dry out each year and they are able to live in standing water at least for some time during the growing season (Heywood 1993). This suggests that PZ3a was influenced by a higher and oscillating lake level in comparison to the previous PZ2 (Fig. 4.6.11).
The samples of PZ3b plot slightly separate from the samples of PZ3a in the DCA (Fig. 4.6.10b) indicating changes in the pollen assemblage. The peak abundance of putative Gentianaceae (*Pistillipollenites*) is particularly noteworthy. The distribution within the succession at Lake PvH indicates that such plants were important in wet herbaceous swamps at the lake side during phases with a higher water level. The onset of Hydrocharitaceae (*Punctilongisulcites microechinatus*) and Nymphaeaceae (*Monocolpopollenites crassiexinuns*, Fig. 4.6.7c) in PZ3b (Fig. 4.6.4) indicates littoral zones of a depth sustaining floating and submersed aquatic plants. This can be related to a further increase of the lake level compared to PZ3a which led to more extended permanently flooded areas at the lake margin (Fig. 4.6.11). A *Nyssa/Taxodium* swamp community still existed around the lake margin since pollen of both genera (*Inaperturopollenites* spp., *Nyssapollenites* spp.) also reached higher percentages in PZ3b.
Within the climax forest surrounding the lake, Juglandaceae and Fagaceae still dominated. *T. liblarensis* (Fagaceae or Leguminosae) and *Tricolpo*(*ro*)*pollenites parmularius* (Eucommiaceae) increased significantly from PZ2 to PZ3a/b. This may only be an apparent increase in parent plant abundance within the vegetation, related to the decrease and disappearance of most of the fern spores. Nevertheless, especially the parent plants of *T. liblarensis* have been considered to be elements of more moist habitats by Riegel et al. (2015). Therefore, an increase of these Fagaceae may also have been related to a rising lake level in combination with a rising groundwater table.
PZ4 is also separated from the other PZ's in the DCA (Fig. 4.6.10b). This is due to the abundance of some fern spores in the lignite layers where they reach values comparable to those in PZ1 and PZ2 indicating that ferns were again widespread around the lake margin. The distribution of aquatic plants such as Nymphaeaceae and Hydrocharitaceae as well as Cupressaceae and Nyssaceae show that a *Nyssa/Taxodium* swamp still existed in behind shallow water habitats at least in parts of the lake. Further typical swamp elements such as Ericaceae (*Ericipites* spp.) or *Sphagnum* (*Stereisporites* sp.) occur for the first time. Therefore, the frequency of herbaceous elements in the palynoflora and the onset of lignite deposition indicate that wet areas were widely distributed around the lake in areas newly formed due to lake shrinkage following a drop in water level (Fig. 4.6.11).
Since spectral analysis of brightness values from the alternation of lignite layers and interbedded grey-green mudstones in LZ4 yielded periodic signals, Hofmann et al. (2005) suggested an orbital control of the lake level related to precession-paced changes in annual precipitation. Erosional structures within the succession of LZ4 (Fig. 4.6.3d) and the complete lack of rooting structures below the lignites prove an allochthonous origin and transport of plant material from the swamp areas into the lake (Hofmann et al. 2005). This indicates repeated erosion and redeposition possibly related to tectonic activity. Therefore, an orbital control for the alternation of lignites and mudstones in relation to fluctuating lake levels as suggested by Hofmann et al. (2005) cannot be proven.
A higher lake level and a profundal depositional environment were established again during PZ5 (Fig. 4.6.11). The succession of bituminous shales within LZ5 indicates an increased water depth due to rapid subsidence of the lake basin (Fig. 4.6.3e). Compared to the pollen

assemblage from the earlier part of bituminous shale deposition (LZ3, PZ3b) significant changes become obvious towards the top. Accordingly, the samples from PZ5 are distinctly separated from the samples of PZ3b in the DCA along the first axis (Fig. 4.6.10b). A change among the dominant elements of the climax forest vegetation is indicated by a strong increase in *Tricolporopollenites microreticulatus* (Oleaceae), *Plicapollis* spp. (Juglandaceae) and *T. liblarensis* (Fagaceae, Leguminosae). These elements therefore plot on the negative side of axis 1 on the DCA, separated from the taxa of the (para)tropical forest, which were dominant within PZ's 3 and 4 (Fig. 4.6.10b).
Plicapollis and *Nudopollis*, two elements of the extinct Normapolles group are now abundant and represent a relict of a warm Cretaceous vegetation (Fig. 4.6.4). The respective plants may have represented an ancestral group of extant fagaleans (e.g., Schöneberger et al. 2001; Friis et al. 2006) which were distributed in warm and dry environments (Daly and Jolley 2015). The distribution of *Plicapollis* and *Nudopollis* therefore indicates that PZ5 was deposited during a less humid phase compared to PZ3b. Accordingly, other Normapolles elements which have been assigned to cooler and more humid environments such as *Interpollis* (Daly and Jolley 2015) still existed in PZ3b and 4 but disappeared in PZ5. The DCA (Fig. 4.6.10b) with the separation of PZ's 3a to 5 from right to left along axis 1 therefore indicates that changes in relative humidity or precipitation were responsible for differences in the composition of the vegetation.
Two different associations can therefore be distinguished within the climax forest and swamp vegetation (Fig. 4.6.10b). During the older PZ's 3a and 3b swamp elements such as Cupressaceae (*Inaperturopollenites* spp., *Cupressacites bockwitzensis*) as well as tropical elements, such as Sapotaceae (*Tetracolporopollenites* spp.) prevailed indicating a warm and wet climate. In the youngest PZ5 other elements were abundant, such as Oleaceae (*T. microreticulatus*) or Juglandaceae (*Plicapollis* spp.), which point to less humid conditions. In both forest and swamp associations however, the dominating elements, such as *T. libarensis, T. cingulum* or *T. parmularius* remained relatively constant in abundance (Fig. 4.6.4) indicating that the general composition of the forest in the vicinity of the lake did not change, except for few taxa.

Conclusions

Compared to other nearby lakes of Eocene age, Lake PvH most probably was not a maar lake, but occupied a small pull-apart basin. Tectonic activity significantly influenced the long-term evolution of the lake basin by causing phases of relatively rapid subsidence resulting in deposition of organic-rich mudstones and bituminous shales. In contrast, shallow water phases with deposition of allochthonous lignite may have been related to periods of quiescent tectonic activity and limited subsidence.
As well as tectonic activity, changes in humidity can be recognized especially through long-term changes within the forest vegetation. In summary, a combination of both, regional tectonic activity and climate change (humidity) had a significant impact on the palaeoenvironment and the evolution of the ecosystem. As a result, the development of the vegetation at PvH differs significantly from that described for the maar lakes in the vicinity, such as Lake Messel, where changes within the vegetation during stable depositional conditions are controlled purely by climate change (Lenz et al. 2011, 2017).
In addition, the palynological results show that Lake PvH is considerably older than previously assumed. Lacustrine sedimentation started in the latest Early Eocene almost coeval with deposition of the Lower Messel Formation at Messel. A mammal age for PvH from the mined part of the succession (Franzen 2006) possibly even ranges into the late Eocene and points to a considerable hiatus between the lake sediments in core PvH and the thick lignite which was originally mined at the top of the succession. The existence of the basin at PvH

may therefore have lasted for more than 7 million years in contrast to less than a million years for the maar lake at Messel.

Acknowledgements and funding
Our research has been carried out as a project financed by the Deutscher Akademischer Austauschdienst (DAAD) under the grant MO207-54900347 including the PhD appointment of the first author. This generous support is gratefully acknowledged. The help of Karin Schmidt, Palaeobotanical Section, Senckenberg Research Institute and Natural History Museum Frankfurt, in sampling and sample preparation is also acknowledged. Core photographs of FIS/HLUG from the core B/97- BK9 were kindly supplied by the Department for Messel Research and Mammalogy, Senckenberg Research Institute and Natural History Museum Frankfurt. We also thank Alan Lord (London/Frankfurt am Main) who kindly checked the manuscript for language and consistency. Finally, we thank 3 reviewers for their comments and suggestions which greatly helped to improve this paper.

References

Bohacs, K.M., Carroll, A.R., Neal, J.E. and Mankiewicz, P.J. (2000). Lake-basin type, source potential, and hydrocarbon character: an integrated sequence-stratigraphic-geochemical framework. In: Gierlowski-Kordesch, E.H. and Kelts, K.R. (eds) *Lake basins through space and time*. AAPG Studies in Geology, 46, 3-34.

Boulter, M.C. and Hubbard, R.N. (1982). Objective paleoecological and biostratigraphic interpretation of Tertiary palynological data by multivariate statistical analysis. *Palynology*, **6**, 55-68.

Campbell, E.O. (1983). Mires of Australasia. *In*: Gore, A.J.P. (ed), *Mires: swamp, bog, fen and moor*. Ecosystems of the world, 4B, 153-180.

Carroll, A.R. and Bohacs, K.M. (1999). Stratigraphic classification of ancient lakes: Balancing tectonic and climatic controls. *Geology*, 27, 99-102.

Collinson, M. E., Manchester, S. R. and Wilde. V. (2012). Fossil fruits and seeds of the Middle Eocene Messel biota, Germany. *Abhandlungen der Senckenberg Gesellschaft für Naturforschung*, 570, 1–249.

Cronquist, A. (1981). *An integrated system of classification of flowering plants.* Columbia University Press, New York**.**

Daly, R.J., Jolley, D.W., Spicer, R.A. and Ahlberg, A., (2011). A palynological study of an extinct arctic ecosystem from the Palaeocene of Northern Alaska. *Review of Palaeobotany and Palynology*, 166, 107-116.

Daly, R.J. and Jolley, D.W. (2015). What was the nature and role of Normapolles angiosperms? A case study from the earliest Cenozoic of Eastern Europe. *Palaeogeography, Palaeoclimatology, Palaeoecology*, 418, 141-149.

DeBusk Jr, G.H. (1997). The distribution of pollen in the surface sediments of Lake Malawi, Africa, and the transport of pollen in large lakes. *Review of Palaeobotany and Palynology*, 97, 123-153.

Fahlbusch, V. (1976). Report on the International Symposium on mammalian stratigraphy of the European Tertiary (München, April 11-14, 1975). *Newsletters on Stratigraphy*, 5, 160-176.

Felder, M. and Gaupp, R. (2006). The δ13C and δ18O signatures of siderite a tool to discriminate mixis patterns in ancient lakes. *Zeitschrift der Deutschen Gesellschaft für Geowissenschaften*, 157, 397-410.

Felder, M. and Harms, F.J. (2004). Lithologie und genetische Interpretation der vulkano-sedimentären Ablagerungen aus der Grube Messel anhand der Forschungsbohrung Messel 2001 und weiterer Bohrungen (Eozän, Messel-Formation, Sprendlinger Horst, Südhessen). *Courier Forschungsinstitut Senckenberg*, 252, 151–206.

Felder, M., Harms, F.J. and Liebig, V. (2001). Lithologische Beschreibung der Forschungsbohrungen Groβ-Zimmern, Prinz von Hessen und Offenthal sowie zweier Lagerstättenbohrungen bei Eppertshausen (Sprendlinger Horst, Eozän, Messel-Formation, Süd-Hessen). *Geologisches Jahrbuch Hessen*, 128, 29- 82.

Franzen, J.L. (2006). *Eurohippus parvulus parvulus* (Mammalia, Equidae) aus der Grube Prinz von Hessen bei Darmstadt (Süd-Hessen, Deutschland). *Senckenbergiana lethaea*, 86, 265-269.

Friis, E.M., Raunsgaard Pederse, K. and Schöenberger, J. (2006). Normapolles plants: a prominent component of the Cretaceous rosid diversification. *Plant Systematics and Evolution*, 260, 107–140.
Galloway, J.M., Tullius, D.N., Evenchick, C.A., Swindles, G.T., Hadlari, T. and Embry, A. 2015. Early Cretaceous vegetation and climate change at high latitude: Palynological evidence from Isachsen Formation, Arctic Canada. *Cretaceous Research*, 56, 399-420.
Gauch, A.G. 1982. *Multivariate analysis in community ecology*. Cambridge University Press, Cambridge.
Gruber, G. and Micklich, N. 2007. *Messel - Tresures of the Eocene. Book to the Exhibition "Messel on Tour".* Hessisches Landesmuseum Darmstadt, Darmstadt.
Hammer, Ø., Harper, D.A.T. and Ryan, P.D. (2001). PAST: Paleontological Statistics Software Package for Education and Data Analysis. *Palaeontologia Electronica*, 4**,** http://palaeo-electronica.org/ 2001_1/past/issue1_01.htm.
Harms, F.J. With contributions of Wallner, H. and Jacoby,W.R. (1999). *Karte zur Verbreitung der Messel-Formation/Faltblatt Welterbe Grube Messel. Map, back side with comment*. Hessisches Landesamt für Bodenforschung, Wiesbaden.
Harms, F.J. (2005). Ehemaliger Braunkohlen-Tagebau "Grube Prinz von Hessen", Darmstadt, auf historischen Fotos. *Naturwissenschaftlicher Verein Darmstadt – Bericht N.F.* 28, 57-80.
Harms, F.J., Aderhold, G., Hoffmann, I., Nix, T. and Rosenberg, F. (1999). Erläuterungen zur Grube Messel bei Darmstadt, Südhessen. *Schriftenreihe der Deutschen Geologischen Gesellschaft*, 8, 181-222.
Harrington, G., Kemp, S. and Koch, P. (2004). Palaeocene–Eocene paratropical floral change in North America: responses to climate change and plant immigration. *Journal of the Geological Society*, 161, 173-184.
Heywood, V.H. (1993). *Flowering plants of the world. Updated edition*. Oxford University Press, New York.
Hill, M.O. and Gauch, H.G. (1980). Detrended Correspondence Analysis: an improved ordination technique. *Vegetatio*, 42, 47-58.
Hochuli, P.A. (1979). Ursprung und Verbreitung der Restionaceen. *Vierteljahrsschrift der Naturforschenden Gesellschaft in Zürich*, 124, 109-130.
Hofmann, P., Duckensell, M., Chpitsglous, A. and Schwark, L. (2005). Geochemical and organic petrological characterization of the organic matter of lacustrine Eocene oil shales (Prinz von Hessen, Germany): reconstruction of the depositional environment. *Paleolimnology*, 33, 155–168.
Jacoby, W. (1997). Tektonik und Eozäner Vulkanismus des Sprendlinger Horstes, NE-Flanke des Oberrheingrabens. *Schriftenreihe der Deutschen Geologischen Gesellschaft*, 2, 66–67.
Jacoby, W., Wallner, H. and Smilde, P. (2000). Tektonik und Vulkanismus entlag der Messel-Störungszone auf dem Sprendlinger Horst: Geophysikalische Ergebnisse. *Zeitschrift der Deutschen Gesellschaft für Geowissenschaften*, 151, 493-510.
Jacoby, W., Sebazungu, E., Wallner, H., Gabriel, G. and Pucher, R. (2005). Potential field data for the Messel Pit and surroundings. *Courier Forschungsinstitut Senckenberg*, 255, 1–9.
Janssen, C.R. and Birks, H.J.B. (1994). Recurrent groups of pollen types in time. *Review of Palaeobotany and Palynology*, 82, 165–173.
Juggins, S. (2007). *C2 Software for ecological and palaeoecological data analysis and visualization. User guide Version,* 1.5, 73.
Kaiser, M.L. and Ashraf, R. (1974). Gewinnung und Präparation fossiler Pollen und Sporen sowie anderer Palynomorphae unter besonderer Berücksichtigung der Siebmethode. *Geologisches Jahrbuch*, 25, 85–114.
Krumbiegel, G., Rüffle, L. and Haubold, H. (1983). *Das eozäne Geiseltal, ein mitteleuropäisches Braunkohlevorkommen und seine Pflanzen- und Tierwelt*. Neue Brehm-Bücherei, 273, A. Ziemsen, Wittenberg.
Krutzsch, W. (1966). Die sporenstratigraphische Gliederung des Tertiär im nördlichen Mitteleuropa (Paläozän-Mitteloligozän), methodische Grundlagen und gegenwärtiger Stand der Untersuchungen. *Abhandlungen des Zentralen Geologischen Instituts*, 8, 112–149.
Krutzsch, W. (1970). Die stratigraphisch verwertbaren Sporen- und Pollenformen des mitteleuropäischen Alttertiärs. *Jahrbuch für Geologie*, 3, 309-379.

Lenz, O.K. (2005). Palynologie und Paläoökologie eines Küstenmoores aus dem Mittleren Eozän Mitteleuropas Die Wulfersdorfer Flözgruppe aus dem Tagebau Helmstedt, Niedersachsen. *Palaeontographica B*, 271, 1–157.

Lenz, O.K. and Riegel, W. (2001). Isopollen Maps as a tool for the Reconstrauction of a Coastal Swamp from the Middle Eocene at Helmstedt (Northern Germany). *Facies*, 45, 177-194.

Lenz, O.K., Wilde, V. and Riegel, W. (2007). Recolonization of a Middle Eocene volcanic site: quantitative palynology of the initial phase of the maar lake of Messel (Germany). *Review of Palaeobotany and Palynology*, 145, 217 – 242.

Lenz, O.K., Wilde, V. and Riegel, W. (2011). Short-term fluctuation in vegetation and phytoplankton during the middle Eocene greenhouse climate: a 640-kyr record from the Messel oil shale (Germany). *International Journal of Earth Sciences*, 100, 1851-1874.

Lenz, O.K., Wilde, V., Mertz, D.F. and Riegel, W. (2015). New palynology-based astronomical and revised $^{40}Ar/^{39}Ar$ ages for the Eocene maar lake of Messel (Germany). *International Journal of Earth Sciences*, 104, 873-889.

Lenz, O.K., Wilde, V. and Riegel, W. (2017). ENSO-and solar-driven sub-Milankovitch cyclicity in the Paleogene greenhouse world: high resolution pollen records from Eocene Lake Messel, Germany. *Journal of the Geological Society*, 174, 110-128.

Leroy, S., Kazanci, N., İleri, Ö., Kibar, M., Emre, O., McGee, E. and Griffiths, H.I. (2002). Abrupt environment changes within a late Holocene lacustrine sequence south of the Marmara Sea (Lake Manyas, N-W Turkey): possible links with seismic events. *Marine Geology*, 190, 531-552.

Lutz, H., Kaulfuss, U., Wappler, T., Löhnertz, W., Wilde, V., Mertz, D.F., Mingram, J.F., Franzen, J.L., Frankenhäuser, H. and Kozil, M. (2010). Eckfeld Maar: Window into an Eocene terrestrial habitat in Central Europe. *Acta Geologica Sinica*, 84, 984-1009.

Marell, D. (1989). Das Rotliegende zwischen Odenwald und Taunus. – *Geologische Abhandlungen Hessen*, 89: 1-128.

Mai, D:h. (1981). Entwicklung und klimatische Differenzierung der Laubwaldflora Mitteleuropas im Tertiär. *Flora,* 171, 525-582.

Mai, D.H. (1995). *Tertiäre Vegetationsgeschichte Europas—Methoden und Ergebnisse*. Gustav Fischer Verlag, Jena.

Manchester, S.R. (1989). Attached reproductive and vegetative remains of the extinct American–European genus Cedrelospermum (Ulmaceae) from the early Tertiary of Utah and Colorado. *American Journal of Botany*, 76, 256–276.

Mezger, J.E., Felder, M. and Harms, F.-J. (2013). Crystalline rocks in the maar deposits of Messel: key to understand the geometries of the Messel Fault Zone and diatreme and the post-eruptional development of the basin fill. *Zeitschrift der Deutschen Gesellschaft für Geowissenschaften*, 164, 639–662.

Micklich, N. (2012). Peculiarities of the Messel fish fauna and their palaeoecological implications: a case study. *Palaeobiodiversity and Palaeoenvironments*, 92, 585–629.

Nickel, B. (1996). Die mitteleozäne Mikroflora von Eckfeld bei Manderscheid/Eifel. *Mainzer Naturwissenschaftliches Archiv, Beiheft*, 18, 1–121.

Neumann, F.H., Kagen, E.J., Stein, M. and Agnon, A. (2009). Assessment of the effect of earthquake activity on regional vegetation- High- resolution pollen study of the Ein Feshka section, Holocene Dead Sea. *Review of Palaeobotany and Palynology*, 155, 42-51.

Pflug, H. (1986). Palyno-Stratigraphy of the Eocene/Oligocene in the Area of Helmstedt, in North Hessia and in the adjacent southern Range, *In*: Tobien, A. (ed) *Nordwestdeutschland im Tertiär.* Beiträge zur regionalen Geologie der Erde, 38, 567-583.

Pirrung, M. (1998). Zur Entstehung isolierter alttertiärer Seesedimente in zentraleuropäischen Vulkanfeldern. *Mainzer Naturwissenschaftliches Archiv, Beiheft*, 20, 117.

Prentice, I.C. 1(980). Multidimensional scaling as a research tool in Quaternary palynology: a review of theory and methods. *Review of Palaeobotany and Palynology*, 31, 71-104.

Riegel, W., Lenz, O.K. and Wilde, V. (2015). From open estuary to meandering river in a greenhouse world: an ecological case study from Middle Eocene of Helmstedt, Northen Germany. *Palaios*, 30, 304-326.

Riegel, W. and Wilde, V. (2016). An early Eocene Sphagnum bog at Schöningen, northern Germany. *International Journal of Coal Geology*, 159, 57-70.

Schaal, S. and Ziegler, W. (1988). *Messel - ein Schaufenster in die Geschichte der Erde und des Lebens.* Waldemar Kramer, Frankfurt am Main.
Schaarschmidt, F. (1988). Der Wald, fossile Pflanzen als Zeugen eines warmen Klimas, *In*: Schaal, S. and Ziegler, W. (eds) *Messel - ein Schaufenster in die Geschichte der Erde und des Lebens.* Waldemar Kramer, Frankfurt am Main, 27-52.
Schönenberger, J., Pedersen, R.K. and Friis, E.M. 2001. Normapolles flowers of fagalean affinity from the Late Cretaceous of Portugal. *Plant Systematics and Evolution*, 226, 205–230.
Stukins, S., Jolley, D.W., McIlroy, D. and Hartley, A.J. (2013). Middle Jurassic vegetation dynamics from allochthonous palynological assemblages: an example from a marginal marine depositional setting; Lajas Formation, Neuquén Basin, Argentina. *Palaeogeography, Palaeoclimatology, Palaeoecology*, 392, 117-127.
Suc, J.P. and Drivaliari, A. (1991). Transport of bisaccate coniferous fossil pollen grains to coastal sediments: an example from the earliest Pliocene Orb Ria (Languedoc, Southern France). *Review of Palaeobotany and Palynology*, 70, 247-253.
ter Braak, C.J.F. and Looman, C.W.N. (1995). Regression. *In*: Jongman, R.H.G., Ter Braak, C.J.F. and Tongeren, O.F.R. (eds) *Data analysis in community and landscape ecology*. Cambridge University Press, Cambridge, 29–77.
ter Braak, C.J.F. and Smilauer, P. (2002). CANOCO Reference Manual and CanoDraw for Windows User's Guide: Canonical Community Ordination (version 4.5). *Microcomputer Power*, Ithaca, New York.
ter Braak, C.J.F. and Smilauer, P. (2009). Canoco. *Wageningen: Biometris Plant Research International.*
Thiele-Pfeiffer, H. (1988). Die Mikroflora aus dem mitteleozänen Ölschiefer von Messel bei Darmstadt. *Palaeontographica B*, 211, 1–86.
Thomson, P.W. and Pflug, H. (1953). Pollen und Sporen des mitteleuropäischen Tertiärs. Gesamtübersicht über die stratigraphisch und paläontologisch wichtigen Formen. *Palaeontographica B*, 94, 1–138.
Vellekoop, J., Smit, J., van de Schootbrugge, B., Weijers, J.W., Galeotti, S., Damste, J.S.S. and Brinkhuis, H. (2015). Palynological evidence for prolonged cooling along the Tunisian continental shelf following the K–Pg boundary impact. *Palaeogeography, Palaeoclimatology, Palaeoecology*, 426, 216-228.
Wilde, V. (1989). Untersuchungen zur Systematik der Blattreste aus dem Mitteleozän der Grube Messel bei Darmstadt (Hessen, Bundesrepublik Deutschland). *Courier Forschungsinstitut Senckenberg*, 115, 1–123.
Wilde, V. (2004). Aktuelle Übersicht zur Flora aus dem mitteleozänen "Ölschiefer" der Grube Messel bei Darmstadt (Hessen, Deutschland). *Courier Forschungsinstitut Senckenberg*, 252, 109–114.

4-7 Publication 3: Lake level fluctuations and allochthonous lignite deposition in the Eocene pull-apart basin "Prinz von Hessen" (Hesse, Germany) - A palynological study.

Accepted in Syntheses in Limnogeology, Rosen, M.R., Finkelstein, D., Park Boush, L., Pla-Pueyo, S. (eds.): Limnogeology: Progress, challenges and apportunities: A tribute to Beth Gierlowski-Kordesch, Chapter 3. Springer Nature article in press.

Maryam Moshayedi[1*], Olaf K. Lenz[1, 2], Volker Wilde[3], Matthias Hinderer[1]
[1]Technische Universität Darmstadt, Institute of Applied Geosciences, Applied Sedimentology, Schnittspahnstrasse 9, 64287 Darmstadt, Germany.
[2]Senckenberg Gesellschaft für Naturforschung, General Directorate, Senckenberganlage 25, 60325, Frankfurt am Main, Germany.
[3]Senckenberg Forschungsinstitut und Naturmuseum, Sektion Paläobotanik, Senckenberganlage 25, 60325, Frankfurt am Main, Germany.

Author Contributions

Conceptualization: M. Moshayedi, Olaf K. Lenz, Volker Wilde, M. Hinderer
Data Curation: M.Moshayedi
Formal Analysis: M. Moshayedi
Funding Acquisition: M. Moshayedi
Investigation: M. Moshayedi,
Methodology: M. Moshayedi, Olaf K. Lenz, Volker Wilde
Project Administration: Olaf K. Lenz, Volker Wilde, M. Hinderer
Resources: M. Hinderer, V. Wilde
Validation: M. Moshayedi
Visualization: M. Moshayedi
Writing – Original Draft Preparation: M. Moshayedi
Writing – Review and Editing: Olaf K. Lenz, V. Wilde

Abstract
High resolution palynological analysis of 52 core samples from a distinct part of the lacustrine filling of the Eocene pull-apart basin "Grube Prinz von Hessen" in Southwest Germany has been applied to recognize driving factors responsible for changes in vegetation and environment. The 15 m studied interval is characterized by a specific alternation of lignite beds and mudstones which were deposited when the lake had reached its smallest extent. The diverse and well-preserved palynoflora shows that the shoreline and the marginal swamp around the lake were dominated by herbaceous and woody swamp communities, whereas the forest association in the hinterland was mainly dominated by Juglandaceae and Fagaceae. Non-metric multidimensional scaling and Q- and R-mode cluster analyses of the microflora reveal strong differences between the palynomorph assemblages of lignite and mudstone beds. The situation in the vicinity of the lake was influenced by tectonic activity, such as earthquake tremor, resulting in the redeposition of lignite and mudstone. Nevertheless, the same subordinate trend in the vegetation is obvious in the microflora of both lithologies. Slight qualitative changes may be explained by slightly decreasing temperature and precipitation during the deposition of the studied section. Therefore, changes in the paleoenvironment and the ecosystems were mainly controlled by tectonic activity, but some influence of climate change may also be noted.

Key words: Central Germany, Paleogene, palynology, lacustrine sediments, climate change, tectonic activity

Introduction

The Sprendlinger Horst in Southwest Germany consists of a Palaeozoic metamorphic and magmatic basement with a Rotliegend (Lower Permian) sedimentary cover (Marell 1989), and represents the northern extension of the Odenwald basement which is flanking the Upper Rhine Graben to the northeast (Fig. 4.7.1). Several small, isolated basins filled by lacustrine sediments of Paleogene age are known from the area, some of which have been studied from drill cores. Most of them represent the filling of maar-type volcanic structures (e.g., Jacoby 1997; Harms et al. 1999; Jacoby et al. 2000; Felder and Harms 2004). This includes the Eocene maar lake of Messel, which is well-known for the perfect preservation of fossils and was in the focus of numerous palaeoenvironmental studies (e.g., Schaal and Ziegler 1988; Gruber and Micklich 2007; Lenz et al. 2007, 2011; Collinson et al 2012; Smith et al. 2018).
Another Eocene record on the Sprendlinger Horst which has been cored is the lacustrine filling of Lake "Prinz von Hessen" (PvH), 5 km northeast of Darmstadt (Hesse, Germany) and 2 km southwest of the maar structure of Messel (Fig. 4.7.1). Nevertheless, in contrast to other Paleogene records on the Sprendlinger Horst which are of phreatomagmatic origin and contain sediments of deep meromictic lakes, the structure at Lake PvH represents a more shallow pull-apart basin (Felder et al. 2001; Hofmann et al. 2005; Felder and Gaupp 2006; Moshayedi et al. 2018).
Because qualitative and quantitative analyses of pollen and spores are especially suited for the reconstruction of plant communities and their evolution (Frederiksen 1996), our palynological study of the lacustrine succession at PvH provides a rare insight into the evolution of a vegetation around a basin that was mainly influenced by tectonic activity and, therefore, experienced a complex pattern of deposition and subsidence. We have shown not only the long-term evolution of the lake, but also that the ecosystem around it had been controlled by tectonic activity resulting in phases of relatively rapid subsidence and deposition of organic-rich mudstone and bituminous shale (Moshayedi et al. 2018). Shallow water phases with deposition of lignite can be related to periods of quiescent tectonic activity and limited subsidence. However, long-term changes in the composition of the forest vegetation at Lake PvH can be attributed to a change in humidity (Moshayedi et al. 2018). Therefore, a

combination of both, regional tectonic activity and climate change (humidity) had a significant impact on the palaeoenvironment and the evolution of this ecosystem (Moshayedi et al. 2018).

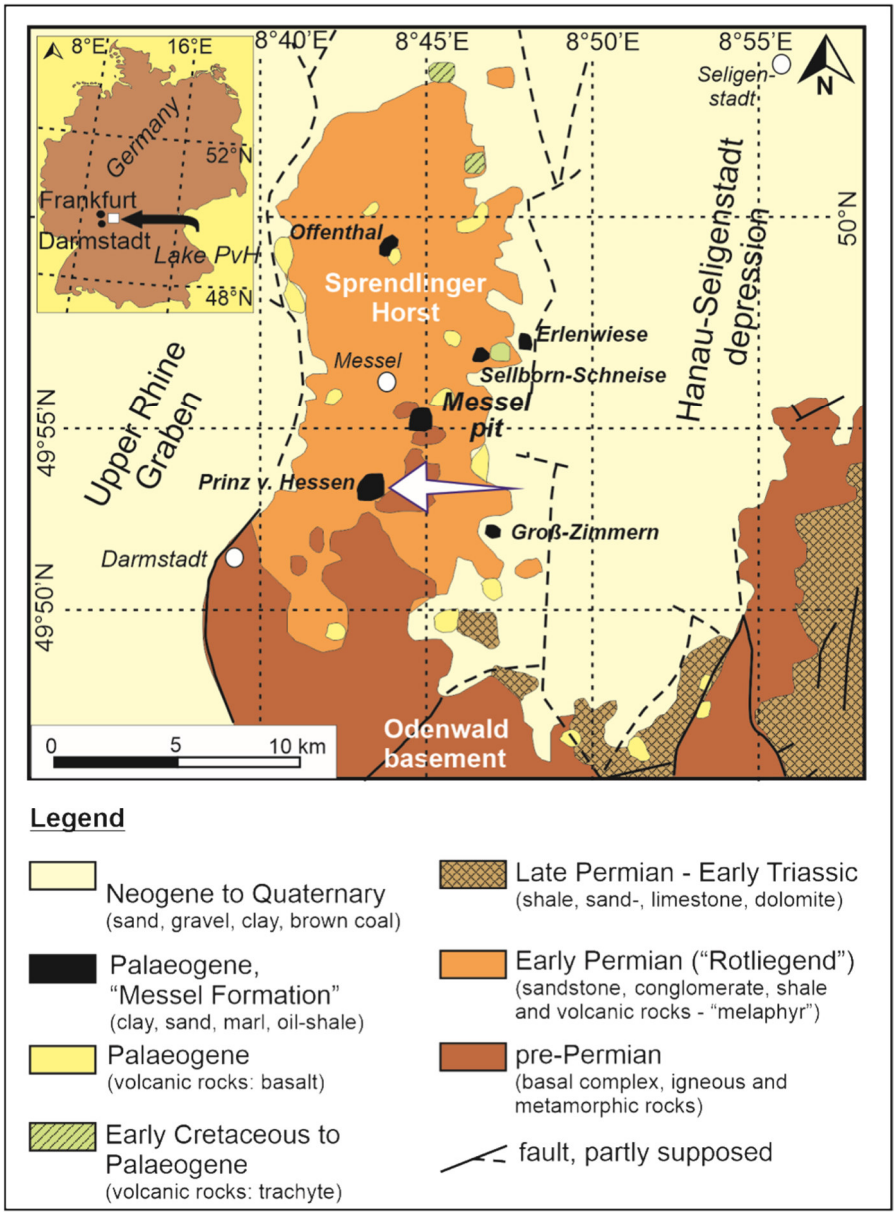

Fig. 4. 7. 1. Geological map of the Sprendlinger Horst (Southwest Germany) showing the location of Eocene Lake Prinz von Hessen (PvH) and other Palaeogene sites in the area (modified after Harms et al. 1999 and Lenz et al. 2007).

Here, we present a high resolution palynological study of a specific part of the lacustrine succession of Lake PvH, which is characterized by alternating beds of lignite and mudstone, representing a shallow phase of the lake`s evolution. Orbital control of changes in annual precipitation and related lake-level fluctuations have been suggested as a possible trigger for the regular alternation of lignite and mudstone beds (Hofmann et al. 2005). We have tested if this alternation in lithofacies may serve as a record for orbitally controlled vegetational change in the Paleogene greenhouse system, or if other factors influenced the sedimentary environment and the composition of the vegetation.

Geological setting

In contrast to the lacustrine fillings of maar-type volcanic structures, such as those at Messel or Offenthal (e.g., Harms et al. 1999; Jacoby et al. 2000; Felder and Harms 2004), PvH is special among the Paleogene deposits on the Sprendlinger Horst because it does not show the typical succession of lithozones as described for maar lakes by Pirrung (1998). Furthermore, the isotopic values of siderite (δ^{13}Carbon and δ^{18}Oxygen) in the sediments at PvH are significantly lower than typical values for long-lived deep and meromictic maar lakes (Felder and Gaupp 2006), These values fit those typical for open holomictic systems on river deltas or alluvial plains in which the position of the redox boundary is near to the sediment surface (Felder and Gaupp 2006). Therefore, the sedimentary succession discussed here for Lake PvH was deposited in a significantly shallower setting than a typical deep maar lake, and probably filled a small pull-apart basin (Felder et al. 2001; Felder and Gaupp 2006; Moshayedi et al. 2018).

A continuous core was drilled in 1997 in the centre of the lake basin (49°53'56.64" N, 8°43'48.31"E) which has a diameter of 600 to 800 m and was surrounded by sediments of Permian age (Felder et al. 2001). The 150 m long core revealed in the lower 55 m a clast supported, poorly sorted breccia with a mixed allochthonous succession, composed of Permian (Rotliegend) sandstones, granodiorite and other fragments of the crystalline basement (Felder et al. 2001). In the upper 20 m of the breccia frequent lapilli appear. This part is followed by a 95 m succession of lacustrine sediments that were separated in a previous study in five lithozones (Moshayedi et al. 2018).

Previous work

Sedimentology of the lacustrine succession

Based on lithological changes and the description of the fresh core by Felder et al. (2001) the 95 m thick lacustrine succession at PvH has been divided in five lithozones from bottom to top (LZ1-5; Fig. 4.7.2) by Moshayedi et al. (2018).

In LZ1, between 95 m and 64.80 m (Fig. 4.7.2), the sediments are characterized by layers of well bedded to laminated calcareous sand, silt, and clay suggesting proximity to a source of clastic material. The sediment was transported to the lake probably by river(s) and different grainsize depended on changes in discharge rates. Occasional remobilization of the sediment produced graded bedding. LZ1 is comparable with a fluvial–lacustrine facies association (Carroll and Bohacs 1999), typical for an overfilled lake, in which the influx of water and sediment generally exceeds potential accommodation (Moshayedi et al. 2018).

LZ2, between 64.80 and 55.40 m (Fig. 4.7.2), is characterized by frequent changes in lithology and sedimentological processes including the deposition of bituminous shale with interbedded turbidites, grainflows, and mudflows. The first beds of laminated bituminous shale occur at a depth of 60.55 m. A high total sulphur content with an average of 2.5% and the lamination indicate that during this stage the lake was deep enough for a permanent chemocline and sub-oxic to euxinic conditions in its deep hypolimnion (Hofmann et al. 2005). In LZ2 and also in the succeeding LZ 3 the deposition of laminated organic-rich bituminous shale and mudstone (Fig. 4.7.2) with TOC values up to 45% (Hofmann et al. 2005) characterizes a fluctuating profundal (deepwater) facies association with changing lake level (Moshayedi et al. 2018). In such balanced-filled lakes tectonic accommodation equals water and sediment fill (Carroll and Bohacs 1999, Bohacs et al. 2000).

Laminated bituminous shale without bioturbation is typical for the succeeding LZ3, between 55.40 and 44.70 m, and indicates an open lake and increased water depth (Fig. 4.7.2; Moshayedi et al. 2018). Anaerobic conditions in the sediment at the lake bottom and a poorly oxygenated lower part of the water column are indicated by a total sulphur content in the bituminous shale of <1% (Hofmann et al. 2005). In samples above 47.5 m an increasing amount of detrital quartz (Hofmann et al. 2005) may indicate shallowing of the lake.

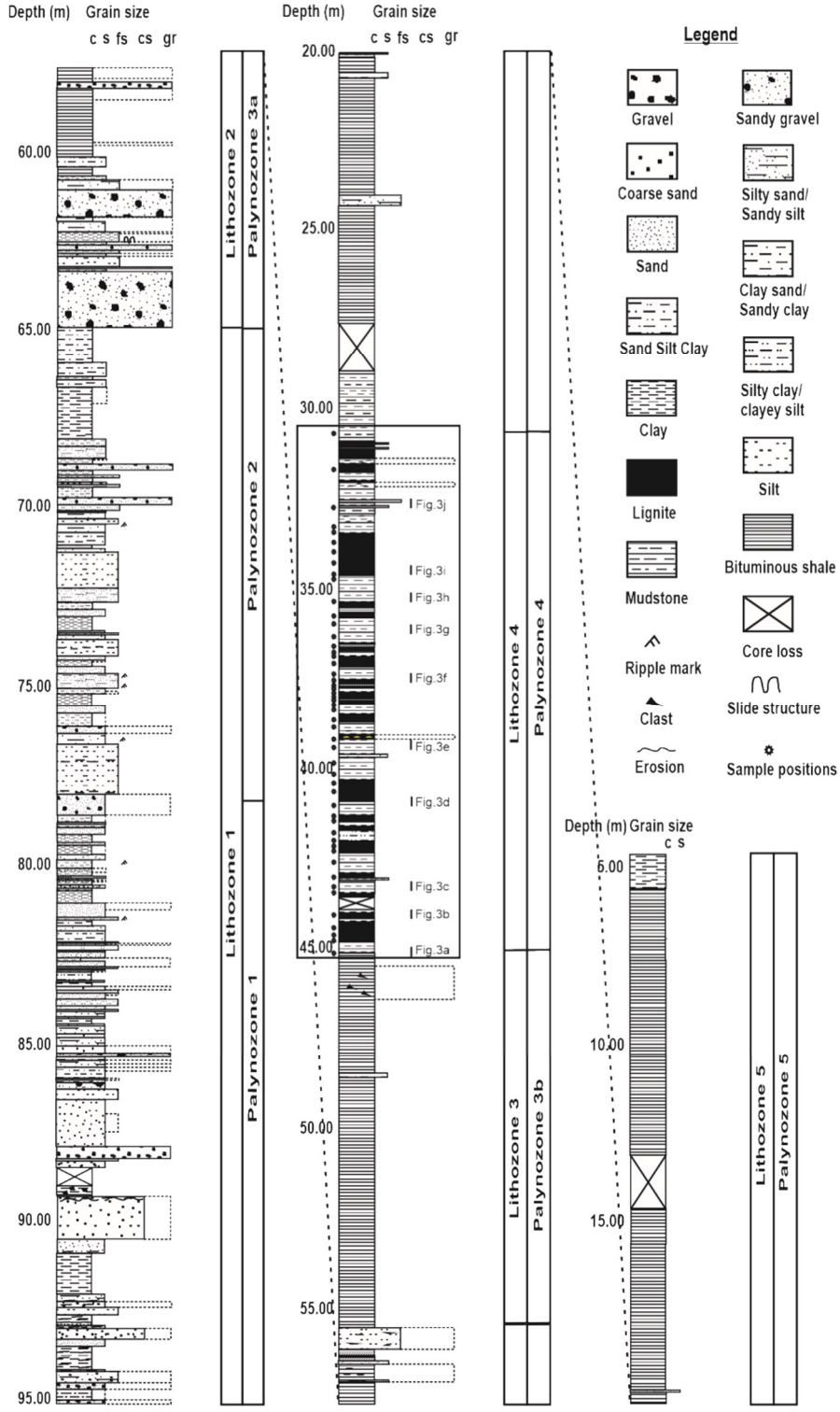

Fig. 4. 7. 2. Generalized section of the "Prinz von Hessen" core showing lithozones and palynozones of Moshayedi et al. (2018). The part of the core that has been studied for the present paper is framed. Within the frame, the position of samples is indicated by black dots, and the position of core images selected for Fig. 3 is shown by grey bars.

LZ4, between 44.70 and 30.82 m (Fig. 4.7.2), which is in the focus of the present study, shows an alternation of at least 20 lignite layers, with thicknesses ranging between 5 and 100 cm, and interbedded grey-green mudstone (Fig. 4.7.3). The TOC content of the lignite is between 50 and 60% (Hofmann et al. 2005). The lignite consists primarily of woody organic matter of the huminite group, which indicates a source either from terrestrial higher plants or

from aquatic macrophytes which lived in the shallow littoral zone (Hofmann et al. 2005). Compared to the lignite, the interbedded massive mudstone is poor in organic matter (<10 % TOC; Hofmann et al. 2005). LZ4 indicates a period with a very low lake level and a change to a more fluvial–lacustrine facies (Moshayedi et al. 2018).
In LZ5, between 30.82 and 4.67 m (Fig. 4.7.2), massive mudstone and sometimes laminated bituminous shale with TOC values <10% (Hofmann et al. 2005) indicate a similar depositional environment as for LZ3. The lignite layers that are typical of LZ4 disappear completely (Fig. 4.7.2), but lignite clasts can be found in some of the mudstones and shales (Hofmann et al. 2005). LZ5 represents a further profundal facies association comparable with LZ2 and 3 (Moshayedi et al. 2018).
The abrupt changes of lithofacies separating the different lithozones suggest that tectonic activity has influenced the evolution of the basin by rapid uplift and subsidence (Moshayedi et al. 2018). This is especially true for the change between LZ's 1 and 2, which records considerable deepening of the lake within a few metres of sediment. The frequent occurrence of mass flows and turbidites, especially at the transitions between the individual facies associations and LZ's, may relate to strong tectonic events such as earthquakes during the history of the lake (Moshayedi et al. 2018).

Palynology
In a palynological study that was designed to unveil both long- and short-term changes in the vegetation over the entire time of deposition of the lacustrine sediments at PvH, five vegetational stages during the deposition time, resulting in five palynozones (PZ1 to 5; Fig. 4.7.2), were recognized (Moshayedi et al. 2018). They show an almost perfect correlation to the lithozones, indicating that sedimentary processes, tectonic activity and the deposition of palynomorphs are depending on each other (Moshayedi et al. 2018).
In PZ's 1 and 2, which encompass the fluvial-lacustrine facies of LZ 1, widespread fern meadows flourishing under wet conditions at the shoreline or in marginal swamps are represented by high numbers of fern spores. They strongly increase between PZ1 and PZ2 without a significant change in lithology and depositional environment. Therefore, this increase is probably not related to taphonomic processes and may indicate a change to more humid conditions from PZ1 to PZ2 (Moshayedi et al. 2018). This is supported by a decrease of pinaceous pollen, because Pinaceae are regarded as more tolerant of less humid conditions and well-drained soils than most of the plants that form components of the regular PvH forest (Moshayedi et al. 2018). The forest was characterized by elements of a climax stage of the Paleogene European vegetation, typical for inland sites of Western and Central Europe during the greenhouse period of the Eocene (Mai 1981, 1995; Schaarschmidt 1988, Wilde 1989, Collinson et al. 2012), such as Fagaceae or Juglandaceae. Different species of Cupressaceae indicate that some swamp forest elements existed at the edge of the lake (Moshayedi et al. 2018).
Compared with the palynomorph assemblages of the fluvial–lacustrine facies association of LZ1 the strong decline or even disappearance of most fern spores is noteworthy in PZ3 (fluctuating profundal facies association; LZ 2). This abrupt decrease is correlated with the change in lithology and therefore coupled to a rapid deepening of the lake (Moshayedi et al. 2018). Therefore, tectonic activity and related changes in the palaeoenvironment at Lake PvH were probably responsible for changes in the vegetation (Moshayedi et al. 2018). A strong peak of Restionaceae as a typical herbaceous swamp element in PZ3 is further evidence for changes in the vegetation at the lakeside. They point to a higher and oscillating lake level (Moshayedi et al. 2018). A higher lake level and extended shallow water areas at the lakeside are also indicated by the distribution of submersed and floating plants such as Hydrocharitaceae and Nymphaeaceae (Moshayedi et al. 2018).

A specific vegetational composition is represented in PZ4, encompassing the alternation of lignite and mudstone beds of LZ4, which are in the focus of our high-resolution study presented here. The high abundance of herbaceous elements in the palynoflora and the onset of lignite deposition indicate that wet areas were widely distributed around the lake in areas newly formed due to a drop in lake level (Moshayedi et al. 2018).
In PZ5 lake level increased and a profundal facies developed again (LZ5). Cupressaceae from the edge of the lake and Fagaceae from the climax vegetation in the vicinity of the lake still are dominating elements during PZ5. While they remained the decrease of Sapotaceae pollen and relicts of a warm Cretaceous vegetation (Normapolles group) from the lower to the upper zones and the simultaneous increase of some juglandaceous taxa point to slight changes in the composition of the vegetation, which probably were related to climate change (Moshayedi et al 2018).

Stratigraphy
In the 1920´s, lignite was mined from the uppermost part of the succession at PvH in an area ca. 250 m east of the drilling site. The presence of *Eurohippus parvulus parvulus*, an early equid, in the mined lignite succession points to a late middle Eocene to middle late Eocene age (European mammal chronology zones MP13-MP16; Franzen 2006). This comparatively thick lignite was not recovered in the core (Moshayedi et al. 2018) and probably represented the final silting-up phase of Lake PvH. Nevertheless, the palynological study of the lacustrine succession revealed a typical Lower Eocene palynomorph assemblage and proved that the lower part of the succession at PvH is considerably older (Moshayedi et al. 2018). Therefore, the lake basin has probably existed for a significantly longer time (~6-8 Ma) than the nearby Eocene maar lakes including Messel (~1 Ma, Lenz et al. 2015).

Methods
Sampling and sample processing
For high resolution palynological analysis, 52 samples were selected from the part of the core between 45 and 30 m depth (LZ 4, Fig. 4.7.2), which is mainly characterized by an alternation of c. 20 lignite beds and interbedded mudstone. Compared to the overview of Moshayedi et al. (2018), the number of analyzed samples for this core segment has been increased by 43 samples. The sample interval is approximately 10 cm and at least one sample in each bed has been analyzed (Fig. 4.7.2).
Palynological preparation followed the standard procedures as described by Kaiser and Ashraf (1974) including treatment with hydrochloric acid (HCl), hydrofluoric acid (HF), and potassium hydroxide (KOH). To remove flocculating organic matter and improve the transparency of the palynomorphs, the residue was briefly oxidized with nitric acid (HNO_3) or hydrogen peroxide (H_2O_2) after sieving with a mesh size of 10 µm. Remaining sample material and slides are stored at the Senckenberg Forschungsinstitut und Naturmuseum, Sektion Paläobotanik, Frankfurt am Main, Germany.

Quantitative palynological analysis
Numerical analyses of palynological data are based on quantitative palynomorph counts. At least 300 individual palynomorphs per sample were identified and counted at 400 times magnification to obtain a representative dataset for statistical analysis. A complete list of all palynomorphs encountered during the present study together with the raw data table is included in the supplementary material. Identification of palynomorphs is based on the systematic-taxonomic studies of Thomson and Pflug (1953), Thiele-Pfeiffer (1988), Nickel (1996), and Lenz (2005). Nevertheless, a relatively high proportion of 10- 20% of the total assemblages is poorly preserved and has been counted as “Varia”. Morphologically similar

sporomorph taxa, which have been assigned to the same parent plant family, were lumped to minimize potential errors in the identification and counting of individual species.
The pollen diagram shows the abundance of the most important palynomorphs in percentages. They are arranged according to their weighted average value (WA regression, Ter Braak and Looman 1996) in relation to depth using the software C2 1.7.6 (Juggins 2007). This arrangement led to a structured pollen diagram showing the major patterns of compositional variation in relation to depth and revealed the different steps in the progression of the plant community (Janssen and Birks 1994). Pollen and spores were calculated to 100%, whereas algae, such as *Botryococcus* and *Ovoidites*, were added as additional percentages (in % of the total sum of pollen and spores).

Statistical analysis
For statistical analyses we used Wisconsin double standardized raw data values (Bray and Curtis 1957; Cottam et al. 1978; Gauch and Scruggs 1979; Oksanen 2007). Hence, the species counts are standardized by dividing the empirical value by the maximum counting value across all samples for each species; then, sample counts are standardized by finding the proportion of each species versus the total sum for each sample. This equalizes the effects of rare and abundant taxa, and removes the influence of sample size on the analysis (Bray and Curtis 1957; Cottam et al. 1978). Nevertheless, rare species with a maximum value <1.5%, which do not show any significant pattern throughout the pollen diagram were excluded from statistical analyses. Remains of algae were included in the numerical analysis because their appearance in parts of the section is important for the definition of individual palyno-phases.
To illustrate compositional differences and ecological trends, and to visualize the level of similarity between samples, non-metric multidimensional scaling (NMDS) with the standardized raw data values and the Bray-Curtis dissimilarity has been implemented (Bray and Curtis 1957; Hair et al. 2010) using the software package PAST 3.06 (Hammer et al. 2001). This ordination method was chosen as the appropriate multivariate model, because NMDS is the most robust unconstrained ordination method in ecology (Minchin 1987) and has been successfully applied to palynological data in previous studies (e.g., Jardine and Harrington 2008, Mander et al. 2010, Broothaerts et al. 2014). NMDS avoids the assumption of a linear or unimodal response model between the palynomorph taxa and the underlying environmental gradients, and also avoids the requirement that data must be normally distributed.
NMDS of the complete data set revealed significant differences between the palynomorph assemblages from the mudstone beds and the lignite. Therefore, further analyses included separate cluster and NMDS analyses of both mudstone and lignite samples. For robust zonation of the pollen assemblages in the lignite and mudstone samples, two-way cluster analyses (Q- and R-mode) were applied resulting in a cluster matrix to identify samples with similar palynomorph contents (Q-mode) and to reveal which pollen-spore taxa group together (R-mode). Bootstrapped Q-mode cluster analysis was established by constrained cluster analysis using the unweighted pair-group average (UPGMA) method and Eucledian distance, whereas R-mode cluster analysis applied the unconstrained UPGMA method with the Euclidean distance (software PAST 3.06, Hammer et al. 2001). We have chosen bootstrapped constrained analysis for Q-mode defined sample clusters to group only stratigraphically adjacent samples during the clustering procedure to identify a zonation in the lithological succession and to test if the multiple phases (clusters) are robust or just produced by change (detailed results of the bootstrapping analysis are presented in the supplementary material).

Results

Sedimentology

In the sedimentary record of core PvH between 45 and 30.50 m, lignite beds with a thickness of 1 cm to 1 m alternate with clay-rich, slightly bituminous mudstones (Felder et al., 2001). The following description of this sequence LZ4 of Moshayedi et al. (2018), is based on the photo documentation and the lithological description of the fresh core by Felder et al. (2001). Fig. 4.7.3 shows only representative parts of the succession, however, the complete photo documentation of LZ4 is included in the online supplementary material.

Generally, the succession of LZ4 is characterized by the lack of any bioturbation. There are no traces of rooting beneath any of the lignite layers (Hofmann et al. 2005; Moshayedi et al. 2018). Up to a depth of 44.70 m the lower part of LZ4 consists of a laminated, partly massive mudstone, sometimes containing clasts of mudstone (Fig. 4.7.3a) and bituminous shale, which indicate reworking and redeposition of sediment from the older LZ3 (Moshayedi et al. 2018). The first cm-thick lignite beds, which alternate with laminated to massive, horizontally bedded mudstone of several centimeters in thickness occur between 44.70 and 44.15 m.

Between 44.15 and 42.92 m laminated mudstone dominates, in which 1 to 5 cm thick lignite beds are irregularly intercalated. The mudstone is predominantly horizontally laminated, but the individual laminae may be crinkly. Sometimes a dip of up to 10° can be observed (e.g., 43.80 m, Fig. 4.7.3b). In particular, the lignite shows traces of reworking, because lignite beds either contain a high portion of clastic material (44.03m, Figure 3b) or show erosional bases (43.15 m; Fig. 4.7.3c). Above a lignite bed between 42.92 and 42.78 m depth, laminated to massive mudstones dominate again with some interbedded lignite streaks of <1 cm thickness up to a depth of 42.20 m. The stratification is primarily horizontal, but loop structures and convolute bedding are common.

Up to a depth of 37.40 m an alternation of nine up to 30 cm thick lignite beds and horizontally laminated mudstone follows. Here, the mudstone is in part recognizable as primary and undisturbed (Fig. 4.7.3e). Nevertheless, the mudstone often incorporates lignite clasts (40.90 - 41.05 m, Fig. 4.7.3d), which indicate reworking and transport. In the thick lignite beds, transport and reworking of the organic material is not clearly recognizable, but some of them are also characterized by an erosive base (e.g., 41.60 m and 41.35 m, see supplementary material). Between 37.40 and 37.02 m, a laminated mudstone follows, which shows reworking including the incorporation of massive mudstone as well as lignite clasts (Fig. 4.7.3f). In the succeeding part of the section up to 36.40 m an alternation of five up to 15 cm thick lignite beds and horizontally laminated mudstone occurs again. In contrast, the massive mudstone between 36.40 m and 35.40 m is characterized by in-situ displacement and mixing of the sediment, indicated by convolute bedding and the incorporation of lignite clasts (Fig. 4.7.3g). Following a lignite bed between 35.40 m and 35.24 m with an erosional base a massive mudstone including frequent laminated mudstone clasts up to gravel size occurs between 35.24 and 34.50 m (Fig. 4.7.3h). In the lower part also a 10 cm thick lignite clast is incorporated in the mudstone (Fig. 4.7.3h). Between 34.50 m and 33.35 m a more than 1 m thick crumbly lignite occurs, that includes up to 5 cm thick irregularly shaped lenses of yellow sandy material (Fig. 4.7.3i). In the succeeding 40 cm a laminated to massive mudstone appears, which includes also cm-thick yellow sandy lenses.

A change in the depositional system occurs between 32.95 m and 32.32 m with an alternation of laminated and massive mudstone and yellow, sometimes graded beds of sand and silt. Parts of this succession are characterized by varying dip directions (32.45; Fig. 4.7.3j). In the following section between 32.32 and 31.70 m thick clasts and lenses of light sandy sediments (32.25; Fig. 4.7.3j), mudstone and lignite appear in a mudstone matrix. The succeeding crumbly lignite between 31.70 m 30.85 m, representing the top of LZ4 (Moshayedi et al. 2018), is also characterized by up to 10 cm thick clasts of laminated to massive mudstone. LZ3 above 30.85 m is represented by massive to laminated dark bituminous shale.

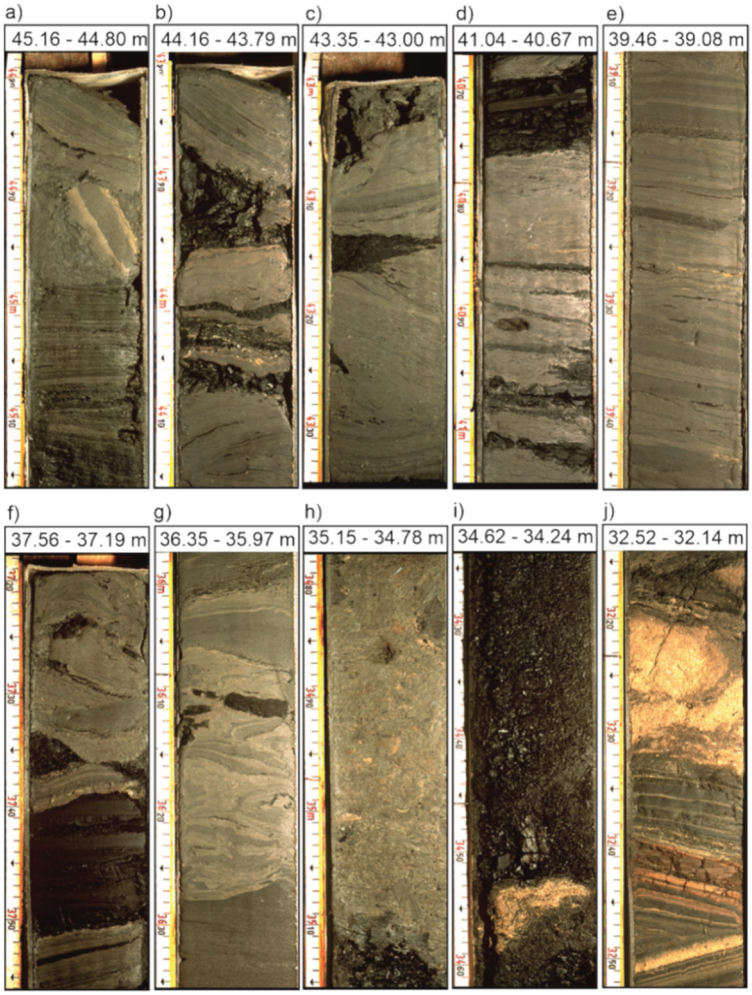

Fig. 4. 7. 3. Selected images of the core illustrating the succession of LZ 4 in the core from PvH between 44.70 and 30.82 m depth (a) 45.16 – 44.18 m. Laminated, partly massive mudstone with a mudstone clast between 45.00 and 44.90 m, (b) 44.16 – 43.79 m. Alternation of mudstone and reworked lignite that contains a high portion of clastic material (e.g., 44.05 – 44.00 m), (c) 43.35 – 43.00 m. Massive mudstone including a lignite clast (43.15 m), (d) 41.04 – 40.67 m. Crinkly laminated to massive mudstone with some lignite clasts and streaks of <1 cm thickness (41.02 – 40.90 m), (e) 39.46 – 39.08 m. Horizontally bedded undisturbed mostly laminated mudstone including rare streaks of organic material, (f) 37.56 – 37,19 m. Reworked mudstone and lignite clasts, (g) 36,35 – 35,97 m. Mudstone with convolute bedding and incorporated lignite clasts, (h) 35,15 – 34,78 m. Reworked massive mudstone including frequent laminated mudstone clasts up to gravel size, (i) 34,62 – 34,24 m. Crumbly lignite including a 5 cm thick irregularly shaped lens of yellow sand, (j) 32,52 – 32,14 m. Alternation of laminated and massive mudstone and yellow, sometimes graded beds of sand and silt with varying dip directions between 32.52 and 32.33 m and massive clasts of light sandy material between 32.32 and 32,15 m. The pictures are photographs of FIS/HLUG (S. Borges, W. Schiller and M. Stryj) from core B/97- BK9: (**a**) 10623.pcd, (**b**) 10620.pcd, (**c**) 10618.pcd, (**d**) 10610.pcd, (**e**) 10604.pcd, (**f**) 10597.pcd, (**g**) 10593.pcd, (**h**) 105899.pcd, (**i**) 10587.pcd, and (**j**) 10580.pcd.

Palynology

Differences between palynomorph assemblages from lignites and mudstones

The pollen diagram (Fig. 4.7.4) shows that most of the palynomorphs occur over the entire interval of LZ4, but some taxa vary significantly in their proportional representation, because there is a strong correlation between lithology and palynomorph content. A Mann-Whitney-U-test reveals that among the 49 taxa or groupings of taxa, which are presented in the pollen diagram, 8 are characterized by significant abundance differences in lignite and mudstone

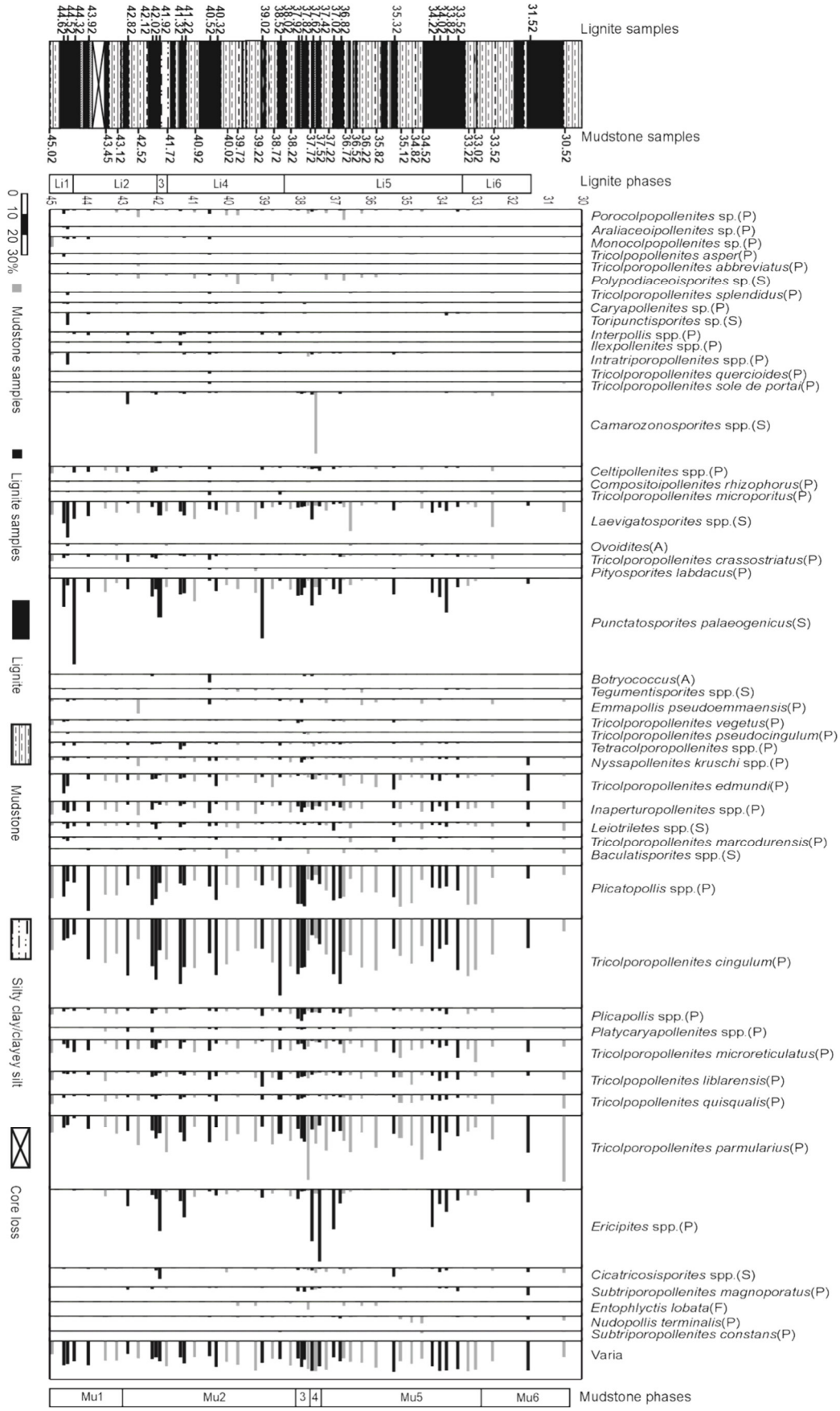

Fig. 4. 7. 4. Pollen diagram of 52 samples from core PvH between 30.52 and 45.02 m depth (LZ 4 of Moshayedi et al. 2018). (A) algae, (P) pollen, (S) spores, (F) fungi. Black bars: lignite samples. Grey bars: mudstone sample.

palynomorph assemblages (Tab. 4.7.1). Some palynomorphs are more dominant in the mudstone beds, e.g., the swamp forest elements *Inaperturopollenites* spp. (Cupressaceae) and *Nyssapollenites* spp. (Nyssaceae), the spores of *Tegumentisporis* spp. (Selaginellaceae) and forest elements, such as *Tricolpo(ro)pollenites parmularius* (Eucommiaceae) and *Porocolpopollenites* spp. (Symplocaceae), while others, such as *Ericipites spp.* (Ericaceae) or fern spores (*Punctatosporites palaeogenicus*; Polypodiaceae), are mostly associated with lignite samples (Tab. 4.7.1). Furthermore, other fern spores such as those of *Polypodiaceoisporites* spp. (Polypodicaeae) and *Baculatisporites* spp. (Osmundaceae) are confined or nearly restricted to the mudstone samples and therefore excluded from the Mann-Whitney-U-test. Therefore, more than 20% of the taxa show significant differences in abundance between lignite and mudstone. However, most palynomorphs from the forest vegetation in the vicinity of the lake, such as the dominating taxa *Tricolporopollenites cingulum* (Fagaceae) or *Plicatopollis* spp. (Juglandaceae), are independent in their abundance from the lithological changes (Tab 4.7.1).

The difference between the composition of the pollen assemblages also is seen in a NMDS plot (Fig. 4.7.5). Samples from lignite and mudstone-dominated beds are characterized by substantially different palynomorph assemblages, because mudstone samples are generally concentrated on the left side while lignite samples are commonly found on the right side of the ordination space (Fig. 4.7.5). However, it is obvious that the lignite beds are fundamentally different in origin from the mudstones. Therefore, besides a different source, sorting of pollen and spores during transport and deposition must be considered (Galloway et al. 2015), which prevents a direct comparison between the palynomorph assemblages of lignite and mudstone samples. For this reason, we performed separate analyses for both lithologies.

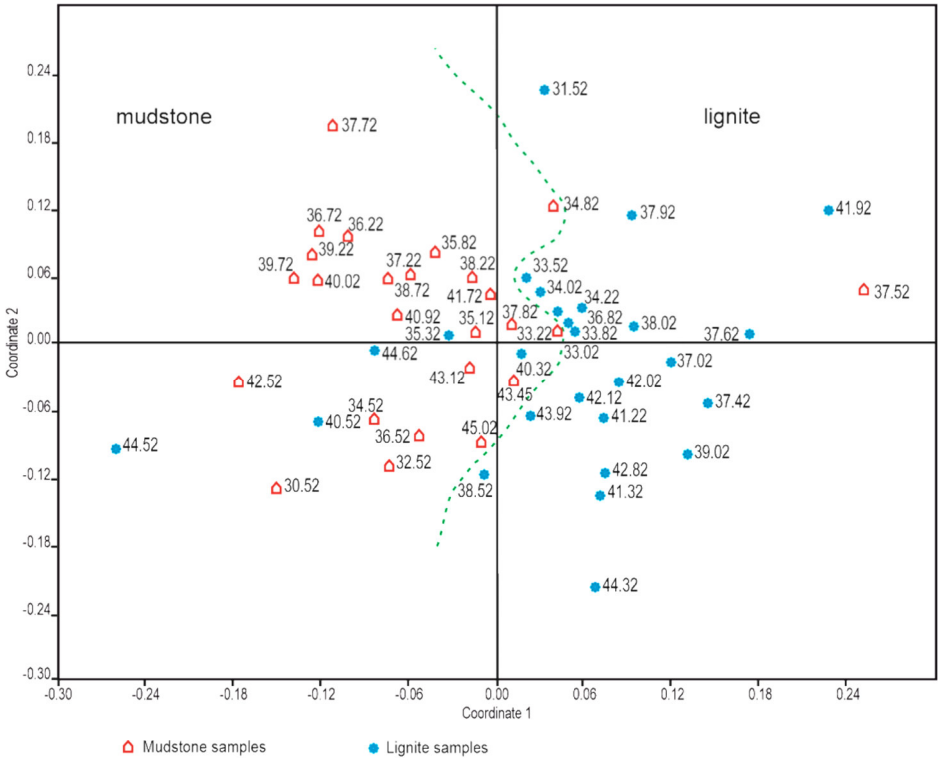

Fig. 4. 7. 5. Non-metric multidimensional scaling (NMDS) plot of palynological data of 52 samples from the succession of lignite and mudstone beds in LZ4 of Moshayedi et al. (2018) using the Bray-Curtis dissimilarity and the Wisconsin double standardized raw-data values. The scatter plot shows the arrangement of samples (numbers correspond to depth in m). Stars: Lignite samples. Pentagons: Mudstone samples.

Table 4. 7. 1. Comparison of species abundances of selected taxa in lignite and mudstone samples. To assess statistical differences Mann-Whitney U-test is used. P-values ≤0.05 (upper 8 species) indicate a significant difference between the abundance of a species in the lignite and mudstone assemblage, whereas p-values >0.05 point to an equal distribution.

Species	Lignite				Mudstone				Mann-Whitney test, u-value	Mann-Whitney test, p-value
	Max value [%]	Mean value [%]	Median value [%]	Standard deviation [%]	Max value [%]	Mean value [%]	Median value [%]	Standard Deviation [%]		
Tricolporopollenites parmularius	17.65	8.62	7.985	3.64	31.52	13.54	12.365	6.61	165	0.001
Porocolpopollenites sp.	2.12	0.34	0.155	0.54	4.8	1.12	0.645	1.25	185	0.004
Punctatosporites palaeogenicus	40.37	9.3	7.43	8.41	11.07	2.79	1.975	2.76	101.5	<0.001
Tegumentisporis spp.	0.54	0.06	0	0.15	1.99	0.39	0.365	0.52	201	0.002
Emmapollis pseudoemmaensis	2.70	0.3	0	0.64	7.03	1.16	0.655	1.49	154	0.0004
Nyssapollenites kruschii spp.	3.92	0.87	0.58	0.89	4.3	1.34	1.28	0.9	215.5	0.02
Inaperturopollenites spp.	5.66	3.09	2.8	1.41	6.65	3.88	3.565	1.29	236	0.05
Ericipites spp.	33.86	7.31	4.385	8.67	3.56	1.35	1.1	1.16	185	0.005
Tricolporopollenites cingulum	36.12	19.59	21.15	7.87	26.95	17.78	17.325	5.41	304	0.54
Celtipollenites spp.	2.9	0.95	0.795	0.95	3.43	0.88	0.58	0.94	331.5	0.91
Plicatopollis spp.	21.22	12.21	10.425	4.39	19.37	10.88	11.045	4.67	272.5	0.23
Plicapollis spp.	5.98	1.68	1.285	1.42	4.23	1.64	1.475	1.02	315.5	0.69
Platycaryapollenites spp.	2.42	0.53	0.4	0.64	2.09	0.56	0.4	0.63	335.5	0.97
Tricolpopollenites liblarensis	7.14	2.26	1.975	1.48	6.36	2.41	2.185	1.4	305.5	0.56
Tetracolporopollenites spp.	3.45	0.77	0.79	0.73	2.02	0.64	0.48	0.43	307	0.58

The palynological composition of the lignite samples

There are at least 20 lignite beds with thicknesses ranging from 5 to 100 cm in the core (Figs. 4.7.2, 4.7.3). The bootstrapped Q-mode cluster analysis reveals that in the 27 lignite samples, seven robust palyno-phases can be distinguished (lignite/Li phases, Figs. 4.7.4, 4.7.6a)

Phase Li 1

The 2 samples from phase Li 1 plot to the right side of the NMDS ordination space and appear clearly separate from the other lignite samples (Fig. 4.7.6b) indicating significant compositional differences. Both samples are from the lower part of the succession between 44.62 and 44.52 m. Most remarkable are the high abundances of *Intratriporopollenites* spp. (Tiliaceae) and *Toripunctisporites* sp. (fern spore of unknown botanical affinity) with up to 6% (Figs. 4.7.4, 4.7.6a). Other fern spores such as *Laevigatosporites* spp. (Polypodiaceae, up to 17%), *Punctatosporites palaeogenicus* (up to 14%), and *Leiotriletes* spp. (Schizaeaceae, up to 3%) are also abundant in this phase. Fern spores compose a total of up to 40% of these assemblages (see supplementary material raw data table).

Phase Li 2

Five samples, between 44.32 and 42.02 m, are combined in phase Li 2 and plot in the upper left part of the NMDS ordination space on the negative side of NMDS axis 1 (Fig. 4.7.6b). The most characteristic taxa are *Interpollis* spp. (unknown botanical affinity, up to 2%) and *Celtipollenites* spp. (Ulmaceae, up to 3%). *Punctatosporites palaeogenicus* (up to 41%) reaches its maximum for the lignite layers, but other fern spores such as *Leiotrilites* spp. (up to 4%), *Laevigatosporites* spp. (up to 9%), and the lycopod spores of *Camarozonosporites* spp. (6%) are frequent at least in some samples (Figs. 4.7.4, 4.7.6a). Fern spores account for a total of up to 60% of these assemblages.

Phase Li 3

One sample from a depth of 41.92 m is characterized by a unique combination of very high values for the spores of *Cicatricosisporites* spp. (Schizaeaceae, 6%) and pollen of *Ericipites* spp. (20%). It plots on the negative lower side of the NDMS ordination space away from the other lignite samples (Figs. 4.7.4, 4.7.6b).

Phase Li 4

Phase Li 4 includes 6 samples between 41.32 and 38.52 m, which plot in the upper part of the NMDS ordination space (Fig. 4.7.6b). Compared to Li 2, *Interpollis* spp. (up to 2%) is relatively frequent, but *Celtipollenites* spp. is of a lower value (Fig. 4.7.6a). Other elements show peak abundances including *Tetracolporopollenites* spp. (Sapotaceae, 4% in 41.32 m), *Tricolporopollenites liblarensis* (Fagaceae, 8% in 39.02m), or the coccal green algae *Botryococcus* (1%).

Phase Li 5

This phase consists of 12 samples between 38.02 and 33.52 m. In the NMDS plot they occur in the lower part of the ordination space mainly at the negative side of NDMS axis 2 (Fig. 4.7.6b). This position shows differences in the composition of the palynoflora compared to the older phases Li 2 and Li 4. Notable is the disappearance of *Interpollis* spp., along with an increase of *Plicatopollis* spp. (up to 18%) and *Inaperturopollenites* spp. (up to 5%). Characteristic and frequent palynomorph taxa are *Ericipites* spp. (up to 35%) and *Tricolporopollenites cingulum* (up to 31%), which reach their highest values for the studied core interval.

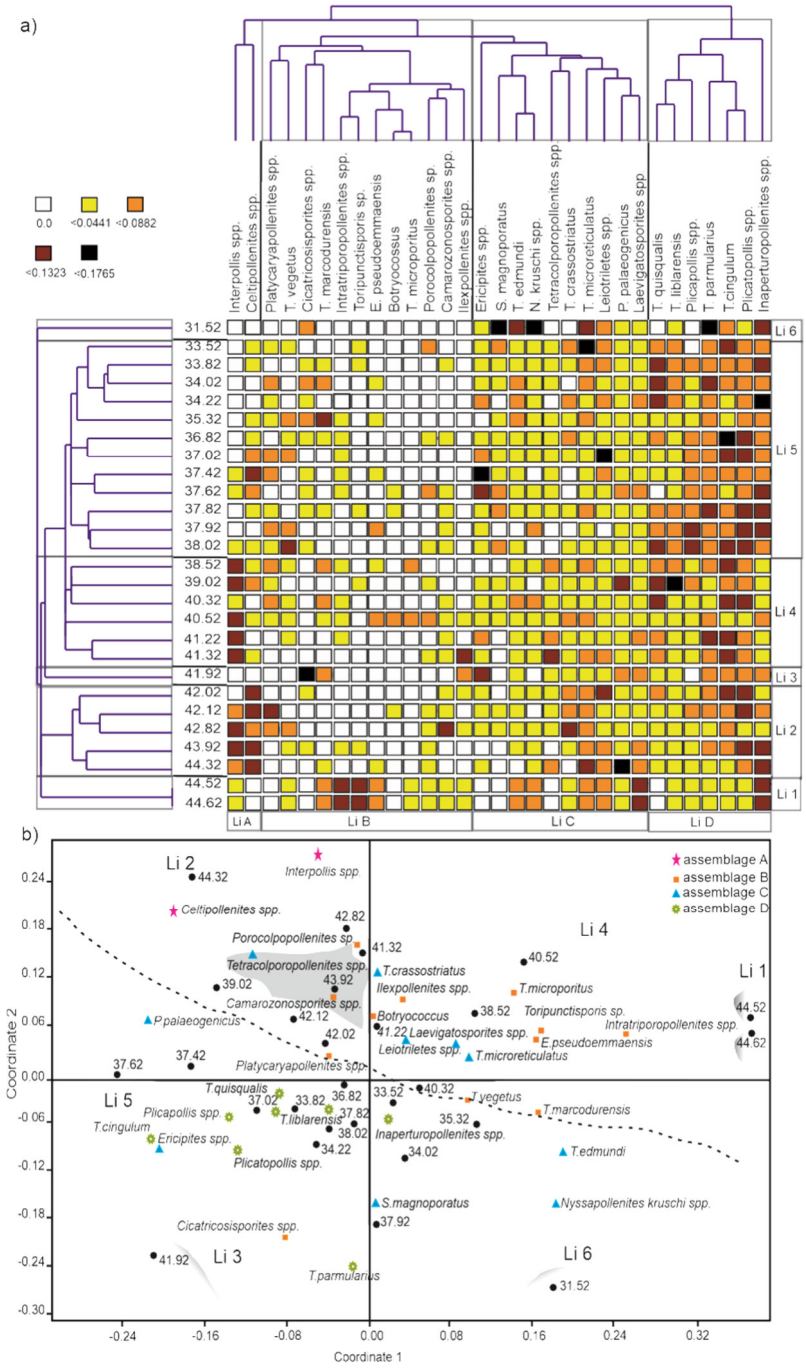

Fig. 4. 7. 6. Numerical analyses of palynological data from lignite samples of LZ4. (a) A combined constrained Q- and unconstrained R-mode cluster analysis of Wisconsin double standardized raw-data values of 27 lignite samples (numbers correspond to depth in m) and 31 palynomorph taxa that occur with at least 1.5% in one sample. Different abundance classes based on the Wisconsin double standardized raw data values are shown in different colors. The darker the color the higher is the proportion of specific palynomorphs within the palynomorph assemblage of a sample; white boxes indicate the absence of a specific taxon. For cluster analysis the unweighted pair-group average (UPGMA) method has been applied together with a Eucledian distance. As a result, 6 palynological phases (Li 1 to Li 6) can be distinguished in the lignite succession, which are related to abundance variations in 4 palynomorph assemblages (Li A to Li D). (b) Non-metric multidimensional scaling (NMDS) of palynological data from 27 lignite samples from LZ 4 of the Eocene Lake PvH using the Bray-Curtis dissimilarity and the Wisconsin double standardized raw-data values. The different palynomorph assemblages (Li A to Li D) are indicated by different symbols, whereas the different palynophases (Li 1 to Li 6) appear in grey. The dotted line indicates the general separation of the succession as based on differences in the composition of the microflora with an older part including phases Li 2 and 4 and a younger part with phase Li 5. Phases Li 1, Li 3 and Li 6 represent individual samples which are characterized by specific palynomorph assemblages clearly different from assemblages of the other lignite samples.

Phase Li 6

The uppermost sample (31.52 m) is similar to the samples from Li 1 and Li 3, and characterized by a specific palynomorph assemblage. The sample plots in the ordination space in the lower right, clearly separate from all other lignite samples (Fig. 4.7.6b). The sample is characterized by *Subtriporopollenites magnoporatus* (unknown botanical affinity, 4%), *Nyssapollenites kruschii* spp. (4%), *Tricolporopollenites edmundii* (Mastixiaceae 8%) and *Tricolpo(ro)pollenites parmularius.* (18%). All of these taxa reach their maximum for the succession of lignite beds here (Figs. 4.7.4, 4.7.6a).

General changes in the composition of the vegetation recorded in lignite samples

The NMDS plot reveals that a younger and an older part can generally be separated in the succession of lignitic layers based on differences in palynomorph assemblages. Samples from Li 1, 2, and 4, between 44.62 and 38.52 m, which plot in the upper part of the ordination space of the NMDS (Fig. 4.7.6b), characterize the older series. They are composed mainly of palynomorph taxa that are clustered in the assemblages Li A, B, and C of the R-mode cluster analysis (Fig. 4.7.6a). In contrast, samples from Li 5 between 38.02 and 31.52 m plot in the lower part of the NMDS ordination space and are mainly composed of palynomorphs that are clustered in assemblage Li D along with some elements of assemblage Li C (e.g., *Ericipites* spp. or *S. magnoporatus*; Fig. 4.7.6a, b). Therefore, a change in the general composition of the vegetation during the deposition of the lignite is obvious. Furthermore, a single sample from the lower part (Li 3) and another one from the top of the record (Li 6) are characterized by a specific microfloral composition clearly different from the other lignite samples.

One of the main differences between the lower phases (Li 1, 2 and 4) and the upper phase Li 5 is the disappearance of *Interpollis* spp. and *Celtipollenites* spp., which appear regularly in low numbers in the older part and cluster in assemblage Li A (Figs. 4.7.4, 4.7.6a). Pollen and spores that are clustered in assemblage Li B occur generally in low numbers in the lignite succession, except for peak abundances in the two lowermost samples. Assemblage Li C is composed of palynomorphs that occur regularly with low to high numbers and include *Ericipites* spp. or *Punctatosporites palaeogenicus*. These taxa vary in frequency throughout the succession of lignites (Fig. 4.7.4) and are independent from the general change in the overall vegetation. The dominant palynomorph taxa are clustered in assemblage Li D. Elements of a forest vegetation, such as juglandaceous pollen (*Plicapollis* spp., *Plicatopollis* spp.) and pollen with fagalean affinity, e.g., *Tricolporopollenites cingulum* and *Tricolpopollenites liblarensis,* as well as pollen from a swamp forest (*Inaperturopollenites* spp.), are generally found in high numbers in the lignite. But, NMDS and cluster analysis show that these elements slightly increase in the younger phase Li 5 (Fig. 4.7.6).

The palynological composition of the mudstone samples

Bootstrapped Q-mode cluster analysis of 25 samples from the mudstones results in 6 robust palynomorph phases (mudstone/Mu phases, Fig. 4.7.7a).

Phase Mu 1

Mu1 includes 3 samples between 45.02 and 43.12 m, which plot in the upper left part of the NMDS ordination space on the negative side of axis 1 (Fig. 4.7.7b). Characteristic taxa are *Monocolpopollenites* spp. (Palmae, up to 5%), *Celtipollenites* spp. (up to 4%), *Tricolporopollenites crassostriatus* (Solanaceae or Gentianaceae, up to 4%), and *Tricolporopollenites vegetus* (Hamamelidaceae, up to 3%), all of which reach their maximum for the mudstone samples (Fig. 4.7.4, 4.7.7a).

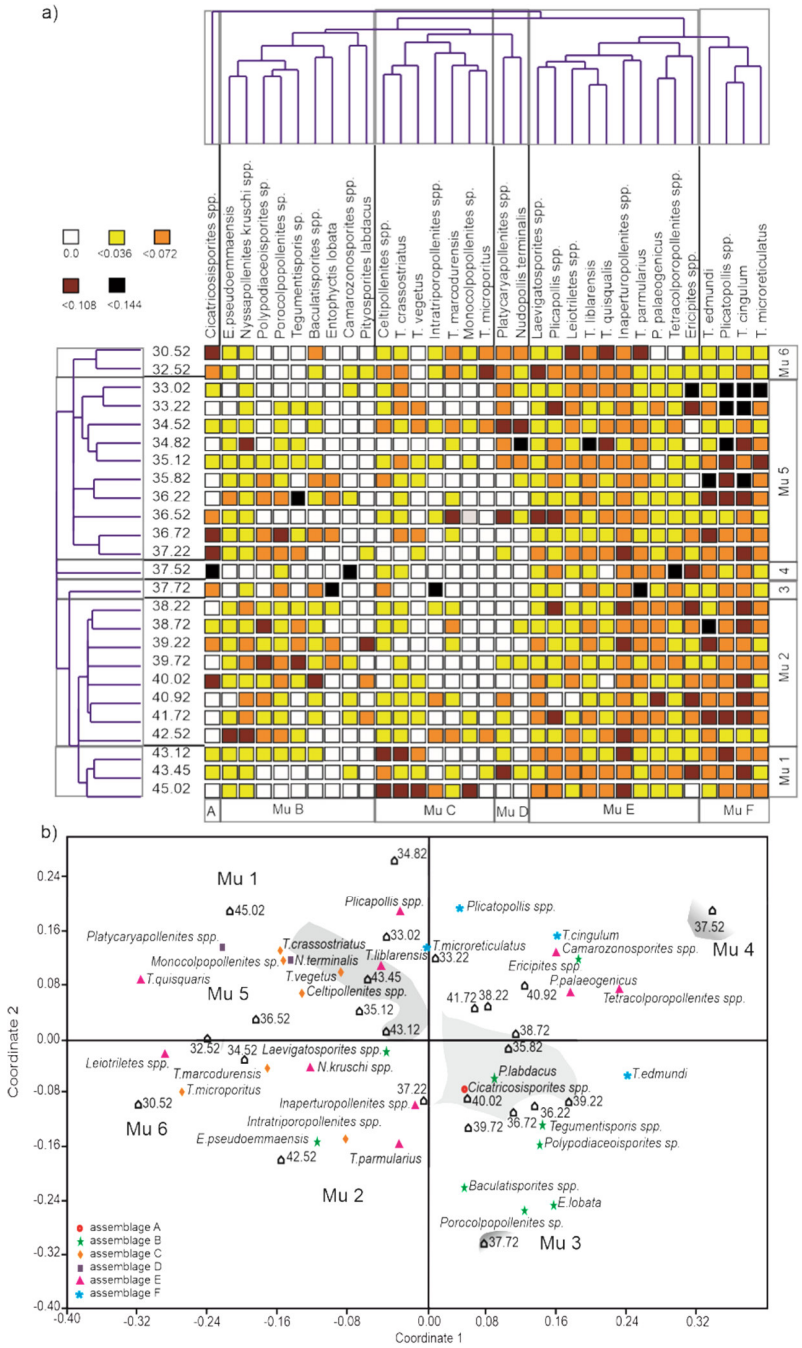

Fig. 4. 7. 7. Numerical analyses of palynological data from mudstone samples of LZ4. (a) A combined constrained Q- and unconstrained R-mode cluster analysis of Wisconsin double standardized raw-data values of 25 mudstone samples (numbers correspond to the depth in m) and 33 palynomorph taxa with a maximum of at least 1.5% in one sample. Different abundance classes based on the Wisconsin double standardized raw data values are shown in different colors. The darker the color the higher is the proportion of specific palynomorphs within the palynomorph assemblage of a sample; white boxes indicate the absence of a specific taxon. For cluster analysis, the unweighted pair-group average (UPGMA) method has been applied together with a Eucledian distance. As a result, 6 palynological phases (Mu 1 to Mu 6) can be distinguished in the mudstone succession, which are related to abundance variations in 6 palynomorph assemblages (Mu A to Mu F). (b) Non-metric multidimensional scaling (NMDS) plot of palynological data of 25 mudstone samples from LZ 4 of the Eocene Lake PvH using the Bray-Curtis dissimilarity and the Wisconsin double standardized raw-data values. The different palynomorph assemblages (Mu A to Mu F) are indicated by different symbols, whereas the different palynophases (Mu 1 to Mu 6) are shaded in grey. Phases Mu1 and Mu 6 plot on the left side of the ordination space, indicating a similar composition of the palynomorph assemblages, whereas phases Mu 2, Mu 3 and Mu 4 are generally on the right side of the ordination space. Phase Mu 5 as a transitional phase between the older phases Mu 2 zo Mu 4 and the youngest phase Mu 6 plot in the center of the ordination space.

Phase Mu 2
Mu 2 is composed of 8 samples collected between 42.52 and 38.22 m. The samples generally plot on the right side of the NMDS ordination space on the positive side of axis 1 (Fig. 4.7.7b). Only the lowermost sample (42.52 m) plots in the lower left of the NMDS ordination space, clearly separate from the other mudstone samples. Compared to the older phase Mu 1 a distinct change in the composition of the microflora is obvious. Most remarkable is the rare, but regular, appearance of palynomorphs that cluster in assemblage Mu B of the R-mode cluster analysis (Fig. 4.7.7a). These include *Polypodiaceoisporites* spp. (up to 6%), *Tegumentisporis* spp. (Selaginellaceae, up to 2%), or the pinaceous pollen *Pityosporites labdacus* (up to 2%). Various species that are combined in assemblage Mu C decrease in proportion compared to phase Mu 1, such as *Celtipollenites* spp., or disappear completely, e.g., *Monocolpopollenites* sp. (Figs. 4.7.4, 4.7.7a).
The separation of the sample in 42.52 m in the NMDS plot from the other samples of phase Mu2 is based on the occurrence of *Emmapollis pseudoemmaensis* (Chloranthaceae, 7%) and *Nyssapollenites kruschii* (5%), which attain their maximum for the succession of mudstone beds here.

Phase Mu 3
A single sample (37.72 m) plots in the upper right corner of the NMDS ordination space far away from all other mudstone samples, also indicating a specific palynomorph composition (Fig. 4.7.7b). The maximum of *Tricolpo(ro)pollenites parmularius* (31%) together with the maximum of *Intratriporopollenites* spp. (2%) in the succession is noteworthy. Furthermore, the freshwater fungus *Entophlyctis lobata* (4%), a saprophytic cytrid that is often associated with algal blooms (Geitler 1962, Bradley 1967), is abundant.

Phase Mu 4
One sample (37.52 m) plots in the NMDS ordination space on the negative end of axis 2 (Fig. 4.7.7b). Significant differences are obvious when compared to the sample 20 cm below especially with regard to a maximum of *Camarozonosporites* spp. (29%), which is almost absent from all other mudstone samples (Fig. 4.7.4). Other palynomorphs characteristic for this sample are *Cicatricosisporites* spp. (3%) and *Tetracolporopollenites* spp. (Sapotaceae, 2%) (Fig. 4.7.7a).

Phase Mu 5
The 10 samples clustered in assemblage Mu 5, between 37.22 and 33.02 m, plot in the center of the NMDS ordination space on both, the negative and positive side of axis 1 (Fig. 4.7.7b). There is a wide overlap in the ordination space with samples from Mu 1 and 2 indicating a similar palynomorph composition. Only a few samples are slightly different.
The samples from 36.52 m and 34.52 m depth, which are plotted on the negative end of NMDS axis 1 (Fig. 4.7.7b), are characterized by peak abundances of rare elements such as *Platycaryapollenites* spp. (Juglandaceae, 2%), *Tricolporopollenites marcodurensis* (Vitaceae, 3%), whereas the sample in 34.82 m, plotted on the positive end of NMDS axis 2 (Fig. 4.7.7b), is characterized by *Nudopollis terminalis* (4%) and *Tricolporopollenites liblarensis* (7%), both showing their maximum for the mudstones (Figs. 4.7.4, 4.7.7a).
In the two uppermost samples of Mu 5 in 33.22 and 33.02 m depth, the dominant pollen of the forest vegetation *Tricolporopollenites cingulum* (up to 27%), *Plicatopollis* spp. (up to 19%), and *Tricolporopollenites microreticulatus* (up to 11%) reach their maximum for the mudstone assemblages.

Phase Mu 6
Two samples from the top of the succession (32.52 and 30.52 m) plot in the NMDS ordination space on the left side on the negative end of axis 1 (Fig. 4.7.7b). There is a notable decrease of elements that dominate the palynomorph assemblage in the upper samples of phase Mu 5, such as *Tricolporopollenites cingulum* or *Plicatopollis* spp. (Figs. 4.7.4, 4.7.7a). In contrast, there is an increase in the fern spore *Cicatricosisporites* spp. and elements associated with cluster Mu E. *Tricolpo(ro)pollenites parmularius* is especially common (32%) in the uppermost sample.

General changes in the composition of the vegetation recorded in the mudstones
The NMDS plot reveals that, similar to the succession of lignite beds, the succession of mudstones in LZ4 can be arranged in a way that indicates a step-wise change in the development of the vegetation. However, a clear separation in a younger and older part as for the lignite assemblages, each with a specific palynological composition, is not recognizable in the mudstone samples, because phases Mu 2 and Mu 5, mainly representing the older respectively the younger part of the mudstone succession overlap in the NMDS plot, which points to a similar palynological composition (Fig. 4.7.7). However, phase Mu 1, including the oldest mudstones in the succession between 45.02 and 43.12 m, plots on the left side of the NMDS ordination space and is mainly composed of palynomorph taxa that group in assemblages Mu C, E and F of the R-mode cluster analysis (Fig. 4.7.7a). In contrast, samples from Mu 2 to Mu 4 between 42.52 and 35.12 m, plot, clearly separated from phase Mu 1, generally on the right side of the NMDS ordination space and are mainly characterized by palynomorphs that cluster in assemblages Mu A and Mu B (Fig. 4.7.7a). This indicates a change in the composition of the vegetation between phases Mu 1 and Mu 2 to Mu 4. Furthermore, the upper samples of phase Mu 5 and both samples from Mu 6 plot on the negative side of NMDS axis 1 in an area together with the oldest phase Mu 1 (Fig. 4.7.7b). This shows that the vegetation in the youngest samples had a composition similar to the vegetation at the beginning of the deposition of the mudstones (= base of LZ4).
Cicatricosisporites spp, the only taxon of Mu A, has a unique distribution in the mudstone succession with peak abundances in phases Mu 4 and Mu 6. Therefore, it is clearly separated from all other taxa in the R-mode cluster analysis (Fig. 4.7.7a). Pollen and spores that cluster in assemblage Mu B occur regularly in low to medium numbers in phases Mu 2 to Mu 5 and are almost restricted to them (Fig. 4.7.7a). These plot in the NMDS ordination space generally on lower right side (Fig. 4.7.7b). The occurrence of polypodiaceous spores (*Polpodiaceoisporites* ssp.) is remarkable in Mu B because they are completely missing in samples from the lignite beds. Their occurence indicates a habitat outside of the peat-forming environments for these ferns. In contrast to Mu B, assemblage Mu C is more prevalent in the oldest and youngest phases Mu 1 and Mu 6. Assemblage Mu D is characterized by only two taxa *Platycaryapollenites* spp. and *Nudopollis terminalis*. Both are typical elements of the youngest phases (Mu 5 and Mu 6) with *N. terminalis* being almost restricted to these phases. Assemblages Mu E and Mu F are composed of the main elements of the forest vegetation and include pollen of the Fagaceae (*Tricolporopollenites cingulum, Tricolpopollenites liblarensis*) and of the juglandaceous alliance (*Plicatopollis* spp. *Plicapollis* spp.). These elements occur regularly in medium to high values in the mudstone. Nevertheless, the values vary independent from the general trends in the composition of the vegetation.

Discussion
Sedimentology
According to Hofmann et al. (2005), the lignite beds from the core of Lake PvH consist primarily of woody organic matter of the huminite group, indicating that terrestrial higher plants or aquatic macrophytes, which lived in the shallow littoral zone of the lake, contributed

organic material. Neither the lignites nor the underlying mudstones show traces of rooting and most of the lignite beds are characterized by erosional contacts at the base (Fig. 4.7.3b). Furthermore, lignite clasts are often incorporated in the mudstones (Figs. 4.7.3 d, f), which indicates an allochthonous origin of the lignitic material by transport from peat-forming environments into the lake. This is also confirmed by the relatively low TOC content of 50 to 60% and a high content of clastic material in the lignite (Hofmann et al., 2005). Lignite accumulation may therefore have included repeated erosional and redepositional events (Hofmann et al. 2005, Moshayedi et al. 2018).
Compared to the lignite beds, the gray-green mudstones are low in organic matter (<10 % TOC) and consist mostly of laminated mudstones, which indicate deposition in a low energy environment. The setting has been interpreted as a shallow water and well-oxygenated site (Hofmann et al. 2005). The same is true for the upper part of the studied succession with finely layered and laminated silt and sand.
Similar to the lignite beds, the clastic material has, at least in part, been redeposited (Fig. 4.7.3). For example, oppositely dipping finely layered to laminated packages occur between 32 and 33 m depth (Fig. 4.7.3j). This may be a result of disturbance and redeposition due to tectonic activity. Convolute bedding as a result of the in place deformation of unconsolidated mudstones may also indicate tectonic activity (Fig. 4.7.3g). Furthermore, individual clasts of remobilized mudstone within the mudstone succession (Figs. 4.7.3a, h) as well as within lignite beds (Figs. 4.7.3i) show that the mudstone has mainly been reworked.
However, parts of the succession are characterized by horizontally laminated mudstones which show no traces of deformation or redeposition (Fig. 4.7.3e). Therefore, during periods of reduced tectonic activity, mudstones were primarily derived from surface transport of clastic material into the lake. In the upper part of the sequence between 34.50 and 33.35 m, in which a massive lignite occurs (Fig. 4.7.3i), lignite-forming swamp areas may have reached their maximum extension in the vicinity of the lake. Accordingly, the deposition of lignitic material predominated over clastic material derived from surface transport.

Vegetational trends in the lignite succession
The pollen diagram and the two-way cluster analyses do not show any taxonomic turnover across the lignite samples throughout the succession (Figs. 4.7.4, 4.7.6a). Changes are mainly restricted to the quantitative composition of the pollen assemblages. However, the NMDS plot indicates that there are slight qualitative changes in the lignite record, e.g., the disappearance of the Normapolles element *Interpollis* spp. in the younger samples (Fig. 4.7.6b). Therefore, the lignite succession can be subdivided in a lower part (e.g., Li 2, Li 4) and an upper part (e.g., Li 5), each represented by a specific palynomorph composition (Fig. 4.7.6b).
Fern spores, such as Polypodiaceae and Schizaeaceae as well as spores of Lycopodiaceae, are especially abundant in the lignite beds (Figs. 4.7.4, 4.7.6a). This points to a wide distribution of herbaceous pteridophytes growing under wet conditions at the shoreline of the lake and in marginal swamps (e.g., Lenz and Riegel 2001, Lenz et al. 2011). Spores of ferns and fern allies occur together with pollen of a forest association mainly dominated by Juglandaceae and Fagaceae representing the typical Paleogene paratropical inland flora of Europe and North America (Mai 1981, 1995; Manchester 1989). Furthermore, a peat-forming swamp with trees such as Cupressaceae und Nyssaceae existed at least in some areas at or near to the lake.
Slight shifts in abundance in the plant assemblages between the lower and upper phases are documented by (1) a general decrease of *Laevigatosporites* spp. and *Punctatosporites palaeogenicus* from the lower to the upper part and (2) the regular appearance of *Cicatricosisporites* spp. only in the upper beds. This suggests that compositional changes occurred in the vegetation at the lake side during the time of deposition which may have been related to a general climate change between the lower and upper part of the succession. A slight decrease in temperature from the older to the younger part is interpreted from the

disappearance of some more (sub)tropical elements (Sanderson and Donoghue 1994; Plunkett et al. 1996; Couvreur et al. 2011) including palms and Sapotaceae which lived in the forest in areas around the lake (Fig. 4.7.4). On the other hand, the Ericaceae (*Ericipites* spp.) as swamp elements occur with notable changes in frequency throughout the lignites, but appear more abundantly in the younger phase Li 5 (Fig. 4.7.4, 4.7.6a). Ericaceae today mainly grow in more temperate regions of the world and in cooler mountainous areas of tropical latitudes (Kron 1996; Kron et al. 2002; Luteyn 2002), frequently preferring wet ground. Their common appearance in the younger part of the lignite succession may point to a slight decrease in temperature. The same is true for the disappearance of the extinct Normapolles element *Interpollis* spp. in the younger phases, which is thought to have preferred warm conditions (Daly and Jolley 2015).
The disappearance of pollen of *Carya* and *Celtis,* which both today prefer more moist habitats and, for example, are important elements of forested wetlands in the Southern United States (Tiner 2017), is noteworthy. This may indicate that less humid climate conditions prevailed in the younger part in phase Li 5. As a consequence, the general vegetation change in the lignite succession of Lake PvH can possibly be related to a gradual change towards slightly less humid and slightly cooler conditions.
The lower phases (Li 1 to Li 4) also include remains of freshwater algae (Fig. 4.7.4). Colonies of the coccal green alga *Botryococcus* are represented by low numbers in four samples, but disappear completely in the upper part (Fig. 4.7.4). *Ovoidites*, a cyst of Zygnemataceae, is found only in one sample of phase Li 1 (Fig. 4.7.4). Even if the overall plankton production was probably very low and/or the well mixed oxic water column prevented the preservation of plankton (Hofmann et al. 2005), the occurrence of algae in the lower phases and their complete disappearance in the upper phases may have been related to changes in water chemistry and nutrient supply in response to decreasing precipitation. Decreasing nutrient availability also may be indicated by an increasing abundance of Ericaceae in the younger part, as these plants frequently prefer nutrient-poor soils (Riegel and Wilde 2016).
Some samples in the sequence of lignite beds are characterized by specific palynomorph assemblages and clearly distinguished as “outliers” from the other assemblages in phases Li 2, 4, and 5 in the Q-mode cluster analysis (Li 1, 3, 6) (Fig. 4.7.6a). The same is seen in the NMDS plot (Fig. 4.7.6b). Nevertheless, the two outliers from Li 1 and the single sample from Li 7, which come from the base and the top of the lignite succession, respectively, fit the general trend of vegetational change. Samples of Li 1 plot along with the older samples from phases Li 2 and Li 4 in the upper half of the ordination space of the NMDS, while the sample of Li 7 is found in the lower part of the NMDS plot together with the samples from the younger phases Li 5 and Li 6 (Fig. 4.7.6b). However, the fact that these samples have a palynomorph composition distinctly different from the other samples may be related to the fact that the lignite beds are of allochthonous origin. Tectonic activity in the small pull-apart basin probably led to repeated earthquake tremor (Moshayedi et al. 20018), resulting in the mobilization of organic detritus or peat and its transport into the center of the lake. This material may have had different sources around the lakeside in which the composition of the local vegetation differed. While the contribution of the zonal forest vegetation to the pollen assemblage did not change, the contribution of local communities increased in these outlier samples. This could explain the abnormal high proportion of fern spores of *Toripunctisporis* sp. in phase Li1 and of *Cicatricosiporites* sp. in the sample from phase Li 3, or the increase in *Nyssa* pollen in phase Li6.

Vegetational trends in the mudstone succession
Six different palynomorph phases in the mudstone succession can be distinguished based on constrained Q-mode cluster analysis (Fig. 4.7.7). The NMDS plot shows that the oldest part of the succession (phase Mu 1) and the youngest phases (upper part of Mu 5 and Mu 6) are

characterized by a similar palynomorph assemblage. These phases plot together on the left side of the ordination space. In contrast, phases Mu 2 to Mu 4 plot generally on the right side of the NMDS ordination space indicating slight changes in the composition of the vegetation. Nevertheless, these changes are a consequence of the occurrence of rare elements such as *Porocolpopollenites* sp. or the pinaceous pollen *Pityosporites labdacus*.

Generally the vegetation, which is represented by the palynomorph assemblages in the mudstones, is similar to the associations found in the lignite beds. A diverse herbaceous vegetation dominated by ferns, such as Polypodiaceae, Osmundaceae and Schizaeaeceae and to lesser extent by Selaginellaceae, was associated with a forest vegetation dominated by Juglandaceae and Fagaceae as well as a *Nyssa/Taxodium* swamp community. However, the general trend towards slightly less humid and slightly cooler conditions during deposition, recognized in the succession of the lignites, is also obvious in the microflora of the mudstone beds. Warm elements, such as Symplocaceae (*Porocolpopollenites* sp.), Sapotaceae, or palms, which occur regularly at least in parts of the older phases (Mu 1 to Mu 5) disappear in the younger part of the succession (Mu 6, Fig. 4.7.7a). Palms, which are mainly distributed in tropical to subtropical climates, have been widely used as indicators for a warm and humid climate (e.g., Greenwood and Wing 1995; Morley 2000, 2003; Walther et al. 2007). In contrast, the Normapolles taxon *Nudopollis terminalis* appears regularly in the upper phases (Mu 5 to Mu 6). The *Nudopollis* parent plants, possibly of juglandaceous affinity, preferred warmer and dryer environments compared to other Normapolles elements (Daly and Jolley 2015). A trend to less humid conditions is supported by the disappearance of the freshwater fungus *Entophlyctis lobata* in the upper beds. Generally, fungi and their spores are common in Paleogene strata during warmer periods at higher latitudes (Elsik 1996), but they are most abundant under relatively humid conditions (Kuhry 1985).

Compared to the lignite samples, which generally can be subdivided in a lower and upper series, the oldest (Mu 1) and the youngest samples (upper part of Mu 5, Mu 6) of the mudstone succession are characterized by relatively similar palynomorph assemblages. Therefore, if changes in pollen spectra were the result of climate the vegetation at the end of the deposition time was distributed under climatic conditions similar to those at the beginning of mudstone deposition. Hence, this could indicate an overall climate cycle.

The NMDS analysis of mudstone beds shows that some samples (Mu 3, 4) are characterized by specific palynomorph assemblages and plot separate from all others in the ordination space (Fig. 4.7.7b). Similar to the “outlier samples” of the lignite succession, these mudstone assemblages follow the general trend and plot in the ordination space next to the successive phases, either on the negative or positive side of the first NMDS axis. Thus, the contribution of abundant pollen from the zonal forest vegetation in these samples is the same compared to the other samples. Differences in the microflora are restricted to changes in the local contribution of the parent vegetation. For example, phase Mu 4 (37.52 m depth) is characterized by a maximum occurrence of *Camarozonosporites* spp. (Lycopodiaceae) which is almost missing in all the other samples. This may indicate that these spores were transported into the lake due to tectonic activity and related redeposition of the sediment from a local source around with abundant growth of lycopods. However, because redeposition cannot be unequivocally proven, other possible factors affecting transport, such as wind direction or intensity are not excluded (Friis-Christensen and Svensmark 1997, Kern et al. 2013).

Comparison of lignite and mudstone palynomorph assemblages

Comparing the palynomorph assemblages of lignite and mudstone samples significant differences may be noted (Tab. 1), because more than 20% of the palynomorph taxa, such as pollen of Cupressaceae and Ericaceae, are significantly more abundant either in mudstone or in lignite samples.

However, in particular the arboreal pollen, which originate from the regional forest, are independent of the lithology in their frequency distribution. This concerns, e.g., fagaceous pollen, such as *Tricolpopollenites liblarensis* or *Tricolporopollenites cingulum*, as well as juglandaceous pollen, such as *Plicatopollis* spp., *Plicapollis* spp. or *Platycaryapollenites* spp. In particular *Plicatopollis* spp. and *T. cingulum* are dominating the palynomorph assemblages at Lake PvH with values up to 21% and 36% (Tab. 1). Although both elements are more prevalent in the lignites, these differences are not statistically significant (Tab. 1). Both the Juglandaceae and the Fagaceae were major elements of the vegetation of the Central European paratropical rainforest during the Lower and Middle Eocene in the region (Nickel 1996, Lenz et al. 2011, Riegel et al. 2015, Riegel and Wilde 2016). At Lake PvH the Fagaceae dominated during the deposition of the studied sediments of LZ 4, but both the juglandaceous and fagaceous pollen show strong frequency fluctuations similar as in Messel. However, an orbital influence as found at Messel (Lenz et al., 2011, 2015, 2017) cannot be proven at Lake PvH because a suitable age model is lacking. Since there is no difference in the general abundance of pollen from main elements of the forest vegetation between lignite and mudstone samples independent from facies changes, a uniform pollen rain from the forest around the lake is documented in the respective sediments at Lake PvH.

Significant differences in palynomorph abundance between lignite and mudstone samples, however, are evident for elements of the local vegetation from the edge of the lake. This may be related to taphonomical processes bringing pollen into the depositional area and to a lesser extent to the changing contribution of different vegetation communities during the deposition time of the lignite and mudstone beds. For example, a *Nyssa/Taxodium* swamp forest community has generally been widespread on the edge of the lake, because the respective pollen can be found in both lignite and mudstone samples. However, since pollen of Cupressaceae and Nyssaceae was not only transported by wind but probably also by runoff from a larger catchment area together with clastic material *Nyssapollenites* spp. and *Inaperturopollenites* spp. occur in the mudstone with significantly higher values. The same applies possibly to pollen of Eucommiacae (*Tricolpo(ro)pollenites parmularius*) and Symplocaceae (*Porocolpopollenites* sp.). A strong influence of surface transport is also supported by the fact that the fern spores *Polypodiaceoisporites* spp. (Polypodicaeae) and *Baculatisporites* spp. (Osmundaceae) are restricted to mudstone samples, because fern spores are generally transported in higher numbers by fluvial and surface transport (DeBusk 1997).

In contrast, pollen of Ericaceae as one of the main elements of the peat-forming vegetation are significantly more abundant in the lignites. Lignitic material is a regular component of the mudstones. This explains that the strong frequency fluctuations of the ericaceous pollen between lignite and mudstone samples are not necessarily related to changes in the abundance of these plants around Lake PvH, but purely on the degree of redeposition of lignitic material. The same applies to the fern spore *Punctatosporites palaeogenicus*, whose parent plants must be regarded as important elements of the lignite-forming community.

Controls of vegetation changes

The frequencies of palynomorph taxa from the mudstone beds and the lignite layers are not directly comparable because sources were different and processes acting during transport and deposition varied. For example, the values of *Tricolporopollenites cingulum* are generally higher in the lignite, while the values for *Tricolpo(ro)pollenites parmularius* are significantly higher in the mudstone (Tab. 1). However, the frequency trends for six of the dominant elements in the microflora (Fig. 4.7.8) almost coincide with a minimum of *Tricolporopollenites cingulum* between 37 and 38 m or maxima of *Tricolpo(ro)pollenites parmularius* between 37 and 38 m and at *c*. 42 m. This illustrates general trends in the development of the vegetation during the deposition of the studied succession.

An overall cyclic trend is possibly suggested by the frequency distribution of the background taxa including a similar microfloral composition at the base and at the top of the studied succession (Fig. 4.7.7). ^

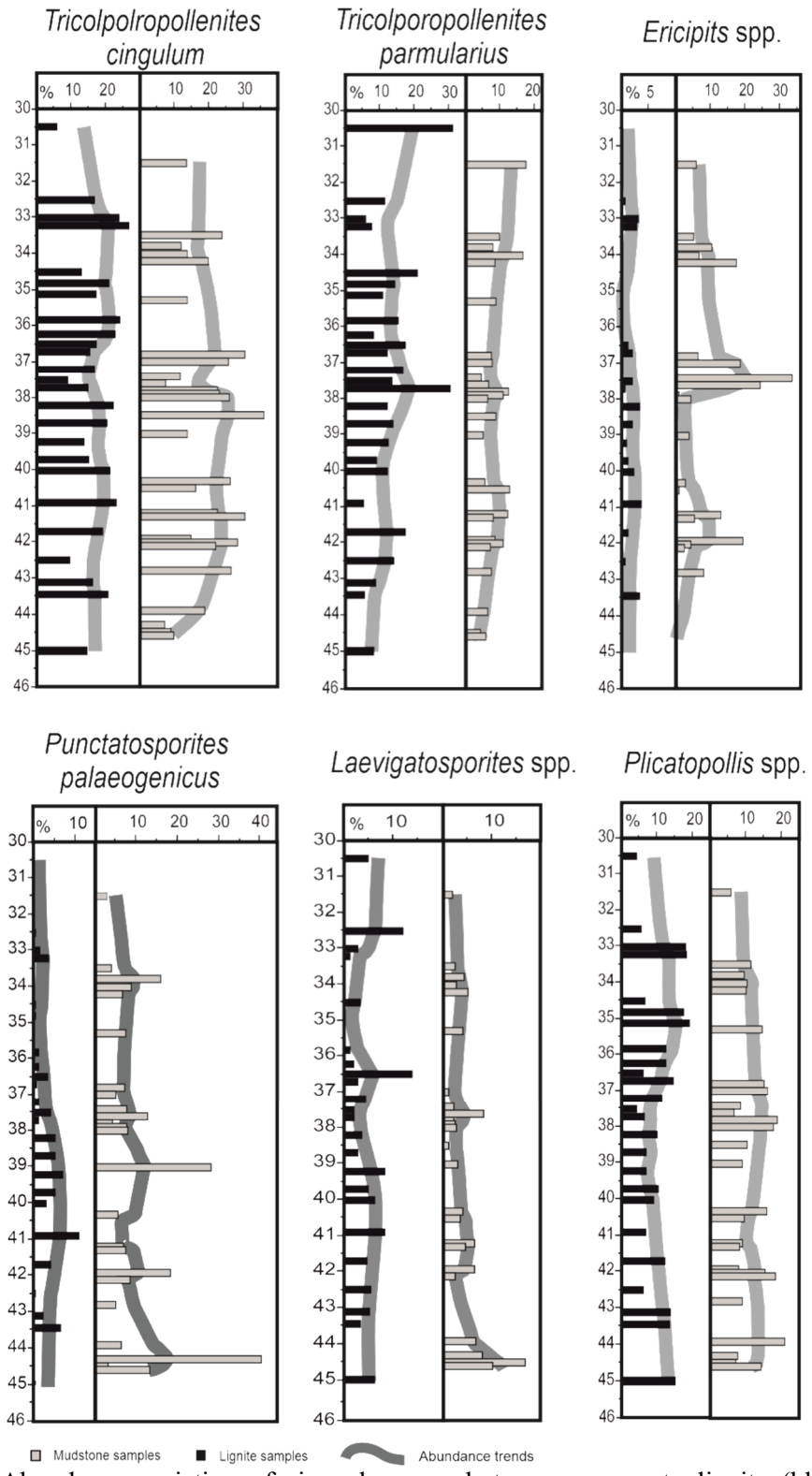

Fig. 4. 7. 8. Abundance variation of six palynomorph taxa common to lignite (black bars) and mudstone (grey bars) samples between 30.52 and 45.02 m depth (LZ4). The grey lines represent the smoothed abundance trends using a 12 point-Gaussian kernel according to Hammer et al. (2001).

Hofmann et al. (2005) assumed that the deposition of the lignites may have been the result of lake level influencing auto-cyclic controls, such as processes that were strictly related to the progressive delivery of sediment to a water filled depression or related to a combination of auto-cyclic, climate-related and tectonic control. However, systematic variation in abundance of the palynomorphs is not correlated to lithology.

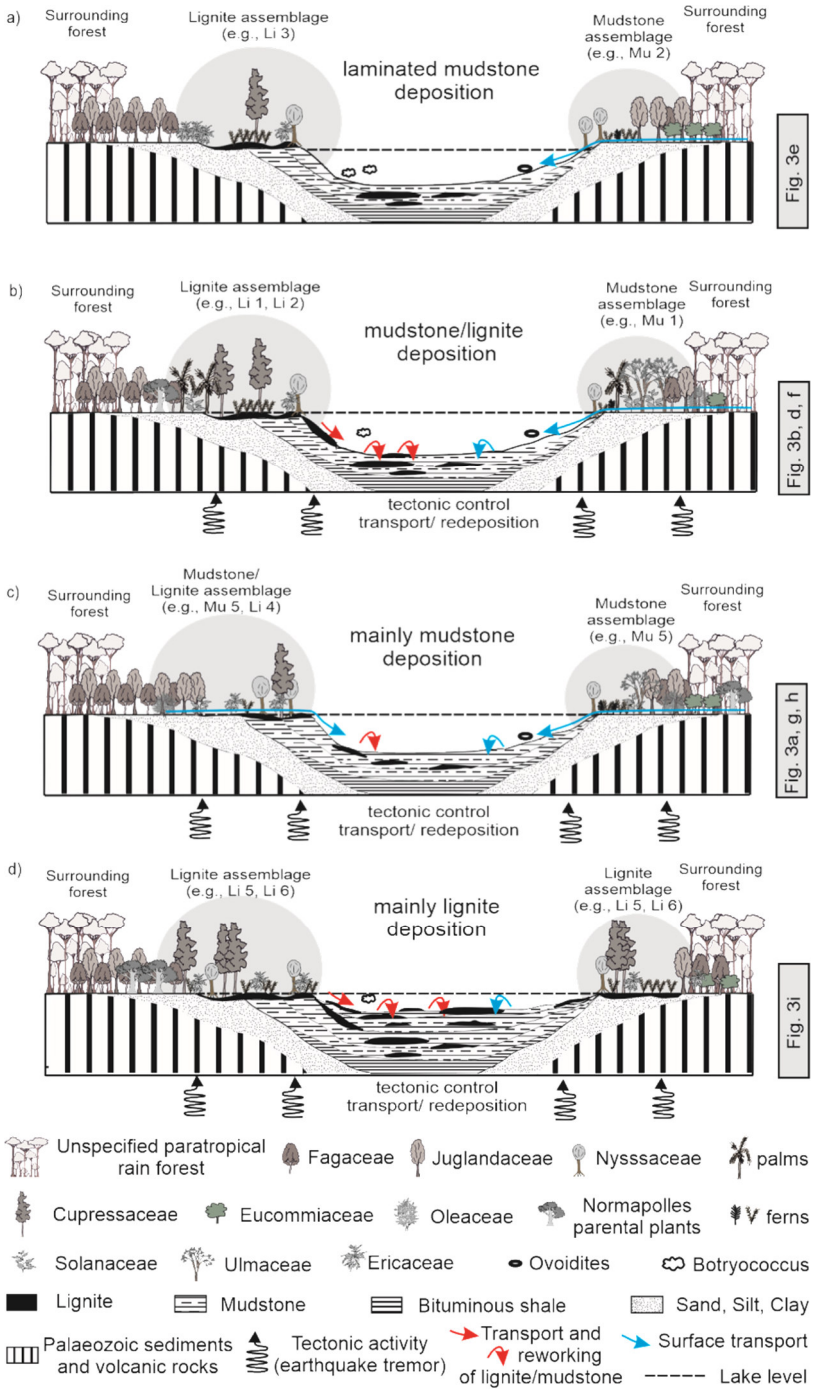

Fig. 4. 7. 9. Four different scenarios for the basin at PvH with regard to tectonic activity and vegetation: (a) Quiescent tectonic activity, (b) Tectonic activity with redeposition of both, lignite and mudstone, (c) Tectonic activity and preferential redeposition of mudstone, (d) Tectonic activity and preferential redeposition of lignitic material (see text for details). For each of the scenarios examples are given by references to core images presented in Fig. 4.7.3. Changes in the vegetation during the (re)deposition of lignite and mudstone are restricted to the local flora at the edge of the lake (shaded). Different Li (lignite) and Mu (mudstone) phases are specified, but it should be noted that the respective assemblages are not directly associated with one of the tectonic scenarios (see text).

The complete absence of rooting (Hofmann et al. 2005) and erosional structures at the base of some lignites support an allochthonous origin for the organic material. This is a strong argument for discontinuities in the sequence in combination with repeated erosion and redeposition of organic material. An orbital control of lake-level fluctuations and related deposition of plant matter (biomass) as suggested by Hofmann et al. (2005) cannot be proven by our study. The palynological investigation of the lignite and mudstone samples may therefore suggest that climate change influenced the composition of the vegetation over time.
Nevertheless, compared to the influence of tectonic activity as recorded by sedimentological evidence (Moshayedi et al. 2018) climate change is of minor importance for the composition of the palynomorph assemblages.
The structure at PvH is aligned in SW-NE direction with three other Eocene basins (Messel, Erlenwiese, Sellborn-Schneise; Fig. 4.7.1) along a major concealed fault, the Messel Fault Zone (MZN; Mezger et al. 2013). Therefore, tectonic events, such as small earthquakes may have occurred frequently during the history of the lake and led to remobilization and transport of marginal deposits into more central parts of the basin at Lake PvH. Fig. 4.7.9 is based mainly on tectonic activity as the main factor influencing facies and palaeoenvironment changes at PvH.
The model distinguishes between 4 scenarios:

(a) *Quiescent tectonic activity*: Predominant surface transport of fine grained clastic material leads to the deposition of laminated mudstones without lignite clasts (Fig. 4.7.3e).
(b) *Tectonic activity with redeposition of lignite and mudstone*: In case of increased tectonic activity, eg, as a result of earthquakes, lignitic material is transported from areas of peat accumulation at the edge of the lake into the basin. At the same time clastic sediments will also be redeposited and in situ displacement occurs (Fig. 4.7.3b, d, f).
(c) *Tectonic activity and redeposition of mudstones*: During phases of reduced peat formation, tectonic activity primarily leads to redeposition and mixing of mudstones with few lignitic clasts (Figs. 4.7.3a, g, h).
(d) *Tectonic activity and redeposition of lignites*: During phases of enhanced peat formation at the edge of the lake, tectonic activity primarily leads to redeposition of lignite (Fig. 4.7.3i) including some clastic material.

The model (Fig. 4.7.9) also includes minor changes in the composition of the vegetation, especially affecting the local habitats in swampy areas at the edge of the lake which are influenced by lake level. At the same time the regional forest vegetation persists. The different vegetational phases (Li and Mu phases) which are summarized in Fig. 4.7.9 show different phases in the evolution of the vegetation probably reflecting a climatic influence. They are not directly linked to one of the tectonic scenarios and here is no specific vegetation associated, for example, with times of quiescent tectonic activity.

Conclusions

The studied 15 meter succession of alternating lignite and mudstone beds comprises only a small part of the lacustrine sequence at Lake “Prinz von Hessen”, but includes the time during which the lake probably had its smallest extent and lowest water level, which led to the establishment of extensive swamp environments and peat accumulation. High-resolution palynology, in combination with statistical analyses, shows that trends in the composition of the vegetation can clearly be identified during this lake phase, although they are masked by distinct facies changes (lignite versus clastic beds). The difference between lignites and clastic beds is reflected by significant differences in abundance for more than 20% of the palynomorphs. However, this is primarily related to taphonomical processes. While pollen and spores from the lignites mainly represent the more local aspect of peat forming

environments around the lake, the mudstone record is derived from surface transport covering a larger catchment area.
Nevertheless, our study shows that the general vegetational trends were consistently expressed throughout both lithologies. Therefore, the study provides insight into the evolution of the vegetation during a short interval of the Paleogene greenhouse phase. A general climate change to slightly cooler and less humid conditions resulted only in minor changes in the qualitative composition of the vegetation. Only few taxa disappear between samples from the lower and upper part of the studied succession. It is therefore obvious that the vegetation, in general, had been robust in composition during the time recorded in the studied lacustrine succession. Only the communities at the lake shore were seriously affected by climate change.
However, our study shows quantitative changes in the vegetation, especially with regard to dominant elements as recorded in the palynoflora and probably recording changes in the dominance of different plant families. This applies especially to the Fagaceae and the Juglandaceae, which were among the most widespread elements of the Central European forests during the Paleogene (Mai 1981). These families alternated in their predominance in the forest vegetation at PvH in a similar way as described for the vegetation at nearby Lake Messel (Lenz et al., 2015). Such changes in the dominance of individual plant families may also have been related to orbitally controlled climate change at PvH, however, this cannot be unequivocally proven without an exact age model for the succession.
Frequent disturbance of the mudstones and an allochthonous origin of the lignitic material suggest that tectonic activity may have had some impact on the paleoenvironment of the lake basin and its surroundings. This is not only evident for the studied short interval, but also for the whole lacustrine sequence of PvH as described by Moshayedi et al. (2018). Tectonic activity is expressed by frequent earthquake tremor as identified by disturbed bedding, frequent evidence for redeposition and several discontinuities in the sedimentary record (Moshayedi et al 2018). In summary, a combination of both, tectonic activity, and, to a minor extent, climate change, were the driving factors for changes in palaeoenvironment and the palaeoecosystems which may have been related to changes in lake level.

Acknowledgements and funding
Our research has been carried out as a project funded by the Deutscher Akademischer Austauschdienst (DAAD) under the grant 110207-54900347 including the PhD appointment of the first author. This generous support is gratefully acknowledged. The help of Karin Schmidt, Palaeobotanical Section, Senckenberg Research Institute and Natural History Museum Frankfurt, in sampling and sample preparation is also acknowledged. Core photographs of FIS/HLUG from the core B/97-BK9 were kindly supplied by the Department for Messel Research and Mammalogy, Senckenberg Research Institute and Natural History Museum Frankfurt. Finally, we thank Robert A. Gastaldo and Carlos Jaramillo for their constructive comments and suggestions, which greatly helped to improve the paper.

References
Bohacs, K.M., Carroll, A.R., Neal, J.E., Mankiewicz, P.J. (2000). Lake-basin type, source potential, and hydrocarbon character: an integrated sequence-stratigraphic-geochemical framework. In: Gierlowski-Kordesch, E.H. and Kelts, K.R. (eds) *Lake basins through space and time*. AAPG Studies in *Geology*, 46: 3-34.
Bradley, W.H. (1967). Two aquatic fungi (Chytridiales) of Eocene Age from the Green River Formation of Wyoming. *American Journal of Botany*, 54: 577-582.
Bray, J.R., Curtis, J.T. (1957). An ordination of the upland forest communities of southern Wisconsin. *Ecological Monographs,* 27: 325-349.
Broothaerts, N., Verstraeten, G., Kasse, C., Bohncke, S., Notebaert, B., Vandenberghe, J. (2014). Reconstruction and semi-quantification of human impact in the Dijle catchment, central Belgium: a palynological and statistical approach. *Quaternary Science Reviews,* 102: 96-110.

Carroll, A.R., Bohacs, K.M. (1999). Stratigraphic classification of ancient lakes: Balancing tectonic and climatic controls. *Geology,* 27: 99-102.
Collinson, M.E., Smith, S.Y., Manchester, S.R., Wilde,V., Howard, L. E., Robson, B.E., Ford, D.S, Marone, F., Fife, J.L., Stampanoni, M. (2012). The value of X-ray approaches in the *study of the Messel fruit and seed flora. Palaeobiodiversity and Palaeoenvironments,* 92(4): 403-416.
Cottam, G., Goff, F.G., Whittaker, R.H. (1978). Wisconsin Comparative Ordination, in Whittaker RH, ed., Ordination of Plant Communities. *Handbook of Vegetation Science*, vol 5-2. Dordrecht, Springer, p 185-213.
Couvreur, T.L.P., Forest, F., Baker, W.J. (2011). Origin and global diversification patterns of tropical rain forest: inferences from a complete genus-level phylogeny of palms. *BMC Biology*, 9: 1-12.
Daly, R.J., Jolley, D.W. (2015). What was the nature and role of Normapolles angiosperms? A case study from the earliest Cenozoic of Eastern Europe. *Palaeogeography, Palaeoclimatology, Palaeoecology,* 418: 141-149.
DeBusk, J.r.G.H. (1997). The distribution of pollen in the surface sediments of Lake Malawi, Africa, and the transport of pollen in large lakes. *Review of Palaeobotany and Palynology,* 97: 123-153.
Elsik, W.C. (1996). Chapter 10, Fungi, *in* Jansonius, J. and McGregor, D.C., eds., Palynology: principles and applications, 1. Houston, TX*, American Association of Stratigraphic Palynologists Foundation*, 296-305.
Felder, M., Gaupp, R. (2006). The δ13C and δ18O signatures of siderite – a tool to discriminate mixis patterns in ancient lakes. *Zeitschrift der Deutschen Gesellschaft für Geowissenschaften* 157, 397-410.
Felder, M., Harms, F.J. (2004). Lithologie und genetische Interpretation der vulkano-sedimentären Ablagerungen aus der Grube Messel anhand der Forschungsbohrung Messel 2001 und weiterer Bohrungen*. Courier Forschungsinstitut Senckenberg,* 252: p 151-203.
Felder, M., Harms, F.J. (2004). Lithologie und genetische Interpretation der vulkano-sedimentären Ablagerungen aus der Grube Messel anhand der Forschungsbohrung Messel 2001 und weiterer Bohrungen (Eozän, Messel-Formation, Sprendlinger Horst, Südhessen). *Courier Forschungsinstitut Senckenberg* ,252: 151–206.
Franzen, J.L. (2006). Eurohippus parvulus parvulus (Mammalia, Equidae) aus der Grube Prinz von Hessen bei Darmstadt (Süd-Hessen, Deutschland). *Senckenbergiana lethaea,* 86: 265-269.
Frederiksen, N.O. (1996). Chapter 29, Vegetational history. Introduction, *in* Jansonius, J. and McGregor, D.C., eds., Palynology: principles and applications, 3. Houston, TX, *American Association of Stratigraphic Palynologists Foundation*, 1129–1131.
Friis-Christensen, E., Svensmark, H. (1997). What do we really know about the sun-climate connection? *Advances in Space Research,* 20: 913–921.
Galloway, J.M., Tullius, D.N., Evenchick, C.A., Swindles, G.T., Hadlari, T., Embry, A. (2015). Early Cretaceous vegetation and climate change at high latitude: Palynological evidence from Isachsen Formation, *Arctic Canada. Cretaceous Research,* 56: 399-420.
Gauch, H.G., Scruggs, W.M. (1979). Variants of polar ordination. *Vegetatio*, 40: 147- 153.
Geitler L (1962) Entwicklungsgeschichte der Chytridiale Entophlyctis apiculata auf der Protococcale Hypnomonas lobata. *Österreichische botanische Zeitschrift,* 109: 138-149.
Greenwood, D.R., Wing, S.L. (1995). Eocene continental climates and latitudinal temperature gradients. *Geology,* 23: 1044-1048.
Gruber, G., Micklich, N. (2007). *Messel—Treasures of the Eocene*. Darmstadt: Hessisches Landesmuseum p 158.
Hair, J.R.J.F., Black, W.C., Babin, B.J., Anderson, R.E. (2010). *Multivariate data analysis*, 7th edition, London, Pearson, p 761.
Hammer, Ø., Harper, D.A.T., Ryan, P.D. (2001). *PAST*: paleontological statistics software package for education and data analysis. Palaeontologia Electronica 4(1): https://palaeo-electronica.org/2001_1/past/issue1_01.htm
Harms, F.J., Aderhold, G., Hoffmann, I., Nix. T., Rosenberg, F. (1999). Erläuterungen zur Grube Messel bei Darmstadt, Südhessen. *Schriftenreihe der Deutschen Geologischen Gesellschaft,* 8: 181-222.
Hofmann, P., Duckensell, M., Chpitsglous, A., Schwark, L. (2005). Geochemical and organic petrological characterization of the organic matter of lacustrine Eocene oil shales (Prinz von Hessen, Germany): reconstruction of the depositional environment. *Paleolimnology,* 33: 155–168.

Jacoby, W. (1997). Tektonik und Eoza¨ ner Vulkanismus des Sprendlinger Horstes, NE-Flanke des Oberrheingrabens. *Schriftenreihe dt. geol*. *Ges*, 2: 66–67.
Jacoby, W., Wallner, H., Smilde, P. (2000). Tektonik und Vulkanismus entlang der Messeler-Sto¨ rungszone auf dem Sprendlinger Horst: geophysikalische Ergebnisse. *Zeitschrift der Deutschen Gesellschaft für Geowissenschaften,* 151–154: 493–510.
Jardine, P.E., Harrington, G.J. (2008). The Red Hills Mine palynoflora: A diverse swamp assemblage from the Late Paleocene of Mississippi, U.S.A. *Palynology,* 32: 183-204.
Janssen, C.R., Birks, H.J.B. (1994). Recurrent groups of pollen types in time. *Review of Palaeobotany and Palynology,* 82: 165–173.
Juggins. S. (2007). *C2 Software for ecological and palaeoecological data analysis and visualization. User guide* Version 1.5: p 73.
Kaiser, M.L., Ashraf, R. (1974). Gewinnung und Präparation fossiler Pollen und Sporen sowie anderer Palynomorphae unter besonderer Berücksichtigung der Siebmethode. *Geologisches Jahrbuch,* 25: 85–114.
Kern, A.K., Harzhauser, M., Soliman, A., Piller, W.E., Mandic, O. (2013). High-resolution analysis of upper Miocene lake deposits: Evidence for the influence of Gleissberg-band solar forcing. *Palaeogeography, Palaeoclimatology, Palaeoecology,* 370: 167–183.
Kron, K.A. (1996). Phylogenetic relationships of Empetraceae, Epacridaceae, Ericaceae. Monotropaceae, and Pyrolaceae: evidence from nuclear ribosomal *18s sequence. Annals of Botany,* 77: 293-303.
Kron, K.A., Powell, E.A., Luteyn, J.L. (2002). Phylogenetic relationships within the blueberry tribe (Vaccinieae, Ericaceae) based on sequence data from matK and nuclear ribosomal ITS regions, with comments on the placement of Satyria. *American Journal of Botany,* 89: 327-336.
Kuhry, P. (1985). Transgression of a raised bog across a coversand ridge originally covered with an oak-lime forest. Palynological study of a middle Holocene local vegetational succession in the Amtsven (northwest Germany). *Review of Palaeobotany and Palynology,* 44: 303-353.
Lenz, O.K. (2005). Palynologie und Paläoökologie eines Küstenmoores aus dem Mittleren Eozän Mitteleuropas Die Wulfersdorfer Flözgruppe aus dem Tagebau Helmstedt, Niedersachsen. *Palaeontographica B*, 271: 1–157.
Lenz, O.K., Riegel, W. (2001). Isopollen maps as a tool for the Reconstruction of a coastal swamp from the Middle Eocene at Helmstedt (Northern Germany). *Facies,* 45: 177-194.
Lenz, O.K., Wilde, V., Riegel, W. (2007). Recolonization of a Middle Eocene volcanic site: quantitative palynology of the initial phase of the maar lake of Messel (Germany). *Review of Palaeobotany and Palynology,* 145: 217–242.
Lenz. O.K., Wilde, V., Riegel, W. (2011). Short-term fluctuation in vegetation and phytoplankton during the middle Eocene greenhouse climate: a 640-kyr record from the Messel oil shale (Germany). *International Journal of Earth Sciences,* 100: 1851-1874.
Lenz, O.K-, Wilde, V., Mertz, D.F., Riegel, W. (2015). New palynology-based astronomical and revised 40Ar/39Ar ages for the Eocene maar lake of Messel (Germany). *International Journal of Earth Science,* 104: 873-889.
Lenz, O.K., Wilde, V., Riegel, W. (2017). ENSO- and solar-driven sub-Milankovitch cyclicity in the Palaeogene greenhouse world; high-resolution pollen records from Eocene Lake Messel, Germany. *Journal of the Geological Society* 174: 110-128.
Luteyn, J.L. (2002). Diversity, adaptation, and endemism in neotropical Ericaceae: biogeographical patterns in the Vaccinieae. *The Botanical Review,* 68: 55-87.
Mai, D.H. (1981). Entwicklung und klimatische Differenzierung der Laubwaldflora Mitteleuropas im Tertiär. *Flora,* 171: 525–582.
Mai, D.H. (1995). *Tertiäre Vegetationsgeschichte Europas—Methoden und Ergebnisse,*. Gustav Fischer Verlag, Jena, p 691.
Manchester, S.R. (1989). Attached reproductive and vegetative remains of the extinct American–European genus Cedrelospermum (Ulmaceae) from the early Tertiary of Utah and Colorado. *American Journal of Botany,* 76: 256–276.
Mander, L., Kürschner, W.M., McElwain, J.C. (2010). An explanation for conflicting records of Triassic–Jurassic plant diversity. *Proceedings of the National Academy of Sciences of the United States of America,* 107: 15351–15356.

Marell, D. (1989). Das Rotliegende zwischen Odenwald und Taunus.- *Geologische Abh. Hessen,* 89: 1-128.
Mezger, J.E., Felder, M., Harms, F.J. (2013). Crystalline rocks in the maar deposits of Messel: key to understand the geometries of the Messel Fault Zone and diatreme and the post-eruptional development of the basin fill. *Zeitschrift der Deutschen Gesellschaft für Geowissenschaften,* 164: 639–662.
Minchin, P.R. (1987). An evaluation of the relative robustness of techniques for ecological ordination. *Vegetation* 69: 89-107.
Morley, R.J. (2000). *Origin and evolution of tropical rain forests*. John Wiley and Sons Chichester: p 362.
Morley, R.J. (2003). Interplate dispersal paths for megathermal angiosperms. Perspectives in Plant Ecology. *Evolution and Systematics,* 6: 5–20.
Moshayedi, M., Lenz, O.K., Wilde, V., Hinderer, M. (2018). Controls on sedimentation and vegetation in an Eocene pull-apart basin (Prinz von Hessen, Germany): evidence from palynology. *Journal of the Geological Society,* 175: 757-773.
Nickel, B. (1996). Die mitteleozäne Mikroflora von Eckfeld bei Manderscheid/Eifel. *Mainzer Naturwissenschaftliches Archiv. Beiheft,* 18: 1–121.
Oksanen, J. (2007). Standardization methods for community ecology. Documentation and user guide for package Vegan, 1.8-6.
Pirrung, M. (1998). Zur Entstehung isolierter alttertiärer Seesedimente in zentraleuropäischen Vulkanfeldern. *Mainzer Naturwissenschaftliches Archiv Beiheft,* 20: 1-117.
Plunkett, G.M., Soltis, D.E., Soltis, P.S. (1996). Higher level relationships of Apiales (Apiaceae and Araliaceae) based on phylogenetic analysis of rbcL sequences. *American Journal of Botany,* 83: 499-515.
Riegel, W., Lenz, O.K., Wilde, V. (2015). From open estuary to meandering river in a greenhouse world: an ecological case study from Middle Eocene of Helmstedt, Northen Germany. *Palaios,* 30: 304-326.
Riegel, W., Wilde, V. (2016). An early Eocene Sphagnum bog at Schöningen, northern Germany. *International Journal of Coal Geology,* 159: 57-70.
Sanderson, M.J., Donoghue, M.J. (1994). Shifts in diversification rate with the origin of angiosperms. *Science,* 264: 1590-1595.
Schaarschmidt, F. (1988). Der Wald, fossile Pflanzen als Zeugen eines warmen Klimas, *In*: Schaal, S. and Ziegler, W. (eds) Messel - ein Schaufenster in die Geschichte der Erde und des Lebens. Waldemar Kramer, Frankfurt am Main, p 27-52.
Schaal, S., Ziegler, W. (1988). *Messel-Ein Schaufensten in die Geschichte der Erde und des Lebens*, Kramer. New York, p 315.
Smith, K.T., Schaal, S.F.K., Habersetzer, J. (2018) Messel – An Ancient Greenhouse Ecosystem. *Senckenberg-Buch 80*, Schweizerbart, Stuttgart, 315p.
Ter Braak, C.J.F., Looman, C.W.N. (1996). Regression. *in* Jongman, R.H.G., Ter Braak, C.J.F., Tongeren, O.F.R., eds., Data analysis in community and landscape ecology. Cambridge, Cambridge University Press, p 29–77.
Thiele-Pfeiffer, H. (1988). Die Mikroflora aus dem mitteleozänen Ölschiefer von Messel bei Darmstadt. *Palaeontographica* B 211: 1–86.
Thomson, P.W., Pflug, H. (1953). Pollen und Sporen des mitteleuropäischen Tertiärs. Gesamtübersicht über die stratigraphisch und paläontologisch wichtigen Formen. *Palaeontographica* B 94: 1–138.
Tiner, R.W. (2017). *Practical considerations for wetland identification and boundary delineation*. In Wetlands, CRC Press, p 129-154.
Walther, G.R., Gritti, E.S., Berger, S., Hickler, T., Tang, Z.Y., Sykes, M.T. (2007). Palms tracking climate change. *Global Ecology and Biogeography,* 16: 801–809.
Wilde, V. (1989). Untersuchungen zur Systematik der Blattreste aus dem Mitteleozän der Grube Messel bei Darmstadt (Hessen, Bundesrepublik Deutschland). *Courier Forschungsinstitut Senckenberg* ,115: 1–123.

4-8 Comparison of core samples and surface samples from the lake basin of Prinz von Hessen

In this chapter the palynomorph assemblages of 6 surface samples are compared with assemblages from core Prinz von Hessen to provide chronological control for the sedimantry sequences in the basin. The results underline age differences between lignites revealed in the core and the lignites that have been mined in the last century in parts of the lake basin. This chapter is considered to be prepared for publication in the near future.

Introduction

Grube Prinz von Hessen is only about 2 km southwest of the Messel pit, which is known as a fossil site and UNESCO World Heritage site and as it was discussed in the previous chapters, that the lacustrine part of core Prinz von Hessen is in some parts of the same age as the lacustrine succession of Lake Messel. Lacustrine sedimentation at Prinz von Hessen started in the latest early Eocene almost coeval with the deposition of the Lower Messel Formation at Messel (Moshayedi et al. 2018). A mammal age for Prinz von Hessen from the mined part of the succession (Franzen 2006) possibly even ranges into the late Eocene and points to a considerable hiatus between the lake sediments in core Prinz von Hessen and the thick lignite which was originally mined at the top of the succession, since the lacustrine succession in core Prinz von Hessen is of uppermost lower Eocene age (Moshayedi et al. 2018). The existence of the basin at Prinz von Hessen may therefore have lasted for more than 7 million years in contrast to less than a million years for the maar lake at Messel. In order to compare lignites from the surface of the lake basin of Prinz von Hessen with the succession in core Prinz von Hessen stratigraphically, 6 lignite samples of the lake surface have been taken from east of the drill site by M. Wuttke (Senckenberg Research Institute and Natural History Museum Frankfurt). The samples analyzed palynologically at TU Darmstadt to see possible relatioships (Fig. 4.8.1). Lithologically the samples are brown coals with or without quartz, which probably belong to the former lignites that were mined at the top of the succession in the eastern part of the lake basin. The surface samples can be used to study the spatial variation of the vegetation. However, a stratigraphic order of the surface samples is not possiible.

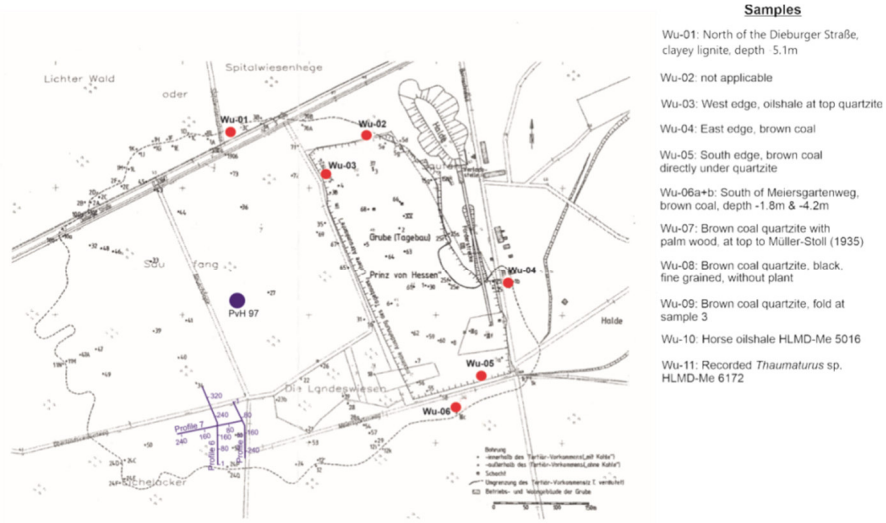

Fig. 4. 8. 1. Locations of the surface samples and scientific core of Prinz von Hessen

Methods

For palynological analysis, 6 brown coal samples were selected from the surface of the lake. Palynological preparation of the samples including treatment with hydrochloric acid (HCl),

hydrofluoric acid (HF) and potassium hydroxide (KOH) followed the standard method as described by Kaiser and Ashraf (1974). After sieving through a 10 µm mesh screen, residues were oxidized using nitric acid (HNO_3) or hydrogen peroxide (H_2O_2) to improve transparency of the palynomorphs.

For each sample one or more slides have been prepared using a mixture of the residue and glycerine jelly. Palynological analysis was undertaken using a transmitted light microscope (Olympus BX40). To obtain a representative dataset for robust statistical analysis, at least 300 individual palynomorphs were counted per sample at ×400 magnification (raw data are included in the Supplementary material). Poorly preserved palynomorphs that could not be identified were counted as 'Varia'. The palynomorphs were mainly identified based on the systematic-taxonomic studies of Thomson and Pflug (1953), Thiele-Pfeiffer (1988), Nickel (1996) and Lenz (2005). In order to detect compositional differences between the surface samples from the lake basin and 47 samples from the lacustrine part of the scientific core Prinz von Hessen, non-metric multidimensional scaling (NMDS; Shepard 1962a, b; Kruskal 1964) has been performed. For this purpose all taxa that did not reach 1% in any of the studied samples have been removed from the analysis. Statistical analysis is based on the raw data, which have been standardized using the Wisconsin double standardization (Bray and Curtis 1957; Cottam et al. 1978; Gauch and Scruggs 1979; Oksanen 2007) as it described by Moshayedi et al. 2020 (in press).

Results

The pollen diagram (Fig. 4.8.2) shows that taxa do not vary significantly in the six studied samples. Spores including Schizaeaceae with species of the genera *Leiotriletes* (up to 10%) and Polypodiaceae (*Polypodiaceoisporites* spp. with 5% and *Laevigatosporites* spp. with 10%) are relatively abundant. Among the dominant elements are juglandaceous (*Plicatopollis* spp., up to 25%) and fagaceous (*Tricolpopollenites cingulum*, up to 50%) pollen. Other characteristic taxa are forest elements of *Tricolpo(ro)pollenites parmularius* (Eucommiaceae, up to 15%) and *Tricolporopollenites edmundi* (Mastixiaceae, up to 5%;). *Celtipollenites* spp. (Ulmaceae, starts with 5%), also occurrs in high numbers. In contrast, swamp elements such as Ericaceae (*Ericipites* spp.) have been observed in few numbers in only one sample.

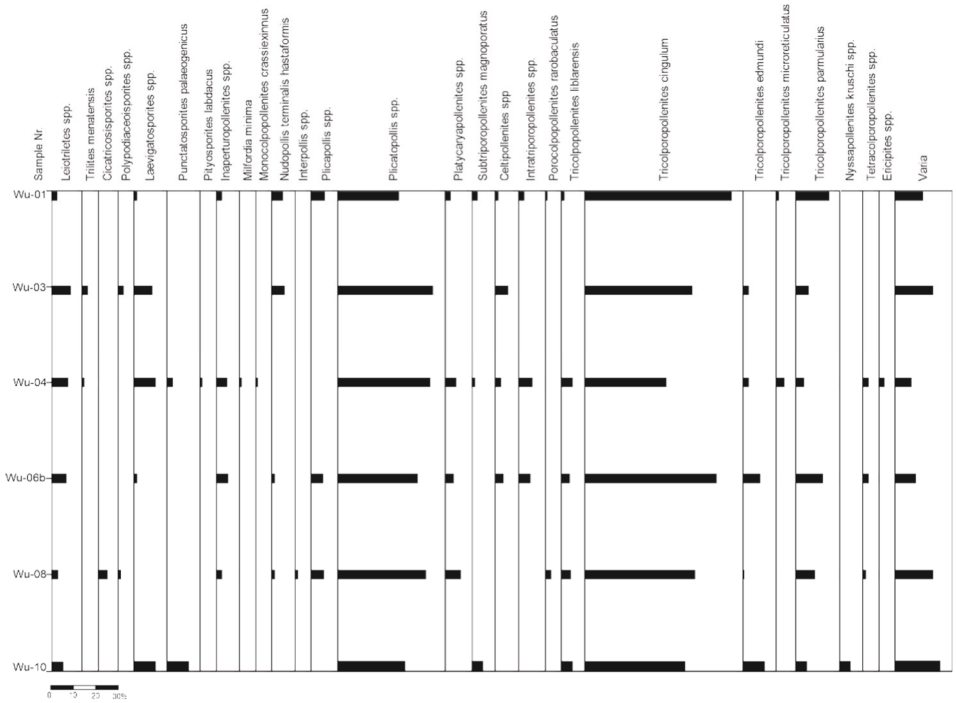

Fig. 4. 8. 2. Pollen diagram showing the abundance of palynomorph in six surface samples.

Discussion

The pollen of Juglandaceae and Fagaceae are dominant elements in the six studied surface samples. They are typical elements of Paleogene floras of Europe and North America (e.g. Manchester 1989). Accordingly, they are common in most of the Central European Eocene pollen floras, such as at Geiseltal (Riegel and Wilde 2016), Eckfeld (Nickel 1996) or Helmstedt (Lenz 2005, Riegel et al. 2015). They are also among the dominant elements within the forest vegetation in the nearby record of Messel (Lenz et al. 2011, 2017). Therefore, similar abundance values in the pollen record of Lake Prinz von Hessen are not surprising. Together with an abundant macrofossil record of Juglandaceae at Messel (Wilde 1989, 2004), this is proof for the dominant role of these plants in the zonal flora on the Sprendlinger Horst during the Eocene. In contrast, macroscopic remains of Fagaceae have never been found at Messel (Wilde 1989, 2004). Therefore, the habitat of the Fagaceae is considered to have been outside the narrow catchment area of Lake Messel (Lenz et al. 2011). The same is most probably true for Lake Prinz von Hessen.

The NMDS shows that there is a clear separation between samples from core Prinz von Hessen and samples from the lake basin at the upper part of the ordination space indicating compositional differences of the pollen assemblages (Fig. 4.8.3). Compared to the assemblage of fluvial –lacustrine facies association with the core Prinz von Hessen (see LZ4 in Moshayedi et al. 2018) the strong decline or even disappearance of most fern spores and completely absence of swamp elements e.g. Ericaceae (Ericipites spp.) are noteworthy. This could indicate a significant change of ecological conditions between both peat forming parts in Lake Prinz von Hessen and less humid conditions during the deposition of the peat at the top of the record. This could mean that surface samples and the lignite part of the core (see LZ4 in Moshayedi et al. 2018) are of the same age and differences may be related to different positions in the swamp forest at the edge or in the centre of the forest. However, there is no lithologic evidence proving that the surface and core samples are of the same age.

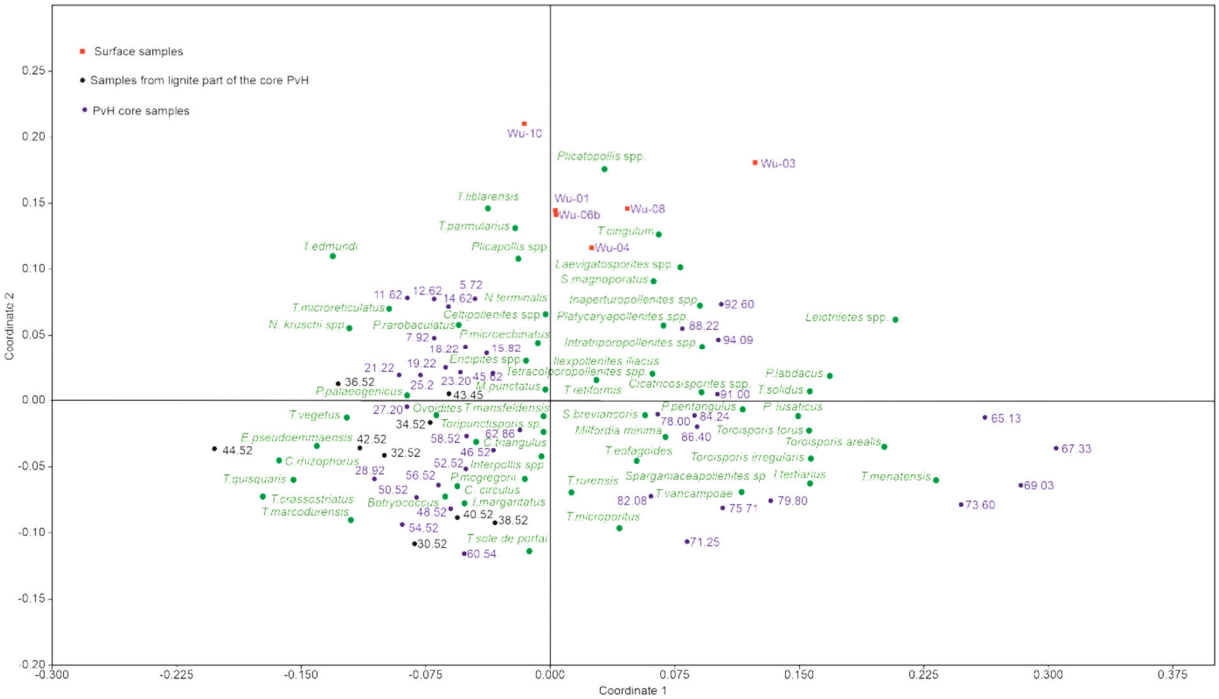

Fig. 4. 8. 3. The NMDS showing a clear separation between samples from core Prinz von Hessen and samples from the lake basin

Seismic profiles of lacustrine sediments in Prinz von Hessen (Fig. 4.8.4) which were kindly provided by the Leibniz Institut für Angewandte Geophysik Hannover (LIAG, formerly GGA, Dr. Buness, Dr. Wonik) show that during the evolution of Lake Prinz von Hessen small basins evolved, which are separated from the main lake basin. The seismic profiles (Fig. 4.8.4) indicate that such a small basin has been cored by the research drilling. This would imply that the succession of lignites in the core is clearly separated and not associated with the lignites that were mined in the eastern part of the Prinz von Hessen basin and which are probably of late Eocene age (Franzen 2006). Therefore, the strong differences of palynomorph assemblages between lignites from the surface and lignites from the core are probably related to age differences between both lignite records and not to the position of the records within the peat forming environment.

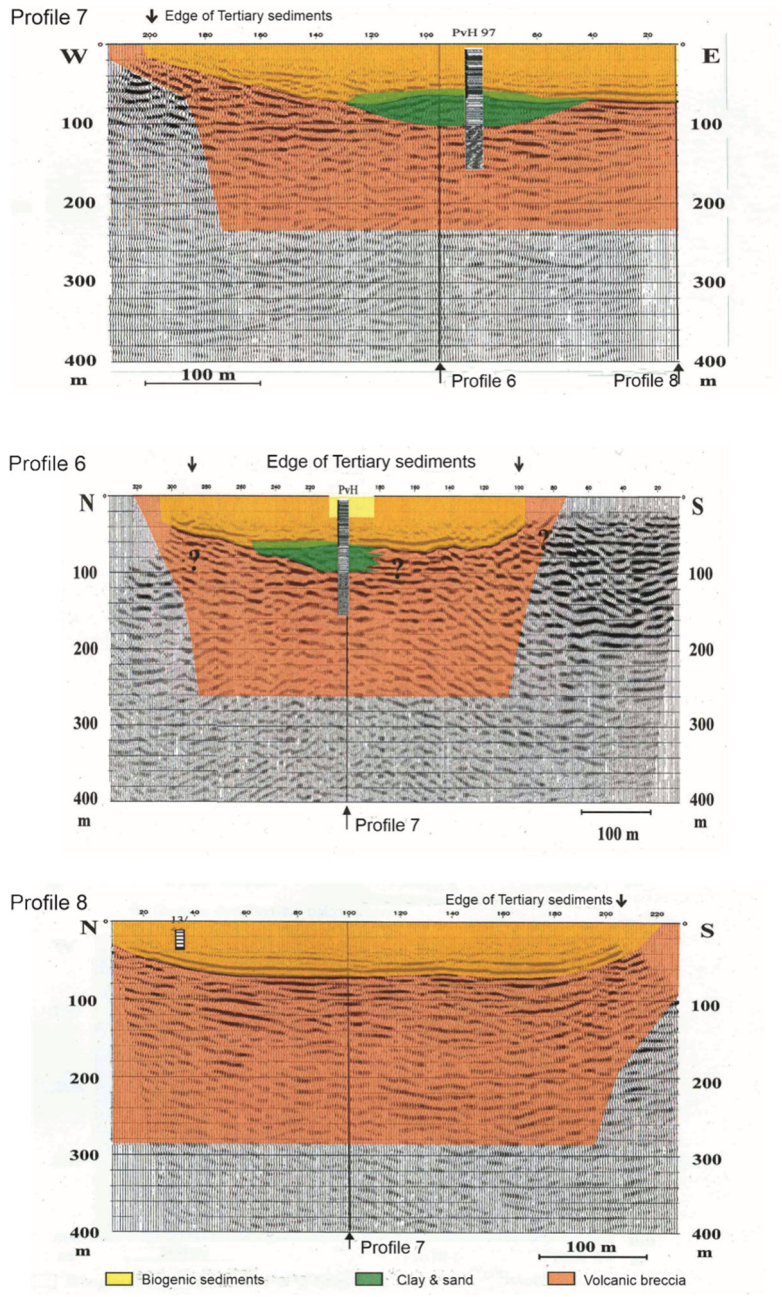

Fig. 4. 8. 4. Seismic profiles of lacustrine sediments in Prinz von Hessen

Conclusion

Significant changes between the palynological assemblages of lake basin samples and samples of core Prinz von Hessen support the age model presented by Moshayedi et al. (2018). Sedimentation at Prinz von Hessen started in the late early Eocene coeval with the Lower Messel Formation. Also the lignite succession within core Prinz von Hessen is therefore of early Eocene age. On the other hand, the mammal age of the mined part at the top of the succession (Franzen 2006) suggests that the peat deposition continued into the late Eocene in other parts of the lake basin. Therefore, a considerable hiatus between the lake sediments in core Prinz von Hessen and the mined lignites at the top of the succession is indicated. There is no palynological proof showing a relationship between the sampled lignites from the mined succession and the lignites in core Prinz von Hessen (LZ 4). In combination with the results of seismic studies it can be proven that the lignites in core Prinz von Hessen and the mined lignites are representing two different peat-forming phases during the evolution of the lake.

References

Bray JR, Curtis JT (1957) An ordination of the upland forest communities of southern Wisconsin. *Ecological Monographs*, 27: 325-349.

Cottam G, Goff FG, Whittaker RH (1978) Wisconsin Comparative Ordination, in Whittaker RH, ed., Ordination of Plant Communities. *Handbook of Vegetation Science*, vol 5-2. Dordrecht, Springer, p 185-213.

Gauch HG, Scruggs WM (1979) Variants of polar ordination. *Vegetatio,* 40: 147- 153.

Moshayedi M, Lenz OK, Wilde V, Hinderer M (2018) Controls on sedimentation and vegetation in an Eocene pull-apart basin (Prinz von Hessen, Germany): evidence from palynology. *Journal of the Geological Society*, 175: 757-773.

Moshayedi, M., Lenz, O.K., Wilde, V., Hinderer, M. (2021): Lake-level fluctuations and allochthonous lignite deposition in the Eocene pull-apart basin “Prinz von Hessen” (Hesse, Germany) - A palynological study. *Syntheses in Limnogeology*, Rosen, M.R., Finkelstein, D., Park Boush, L., Pla-Pueyo, S. (eds.): Limnogeology: Progress, Challenges and Opportunities - A Tribute to Elizabeth Gierlowski-Kordesch, Chapter 3. Springer Nature (in press)

4-9 Publication 4: Volcanos and earthquakes - Their influence on the lower to middle Eocene paleoenvironment on the Sprendlinger Horst (Southwest Germany).

In preparation paper

Maryam Moshayedi[1*], Olaf K. Lenz[1, 2], Jürgen Mutzl[1] Volker Wilde[3], Matthias Hinderer[1]

[1]Technische Universität Darmstadt, Institute of Applied Geosciences, Applied Sedimentology, Schnittspahnstrasse 9, 64287 Darmstadt, Germany.
[2]Senckenberg Gesellschaft für Naturforschung, General Directorate, Senckenberganlage 25, 60325, Frankfurt am Main, Germany.
[3]Senckenberg Forschungsinstitut und Naturmuseum, Sektion Paläobotanik, Senckenberganlage 25, 60325, Frankfurt am Main, Germany.

Author Contributions

Conceptualization: M. Moshayedi, Olaf K. Lenz, Volker Wilde, M. Hinderer
Data Curation: M.Moshayedi, J. Mutzl, Olaf K. Lenz
Formal Analysis: M. Moshayedi
Funding Acquisition: M. Moshayedi
Investigation: M. Moshayedi,
Methodology: M. Moshayedi, Olaf K. Lenz, Volker Wilde
Project Administration: Olaf K. Lenz, Volker Wilde, M. Hinderer
Resources: M. Hinderer, V. Wilde
Validation: M. Moshayedi
Visualization: M. Moshayedi
Writing – Original Draft Preparation: M. Moshayedi
Writing – Review and Editing: Olaf K. Lenz, V. Wilde

Abstract
Palynomorph assemblages of four small Eocene lakes at Messel, Prinz von Hessen, Offenthal and Groß Zimmern on the Spendlinger Horst in Southwest Germany were studied for understanding the evolution of the vegetation in Southwest Germany during Paleogene greenhouse conditions with respect to regional tectonic and volcanic influence. Except for Prinz von Hessen, which is most probably a small pull-apart basin, the other basins are maar lakes and formed as a consequence of phreathomagmatic eruptions. Based on revised $^{40}Ar/^{39}Ar$ dates the eruptions at Offenthal (47.71/47.87 ± 0.3 Ma) and Messel (48.11/48.27 ± 0.22 Ma) are nearly of the same age around the lower/middle Eocene boundary. Palynostratigraphic analyses indicate a lower Eocene age for the studied part of Prinz von Hessen and a Middle Eocene age for Groß Zimmern. Our quantitative palynological studies revealed different pollen and spore assemblages in each basin, but similar general trends in the evolution of the vegetation. The plant succession at the maar lakes started with the progressive recolonization of the area in the vicinity of the craters by pioneering elements such as ferns or Restionaceae and continued into a paratropical rainforest and, finally, a climax vegetation with a dominance of juglandaceous and fagaceous plants. Nevertheless, each basin has its unique story to tell. In Messel the following undisturbed record of about 600.000 years reveals the influence of orbital forcing on the climate and the composition as well as on the diversity of the climax vegetation during the early middle Eocene. A climax vegetation comparable to Messel is not documented at Offenthal mainly due to a significant shorter time period reflected in the respective succession of lake sediments. At Lakes Prinz von Hessen and Groß Zimmern regional tectonic activity had a much higher influence on the paleoenvironment than orbitally controlled climate change.

Introduction

To study the evolution of the paleoenvironment on the Sprendlinger Horst in Southwest Germany the three maar lakes of Messel, Offenthal and Groß Zimmern as well as the pull-apart basin Prinz von Hessen from the Sprendlinger Horst were studied for pollen and spores in the last years (Lenz et al. 2007; 2010; 2011; 2015; Lenz and Wilde 2018; Moshayedi et al. 2018; 2020; 2021; Mutzl (2017). These lakes are part of a series of isolated Paleogene deposits in the area of the Sprendlinger Horst, the northern extension of the Odenwald basement, which forms the northeastern shoulder of the Upper Rhine Graben (Fig. 4.9.1).
It can be assumed that both lakes of Messel (48.27 ± 0.22 Ma based on the FCs age of Kuiper et al. 2008, see Lenz et al. 2015) and Offenthal (47.4 ± 0.3 Ma, Mertz and Renne 2005) are nearly age equivalent. Based on the palynostratigraphic work of Mutzl (2017) it seems likely that Lake Groß Zimmern has a similar age as the adjacent crater lakes of Messel and Offenthal, but this must be confirmed by radiometric dating in the near future. With the comparison of these three adjacent and coeval lakes and the palynostratigraphically dated lower Eocene pull-apart basin Prinz von Hessen (Moshayedi et al. 2018), it is possible to reconstruct the evolution of the vegetation and the paleoclimate on the Sprendlinger Horst across the lower to middle Eocene. Furthermore, a chronostratigraphic scenario for volcanic and tectonic activity in the region can be presented.

Geological background

The Odenwald is part of the Mid-German Crystalline Rise, a magmatic arc formed during the Variscan Orogeny by the collision of the Rhenohercynian and Saxothuringian terranes after the collapse of the Rheic Ocean (Zeh and Will 2010). Miocene uplift of the shoulders of the URG led to the erosion of the Mesozoic and younger sediments that cover most of the basement rocks of the Mid-German Crystalline Rise and exposed Variscan basement (Schumacher 2002, Schwarz and Henk 2005, Ziegler and Dèzes 2005).

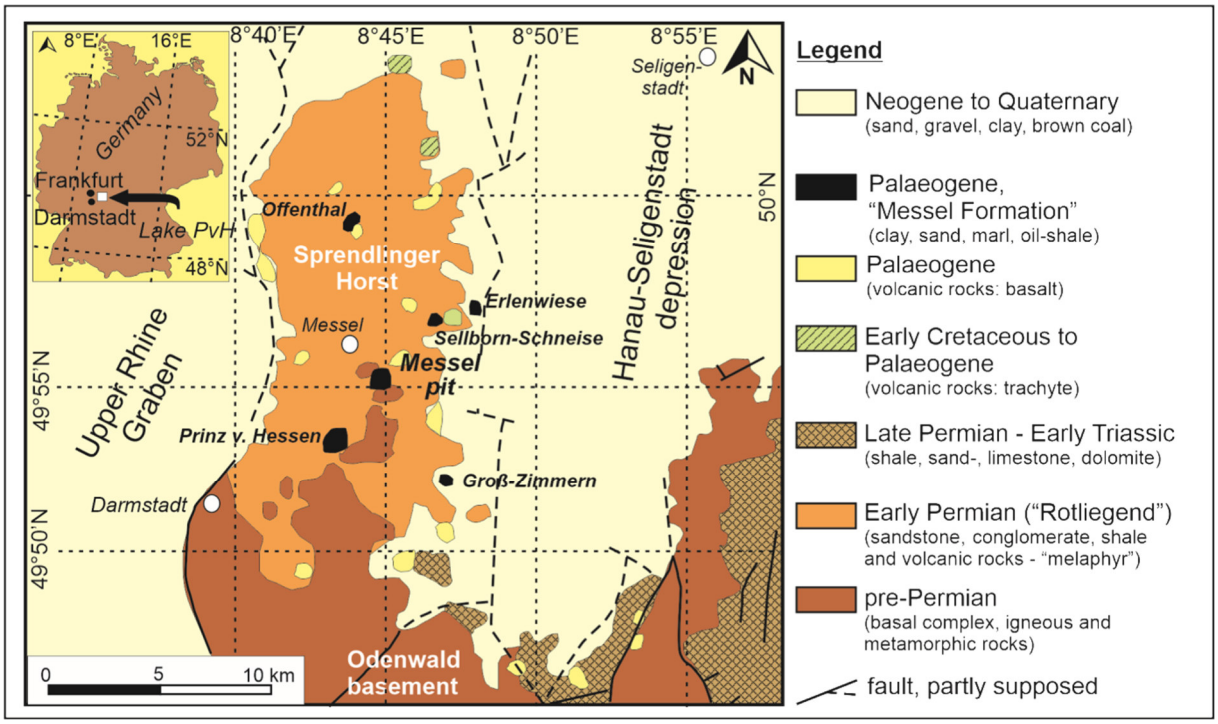

Fig. 4. 9. 1. Geological map of the Sprendlinger Horst (modified after Harms et al. 1999)

The thickness of the Paleozoic cover, including Rotliegend basalts, sedimentary breccias, conglomerates and sandstones, decreases from 250 m in the northern Sprendlinger Horst to zero south of Darmstadt (Marell 1989, Kowalczyk 2001). The southern Sprendlinger Horst is underlain by the Frankenstein Complex and consists of granites, granodiorites, tonalities, diorites and gabbros; the last of latest Devonian to earliest Carboniferous age (ca. 360 Ma; Stein 2001). Mesozoic rocks are followed by a stratigraphic gap that lasts to the early Palaeogene. Eocene extensional tectonics was accompanied by basaltic and trachytic volcanism and local lake deposits, the famous fossil-rich oil shale of Messel, as well as lesser known occurrences at Prinz von Hessen, Gross-Zimmern and Offenthal (Felder et al. 2001).
The Messel and Prinz von Hessen deposits are aligned along a steep gravimetric gradient. Photo lineations within that zone are aligned parallel the Bouguer anomaly isolines (Jacoby et al. 2000, 2005). According to Jacoby et al. (2000) the gravity gradient reflects a 2 km wide, NE–SW-striking sinistral strike-slip fault zone, the so-called Messel Fault Zone (MFZ), which could have originated as a NW-directed thrust fault during the Variscan Orogeny.
The MFZ is thought to be reactivated during the development of the Saar-Nahe Trough in the Permian (Marell 1989) and the Eocene rifting of the URG (Jacoby et al. 2000). 7 km to the SW of the MFZ a transfer zone existed within the URG, acting as a relay ramp connecting half-grabens with different polarity (Derer et al. 2005). The influence of Eocene tectonic activity in the URG on the Sprendlinger Horst is indicated by coeval deposition of the oil shale in Messel (47–45 Ma) and adjacent Prinz von Hessen (Backhaus and Rahnama-Rad 1991, Derer et al. 2005).

Paleogene lacustrine records on the Sprendlinger Horst
The four studied Paleogene lakes represent volcanic and tectonic structures of early to middle Eocene age and their origin have been related to tectonic activity predating the later Rhine Graben system (e.g. Harms et al. 1999; Jacoby et al. 2005).

Lake Prinz von Hessen

Lake Prinz von Hessen had a semi-circular shape with a diameter of 600-800 m and was surrounded by sediments of Permian age (Felder et al. 2001). The character of the basin at Prinz von Hessen remained unclear (Harms 1999; Felder et al. 2001; Jacoby et al. 2005). It has been discussed that it could represent either another maar structure or a small pull-apart basin (Felder et al. 2001, Hofmann et al. 2005). A scientific core with a total thickness of 150 m was drilled in 1997 from the center of the lake basin and has been described by Felder et al. (2001).

The generalized lithologic succession of the core is shown in Fig. 4.9.2. The core can be divided into five lithozones (LZs) which are described by Moshayedi et al. (2018). At the lower part the sediments are characterized by layers of well-bedded clastic sediments composed of laminated carbonate sand, silt and clay (between 95 m and 64.80 m) . Toward the upper part of the core, between 64.80 and 55.40 m, sediments frequently changed to bituminous shales with interbedded turbidites, grainflows and mudflows and finally the rest of the core (about 55 meter) characterized by massive mudstones and laminated bituminous shales without bioturbation which has several meters of alternation of lignite layers and interbedded grey-green mudstones in between. Moshayedi et al. (2018) analyzed the core palynologically, distinguished five lithozones (LZ1-5, Fig. 4.9.2) and proved that the lacustrine filling was deposited in a tectonically controlled small pull-apart basin.

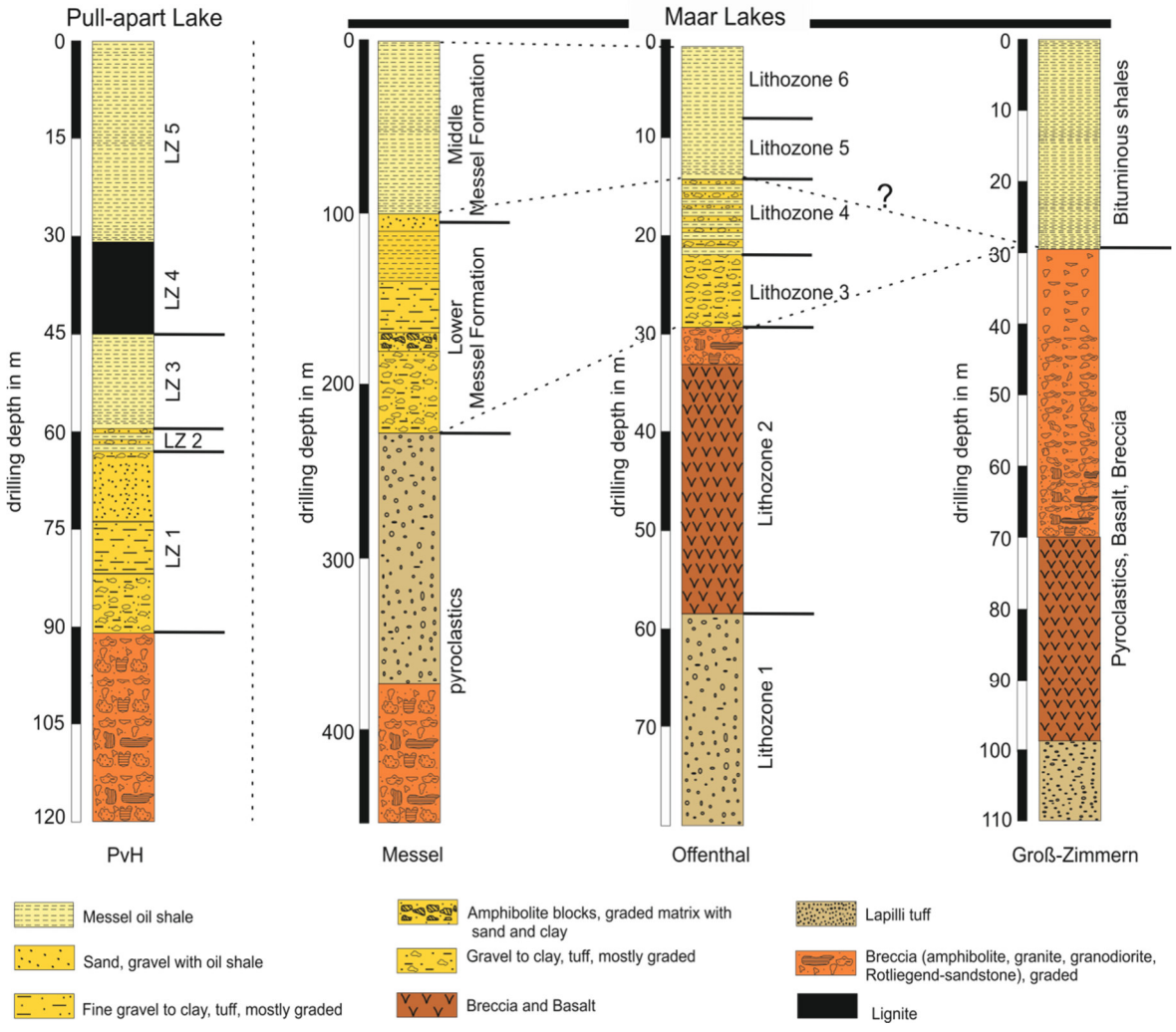

Fig. 4. 9. 2. Generalized sections of the Messel, Prinz von Hessen, Offenthal and Groß Zimmern cores modified after Felder et al. (2001) and Felder and Harms (2004).

Lake Messel

The Messel pit is the most famous isolated Eocene lake on the Sprendlinger Horst and is located about 10 km NE of Darmstadt (Southwest Germany) (Fig. 4.9.1). In 2001 a continuous core was received from a research well in the center of the Paleogene basin at Messel. Starting with typical "Messel oil shale" at the top it shows a differentiated lacustrine succession overlying some volcanoclastics and ends in some kind of vent breccia (Jacoby 1997; Harms et al. 1999; Jacoby et al. 2000; Felder et al. 2001; Felder and Harms 2004; Fig. 4.9.2).

The lowermost part in the core between 433 m and 373 m consists of a diatreme breccia which is overlain by lapilli tuffs to a depth of 228 m. The discovery of these massive volcanoclastic deposits provided final proof that the overlying lake sediments have been deposited within a maar structure that was formed by one or more phreatomagmatic eruptions (Lorenz 2000; Schulz et al. 2002; Harms et al. 2003; Felder and Harms 2004).

The pure mass-flow deposits and pyroclastics are overlain by the Lower Messel Formation (LMF) at a depth of 228 m which is characterized by alternating breccias, tuffs and layers of sand and clay. During that time instability of the crater wall resulted in frequent mass movements as reflected by turbidities and slump deposits in the core and a holomictic conditions existed within the water body. Increasing stability of the crater walls and decreasing turbulence led to the onset of meromictic conditions and the beginning of deposition of oil shale layers in the upper part of LMF at a depth of 140 m. The Lower Messel Formation represents the initial lake phase (Lenz et al. 2007) and is terminated by an "event bed" from the succeeding Middle Messel Formation (MMF) at a depth of 110 m. The MMF is identical with the classical "Messel Oil-shale", the finely laminated highly bituminous shale known for its unique fossil preservation and formed during the predominantly stable meromictic phase of the lake. The MMF is unconformably overlain by the Upper Messel Formation, an intercalation of inorganic claystones of various colors and coal beds restricted to three troughs in the south and east of the basin (Matthess 1966).

Lake Offenthal

Among the Paleogene lacustrine basins on the Sprendlinger Horst Lake Offenthal is one of the smallest with a diameter of only 200 – 400 m (Felder et al. 2001). In order to find unequivocal proof for the origin of the basin, a scientific well (B/98-BK 1E) was drilled 1998 in the center of the basin to penetrate the lake sediments. A total of 80 m was cored of which the lower 51 m consist of volcanic rocks such as lapilli tuff, breccia and basalt that can be separated from a lacustrine succession in the upper 29 m (Fig. 4.9.2). Based on lithological changes Felder et al. (2001) divided the core in seven lithozones (LZ 1 to LZ 7), the lower two of them (LZ1 and 2; Felder at al. 2001) of purely volcanic origin. The lacustrine sediments, that became the focus of our palynological study (Moshayedi et al. 2020, Fig. 4.9.2), can be divided into four lithozones (Felder et al. 2001; Lithozone 3 to 6). A first bituminous siltstone marks the boundary between LZ 3 and 4. In LZ5 bituminous shales are dominant (Felder et al. 2001). The same as for LZ 5 also applies to LZ 6 between 8.25 and 1.8 m. However, in contrast to LZ 5, the bituminous shales are often finely laminated and frequently interspersed with siderite laminae (Felder et al. 2001).

Lake Groß Zimmern

Groß Zimmern is another small Paleogene maar lake in this area and is generally characterized by a similar lithological succession compared to the records of Lake Messel and Lake Offenthal (Felder et al. 2001). A scientific well has been drilled in 1997. Among the 116 m core the lower 80 m can be divided in four lithozones (Felder et al. 2001) which consist of pyroclastics, basalt and breccia. The overlying 32 m are lacustrine deposits (Fig. 4.9.2) and are composed of bituminous shales separated into two parts (lithozones 5 and 6, Felder et al.

2001). Sedimentological evidence indicates that the core is completely disturbed which is reflected by turbidities, slumps and erosional structures through the succession. In contrast to Messel and Offenthal the lacustrine succession starts directly with bituminous shales that were deposited under meromictic conditions.

Material and methods

Sampling

The present study is primarily based on published data of 114 samples from the LMF (Lenz et al. 2007), 468 samples from the MMF (Lenz et al. 2011), 99 samples from Lake Prinz von Hessen (Moshayedi et al. 2018, 2021), 68 samples from Lake Offenthal (Moshayedi et al. 2020) and 19 samples from Lake Groß Zimmern (Mutzl 2017). Therefore, a total of 768 samples has been analyzed. Samples were selected on the basis of lithology, especially including dark sediments in which a sufficient content of organic material could be expected and they were prepared using standard palynological extraction techniques as described by Kaiser and Ashraf (1974). About 300 palynomorphs were counted per sample. Nevertheless, between 10% to 15% of the total assemblage (Lenz et al. 2007, 2011; Moshayedi et al. 2018. 2020, Mutzl 2017) could not be determined and was recorded as "varia". Therefore 220 to 280 individual counts have been used per sample for palynological investigations.

Non-metric multidimensional scaling (NMDS)

To illustrate compositional differences and ecological trends between different vegetation assemblages from Messel, Prinz von Hessen, Offenthal and Groß Zimmern, NMDS (Shepard 1962 a, b; Kruskal 1964) was performed using the software PAST (Hammer et al. 2001). NMDS is the most robust unconstrained ordination method in ecology (Minchin 1987). For NMDS we used the Bray-Curtis dissimilarity and the Wisconsin double standardized raw data values (Bray and Curtis 1957; Gauch and Scruggs 1979; Oksanen 2007). Wisconsin standardization scales the abundance of each taxon to its maximum value and represents the abundance of each taxon by its proportion in the sample (Mander et al. 2010). This removes the influence of sample size on the analysis and equalizes the effects of rare and abundant taxa on clustering and NMDS (Van Tongeren 1995; Jardine and Harrington 2008).

Results

In order to reveal similar palaeoecological trends and changes in the composition of the vegetation around the four the lakes NMDS has been applied on the standardized palynological data set (Fig. 4.9.3). The scatter plot of the first two axes of the NMDS shows the arrangement of 780 samples from the four Paleogene lakes at Messel, Prinz von Hessen, Offenthal and Groß Zimmern.

Samples from the Prinz von Hessen group separately in the ordination space on the right end of the NMDS plot indicating a significant difference in composition between palynomorph assemblages of Prinz von Hessen and samples from the other cores (Fig. 4.9.3). There is a clear separation between samples from Prinz von Hessen and samples from Offenthal as well as Groß Zimmern on the right side of the diagram with positive values indicating that each lake has its own specific palynomorph composition. Samples of core Groß Zimmern are separated in two groups that may be related to the disturbance of the lithological succession at Groß Zimmern (Fig. 4.9.3). Samples of the LMF are plotted nearly at the center of the NMDS ordination space. However, samples from the lower part of the LMF on the positive side of the ordination space can be clearly distinguished from samples of the upper part of the LMF and the succeeding MMF on the negative side of the ordination space. This is in general identical with a separation of samples from the lower part of the LMF or Early Initial Lake Phase (EILP) and samples from the upper part of the LMF or Late Initial Lake Phase (LILP) (Lenz et al. 2007; Fig. 4.9.3). Lenz et al. (2011) showed that the floral development within the

MMF can be divided into three phases emphasizing that changes in the composition of vegetation were gradual. All the samples from the MMF are plotted on the negative side of NMDS ordination space (Fig. 4.9.3).

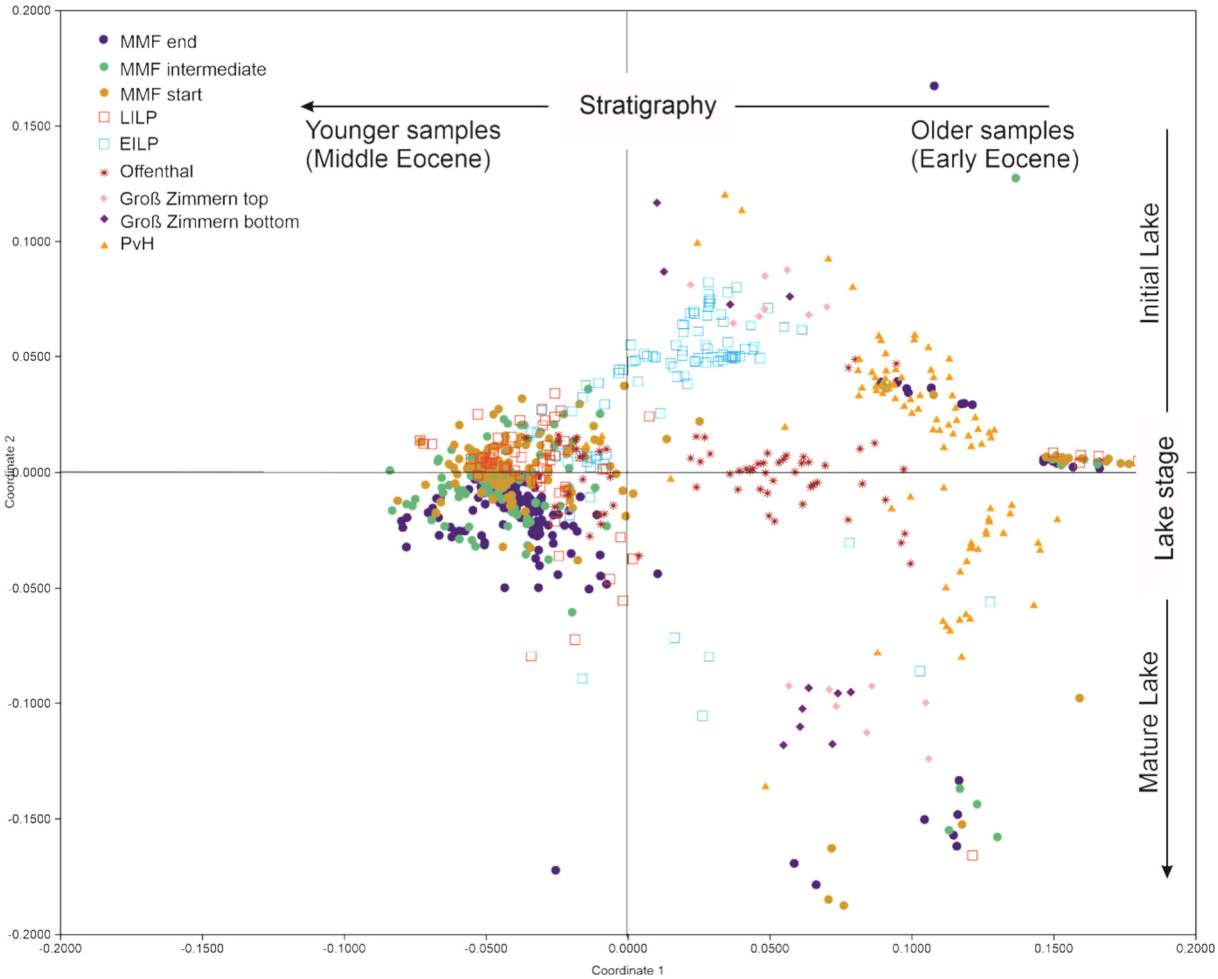

Fig. 4. 9. 3. Non-metric multidimensional scaling (NMDS) of palynological data of 780 samples from the lacustrine succession of the Messel, Prinz von Hessen, Offenthal and Groß Zimmern lakes using the Bray-Curtis dissimilarity and the Wisconsin double standardised raw data values. Scatter plot of the first two axes showing the arrangement of samples.

The NMDS plot of taxa (Fig. 4.9.4) show that there is a group of palynomorphs which are plotted on the positive side of the first NMDS axis. Especially fern spores and other pioneering taxa (Fig. 4.9.4) are therefore abundant in samples which are plotted on the same side of the ordination space. On the other hand taxa, such as pollen of Juglandaceae and Fagaceae, are plotted on the negative left side of the first NMDS axis that indicates a dominance of these palynomorphs in samples of the MMF.

Discussion

Lake Messel and Offenthal are generally characterized by a similar succession of lithological units starting with volcanic rocks (Fig. 4.9.2) providing proof that the respective lake sediments have been deposited within maar structures which were formed by one or more phreatomagmatic eruption(s) (Felder et al. 2001; Liebig 2002; Felder and Harms 2004). The lacustrine succession at Groß Zimmern is completely mixed and it is obviously overturned (initial elements in the upper part of the succession as nicely shown by the NMDS) which may be due to slope failure, possibly caused by limnic eruption(s) (according to Mutzl 2017). However it has been also deposited in a maar structure whereas Prinz von Hessen represents

not a maar lake but a pull-apart basin (Fig. 4.9.2; Moshayedi et al. 2018). In order to compare the vegetation around these lakes, NMDS was carried out including 780 samples from all lakes.

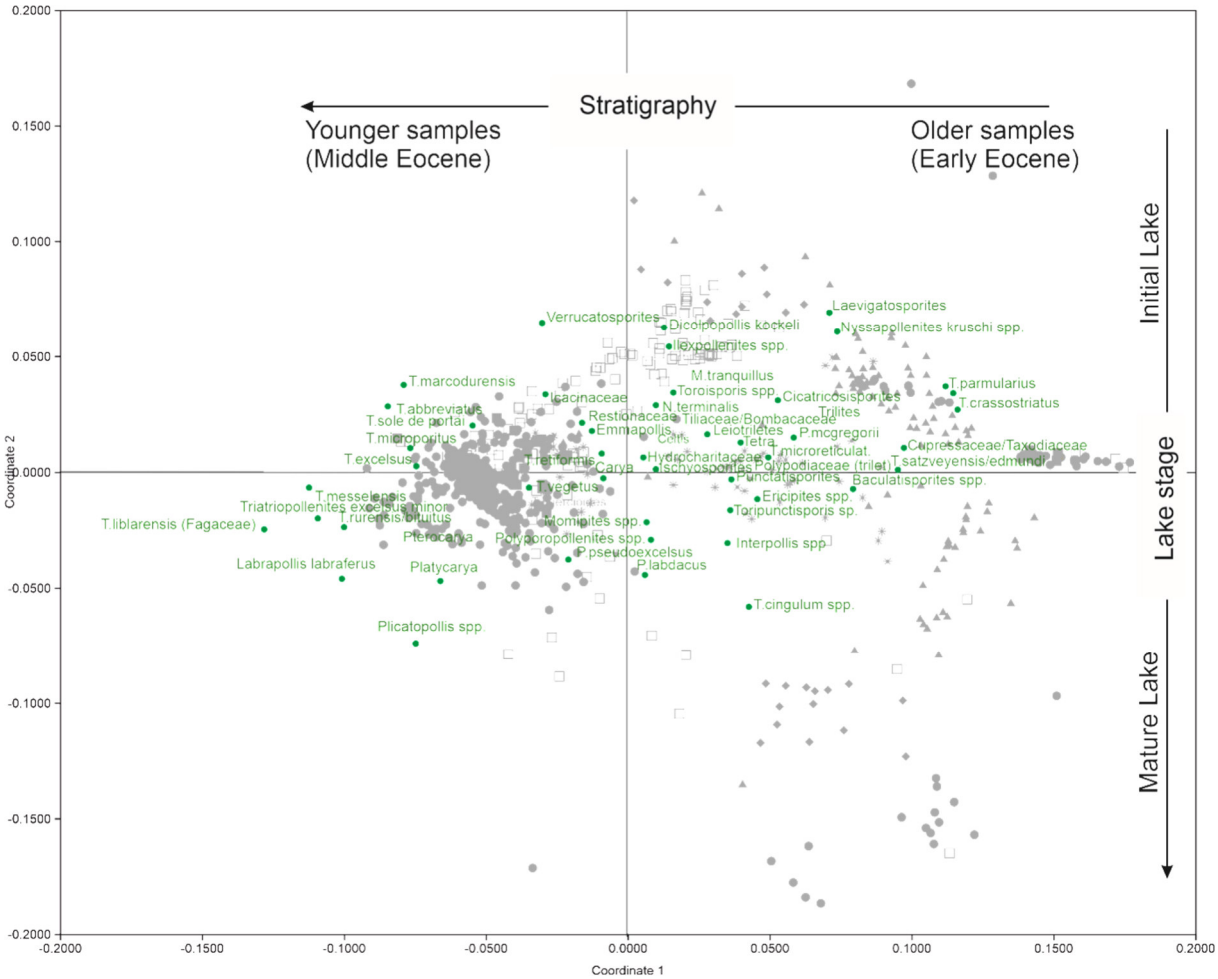

Fig. 4. 9. 4. Non-metric multidimensional scaling (NMDS) of palynological data of 780 samples from the lacustrine succession of the Messel, Prinz von Hessen, Offenthal and Groß Zimmern lakes using the Bray-Curtis dissimilarity and the Wisconsin double standardised raw data values. Scatter plot of the first two axes showing the arrangement of taxa. The dots represent the different samples.

NMDS shows that there is a continuous change in the composition of vegetation during the different lake phases at Messel, because the samples from the LMF group separately in the ordination space at the middle of the NMDS ordination space (Fig. 4.9.3), indicating a significant difference in composition between the palynomorph assemblage of the LMF and MMF. This is mainly related to the disappearing of most of the fern spores toward the MMF. During the MMF especially forest plants such as those from the Juglandaceous became dominant (Fig. 4.9.4). Toward the MMF palynomorphs of the initial pioneering vegetation, such as most of the ferns, disappear almost entirely (Fig. 4.9.4) and reflects the change from a purely pioneering vegetation to a thermophilic forest successively invading the area around the crater as well as the lake margin (Fig. 4.9.5). Thermophilic forest reached a climax state in the MMF as indicated by a strong increase of forest elements such as Fagaceae (*Tricolporopollenites cingulum*) and Juglandaceae (*Plicatopollis* spp.) (Lenz et al. 2007; 2011; 2015; 2017; 2018).
Samples of Prinz von Hessen are plotted at the right end of the first NMDS axis. Similar to Messel the pollen assemblage at Prinz von Hessen is in the lowermost part characterized by a diverse fern spore community indicating extended fern meadows flourishing during the initial

part of the lake evolution (Fig. 4.9.4). Compared with the pollen assemblage from the earlier part of Prinz von Hessen significant changes become obvious towards the top of the succession indicating a community of the (para)tropical forest dominated by elements of a climax stage of the Paleogene European vegetation (Moshayedi et al. 2018) such as Fagaceae (*Tricolpopollenites liblarensis, Tricolporopollenites cingulum*) and Juglandaceae (*Plicapollis* spp., Plicatopollis spp.). This indicates that the regional climax vegetation already existed in the vicinity of Lake Prinz von Hessen during the initial phases of lake development (Fig. 4.9.5; Moshayedi et al. 2018). However, the climax vegetation at Prinz von Hessen and Messel are characterized by significant compositional differences as shown by the NMDS. Therefore, a general compositional difference between the lower and middle Eocene vegetation in the area is indicated.

Fig. 4. 9. 5. Comparison of the lake stages at Messel, Prinz von Hessen, Offenthal and Groß Zimmern.

Samples from Lake Offenthal are plotted mainly in the center of the ordination space (Fig. 4.9.3). The NMDS reveals that palynomorph assemblages from Offenthal are different compared to the assemblages of Messel and Prinz von Hessen (Fig. 4.9.3, 4.9.4), because the samples are separated in the ordination plot. This indicates that the composition of the vegetation was different in the crater areas at Offenthal and Messel as well at the lake margin at Prinz von Hessen. However the recolonization of the devastated areas at Messel and Offenthal followed a similar pattern indicated by palynological assemblages that reflect typical vegetation communities for the recolonization of Eocene maar lakes (Moshayedi et al. 2018; 2020). A fundamental difference between the successions become obvious in the NMDS by the fact that the samples from the MMF are plotted on the left side of the ordination space clearly separated from the samples of the other records (Fig. 4.9.3). During the MMF, at Messel, a robust climax vegetation existed for several hundred thousand years which was characterized by pollen assemblages without significant qualitative changes (Lenz et al. 2011; Lenz and Wilde 2018). Only quantitative changes in the dominance of individual pollen species occurred. Such a vegetation, which can be attributed to a climax phase and which follows the recovery phase in a natural vegetational succession by absence of further disturbance of the crater area is not documented in Offenthal (Fig. 4.9.5). The climax vegetation at Messel is dominated especially by fagaceous (*Tricolporopollenites cingulum*, *Tricolpopollenites liblarensis*) and juglandaceous (e.g. *Plicatopollis* spp. and *Plicapollis* spp.) plants (Lenz et al. 2011; Lenz and Wilde 2018). Although these pollen taxa are also very common in other sites they are not as dominant as in Messel indicating that the final climax phase is not reached in Offenthal (Fig. 4.9.5).
NMDS reveals a stratigraphic order of the four lacustrine records. Based on $^{40}Ar/^{39}Ar$ dates the eruptions at Messel (48.2 ± 0.3 Ma, Lenz et al. 2015) and Offenthal (47.8 ± 03 Ma, Mertz

and Renne 2005; Moshayedi et al. 2020) are nearly of the same age around the lower/middle Eocene boundary. Based on our palynostratigraphic study (Mutzl 2017) it seems also likely that Lake Groß Zimmern has a similar age as the adjacent crater lakes of Messel and Offenthal (Fig. 4.9.6). However, this must be confirmed by radiometric dating in the near future. The palynostratigraphic study of Prinz von Hessen indicates that Lake Prinz von Hessen is some million years older than Messel (Moshayedi et al. 2018). Therefore, the differences between the ecosystems at Prinz von Hessen (lower Eocene) and Messel (middle Eocene) are probably related to stratigraphically based compositional differences in the climax vegetation.

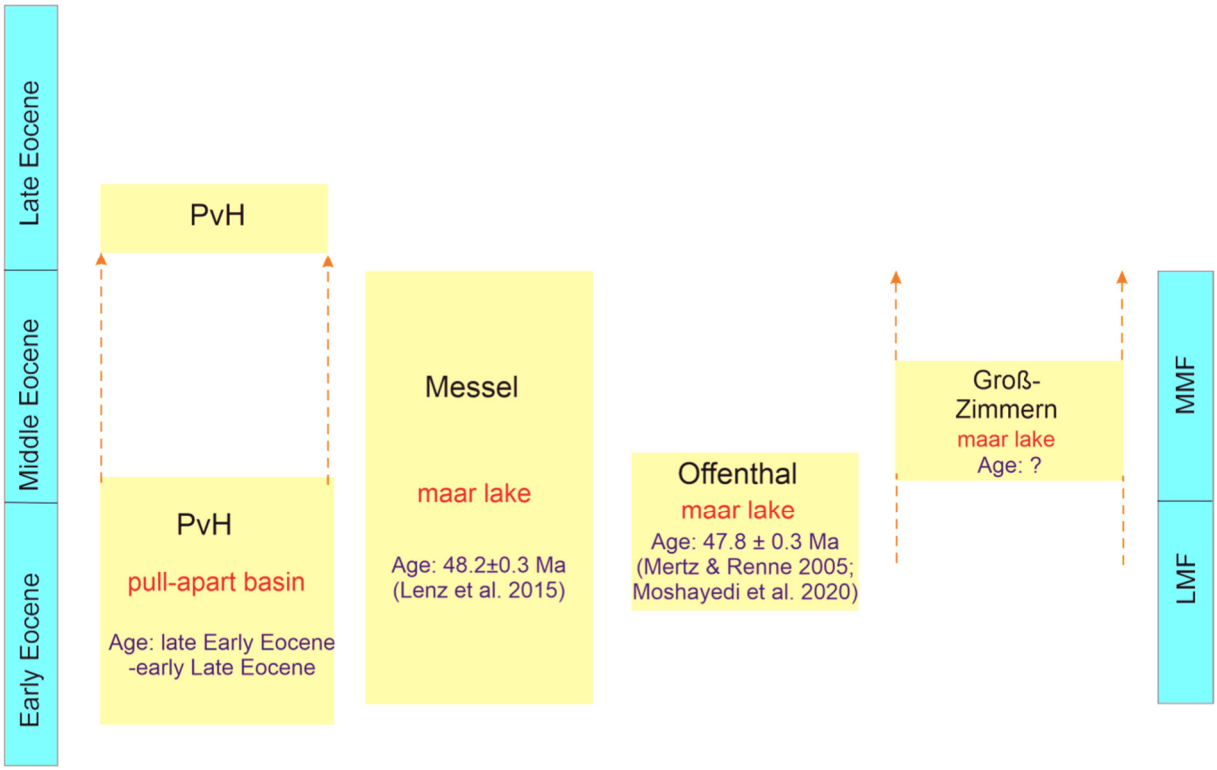

Fig. 4. 9. 6. Age model for the lakes at Messel, Prinz von Hessen, Offenthal and Groß Zimmern.

Conclusion

Except Prinz von Hessen, which is a small pull-apart basin, the other studied basins on the Sprendlinger Horst are maar fillings and formed as a consequence of phreathomagmatic eruptions. Based on revised 40Ar/39Ar dates the eruptions at Offenthal and Messel are nearly of the same age around the Lower/Middle Eocene boundary. Quantitative palynological analyses revealed different pollen and spore assemblages for each basin, but similar general trends in the evolution of vegetation can be recognized in all of the basins. Each of the maar lakes show a similar pioneering stage, followed by the progressive development of a paratropical forest. A terminal climax vegetation is only documented at Messel. The succession at Lake Groß Zimmern was completely mixed after deposition due to tectonic activity or CO2 outburst (Mutzl 2017).

NMDS reveals that there are two main factors controlling the composition of the palynomorph assemblages. The first factor is the stratigraphic influence because the records from the uppermost lower Eocene (Prinz von Hessen), from the lower/middle Eocene boundary (Offenthal, LMF) and the middle Eocene (MMF) are nicely arranged in stratigraphic order along axis one in the NMDS ordination space indicating that the pioneering as well as the climax vegetation was specific for each of the time intervals captured by the different records. The most important differences in the pioneering vegetation

are related to the composition of the fern communities at Messe and Offenthal (Moshayedi et al. 2020). Differences in the composition of the climax vegetation at Messel and Prinz von Hessen are based on the dominance of Fagaceae in the MMF (Moshayedi et al. 2018, Lenz et al. 2011). Factor 2 is the maturity of the lake because during the initial stages and the late stages of the different lakes strong differences in the palynomorph assemblages are obvious. The general evolution of the vegetation is the same in these disturbed areas on the Sprendlinger Horst, starting with a pioneering vegetation and ending with a robust climax vegetation. However, each of the records has a specific story, which is influenced by these two factors.

References

Backhaus, E., and Rahnama-Rad, J. (1991). Die Rutschgefährdung der Messel-Formation (Fundstätte Messel; Mittel-Eozän). Einflüsse der Tektonik, der Hydrogeologie und der Materialeigenschaften der Gesteine. *Cour. Forsch.-Inst. Senckenberg*, 139, 1-69.

Bray, J.R., Curtis, J.T. (1957). An ordination of the upland forest communities of southern Wisconsin. *Ecological Monographs*, *27*, 325-349.

Derer, C. E., Schumacher, M. E., and Schäfer, A. (2005). The northern Upper Rhine Graben: basin geometry and early syn-rift tectono-sedimentary evolution. *International Journal of Earth Sciences*, 94(4), 640-656.

Felder, M., Harms, F.J. (2004). Lithologie und genetische Interpretation der vulkano-sedimentären Ablagerungen aus der Grube Messel anhand der Forschungsbohrung Messel 2001 und weiterer Bohrungen. *Courier Forschungsinstitut Senckenberg*, 252, p 151-203.

Felder, M., Harms, F.J. and Liebig, V. (2001). Lithologische Beschreibung der Forschungsbohrungen Groβ-Zimmern, Prinz von Hessen und Offenthal sowie zweier Lagerstättenbohrungen be Eppertshausen (Sprendlinger Horst, Eozän, Messel-Formation, Süd-Hessen). *Geologische Jahrbuch Hessen*, 128, 29–82.

Hammer, Ø., Harper, D.A.T. and Ryan, P.D. (2001). PAST: Paleontological Statistics Software Package for Education and Data Analysis. *Palaeontologia Electronica*, 4**,** http://palaeo-electronica.org/ 2001_1/past/issue1_01.htm.

Harms, F.-J. (1999) mit Beitr. von Wallner, H. and Jacoby, W.: Verbreitungder Messel-Formation und der Tiefenlage der Basis desDeckgebirges (Miozän, Pliozän und Quartär) am Ostrand des Sprendlinger Horst es.–1 Kt. Hessisches Landesamt für Bodenforschung.

Harms FJ, Aderhold G, Hoffmann I, Nix T, Rosenberg F (1999) Erläuterungen zur Grube Messel bei Darmstadt, Südhessen. Schriftenreihe der Deutschen Geologischen Gesellschaft 8: 181-222.

Harms, F. J., Nix, T., and Felder, M. (2003). Neue Darstellungen zur Geologie des Ölschiefer-Vorkommens Grube Messel. *Natur und Museum*, 133(5), 140-148.

Hofmann, P., Duckensell, M., Chpitsglous, A. and Schwark, L. (2005). Geochemical and organic petrological characterization of the organic matter of lacustrine Eocene oil shales (Prinz von Hessen, Germany): reconstruction of the depositional environment. *Paleolimnology*, 33, 155–168.

Jardine, P. E., and Harrington, G. J. (2008). The Red Hills Mine palynoflora: A diverse swamp assemblage from the Late Paleocene of Mississippi, *USA. Palynology*, *32(1)*, 183-204.

Jacoby, W. (1997). Tektonik und Eozäner Vulkanismus des Sprendlinger Horstes, NE-Flanke des Oberrheingrabens. *Schriftenreihe der Deutschen Geologischen Gesellschaft*, 2, 66–67.

Jacoby, W., Wallner, H. and Smilde, P. (2000). Tektonik und Vulkanismus entlag der Messel-Störungszone auf dem Sprendlinger Horst: Geophysikalische Ergebnisse. *Zeitschrift der Deutschen Gesellschaft für Geowissenschaften*, 151, 493-510.

Jacoby, W., Sebazungu, E., Wallner, H., Gabriel, G. and Pucher, R. (2005). Potential field data for the Messel Pit and surroundings. *Courier Forschungsinstitut Senckenberg*, 255, 1–9.

Kaiser, M.L. and Ashraf, R. (1974). Gewinnung und Präparation fossiler Pollen und Sporen sowie anderer Palynomorphae unter besonderer Berücksichtigung der Siebmethode. *Geologisches Jahrbuch*, 25, 85–114.

Kowalczyk, G. (2001). Permokarbon des Sprendlinger Horstes und der westlichen Wetterau (Exkursion I am 20. April 2001). *Jahresberichte und Mitteilungen des Oberrheinischen Geologischen Vereins*, 211-236.

Kruskal, J.B. (1964). Nonmetric multidimensional scaling: a numerical method. *Psychometrika*, *29*, 115-129.
Kuiper, K.F., Deino, A., Hilgen, F.J., Krijgsman, W., Renne, P.R., Wijbrans, J.R. (2008). Synchronizing rock clocks of Earth history. *Science*, 320, 500–504
Lenz, O.K., Wilde, V. and Riegel, W. (2007). Recolonization of a Middle Eocene volcanic site: quantitative palynology of the initial phase of the maar lake of Messel (Germany). *Review of Palaeobotany and Palynology*, 145, 217 – 242.
Lenz, O.K., Wilde, V., Riegel, W., Harms, F.J. (2010). A 600 k.y.record of El Niño-Southern Oscillation (ENSO): Evidence for persisting teleconnections during the Middle Eocene greenhouse of Central Europe. *Geology*, 38(7), 627-630.
Lenz, O.K., Wilde, V. and Riegel, W. (2011). Short-term fluctuation in vegetation and phytoplankton during the middle Eocene greenhouse climate: a 640-kyr record from the Messel oil shale (Germany). *International Journal of Earth Sciences*, 100, 1851-1874.
Lenz, O.K., Wilde, V., Mertz, D.F. and Riegel, W. (2015). New palynology-based astronomical and revised $^{40}Ar/^{39}Ar$ ages for the Eocene maar lake of Messel (Germany). *International Journal of Earth Sciences*, 104, 873-889.
Lenz, O.K., Wilde, V. and Riegel, W. (2017). ENSO-and solar-driven sub-Milankovitch cyclicity in the Paleogene greenhouse world: high resolution pollen records from Eocene Lake Messel, Germany. *Journal of the Geological Society*, 174, 110-128.
Lenz, O. K., and Wilde, V. (2018). Changes in Eocene plant diversity and composition of vegetation: the lacustrine archive of Messel (Germany). *Paleobiology*, 44(4), 709-735.
Liebig, W. 2002. Neuaufnahme der Forschungsbohrungen KB 1,2, 4, 5, und 7 von 1980 aus der Grube Messel (Sprendlinger Horst, Stidhessen). – *Kaupia*, 11: 3-68
Lorenz, V. (2000). Formation of maar-diatreme volcanos. *Terra Nostra 2000/6*: 284-291
Mander, L., Kürschner, W.M., McElwain, J.C. (2010). An explanation for conflicting records of Triassic–Jurassic plant diversity. *Proceedings of the National Academy of Sciences of the United States of America*, 107, 15351–15356.
Marell, D. (1989). Das Rotliegende zwischen Odenwald und Taunus: *Geologische Abhandlungen Hessen*.
Matthess, G. (1966). Zur Geologie des Ölschiefervorkommens von Messel bei Darmstadt: Abhandlungen des Hessischen Landesamtes für Bodenforschung
Mertz, D.F., and Renne, P.R. (2005). A numerical age for the Messel fossil deposit (UNESCO World Heritage Site) derived from 40Ar/39Ar dating on a basaltic rock fragment. *Courier Forschungsinstitut Senckenberg*, 255, 67-75.
Minchin, P.R. (1987). An evaluation of the relative robustness of techniques for ecological ordination. *Vegetation*, 69, 89-107.
Moshayedi, M., Lenz, O.K., Wilde, V., Hinderer, M. (2018). Controls on sedimentation and vegetation in an Eocene pull-apart basin (Prinz von Hessen, Germany): evidence from palynology. *Journal of the Geological Society*, 175, 757-773.
Moshayedi, M., Lenz, O.K., Wilde, V., Hinderer, M., 2020. The recolonization of volcanically disturbed habitats during the Eocene of Central Europe: The maar lakes of Messel and Offenthal (SW Germany) compared. Palaeobiodiversity and Palaeoenvironments, 100, 951–973 (2020). https://doi.org/10.1007/s12549-020-00425-4
Moshayedi, M., Lenz, O.K., Wilde, V., Hinderer, M. (2021): Lake-level fluctuations and allochthonous lignite deposition in the Eocene pull-apart basin “Prinz von Hessen” (Hesse, Germany) - A palynological study. *Syntheses in Limnogeology*, Rosen, M.R., Finkelstein, D., Park Boush, L., Pla-Pueyo, S. (eds.): Limnogeology: Progress, Challenges and Opportunities - A Tribute to Elizabeth Gierlowski-Kordesch, Chapter 3. Springer Nature (in press)
Mutzl, J., (2017). Klima und Vegetationsdynamik während der eozänen Treibhausphase in Mitteleuropa: Palynologische Untersuchungen der lakustrinen Sedimente aus dem Maar-See von Groß Zimmern. Masrearbeit, Institut für Angewandte Geowissenschaften, TU Darmstadt.
Oksanen, J. (2007). Standardization methods for community ecology. Documentation and user guide for package Vegan, 1.8-6.
Schumacher, M. E. (2002). Upper Rhine Graben: role of preexisting structures during rift evolution. Tectonics, 21(1), 6-1

Schulz R, Harms FJ, Felder M (2002) Die Forschungsbohrung Messel 2001: Ein Beitrag zur Entschlüsselung der Genese einer Ölschieferlagerstätte. *Z Angew Geol*, 48:9–17

Shepard, R.N. (1962a). Analysis of proximities: Multidimensional scaling with an unknown distance function. I. *Psychometrica*, *27*, 125–140.

Shepard, R.N. (1962b). Analysis of proximities: Multidimensional scaling with an unknown distance function. II. *Psychometrica*, 27, 219–246.

Schwarz, M., and Henk, A. (2005). Evolution and structure of the Upper Rhine Graben: insights from three-dimensional thermomechanical modelling. *International Journal of Earth Sciences*, 94(4), 732-750.

Stein, E. (2001): Die magmatischen Gesteine des Bergsträßer Odenwaldes und ihre Inplatznahme-Geschichte. – Jber. Mitt. Oberrhein. *Geol*. Ver., N.F., 83, 267–283.

Van Tongeren, O. F. (1995). Data analysis or simulation model: a critical evaluation of some methods. *Ecological modelling*, 78(1-2), 51-60.

Zeh, A., and Will, T. M. (2010). The mid-German crystalline zone. Pre-Mesozoic Geology of Saxo-Thuringia–from the Cadomian Active Margin to the Variscan Orogen. Schweizerbart, Stuttgart, 195-220.

Ziegler, P. A., and Dèzes, P. (2005). Evolution of the lithosphere in the area of the Rhine Rift System. *International Journal of Earth Sciences*, 94(4), 594-614.

5- Conclusion and outlook

Based on the palynological studies a number of general conclusions can be drawn on the evolution of palaeoclimate and palaeoenvironment during the Paleogene greenhouse on the Sprendlinger Horst:

1) Palynomorphs are of high importance for studying deep time terrestrial records. Pollen assemblages can be used to answer biostratigraphic questions, to enable correlation between geographically separated regions and allow the reconstruction of the palaeoenvironment as well as the paleoclimate. The study of palynomorphs is also essential for understanding the plant evolution. But the requirement is always a high resolution palynological study of the sedimentary successions. These studies generate large amount of data. Therefore, it is vital to evaluate the data by different multivariate statistical methods to simplify the interpretation of the data and identify hidden structures in the data set. Investigations of isolated samples are suitable for answering stratigraphic questions (chapter 4-8), but high-resolution studies are needed for analyzes of paleoenvironment and paleoclimate in order to get an robust insight in the composition of the vegetation because facies conditions or changes in the depositional area have a high impact on the composition of the pollen assemblages (chapter 4-7).
2) Palynological analyses are especially suited for chronostratigraphic correlation and dating of sedimentary records when absolute radiometric dating is not possible due to the lack of appropriate material. As an example, based on the palynological study of the lacustrine succession of Lake Prinz von Hessen it could be proven that the lake is considerably older than previously assumed based on the association of pollen and spores (chapter 4-6; 4-8; Moshayedi et al. 2018).
3) The lacustrine filling of maar lakes are perfect archives for the preservation of paleoenvironmental information due to meromictic conditions caused by a comparatively great water depth in combination with a relatively small size of the lake. Anoxic conditions in the bottom water facilitate the extraordinarily good preservation of fossils and allow high resolution paleoenvironmental studies, because the basin is often filled by undisturbed and finely laminated (varved) sediments. Perfect examples are the highly resolved pollen records from the oil shale of Messel and Offenthal which provide insights into the dynamics of pioneering and climax vegetation and thus serve as records for vegetation changes and their potential cyclicity within the last greenhouse system (Moshayedi et al. 2020).
4) Based on the comparison of palynological assemblages as preserved in different localities on the Sprendlinger Horst similar processes during the recolonization of the volcanically disturbed sites can be recognized (chapter 4-9). However, each locality is characterized by a specific palynomorph assemblage which is slightly different from the others, indicating the influence of local conditions (for example size of the lakes), which influenced the pioneering vegetation.
5) The palynological studies reveal that different factors have influenced the evolution of the vegetation on the Sprendlinger Horst. For example, the Messel Oil shale provides an important reference for understanding the effect of orbital forcing on the composition and diversity of the vegetation in an equable warm climate (Lenz et al. 2011, 2017; Lenz and Wilde 2018) whereas in Prinz von Hessen tectonic activities significantly influenced the long-term evolution of the lake and the vegetation and are more important than climate variations. Frequent disturbance of the lacustrine succession and an allochthonous origin of the lignitic material suggest that tectonic activity had some impact on the paleoenvironment of the lake basin and its surroundings (Moshayedi et al. 2018, 2021).

Annually laminated sediments of Quaternary maar lakes have been widely used as ideal archives of vegetation response to climate and environmental change. The similar studies of temporally highly resolved pollen records from the Eocene lacustrine records on the Sprendlinger Horst prove that it is possible to reconstruct the vegetation and the paleoclimate in detail also for the Paleogene in Central Europe. Especially the maar lake records provide perfect insight into the dynamics of a climax vegetation. However, to link Paleogene and Quaternary records it is also important to extend the palynological studies of the Sprendlinger Horst to younger deposits in Central Europe to complete the picture of the terrestrial evolution of the vegetation in this region.

For example, the finely laminated and possibly varved lacustrine filling of the maar lake of Bärnau (western Eger rift, Upper Palatinate, Bavaria, Germany) which is expected to be of Miocene to Pliocene age, have the potential to become an important archive for Neogene climate and climate cyclicity. This would be bridging the gap between high resolution palynological studies of the Paleogene greenhouse and the Quaternary icehouse systems. Therefore, Lake Bärnau may be an important reference for understanding the effects of orbital forcing on vegetation under the warm climate of the younger Neogene. Equivalent to Lake Messel, the observed cycles in vegetation changes may closely correspond to orbitally controlled climate variation in the range of the Milankovitch frequency band (eccentricity, obliquity and precession) and -to some extent- to sub-Milankovitch periodicity. Therefore, a postdoctoral project has been planned for a high-resolution palynological study of Lake Bärnau.